The University Of Sheffield.

UNIVERSITY OF SHEFFIELD

FACULTY OF MEDICINE, DENTISTRY AND HEALTH

INFECTION, IMMUNITY AND CARDIOVASCULAR DISEASE DEPARTMENT

Identification of new miRNAs and genes networks in the pathogenesis of Autosomal Dominant Polycystic Kidney Disease (ADPKD)

Author: Laura Vergoz

Supervisors: Prof Albert Ong and Dr Andrew Streets

A thesis submitted in partial fulfilment of the requirements
for the degree of Doctor of Philosophy

September 2017

Abstract

Autosomal Dominant Polycystic Kidney Disease is the most common inherited renal disorder caused by germline mutations in *PKD1* or *PKD2*. However its phenotype can be highly variable between individuals suggesting that genetic, epigenetic and environmental factors can influence disease expression. miRNAs are small non-coding nucleic acids that post-transcriptionally regulate mRNA and whose role in other human diseases has been widely studied. We hypothesised that specific miRNAs could similarly modulate ADPKD pathogenesis and aimed to identify gene targets for these miRNAs, characterising their role in ADPKD and uncovering the mechanisms underlying their dysregulation.

This thesis focused on mir-193b-3p and mir-582-5p, identified from a parallel mRNA-miRNA microarray. Prediction algorithms and bioinformatics tools allowed the selection of putative mRNA targets for both miRNAs, whose enrichment was validated by RT-PCR in several ADPKD models and confirmed by Western blotting. Interactions between miRNAs and their respective targets were analysed using dual-reporter luciferase assays and RT-PCR post-transfection, while 3-dimensional cyst assays were used to study the roles of these genes on the disease phenotype.

ERBB4, *CALB1* and *PIK3R1* were found to be targets for mir-193b-3p *in vitro*. Furthermore, anoctamin-1 and PI3K-p85α were enriched in several models of ADPKD and their knock-down reduced cyst expansion *in vitro*. The down-regulation of two other miRNAs, mir-192-5p and mir-194-5p was confirmed in ADPKD mice, and all showed gender-related differences in expression. Finally, I found that miRNAs maturation was altered in disease and associated with a reduced TRBP expression.

These results suggest that dysregulated miRNAs play a likely role in ADPKD by modifying the expressivity of genes regulating several major pathways. An abnormality in miRNA maturation in particular mediated by TRBP deficiency may be at the centre of this dysregulation. These new miRNAs and their validated targets represent potential novel candidates for developing new drug treatments or biomarkers in ADPKD.

Acknowledgements

I would like to thank my two supervisors for their support throughout my project. I am grateful to Prof Albert Ong for giving me this opportunity as well as providing guidance and intellectual support which allowed me to learn a lot about the field and progress as a researcher. Dr Andrew Streets performed the preliminary experiments at the origin of my project, advised me on the technical aspects of my research and was available to answer my questions when needed. Many thanks to both of them without whom I would not have been able to do my PhD.

This project would not have been possible without the Marie Curie ITN EU-FP7/2007-2013, who funded my research under the grant agreement no. 317246. Being part of the TranCYST group was a rewarding experience that allowed me to collaborate with excellent researchers and regularly attend meetings across Europe to present my work. In particular I would like to thank Prof Dorien Peters, Dr Peter-Bram 't Hoen and Tareq Malas in Leiden University for their invaluable input and collaboration which helped my project progress in the right direction.

Many thanks to all my colleagues within the academic unit of Nephrology and the Kidney Genetics group for their moral and professional support during the course of my PhD and whom I enjoyed working with. I am especially grateful to Dr Morgane Lannoy whose input was essential in the progression of my project and to Lisa Chang and Fiona Wright for their technical advices.

These past few years in Sheffield were not only an exceptional professional development opportunity but also an enriching human experience. I owe this to the many friends I have made here, who allowed me to learn about other cultures and to grow up as a person whilst becoming a better scientist. I am thankful for their presence in the good and the more difficult moments. Thank you also to my friends in France whose friendship has been essential to my life for such a long time and has not been affected by distance.

Enfin, un grand merci à toute ma famille, en particulier mes parents, frère et soeurs, pour avoir cru en moi et soutenu mes choix même lorqu'ils impliquaient de m'éloigner d'eux. Merci de me permettre de réaliser mes rêves et d'avoir toujours été un soutien inconditionnel. Je pense également à tous ceux, qu'ils soient toujours là ou qu'ils nous aient quittés, qui m'ont encouragée et que j'espère avoir rendus fiers.
Vous êtes ma maison, mes repères et le vent qui me porte.

Contents

List of Tables

List of Figures

Publications

Parallel microarray profiling identifies *ErbB4* as a determinant of cyst growth in ADPKD and a prognostic biomarker for disease progression

Andrew J. Streets, Tajdida A. Magayr, Linghong Huang, Laura Vergoz, Sandro Rossetti, Roslyn J. Simms, Peter C. Harris, Dorien J. M. Peters, Albert C. M. Ong

Abstract

Autosomal dominant polycystic kidney disease (ADPKD) is the fourth most common cause of end-stage renal disease. The disease course can be highly variable and treatment options are limited. To identify new therapeutic targets and prognostic biomarkers of disease, we conducted parallel discovery microarray profiling in normal and diseased human *PKD1* cystic kidney cells. A total of 1,515 genes and 5 miRNA were differentially expressed by more than twofold in *PKD1* cells. Functional enrichment analysis identified 30 dysregulated signaling pathways including the epidermal growth factor (EGF) receptor pathway. In this paper, we report that the EGF/ErbB family receptor *ErbB4* is a major factor driving cyst growth in ADPKD. Expression of *ErbB4 in vivo* was increased in human ADPKD and *Pkd1* cystic kidneys, both transcriptionally and posttranscriptionally by mir-193b-3p. Ligand-induced activation of *ErbB4* drives cystic proliferation and expansion suggesting a pathogenic role in cystogenesis. Our results implicate *ErbB4* activation as functionally relevant in ADPKD, both as a marker of disease activity and as a new therapeutic target in this major kidney disease.

American Journal of Physiology - Renal Physiology

Published 1 April 2017 Vol. 312 no. 4, F577-F588 DOI: 10.1152/ajprenal.00607.2016

A systems biology approach identifies reciprocal changes in mir-193b-3p and *PIK3R1* as drivers of cyst growth in ADPKD

L Vergoz, AJ Streets, T Malas, M Lannoy, PA 't Hoen, DJM Peters, and ACM Ong

Autosomal dominant polycystic kidney disease (ADPKD) is the most common inherited cause of end-stage renal disease worldwide. *PKD1* and *PKD2* mutations are present in most patients with clear genotype-phenotype correlations. However, the intrafamilial phenotypic variability in some pedigrees suggests the influence of non-allelic factors. Non-coding RNAs e.g. microRNAs are known to play a major role in health and disease (including PKD) via control of mRNA stability or translation. We recently conducted a parallel mRNA/miRNA array study which found mir-193b-3p, among others, downregulated in human ADPKD cells (Streets et al, 2017), associated with dysregulation of the ErbB4/EGF pathway. To select other relevant genes regulated by mir-193b-3p, we compared our human mRNA dataset with mRNA expression data from *Pkd1* mutant mice (Malas et al., 2017). Dual-reporter luciferase assays with native and mutant seed sequences and immunoblotting were used to demonstrate functional binding of mir-193b-3p to the 3'UTR of *PIK3R1* mRNA. IGF-1 stimulation of human ADPKD cystic cells in 2D and 3D cultures characterized the role of *PIK3R1* in Akt or ERK signaling and on cyst growth. *PIK3R1* was selected as a strong candidate gene and shown to be upregulated ≈3-fold in human cells and mouse *Pkd1* kidney tissue. In parallel, the catalytic subunit PIK3CA was also overexpressed suggesting the most common PI3K enzyme combination is upregulated in ADPKD cells. A functional interaction between *PIK3R1* and mir-193b-3p was confirmed by luciferase assays and immunoblotting. Knockdown of *PIK3R1* or PI3K chemical inhibitors significantly reduced cyst growth in ADPKD cells and influenced Akt and ERK activation by IGF-1. We report that *PIK3R1* and one of its catalytic subunits are upregulated in ADPKD and confirm that it is a target for mir-193b-3p. The role of PIK3R1/PIK3CA in driving cyst growth in ADPKD was functionally linked to hyperactivation of Akt and ERK. The co-regulation of *PIK3R1* and *ErbB4* by mir-193b-3p supports the development of PI3K and ErbB4 inhibitors or mir-193b-3p activators for the treatment of ADPKD.

Poster presented at the ASN Kidney Week 2017 (2nd Nov - 5th Nov 2017, New Orleans, USA)

List of Abbreviations

ACE	Angiotensin converting enzyme
ActD	Actinomycin D
ADPKD	Autosomal Dominant Polycystic Kidney Disease
AGO1-4	Argonaute 1-4
ANO1 (TMEM16A)	Anoctamin 1 (Transmembrane protein 16 A)
APS	Ammonium persulfate
AR	Androgen receptor
Bicc1	Bicaudal C1
BrdU	Bromodeoxyuridine
BSA	Bovine serum albumine
CaCC	Calcium-activated chloride channels
CALB1	Calbindin 1
cAMP	cyclic adenosine 3',5'-cyclic monophosphate
CFTR	Cystic fibrosis transmembrane conductance regulator
CKD	Chronic kidney disease
CLIC5	Chloride intracellular channel 5
DAB	3, 3'-diaminobenzidine
DCT	Distal convoluted tubule
DCP	Decapping protein
ddH2O	double distilled water
DDX	Dead-box protein
DHT	Di-hydro testosterone
DMEM	Dulbecco's modified eagle medium
DMSO	Dimethyl sulfoxide
dNTP	deoxynucleoside triphosphate
E2	17 β-estradiol
ECL	Enhanced chemiluminescence
EDC	Enhancer of decapping
EDTA	Ethylene diamine tetra-acetic acid
EGF	Epidermal growth factor
eGFR	estimated glomerular filtration rate
EGFR	Epidermal growth factor receptor
EMT	Epithelial-mesenchymal transition
ER	Endoplasmic reticulum
ERBB4	Erb-B2 receptor tyrosine kinase 4
ERK	Extracellular signal-regulated kinase
ESR1-2	Estrogen receptor 1-2

ESRD	End-stage renal disease
FBS	Fetal bovine serum
GFP	Green fluorescent protein
GSK3β	Glycogen synthase 3β
HC	Hydrocortisone
HEK293	Human embryonic kidney cells
HNF1β	Hepatic nuclear factor 1β
HRP	Horseradish peroxidase
IFN	Interferon
IgAN	IgA nephropathy
IGF-1	Insuline-like growth factor-1
IHC	Immunohistochemistry
ITS	Insulin-Transferrin-Selenite
JAK/STAT	Janus kinase / Signal transducer & act. of transcription
kb	kilobase
kDa	kiloDalton
KO	Knock-out
LB	Lysogeny broth
LoH	Loop of Henle
LRR	Leucin-rich repeat domain (PC1)
LVH	Left ventricular hypertrophy
L-G	L-Glutamine
MCPIP1	Monocyte chemotactic protein-induced protein 1
MDRD	Modification of diet in renal disease
miRNA	micro-ribonucleic acid
mTOR	Mammalian target of rapamycin
NaCl	Sodium chloride
NaOH	Sodium hydroxide
NRG-1	Neuregulin 1
NSAID	Nonsteroidal anti-inflammatory drug
nt	nucleotide
P/S	Penicillin / Streptomycin
PBMC	Peripheral blood monolayer cells
PBS	Phosphate-buffered saline
PC1/2	Polycystin 1/2
PCP	Planar cell polarity
PCT	Proximal convoluted tubules
PI	Protease inhibitor
PI3K	Phosphoinositide-3-kinase
PIK3R1	Phosphoinositide-3-kinase regulatory subunit 1
PKD1-2	Polycystic kidney disease 1-2
Pre-miRNA	Precursor miRNA

Pri-miRNA	Primary miRNA
PTEN	Phosphatase and tensin homolog
PTGER2	Prostaglandin E receptor 2
PVDF	Polyvinylidene difluoride
RAAS	Renin-angiotensin aldosterone
RCC	Renal cell carcinoma
REJ	Receptor for egg jelly (PC1)
RFP	Red fluorescent protein
RISC	RNA-induced silencing complex
RNase	Ribonuclease
(sq) RT-PCR	(semi-quantitative) Real-time polymerase chain reaction
S6K2	Ribosomal S6 kinase 2
SCR	Serum creatinine
SDS-Page	Sodium-dodecylsulfate-polyacrylamide gel electrophoresis
siRNA	small interferent ribonucleic acid
SOC	Super optimal broth with catabolite repression
T3	Tri-iodo-thyronine
TAE	Tris base, acetic acid, EDTA
TBST	Tris-buffered saline with Tween
TGF-β	Transforming growth factor β
TOP	Tetraginak opening for polycystin (PC2)
TRBP	HIV-1 TAR RNA binding protein
UTR	Untranslated region
VEGF	Vascular endothelial growth factor
VPV2R	Vasopressin V2 antagonist
WB	Western blot
Wnt	Wingless-Type MMTV Integration Site Family, Member 1
WSC	Cell wall integrity and stress response component (PC1)
WT	Wild type
XPO5	Exportin 5
XRN1	5'-3' exoribonuclease 1
ZEB	Zinc-finger E-box-binding homeobox 1
ZFD	Zinc finger domain

Chapter 1

Introduction

1.1 The kidney, an essential organ for the cleaning of blood and water reabsorption, can be affected by Chronic Kidney Disease

The kidneys are major organs responsible for the filtration of waste from the blood and the production of urine. They are essential to regulate electrolytes concentrations and maintain acid base homeostasis.

1.1.1 Anatomy and physiology of the kidney

The kidneys are two bean-shaped organs placed on both sides of the posterior abdominal area. A Danish study reported a median renal length of about 11 cm and a total renal volume of about 140 cm^3 (134 cm^3 for the right side and 146 cm^3 for the left side). The kidneys were significantly larger in men than women and significantly thicker and wider in older subjects (30 year-old vs. 50 year-old, and 50 year-old vs. 70 year-old) (Emamian et al., 1993). The average kidney weight is 130 g, with a difference between right and left kidneys (129 g and 137 g on average, respectively) (Molina and DiMaio, 2012).
A cross-section of a kidney (see Figure 1.1) presents the two main vessels arriving (renal artery) and leaving (renal vein) the organ, as well as the complex network of nephrons composing the kidney. Nephrons are the functional units of the kidney. They are typically about 30 to 55 mm long and are closed on one end by the Bowman's capsule containing the glomerulus, both structures together forming the renal corpuscle.
Glomeruli are supplied by a network of microscopic capillaries that are the first intermediates for the blood filtration function by the kidneys. The glomerular filtration barrier filtrates proteins based on charge and size (<68 kDa) from the blood of the afferent arteriole through the glomeruli capillaries into the Bowman's capsule (Kurts et al., 2013).
Glomerular filtrate is then processed first by the proximal convoluted tubule (PCT) lying in the renal cortex, lined with cuboidal epithelial cells that show irregular outline (Krstic, 1997) giving it a large area for its reabsorption properties. The PCT actively transports Na^+ ions (it reabsorbs $\approx$ 70 % of the filtered NaCl), water (typically reabsorbs 70 % of the filtered water), amino acids (100 %), glucose (100 %) and other carbohydrates, hence regulating the osmolality of the plasma by multiple regulatory complexes involving proteins such as SGLT2 or aquaporin 1 (Zhuo and Li, 2013).

The compounds not reabsorbed by the proximal tubules then pass through the loop of Henle (LoH) that dives into the renal medulla where ≈15-25 % of the total Na^+ and Cl^- ions as well as water are reabsorbed into the interstitial fluid. The descending and ascending limbs of the loop of Henle perform opposite functions: while the descending section passively filtrates water, the ascending section actively reabsorbs NaCl into the medullary interstitium. Therefore, the loop of Henle acts as a counter-current multiplier: the osmotic gradient generated from the active release of ions from the ascending limb of the LoH will lead to the passive release of water from the descending limb, hence to the concentration of urine and the limitation of its volume. The LoH is thus a major actor of the water reabsorption from the kidney (Mount, 2014).

The tubule then re-enters the cortex and forms the distal convoluted tubule (DCT). The DCT epithelium is composed of a single layer of cuboidal cells, smaller than those of the PCT, with no brush border conferring it a larger lumen. These cells are rich in mitochondria that produce enough ATP for the DCT to exert its function of actively transporting electrolytes, essentially Ca^{2+}, K^+, Mg^{2+} and Na^+ (≈ 5-10 % of the total sodium originally filtered from the blood) (Subramanya and Ellison, 2014).

The compounds that have not been reabsorbed into the interstitial fluid, mainly water and waste products, then enter the collecting duct that leaves the cortex to go into the medulla and will eventually merge with others to former the ureter from which the urine will be transported to the bladder for future excretion. The vasopressin hormone (also called antidiuretic hormone) acts on the collecting tubule's water permeability and thus helps adjust the concentration of the excreted urine, through processes mainly involving adenylate cyclase, increases in cAMP and subsequent phosphorylation of aquaporin 2 channels (Boone and Deen, 2008).

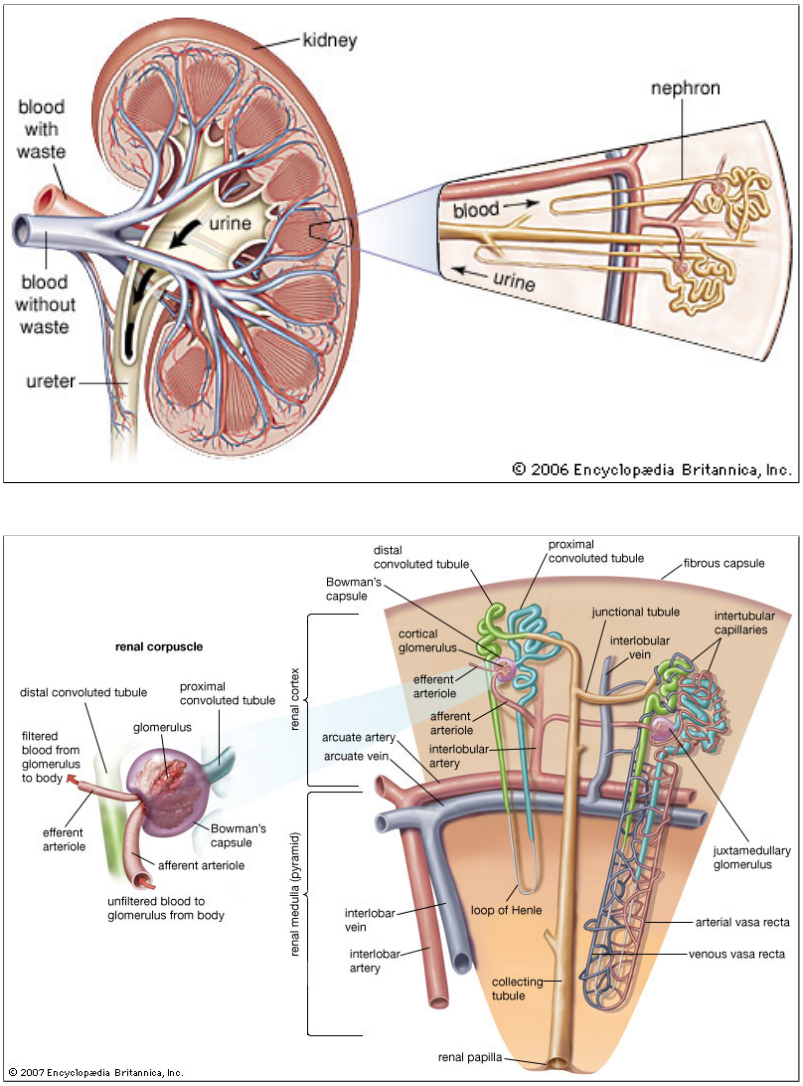

Figure 1.1: **Anatomy of the kidney.**
Top panel: cross-section of a kidney presenting the blood vessels, ureter and multiple nephrons composing the organ. Bottom panel: detail of a nephron including the renal corpuscle, tubules and vessels.
By courtesy of Encyclopaedia Britannica, Inc., copyrights 2006 & 2007; used with permission.

On a typical day, with a fluid intake of about 2 litres, the one to two million nephrons of the kidney produce $\approx$ 150 L of filtrate from plasma, *i.e.* 100 mL/min. Over 90 % of this filtrate is reabsorbed by the body, leading to the production of $\approx$ 1.5 L of urine per day (Tack, 2010). This volume can naturally vary with water intake, physical exercise, vasopressin expression levels or age of the individual.

The typical test used to evaluate the integrity of the kidneys function in a patient is the calculation or estimation of the Glomerular Filtration Rate. The Modification of Diet in Renal Disease (MDRD) study's formula was until recently the most used method that evaluated GFR depending on four variables: serum creatinine concentration, gender, age and ethnicity (NKF, 2002). Indeed, creatinine is a waste amino acid product from the muscles and is normally filtered by the glomerulus and secreted by PCT cells (Stevens et al., 2006). Measuring the clearance of creatinine by the kidney can thus be an indicator of its function. Typically, creatinine clearance levels are between 100 and 130 mL/min for women and 110-150 mL/min for men (Gowda et al., 2010). The MDRD formula also takes into consideration the body surface area's average value of 1.73 m^2.

More recently, another formula called CKD-EPI (Chronic Kidney Disease Epidemiology Collaboration) was developed in order to improve eGFR calculation and was demonstrated to be more accurate than the MDRD formula in a very large cohort of over 1.1 million participants (Levey et al., 2009; Matsushita et al., 2012). It is now the most used eGFR calculation formula in clinic and is as follows:

$$eGFR = 141 \times \min\left(\frac{S_{\mathrm{CR}}}{\kappa}\right)^{\alpha} \times \max\left(\frac{S_{\mathrm{CR}}}{\kappa}\right)^{-1.209} \times (0.993)^{Age} \times (1.018_{\,if\ female}) \times (1.159_{\,if\ black})$$

with serum creatinine (S_{CR}) concentrations in mg/dL, κ = 0.7 for females / 0.9 for males, α = -0.329 for females / -0.411 for males, min = minimum of S_{CR}/κ, or 1 and max = maximum of S_{CR}/κ, or 1. A normal eGFR value is above 90 mL of fluid filtered /min/1.73 m^2 for an adult and 100 mL/min/1.73m^2 for a child under 2 years of age. The eGFR rates can for example help to classify the kidney function of chronic kidney disease (CKD) patients in 6 stages, ranging from stage 0 (GFR >90 mL/min/1.73m^2, normal kidney function) and stage 1 (GFR >90 mL/min/1.73m^2, normal rate with signs of damage) to stage 5 (GFR <15 mL/min/1.73^2, kidney failure) (Stevens et al., 2006).

The limitations of the GFR estimates are factors other than kidney conditions that can affect creatinine levels, including muscle mass, chronic illnesses such as cancer, or diet (Stevens et al., 2006). Hence, other markers such as urea or proteinuria are usually measured along with creatinine in order to get the most complete diagnosis (Gowda et al., 2010).

1.1.2 Chronic kidney disease (CKD) is a major global health issue

The National Kidney Foundation released guidelines that provide a definition of Chronic Kidney Disease and its stages: it regroups the conditions causing kidney damage and affecting its function, regardless of the diagnosis (type of disorder) (NKF, 2002). As stated above, the different stages of CKD are determined using the GFR, and extra laboratory tests and a clinical diagnosis help to understand the causes of renal damage and potential associated risk factors and treatments. The difference between chronic kidney disease and acute kidney disease is that the former is diagnosed after at least two tests made three months apart to confirm the progressive loss of kidney function (Martinez-Castelao et al., 2014), which is one of the criteria from the current guidelines for diagnosing CKD.

Chronic kidney disease is considered an important public health issue with a prevalence estimated to 10 % of the population, with higher risks for women, African Americans and South East Asians (Levey and Coresh, 2012). In 2011, it was estimated to affect 2.6 million people in the UK, *i.e.* 6.1 % of the population over 16 years old (Public Health England report, 2014). As age is one of the factors of progression of CKD, the proportion of people affected by the disease is predicted to increase with the growing number of elderly populations (Thomas et al., 2008).

The symptoms of chronic kidney disease, when they exist, can be back pain, tiredness, poor appetite, swelling of feet or ankles, or changes in the urination pattern for example (NHS, 2016b; Mayo Clinic, 2016). However at early stages, patients often present no symptoms, and the disease is suspected or diagnosed during the assessment of other disorders. The possible causes of this condition are multiple and very heterogeneous: up to two-thirds of cases are linked to diabetes and hypertension, but it can also be the result of infectious diseases (pyelonephritis), inflammation (glomerulonephritis), long-term use of certain drugs such as NSAIDs, obstructions caused by tumours or kidney stones, or inherited kidney diseases such as Autosomal Dominant Polycystic Kidney Disease (ADPKD, topic of the present thesis) (NKF, 2002; Levey et al., 2007; Perico and Remuzzi, 2012). This disparity between the potential causes of CKD make it difficult to diagnose and requires multiple tests to identify the underlying disorder responsible for renal damage in the patient (Levey and Coresh, 2012; Martinez-Castelao et al., 2014).

Figure 1.2 presents the framework of the development, evolution and complications of chronic kidney disease as well as the therapeutic interventions undertaken to try and slow down the progression or ease the symptoms.

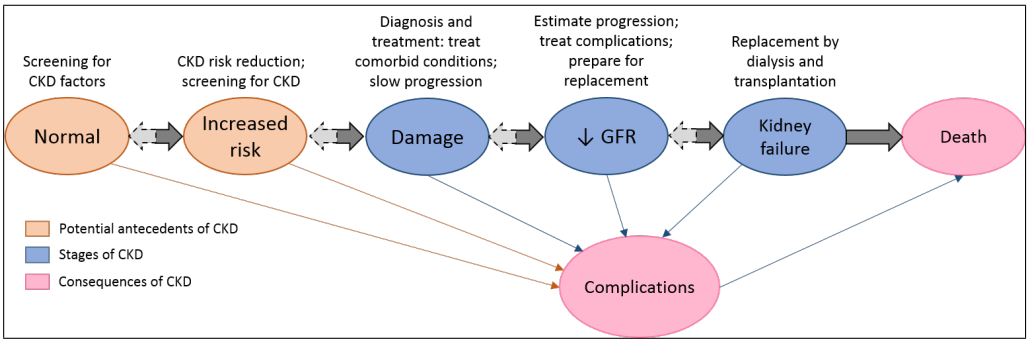

Figure 1.2: **Conceptual model for chronic kidney disease.**
Framework of development, progression, and complications of CKD and therapeutic interventions. Interventions for each stage are presented above the frames. The thick arrows between the frames represent the risk factors that can be detected or influenced by intervention. The dashed arrows represent a remission less frequent than progression. The complications regroup all the complications directly linked to CKD or to adverse effects of its treatment, for example cardiovascular disease or complications from decreased GFR.
Adapted from the National Kidney Foundation report from 2002 with permission from Springer publisher, available upon request.

The main complications of CKD are kidney failure resulting from end-stage renal disease (ESRD) and cardiovascular complications. Depending on the cause of CKD, kidney failure will happen at different times: while some patients may never experience it as the disease will progress slowly, others will need replacement therapies within months of being diagnosed (Levey and Coresh, 2012). Cardiovascular complications include left ventricular hypertrophy (LVH) that worsens with the decline in eGFR and thus has a high prevalence in patients on dialysis, cardiac inflammation, increased risks of ischaemia and myocardial fibrosis leading to heart failure (Thomas et al., 2008, Di Lullo et al., 2015). Other various complications of chronic kidney disease are anaemia, mostly caused by the defective production of erythropoietin by the kidney, bone and mineral disorders caused by hyperphosphataemia but also dyslipidaemia and nutritional issues (Thomas et al., 2008, Lee et al., 2017).

Because the underlying cause of CKD can be of multiple aetiologies, the therapeutic interventions need to focus on treating the cause, where possible, and on reducing its symptoms. Dietary changes are recommended to most CKD patients: control of diabetes, regulation of sodium and potassium intake or vitamin D supplementation are essential to slow the disease progression and development of complications. Hypertension can be controlled by drugs such as angiotensin-converting enzyme (ACE) inhibitors and swelling reduced by diuretics (Mayo Clinic, 2016; Martinez-Castelao et al., 2014).
Pain in CKD can be of different nature; it is mostly musculoskeletal but it can also often be neuropathic. Pharmacokinetics of analgesics can be affected by CKD, making it difficult to adapt the treatment to each individual (Davison et al., 2014). Acetaminophen, a non-opioid analgesic, is commonly used in first instance in cases of mild pain. Patients with mild pain levels will be prescribed this analgesic added to an opioid class II such as codein or tramadol, and the ones with severe pain will get prescribed stronger opioids such as morphine or methadone (Brown et al., 2014). Adjuvants can be added to the treatment depending on the type of pain: tricyclic antidepressants will help with chronic pain, while anticonvulsants will aim at soothing neurological pain, and muscle relaxants, bisphosphonates and corticosteroids will treat musculoskeletal, bone and inflammation-related pain (Cline, 2004).
Finally, when the stage of kidney failure is reached, the only options are to undergo kidney-replacement therapies such as haemodialysis to artificially filter the patient's blood and eventually kidney transplantation (Mayo Clinic, 2016; NHS, 2016b).

Chronic kidney disease is thus a global public health problem affecting many patients in the world. While treatments for the major causes of CKD (diabetes and hypertension) are well developed and rather easy to control, other pathologies leading to chronic kidney disease such as inherited disorders are more difficult to manage as the patients tend to be diagnosed later and the condition itself is usually the result of multiple deficient biological elements and physiological mechanisms.
Among these pathologies, Autosomal Dominant Polycystic Kidney Disease is a complex disorder that involves genetic, epigenetic and environmental factors which are still far from being understood.

1.2 ADPKD – Autosomal Dominant Polycystic Kidney Disease

1.2.1 General facts

Autosomal Dominant Polycystic Kidney Disease (ADPKD) is the most common inherited renal disorder, affecting over 12 million people worldwide, with a prevalence of ca. 1/1,000 (Torres and Harris, 2009; Tan et al., 2011). The main manifestation of the disease is the development of renal cysts leading to a characteristic enlargement of the patients' kidneys. This enlargement can result in kidneys that are 4 times larger (40 cm compared to 11 cm) and up to 15 times heavier (7-8 kg vs. 500 g) in ADPKD patients compared to healthy controls (Pei, 2006). The size and number of cysts increases with age (prevalence 58 % at age 15-25 years, compared to 94 % at age 35-46 years) (Bae et al., 2006), eventually leading to CKD and end stage renal disease (ESRD) in 50 % of patients by the age of 60 and the need for kidney transplantation. Typically the disease manifests around 20 to 40 years of age; however some children have been reported with symptoms (Selistre et al., 2012; Peral et al., 1996). Paediatric patients usually have renal cysts but rarely present extra-renal cysts (Li, 2015). Some studies have shown a higher incidence of the disease in men compared to women in Japan, USA and Europe (Torres and Harris, 2009).

The cysts are disorganized fluid-filled structures arising via several mechanisms: cells form spheres in shape rather than tubes because of a change in the axis of cell division, planar cell polarity and fluid secretion into the lumen of these structures (Fischer et al., 2006). Cysts can originate from any nephron segment and generally are associated with cell infiltration, interstitial fibrosis, non-functional nephrons and a disrupted renal parenchyma (Chang and Ong, 2008). Cell proliferation is increased, which allows the cysts to grow rapidly. The enhanced fluid secretion originates from a change in epithelium characteristics: accumulation of cAMP leads to increased Cl^- transport (notably via CFTR) into the tubular lumen, creating an osmotic disequilibrium and accumulation of fluids in the cyst (Grantham, 1996). Gene dosage is important in the variability of cystogenesis level between patients: a threshold model has recently been suggested in which the level of PC1 or PC2 protein expression determines the severity of disease (Saigusa and Bell, 2015; Ong and Harris, 2015).

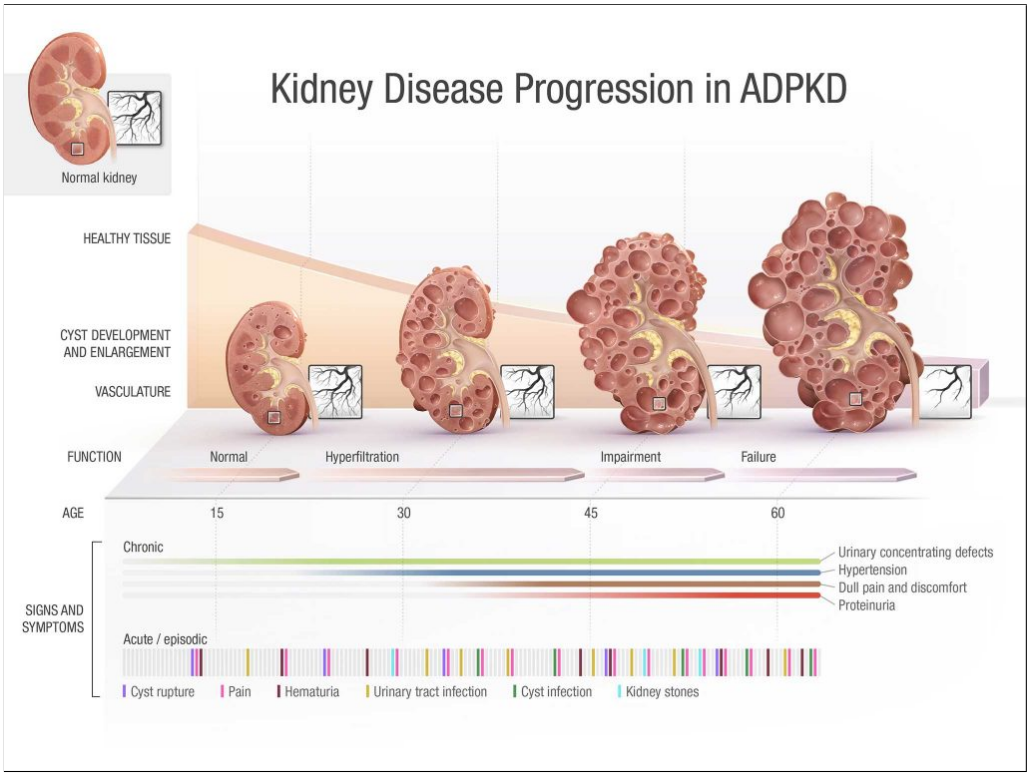

Figure 1.3: **Representation of ADPKD kidney evolution.**
Following multiple initiation hits, cysts start to develop in the kidney, which marks the apparition of acute symptoms such as pain and urinary tract infections. The more chronic symptoms such as hypertension and proteinuria linked with healthy tissue and vasculature integrity progress with the multiplication and growth of the cysts, before reaching the stage of chronic kidney disease and eventually renal failure requiring renal replacement therapies.
Adapted from the PKD Foundation charity website with permission.

Mostly present in the kidney, cysts can also be detected in the liver, pancreas, spleen, arachnoid membrane or seminal vesicles (Torres and Harris, 2009). Among other extra-renal manifestations of ADPKD are cardiac valve defects, intracranial arterial aneurysms and hypertension (Tan et al., 2011). The presence of PC1 and PC2 in endothelium and vascular smooth muscles could be a factor leading to vascular abnormalities (Nauli et al., 2008).

Symptoms and diagnosis ADPKD is often asymptomatic for many years before the first signs of pain or hypertension. The typical symptoms of ADPKD are pain in the back or the side, frequent headaches, urinary tract infections, high blood pressure and eventually an enlarged abdomen, haematuria and/or kidney stones (NHS, 2016a; Mayo Clinic, 2017). However, because of their rather non-specific characteristics, these symptoms are usually not sufficient to diagnose ADPKD. The most lethal complications of this disease are intracranial aneurysms and cerebrovascular events linked to uncontrolled hypertension. The former occur in 16 % of patients with a family history of ADPKD and hypertension is present in $\approx$ 80 % of patients (Cagnazzo et al., 2017).

The diagnosis of ADPKD is mainly made by imaging patients known to be at risk or with typical symptoms. Kidney ultrasound is usually the method of choice as it is inexpensive and safer than other imaging techniques (MRI and CT scan) (Pei et al., 2009). The criteria for diagnosing ADPKD from sonographic imaging are age-specific. Indeed, as indicated in Table 1.1, the younger the patient the less cysts need to be identified in order to suspect or confirm ADPKD (Ravine et al., 1994; Saigusa and Bell, 2015).

Table 1.1: Unified criteria for diagnosis of ADPKD by ultrasound (patient with family history but genotype unknown)

Age (years)	Number of kidney cysts
15-39	$\geq$ 3 total (uni- or bilateral)
40-59	$\geq$ 2 in each kidney
$\geq$ 60	$\geq$ 4 in each kidney
$\geq$ 40	$\leq$ 2 total, excludes disease

Diagnosis cannot be exclusively based on symptoms as other disorders than ADPKD can cause pain and cysts growth or kidney enlargement. For example, Acquired Kidney Disease (AKD) is characterised by cysts formation but no enlargement of the kidneys, while Medullary sponge kidney is characterised by the presence of kidney cysts but rarely progresses to ESRD, and Autosomal Recessive Polycystic Kidney Disease (ARPKD) has an earlier onset and is often responsible for growth failure (Halvorson et al., 2010; Li, 2015). The following Table 1.2 summarises the differential diagnosis for a few kidney diseases other than ADPKD.

Table 1.2: Differential diagnosis of ADPKD.
Adapted with permission from Alves et al. ('Polycystic Kidney Disease' - Chapter 1) 2015, under CC-BY 4.0 license.

Condition	Gene	Inheritance	Prevalence	Differentiating symptoms or signs
'Simple' renal cysts	–	Acquired	Frequent	Normal renal function. Normal looking kidney
Acquired Kidney Disease	–	Acquired	Frequent	Multiple renal cysts and small to normal-sized kidneys
Medullary cystic kidney disease	*MCKD1-2*	Autosomal Dominant	Unknown	Interstitial fibrosis in kidney biopsy. Slow progressive renal failure (ESRD rare)
ARPKD	*PKHD1*	Autosomal Recessive	1/ 20,000	Mostly early onset. Potter's phenotype: pulmonary hypoplasia, spine deformities etc.

As it is an expensive analysis, DNA diagnostic is still mostly reserved to cases where a definitive diagnosis is needed such as potential live kidney donors from the same family (Huang et al., 2009).

It has recently been reported that mutations of *PKD1* may lead to a switch in glucose metabolism, resulting in higher apoptotic rates and decreased proliferation in glucose-depleted mutant cells compared to normal (Rowe et al., 2013). The concentrations of glucose become higher as the glycolysis rates increase, notably activating several major pathways such as the mTOR complex or the chloride channel anoctamin 1 (Rowe et al., 2013; Kraus et al., 2016). There is also evidence of deregulated lipid metabolism (Mao et al., 2014). Indeed, Menezes et al. performed genome wide transcript profiling on a conditional *Pkd1* knock-out mouse model, and identified differentially expressed genes between WT and ADPKD mice that were regulators of lipids metabolism. They also showed that *Pkd1* knock-out renal epithelial cells presented an intrinsic defect in fatty acid oxidation, and that increasing fat in the animals' diet, even by a small amount, was enough to worsen the disease's severity (Menezes et al., 2016). Similarly, Klawitter et al. reported defects in fatty acids metabolism of ADPKD patients (Klawitter et al., 2013).

Current management and future therapies for ADPKD Until recently, there was no cure for ADPKD in terms of a disease-modifying drug. The main aim of treatments was to reduce symptoms and limit morbidity from complications.

A number of potential new therapies have now been or are currently tested, all of them targeting the main pathways implicated in the development of ADPKD; cAMP, CFTR and mTOR (see below).

cAMP is increased in ADPKD possibly by dysregulation of Ca^{2+}. Vasopressin V2 antagonists (VPV2R) and Somatostatin have been shown to reduce this pathological accumulation of cAMP with promising results (Torres et al., 2004; Ruggenenti et al., 2005). As an example, the TEMPO 3:4 phase 3 clinical trial carried on 1,445 patients showed that the vasopressin V2 antagonist Tolvaptan slows the decline in kidney function by reducing the total kidney volume increase by about 1.99 % in CKD1 patients and 3.12 % in CKD2 patients (Torres et al., 2012, 2016). This molecule also presents the advantage of being well tolerated (Boertien et al., 2013; Torres et al., 2016). Tolvaptan was the first pharmaceutical agent approved for treatment against ADPKD and is now commercialised under the trademarked name Jinarc® in the European Union, Switzerland, Japan, Korea and Canada (Gansevoort et al., 2016). The US regulatory agency, the Food Drug Administration, has asked for more data about efficacy and safety as some concerns were raised over liver tolerance and long term efficiency (Torres et al., 2016). However, the TEMPO 4:4 trial recently reported a sustained beneficial effect of this drug on eGFR which suggested a disease-modifying effect, despite limitations such as loss of randomisation resulting in an unexpected loss of the effect on total kidney volume over time (Torres et al., 2017). The ERA-EDTA recently released some recommendations on the use of Tolvaptan including contraindications and inclusion criteria in order to limit the use of this drug to the patients the most likely to benefit from the treatment (Gansevoort et al., 2016).

Other molecules targeting the cAMP pathway are also under trial, such as long-acting somatostatin analogues. Binding to somatostatin receptors is known to inhibit cell proliferation and secretion of several hormones such as insulin and glucagon and of growth factors such as IGF-1 and VEGF (Pyronnet et al., 2008).

Somatostatin also inhibits the generation of cAMP and cell proliferation in several models of the disease (Friedlander and Amiel, 1986). Therefore, synthetic peptides targeting the same receptor as somatostatin but with a longer half-life (octreotide and pasireotide) were developed and tested during small-scale studies on ADPKD patients. The results of these studies were encouraging, suggesting a reduction of liver and kidney volume in the first year of treatment and a good tolerance towards the drugs (Ruggenenti et al., 2005; Hogan et al., 2010). A longer-term study showed a significant reduction of total kidney volume in patients treated with octreotide compared to the placebo group and a stabilisation of the eGFR over 3 years (Caroli et al., 2013), opening doors to larger trials involving more patients and longer time-scales. Finally, a Tolvaptan plus pasireotide combination treatment showed additive effects of these two drugs in a hypomorphic *Pkd1* mouse model, and suggests that combination therapy could be a strong option in future treatments of ADPKD patients (Hopp et al., 2014).

Another major pathway, Akt/mTOR, is linked to the PC1/PC2 complex and its deregulation leads to an excessive cell growth (Shillingford et al., 2006). Treatments targeting this pathway, such as rapamycin (Sirolimus), aim to reduce cell proliferation, but so far clinical trials have given contradictory results and this option has not been validated (Jardine et al., 2013; Ponticelli and Locatelli, 2010). Indeed, although low doses of rapamycin improved short term renal function of ADPKD patients (Braun et al., 2014), adverse effects were observed in many patients and early trial termination of the SIRENA 2 study was recommended, added to the lack of efficiency of this drug on total kidney volume (Ruggenenti et al., 2016). Hence, new ways of targeting the Akt/mTOR pathway as treatments for ADPKD still need to be identified.

CFTR (Cystic Fibrosis Transmembrane Conductance Regulator) is a Cl^- transporter localised across epithelial cell membranes (Terryn et al., 2011), regulated by cAMP. Some potential therapies such as thiazolidinones, glycine and malonic acid hydrazides or pyrimido-pyrrolo-quinoxalinediones are targeting this mechanism to limit the fluid accumulation in the cysts with encouraging results in mice models of ADPKD (Yang et al., 2008a).

Other strategies and targets are currently being investigated in pre-clinical or clinical studies and gave promising results so far. Among them, Triptolide was found to act as a PC2 agonist and to reduce kidney cysts in rodents (Leuenroth et al., 2008), and Bosutinib - an Src tyrosine kinase inhibitor - was shown to reduce renal cysts number and volume in rodents (Elliott et al., 2011).

The management of ADPKD symptoms and complications involves many complementary treatments. As hypertension is a major cause of death in ADPKD patients, a good blood pressure control is essential, especially in patients with large kidneys. As said above, renin-angiotensin-aldosterone (RAAS) inhibitors such as angiotensin-converting enzymes (ACE) inhibitors are the classic treatments for this condition as renin and angiotensin are abundantly present in dilated tubules and cysts (Loghman-Adham et al., 2004). Recently, the HALT-PKD study studied the effects of the ACE inhibitors in ADPKD patients and concluded that these drugs could control hypertension in 70 % of them and that the rate of increase in kidney volume was reduced by 14 % in younger patients. ACE inhibitors, however, did not have a significant impact on eGFR (Schrier et al., 2014; Torres et al., 2014). Pain management may require analgesia using the drugs mentioned in the PKD section above (*i.e.* acetaminophen in first instance, codein and eventually morphine) but can be difficult to treat and surgical interventions can be considered in some specific cases (Bansal and Kapoor, 2014). Kidney transplantation is considered when patients develop ESRD and is not associated with more complications than in other diseases (Pirson et al., 1996). However, kidney replacement does not prevent the development of extra-renal manifestations such as liver cysts or intracranial aneurysms. While somatostatin analogues have been shown to reduce the growth of hepatic cysts, they still have not been approved as a treatment and are only being currently used in advanced clinical trials (Caroli et al., 2013). Intracranial aneurysms are mostly treated using a surgical technique called clipping, consisting in permanently clipping a small titanium ring at the base of the aneurysm in order to isolate it from the normal blood flow (Cagnazzo et al., 2017).

The following figure (Figure 1.4, from Salvadori and Tsalouchos (2017)) depicts the main pathway-targeting therapies currently considered important in cystic pathogenesis.

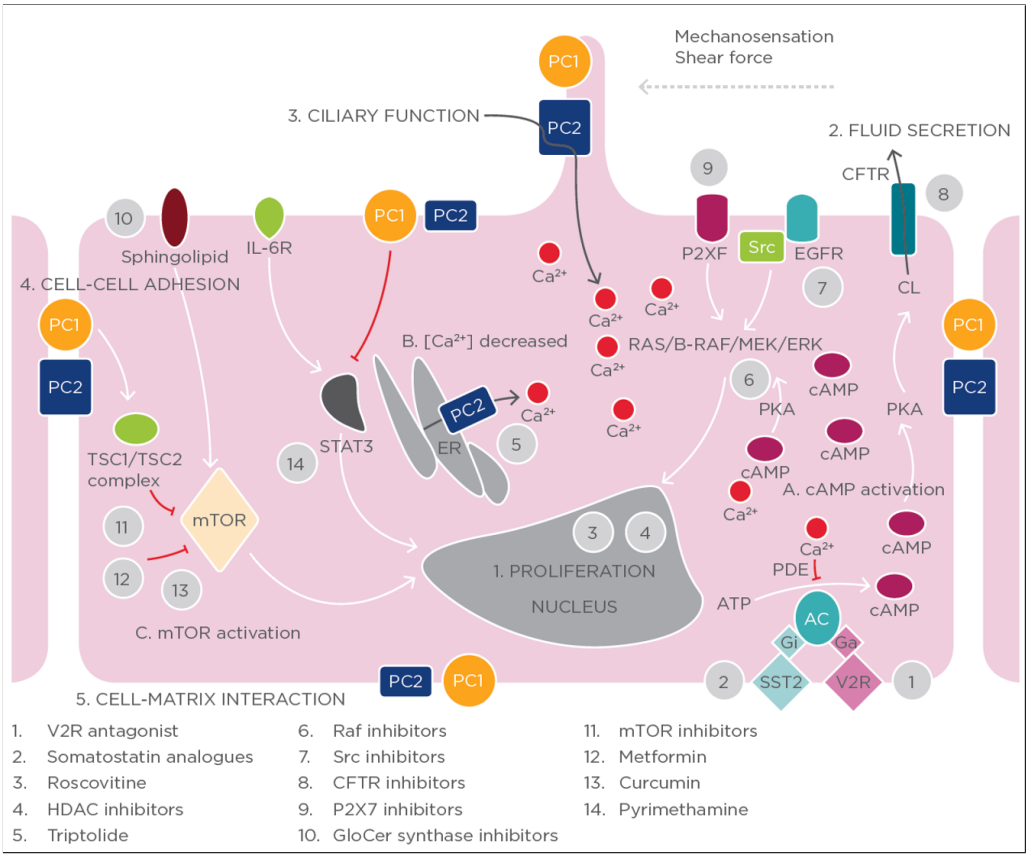

Figure 1.4: **Main pathways linked to ADPKD and their targeting therapies.**
cAMP: cyclic adenosine monophosphate / CFTR: cystic fibrosis transmembrane regulator / EGFR: epidermal growth factor receptor / ER: endoplasmic reticulum / ERK: extracellular-signal regulated kinase / GlcCer: glucosylceramide / HDAC: histone deacetylase / IL-6: interleukin-6 receptor / MEK: mitogen activated protein kinase / mTOR: mammalian target of rapamycin / PC: polycystin / PDE: phosphodiesterase / PKA: protein kinase A / SR: somatostatin receptor / TSC: tuberous sclerosis / V2R: vasopressin V2 receptor.
Reused with permission from Salvadori and Saluchos, Eur Med J 2017, under CC-BY-NC 4.0 license.

1.2.2 The *PKD* genes

ADPKD is caused by germline mutations in one of two genes: *PKD1* (85 % of cases) and *PKD2* (15 %). Some studies had suggested the existence of a third locus (Turco et al., 1996; Ariza et al., 1997), but this has since been contradicted (Paul et al., 2014). Recently, mutations in *GANAB*, encoding the glucosidase II alpha subunit, were reported to cause ADPKD with a milder phenotype than *PKD1* and *PKD2* and to account for ≈0.3 % of all cases of ADPKD (Porath et al., 2016).

Polycystic Kidney Disease 1 (*PKD1*) *PKD1* is located on chromosome 16p3.3 (base pairs 2,088,707 to 2,135,897) and has 46 exons. The Ensembl Genome Database (see www.ensembl.org) describes 40 different transcripts (splice variants), 9 of them coding for a protein. As of June 22nd 2017, the ADPKD mutation database (accessible from http://pkdb.mayo.edu/) referenced 1,273 germline mutations of *PKD1* deemed "pathogenic". These mutations can be deletions, substitutions or frameshifts and can appear all along the *PKD1* sequence. *PKD1* encodes a large membrane protein: polycystin 1 (PC1). It is a 462 kDa protein, 4,303 amino acids long, with an extracellular domain (N-terminal) containing the first 3,000 amino acids, a transmembrane domain and an intracellular domain (C-terminal) (Hughes et al., 1995) (see Figure 1.5). The large size of this protein and the existence of six highly homologous pseudogenes (99 % identity) make it difficult to sequence (Li, 2015).

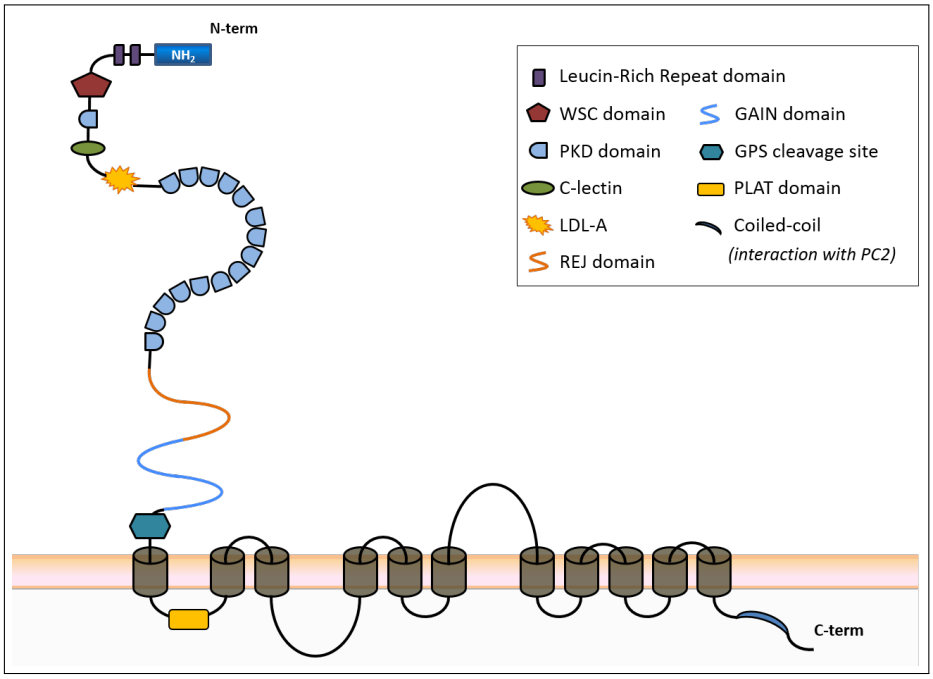

Figure 1.5: **Polycystin 1 protein.** PC1 is composed of three main domains: an extracellular N-terminal tail containing 16 PKD domains, an intra-membrane domain that crosses the membrane 11 times, and an intracellular C-terminus, site of interaction with PC2.

The extracellular N-terminus of the protein contains various structural domains (LRR, WSC, C-lectin, LDL-A, PKD, REJ, GAIN and GPS) which give it the ability to perform multiple different functions. The two Leucin-Rich Repeats (LRR) are involved in PC1's cell adhesion and its interaction with the extracellular matrix and other proteins

(Kobe and Kajava, 2001; Malhas et al., 2002). The cell wall integrity and stress response component (WSC) domain has been reported to interact with several members of the Wnt pathway (along with the LRR domain) and carbohydrates (Ponting et al., 1999; Kim et al., 2016). The C-lectin domain suggests that the protein can bind carbohydrates in a Ca^{2+} dependent-manner (Weston et al., 2001). The presence of the LDL-A region, coded by exon 10 of the *PKD1* gene, suggests an interaction of PC1 with LDL-related molecules and carbohydrates (Babich et al., 2004). Following these motifs, 15 PKD domains associated with an extra repeat a few exons upstream of the C-type lectin domain, compose about 30 % of the PC1 protein and form an immunoglobulin-like domain (Bycroft et al., 1999). Homophilic interactions between the PKD domains have been demonstrated to mediate cell-cell interactions and communication (Streets et al., 2003, 2009). The receptor for egg jelly (REJ) is essential for the cleavage of polycystin and may be involved in Ca^{2+} signalling functions of the proteins (Qian et al., 2002; Babich et al., 2004). The GAIN domain, first crystallised by Araç et al., is a highly conserved 320-residue region and contains a motif of 50 residues mediating the N-terminal cleavage of PC1; the G protein-coupled receptor proteolytic site (GPS) (Arac et al., 2012; Qian et al., 2002). The N-terminal fragment then remains covalently associated with the C-terminal fragment. The functional role of this cleavage still remains to be fully defined but it was suggested it is essential for the homeostasis of distal nephrons and PC1 trafficking and that missense mutations of *PKD1* inhibiting this process result in ADPKD in human (Qian et al., 2002; Kim et al., 2014a; Trudel et al., 2016). Globally, the N-terminal domain plays a role in cell-matrix or cell-cell adhesion (Qian et al., 2005).

There are eleven predicted transmembrane domains separated by extracellular and intracellular loops, the roles of which are not fully determined. Our group recently reported that the polycystin-1 lipoxygenaseα-toxin (PLAT) domain, a signature domain of the polycystins family because of its highly conserved sequence and identification in over 1000 proteins (Ponting et al., 1999), binds to Ca^{2+} and β-arrestins via protein kinase A (PKA)-mediated phosphorylation, leading to PC1 endocytosis (Xu et al., 2016).

Finally, the intracellular C-terminal domain is composed of the last 200 amino acids and contains a coil-coiled region which mediates interaction between PC1 and PC2. Some groups have reported that the C-terminal tail can be cleaved to release either a 15 kDa or a 30 kDa fragment that translocates to the nucleus. Because of its interactions with p100 and STAT6, this PC1 fragment could potentially directly regulate gene transcription (Lal et al., 2008; Low et al., 2006). The coil-coiled domain interacts with polycystin 2 and a G-protein activation motif (Parnell et al., 1998, 2002).

Polycystin-1 is widely expressed, from the epithelial cells of the renal tubules to the pancreas, brain, intestine and other tissues. It is localised essentially in the membrane of the primary cilium but also in the plasma membrane where it plays a role in cell-cell adhesion (adherens and tight junctions, desmosomes) (Newby et al., 2002; Yoder et al., 2002).

Mouse models of ADPKD include knock-outs of *Pkd1*; however other animals have been studied to overcome the limitations of the murine model. The amphibian homologue of *Pkd1* (in Xenopus) has 60 % of homology with the human gene (Burtey et al., 2005). The dog and pig *Pkd1* genes have 81 % of homology (He et al., 2011a, 2013), whereas the mouse gene has 78 %. In general, *Pkd1* is well conserved among species (see Figure 1.6), meaning that animal models other than mouse/rat could be used to study ADPKD.

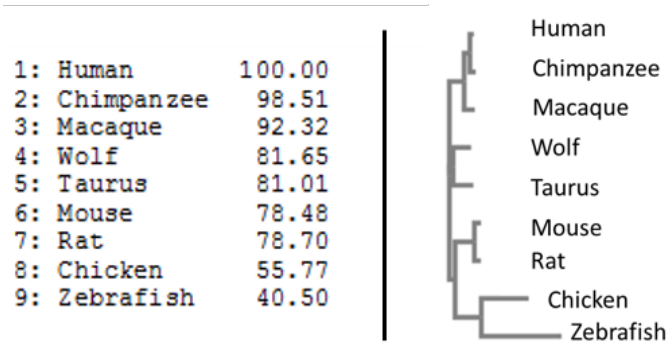

Figure 1.6: **Conservation of *PKD1* across species.**
Percentages of homology between the PC1 protein in Human vs. other species (left). Phylogenetic tree for the PC1 protein (right). Source: ClustalW2 alignment tool (www.ebi.ac.uk).

Polycystic Kidney Disease 2 (*PKD2*) *PKD2* (4q22.1) is a 15-exon, 70 kb long gene (base pairs 88,007,646 to 88,077,778). According to Ensembl, it has seven transcripts, three of them coding for a protein. As of June 22nd 2017, 202 *PKD2* germline mutations were described as "pathogenic" (http://pkdb.mayo.edu/).

PKD2 codes for the transmembrane protein polycystin-2 (PC2). This 968 amino acid protein (109 kDa) has six transmembrane domains homologous to those of PC1, and intracellular N- and C-termini (Wilson, 2001) (see Figure 1.7).

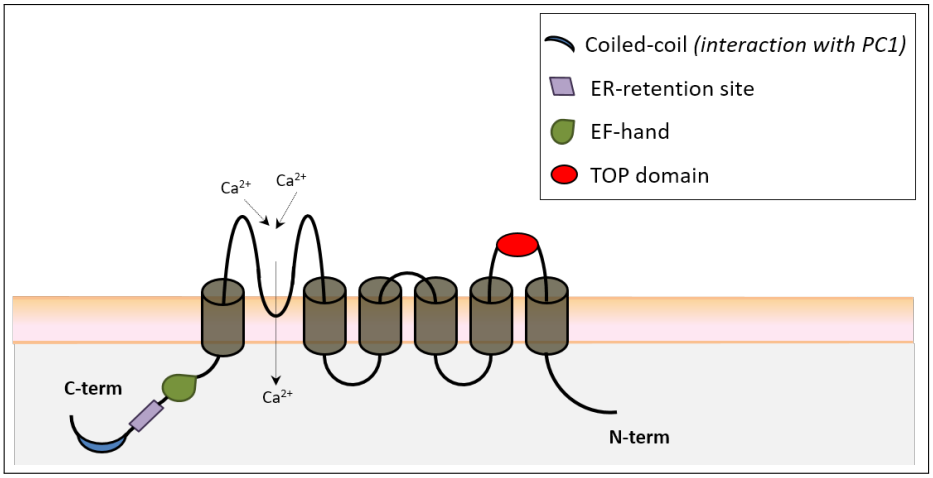

Figure 1.7: **Polycystin 2 protein.** PC2 is composed of an intracellular N-terminus, six transmembrane domains , the TOP (tetragonal opening for polycystins) domain, an EF-hand motif binding to Ca^{2+}, an ER-retention domain restricting its trafficking to the cell surface and an intracellular C-terminus, site of interaction with PC1.

PKD2 is expressed in the kidney but also in various other organs. The protein is localised in the primary cilium with PC1, the apical monocilium, mitotic spindles and in intracellular compartments such as Golgi and ER (Nauli et al., 2003; Yoder et al., 2002). PC2 is maintained in these specific locations by several proteins. The ER-localisation is regulated by the binding of the PC2 C-terminus to PACS-1 and PACS-2 (Phosphofurin Acidic Cluster-Sorting protein) (Köttgen and Walz, 2005). The N-terminal tail of PC2 can also regulate its localisation in the primary cilium via the R6VxP motif (Geng et al., 2006) or in the mitotic spindle via mDia1 (Rundle et al., 2004). Streets et al. demonstrated that Glycogen Synthase Kinase 3 (GSK3) phosphorylates Ser76 (N-terminal region of PC2), which is essential for the retention of PC2 at the plasma membrane (Streets et al., 2006). PIGEA-14 (PC2-Interactor, Golgi and ER-Associated protein) controls the movement of

PC2 from the ER to the Golgi, by binding its C-terminal tail (Hidaka et al., 2004).

The structure of polycystin 2 is still being investigated. PC2 interacts with PC1 via its coil-coiled domain in the C-terminus and can also form homodimers via this region. The main role of PC2 is to act as a non-selective Ca^{2+} channel (Allen et al., 2006). The ER-retention site located near the coiled-coil domain is thought to inhibit its trafficking to the cell surface (Cai et al., 1999; Delmas et al., 2004). The EF-hand motif of PC2 forms a pocket-like structure that binds to Ca^{2+} ions and participates in the change of conformation of this protein depending on calcium concentration by mechanisms not yet fully understood (Allen et al., 2014). Shen et al. were the first to report the presence of what they called a polycystin domain, covalently linked to the first and second helices, and suggested a role of this domain in channel assembly and modulation (Shen et al., 2016). Grieben et al. recently performed the first crystallisation of the full closed version of the protein, giving more insights into its structure and function. They confirmed the existence of the polycystin domain, which they renamed TOP domain (standing for Tetragonal Opening for Polycystins). This region is on the extracellular surface when polycystin 2 is localised in the plasma membrane and its glycosylation is essential for the trafficking and stability of PC2 (Hofherr et al., 2014). Furthermore, Wilkes et al. recently reported the presence of two PC2 conformational states; an 'open' conformation where the lipid-mediated interaction between the TOP and C-terminal domain lead to a larger opening of the funnel and a more 'closed' state which is suggested to restrict the passage of ions such as Ca^{2+}, Na^{+} and K^{+} (Wilkes et al., 2017).

PC2 has homologies with the transient receptor potential family (TRP) (hence its other name, TRPP2) and channel opening is regulated by Ca^{2+} (Vassilev et al., 2001; Giamarchi et al., 2006). Ca^{2+} entry is thought to be mediated through a pore formed between the fifth and sixth transmembrane domains of the protein (Grieben et al., 2016). PC2 can also regulate the cytosolic Ca^{2+} levels indirectly by functional interactions with other Ca^{2+} channels; e.g. IP3R and ryanodine receptor (Sammels et al., 2010; Anyatonwu et al., 2007).

The PC1/PC2 heterodimer The heterodimer formed by the association between PC1 and PC2 in the primary cilium forms a non-selective mechanoreceptor for Ca^{2+} (Yoder et al., 2002). The cilium is a mechanosensory structure present in cells and essential for normal development notably because of its role in Hedgehog signalling, involved in cell differentiation (Ingham and McMahon, 2001; Huangfu et al., 2003). It is composed of a basal body from which originate the microtubules and fibers forming its structure (Singla and Reiter, 2006). Intraflagellar transport (IFT) is a bidirectional transport system driven by kinesins (anterograde transport, Kozminski et al., 1995) and dyneins (retrograde transport to the cell body, Pazour et al., 1998). The flow bending of the primary cilium is sensed by PC1 which is thought to undergo cleavage and structural rearrangement when forming an heteromeric complex with polycystin 2, which leads to the activation of the Ca^{2+} channel function of PC2 (Nauli et al., 2003; Delmas et al., 2004; Singla and Reiter, 2006). Nauli et al. suggested that the first PKD domain of PC1 as well at what is now known as the TOP domain as PC2 are responsible for this mechanosensor and channel functions of the PC1/PC2 complex, as blocking of these regions by specific antibodies led to the inhibition of the Ca^{2+} influx mediated by this complex (Nauli et al., 2003). Interestingly, each protein can have regulatory effects on the other (Newby et al., 2002), the binding of PC1 to PC2 being essential to its maturation in ADPKD mice models (Gainullin et al., 2015).

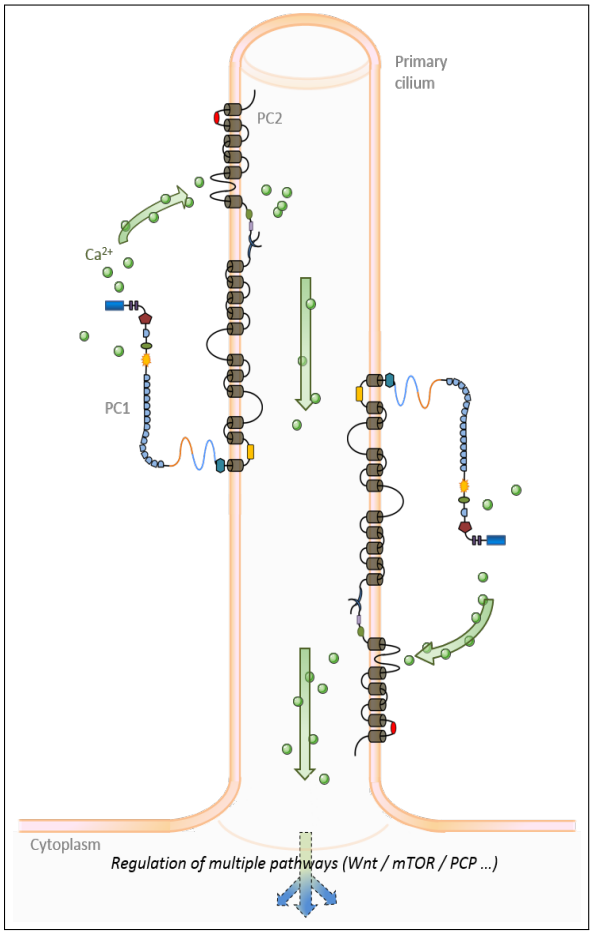

Figure 1.8: **The PC1/PC2 protein in the primary cilium.**
Once colocalised in the primary cilia, PC1 interacts with PC2 via their coiled-coil domain. It acts as a sensor for the calcium influx and activates PC2 which will then open a Ca^{2+} channel and allow calcium entry into the lumen of the cilium. The calcium will then participate in the regulation of multiple pathways such as Wnt, mTOR and modulate planar cell polarity.

Post-translational modifications of the dimer have been shown to modulate its activity. For example, five serine residues were reported to be phosphorylation sites for PC2 and to regulate major processes such as surface localisation and trafficking, regulation of PC2 by Ca^{2+} and Ca^{2+} permeability (Cai et al., 2004; Köttgen et al., 2005; Streets et al., 2006, 2013). Furthermore, ubiquitination of both PC1 and PC2 from the binding of different ubiquitin-ligases (*e.g.* Taz) results in their degradation by the proteasome. The phosphorylation and subsequent degradation of Taz, a protein known to regulate the degradation of β-catenin and thus activate the Wnt pathway, has been shown to lead to an abnormal accumulation of PC2 and the formation of cystic nephrons (Tian et al., 2007; Yim et al., 2011).

The PC1/PC2 complex has been implicated in interacting with various cellular signalling pathways. Indeed, it has been linked to regulation of cell proliferation and differentiation – negatively controlling cell growth via the mTOR or STAT1/p21 pathways, to G-proteins activation, and to both the canonical and non-canonical Wnt pathways (Chapin and Caplan, 2010). The link between PC1/PC2 and these essential pathways is critical to understand the cystic pathogenesis (Newby et al., 2002). The loss of planar cell polarity could be caused by the activation of Wnt signalling and inhibition of non-canonical Wnt signalling, which would lead to the metamorphosis of tubular structures into cysts (Fischer et al., 2006). In healthy cells, PC1/PC2 inhibits mTOR and thus limits cell proliferation, partly explaining the aberrant cell growth and apoptosis in ADPKD kidneys. A recent study described the presence of a feedback loop between mTOR and PC1, the inhibition of mTOR by PC1 leading to a down-regulation of the polycystin in return. The over-expression or over-activation of the mTOR pathway led to a strong inhibition of PC1 hence the formation of cysts in the kidney (Pema et al., 2016), confirming that a tight regulation of PC1 levels is key to preventing cystogenesis. Furthermore, a pathogenic mutation of either PC1 or PC2 leads to an inactive mechanoreceptor and a deregulation of Ca^{2+} influx. Typically, cystic cells show lower intracellular calcium concentrations and depleted ER calcium stores (Xu et al., 2007), potentially leading to increased levels of cAMP. This is in accordance with the fact that calcium acts as a regulator of cAMP concentrations. Increases in cAMP have been shown to stimulate cystic cell proliferation (Torres and Harris, 2014).

Interestingly, the PC1/PC2 heteromeric complex has also been reported to be present in organs other than the kidney and to be involved in disorders in these other locations. For example, in the vascular system, endothelial *Pkd1*$^{null/null}$ and *Pkd2*$^{-/-}$cells lose their ability to synthesise nitric oxide, which might lead to the high blood pressure (Nauli et al., 2008; Aboualaiwi et al., 2009) commonly found in ADPKD patients. Furthermore, these two proteins were reported to be essential to the integrity of blood vessels and heart of different *Pkd1* and *Pkd2* knock-out mice models (Kim et al., 2000; Wu et al., 2000).

Additionally, *Pkd1*- and *Pkd2*-deficient mice exhibited oedema suggested to be caused by defects in their lymphatic system including reduced vessels branching, defective directional migration and front-rear polarity of their endothelial cells (Outeda et al., 2014). Finally, Xiao et al. reported the presence of cilia and expression of PC1/PC2 in osteoblasts/osteocytes and suggested that polycystin 1 plays a role in bone development and bone formation mediated by these specific cells (Xiao et al., 2006). This was the first hint that the polycystins may be involved in bone development and that their deregulation may participate in bone turnover in some ADPKD patients.

***PKD* genes mutations and mechanisms of ADPKD pathogenesis** .

With respective median ages at ESRD onset of 54.3 and 74.0 years, a *PKD1*-profile ADPKD has a much poorer renal prognosis than *PKD2*-ADPKD (Hateboer et al., 1999; Cornec-Le Gall et al., 2013). This is not due to a faster cyst growth but to an increased number of cysts (Harris et al., 2006). Both ADPKD genes are highly heterogeneous and mutations can occur along the whole gene (Rossetti et al., 2001). Mutations of *PKD1* and *PKD2* can be classified in two categories: truncating mutations (frameshift, non-sense, rearrangement or splicing) and non-truncating mutations (missense, indel). The severity of the disease has been linked to the type of mutation and not to its location on the gene (Cornec-Le Gall et al., 2013) (see Figure 1.9), with a delayed onset of ESRD by 12 years in the patients carrying a non-truncating mutation of *PKD1*.

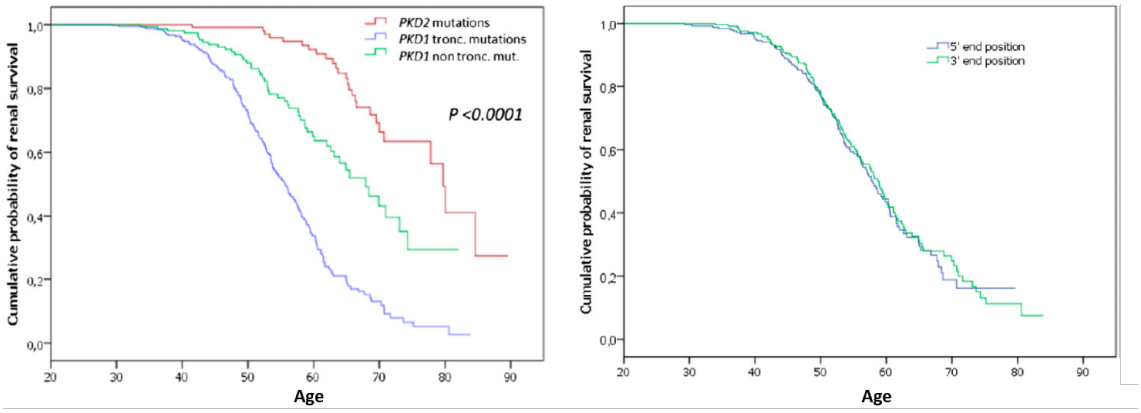

***Figure 1.9:* Renal survival of patients carrying different mutations.**
(left) Comparison of renal survival in *PKD1* truncating mutation, non truncating mutations and *PKD2* mutation carriers. (right) No effect of the position of the mutation could be shown . *From Cornec-Le Gall et al. JASN 2013 (reused with permission from American Society of Nephrology publisher, available upon request).*

The timing of *Pkd1*-inactivation has been shown to be critical for the development of renal cysts. Whereas an inactivation of *Pkd1* in mice at postnatal day 2 will lead to a cystic enlarged kidney by two weeks, the same inactivation in 6 weeks old mice will induce cysts only after 6 months, which proves the essential role of *Pkd1* for tubular integrity with the different impact of the mutation depending on the timing of onset (Piontek et al., 2007). Another study demonstrated a difference in the cystic development between newborn mice and adult mice, the latter showing a milder phenotype (Lantinga-van Leeuwen et al., 2007). This difference could be explained by an impact on different pathways between early and late inactivation.

An important aspect of ADPKD pathogenesis is that a germline mutation in one of the two *PKD* genes is not the only determinant of ADPKD progression and cyst formation: this mutation has to be associated to a sporadic event to induce the disease ("two-hits hypothesis") (Qian et al., 1996; Watnick et al., 1998; Pei et al., 1999; Pei, 2001). Indeed, although all the cells forming the ADPKD patients' kidneys carry the same germline mutation, only a small proportion of them will become cystic. Furthermore, within the same family the symptoms and severity of the disease can be highly variable. A study of 1996 showed that twins carrying the same *PKD1* mutation presented significantly different phenotypes (Peral et al., 1996), indicating that the "sporadic events" can be *PKD* genes-independent factors such as environment, epigenetics or regulators of gene transcription (miRNAs, see below). However this difference in phenotype is much stronger between siblings than between identical twins (Persu et al., 2004). Thus, genetic factors such as somatic mutations are also of importance in ADPKD progression. Both mutations could affect different genes, and cysts can develop with a germline mutation of *PKD1* and a somatic mutation of *PKD2* (Koptides et al., 2000) or vice-versa (Watnick et al., 2000) (transheterozygosity).

Another theory about cyst formation, called "haploinsufficiency", states that the level of PC1 or PC2 correlates with the degree of cysts formation (Lantinga-van Leeuwen et al., 2004). This could explain the difference in phenotypes depending on the mutation of *PKD1* mentioned above (Cornec-Le Gall et al., 2013). There are suggestions that the threshold under which cysts formation is triggered varies depending on the cell type,

nephron segment or organ (Raphael et al., 2009; Ong and Harris, 2015). Furthermore, some genes that directly interact with PC1 or PC2 as well as miRNAs targeting their mRNA were suggested to be responsible for this reduction of the polycystins dosage in the kidney. For example, HNF-1β has been reported to interact with *Pkd2* and directly regulate its transcription (Gresh et al., 2004), and patients carrying deleterious mutations in this gene along with a defective *PKD1* allele present a more severe phenotype (Bergmann et al., 2011). Furthermore, a model of *Pkd1*$^{del34/del34}$ null mice showed a strong reduction of cysts formation when another gene, *Pax2*, was also mutated and its protein was expressed in reduced amounts (haploinsufficiency). Because the authors also showed that *Pax2* expression was repressed by PC1 in MDCK cells, they suggested that the increased levels of Pax2 resulting from a germline mutation of *Pkd1* and thus its reduction could act as a second hit influencing the pathogenesis and phenotype of ADPKD (Stayner et al., 2006). Qin et al. reported the same increased expression of *Pax2* in *Pkd1*$^{-/-}$ mice but linked it to the over-expression of the *Wnt7a* and *Wnt7b* genes, itself caused by an increased cAMP signalling or the mutation of a protein involved in the ciliary IFT system; IFT20 (Qin et al., 2012). All these taken together suggest that the control of Pax2 expression levels or those of its regulating proteins could potentially be an option for the development of therapies against ADPKD.

Regarding miRNAs, Patel et al. reported that targeted deletion of the Dicer protein involved in miRNAs maturation (see below) led to the down-regulation of miRNAs such as mir-200 hence to an up-regulation of *Pkd1* and the production of cysts-like structures (Patel et al., 2012). Another example is the mir-17$\sim$92 family, up-regulated in ADPKD, and whose inactivation in mice improved renal function and delayed cysts growth (Patel et al., 2013). Anti-mir-17 treatments performed in *Pkhd1/Cre;Pkd2*$^{F/F}$ (*Pkd2*-KO) mice were found to efficiently reduce cysts formation (Hajarnis et al., 2017), suggesting that this cluster of miRNAs could be developed as ADPKD treatments in the future.

An increased sensitivity of *PKD1* or *PKD2* mutant kidneys to injury has also been reported to be a factor influencing cysts formation and progression in ADPKD patients which suggest that the second hit does not necessarily occur at the genetic level, or that a 'third hit' can exist and worsen the phenotype (Takakura et al., 2009).

Generally, it is thought that multiple genetic and environmental events occur and promote cysts growth and multiplication (Ong and Harris, 2015).

Figure 1.10 summarises the mechanisms suggested to induce cysts formation and influence their progression, as well as the impact on these cysts' growth on the surrounding tissues, *i.e.* the progressive fibrosis of the renal tissue and the infiltration of immune cells at late stages.

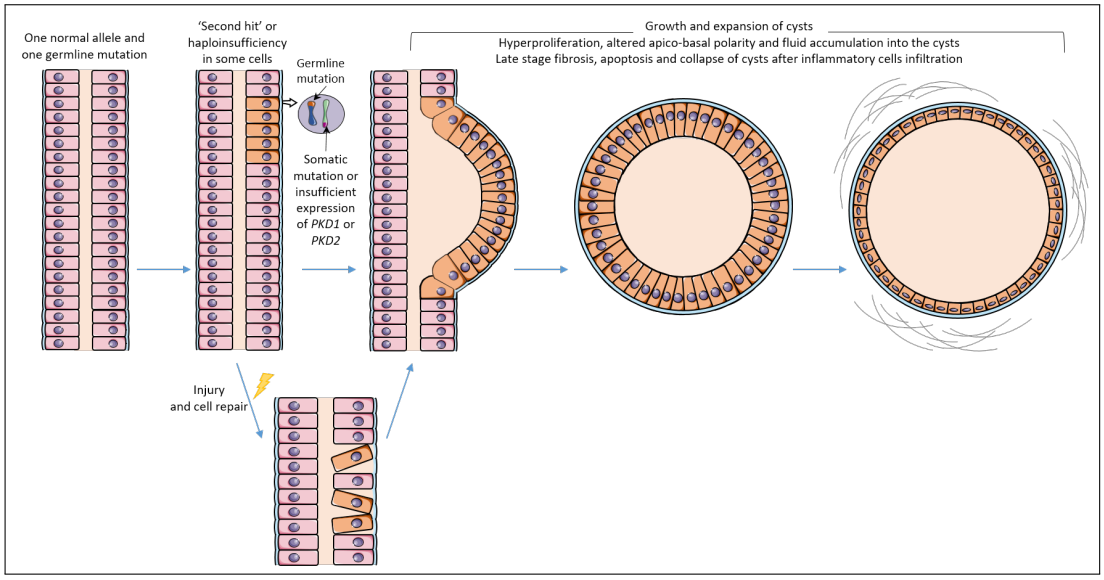

Figure 1.10: **Mechanisms of cysts formation and progression in ADPKD.**
All the epithelial cells contain one normal and one mutated *PKD1* or *PKD2* allele. Cysts initiation occurs when the polycystins expression levels drop below a critical threshold, or under pressure from a somatic mutation ('second-hit'). The cysts progress at variable speed, which can be accelerated by injury and cells repair. Multiple affected pathways lead to parallel hyperproliferation, polarity changes and fluid transport, hence to complete cysts formation which will locally stress adjacent tissues, inducing more injury and an increased fibrosis of the renal tissue, as well as the infiltration of immune cells and the multiplication of complications from the disease.

A detailed characterisation of the multiple sporadic factors linked to ADPKD will improve our understanding of the disease and enable more effective treatment strategies in the future.

1.3 Micro-RNAs: new tools in the characterisation of factors inducing ADPKD

1.3.1 Biogenesis and functions of the miRNAs

Definition Micro-RNAs (miRNAs) are a family of recently discovered nucleic acids which act as regulators of genes expression. The first miRNA was described in 1993 by Rosalind Lee, Rhonda Feinbaum and Victor Ambros, who were working on the larval development of *C. elegans*. They discovered that a gene involved in the timing of development called lin-4 was coding for small RNAs instead of a protein (Lee et al., 1993). Since this major discovery, hundreds of miRNAs have been characterised in various organisms, from *Arabidopsis thaliana* (Llave et al., 2002), *Drosophila melanogaster* (Schertel et al., 2012), zebrafish (Wienholds et al., 2005) and *Xenopus laevis* (Tang and Maxwell, 2008). The miRNA database, miRBase (mirbase.org), referenced only 218 different miRNAs in December 2002 and more than 28,000 (1,881 human) as of June 2017 (Kozomara and Griffiths-Jones, 2014) which shows the tremendous interest in these nucleic acids since their discovery. The current consensus for the definition of a miRNA regroups several criteria such as: an homogeneity of 5' end, a phylogenetic conservation, a 3' overhang structure in the miRNA duplex (proves a processing mediated by RNase III), abundant sequencing reads and proofs of association with Argonaute (Ha and Kim, 2014). MiRNAs differ from small interfering RNAs (siRNAs) by their nuclear process; miRNAs are generated from short hairpin RNAs processed by the RNase III proteins Drosha and then Dicer whereas siRNAs are issued from long double-stranded RNAs and only cleaved by Dicer. Furthermore, while both siRNAs and miRNAs regulate genes translation (the former by endonucleolytic cleavage, the latter by translational repression or degradation of mRNA, Valencia-Sanchez et al., 2006), siRNAs also have a role in the defence against viruses (Ghildiyal and Zamore, 2009). Finally, siRNAs are fully complementary to their mRNA target, which confers them a specificity of action, whereas miRNAs are only partially complementary to the mRNA and therefore are able to target multiple genes (Lam et al., 2015).

MiRNAs are short (≈22 nucleotides), non-coding, single-stranded RNAs. They regulate gene expression post-transcriptionally mostly by targeting their mRNA's 3'UTR (untranslated region at the 3' end) and are responsible for the integrity of most major pathways such as cell proliferation, cell growth, development, metabolism and homeostasis (Ameres and Zamore, 2013). Sequences coding for miRNAs are thought to represent 1 to 3 % of the mammalian genome (Bartel, 2004), and as each miRNA is predicted to target several hundreds of mRNAs, more than half of the protein-coding genes are predicted to be regulated by these elements in humans (Friedman et al., 2009).

MiRNAs promoters Because their genes are mostly distant from the protein-coding genes, it has been suggested that miRNAs derive from their own transcription units (Lagos-Quintana et al., 2001). 68 % of the human miRNA genes found in miRBase are intergenic, while 12 % are intronic and the rest are located in UTR, lncRNA or coding regions of protein-coding genes (Cammaerts et al., 2015). The characterisation of miRNAs promoters and the role of transcription factors on their expression is still not well known, and only a small number of transcription starting sites (TSS) have been confirmed (Zhao et al., 2017). Several promoter-prediction or recognition algorithms have been developed over the past few years. They have based their analyses on histone markers (*CoreBoost_HM*, Wang et al., 2009c), RNA polymerase II binding (*MicroTSS*, Georgakilas et al., 2014), single or combinations of genome sequence features such as similarity with pol II promoters (*CoVote*, Zhou et al., 2007), TATA and CCAT boxes (Fujita and Iba, 2008) or CpG islands density and conservation scores (*promiRNA*, Marsico et al., 2013), or nucleosome-free regions identified by high-throughput sequencing (Marson et al., 2008). A few databases are currently listing promoters from miRNAs, the most extensive one being miRGen (accessible from http://www.microrna.gr/mirgen, Alexiou et al., 2009) and its derivative DIANA-mirGen v.3.0 (Georgakilas et al., 2016) with 812 human and 386 mouse miRNAs recorded (Zhao et al., 2017).

Biogenesis of mammal miRNAs As seen in Figure 1.11, they are transcribed by RNA polymerase II as long precursor transcripts; the primary-miRNAs (pri-miRNAs), stem-loop structures of ≈80 bases (Lee et al., 2004b).

Several factors have been reported to regulate the expression of some miRNAs, such as MYC, p53, ZEB1/2 and MYOD1 (Kim et al., 2009; Krol et al., 2010) or epigenetic modifications such as histones modification or methylation of the DNA (Yu et al., 2005; Liu et al., 2016). In some cases, a single promoter initiates the co-expression of multiple (polycistronic) miRNAs usually located close to each other (Kim et al., 2009).

The pri-miRNA stem-loop is then cleaved by the microprocessor complex in the nucleus and gives rise to the precursor-miRNA (pre-miRNA, ≈60 bases, see Denli et al., 2004). The microprocessor complex comprises the double-stranded RNA-binding protein DGCR8/Pasha (Landthaler et al., 2004) and the RNase III enzyme Drosha (Lee et al., 2003), composed of one RNA-binding domain and two RNase III domains, each cutting a different strand of the pri-miRNA (Blaszczyk et al., 2001). Interestingly, Drosha can excise several pre-miRNAs from one miRNA, which suggests that several targets of the same pathway could be regulated at the same time (Denli et al., 2004; Gregory et al., 2004). DGCR8 interacts with Drosha via its C terminus and with the pri-miRNA via its RNA-binding domains and via its heme-binding domain, heme being an essential cofactor for the processing of pri-miRNAs (Yeom et al., 2006; Quick-Cleveland et al., 2014). The microprocessor complex cleaves the miRNA at ≈22 bp from the loop and ≈11 bp from the region where the two strands separate (Han et al., 2006; Zeng et al., 2005).
The microprocessor complex-mediated miRNA cleavage is regulated by multiple factors. For example, the two proteins Drosha and DGCR8 co-regulate each other by a feedback loop: Drosha cleaves *DGCR8*'s mRNA which leads to its destabilisation (Kadener et al., 2009), and DGCR8 participates in Drosha's stability by protein-protein interactions (Yeom et al., 2006; Han et al., 2009). Acetylation of Drosha will inhibit its degradation (Tang et al., 2013) and GSK3β-mediated phosphorylation is essential to its nuclear localisation and enhances miRNAs biogenesis (Fletcher et al., 2017). Furthermore, phosphorylation of DGCR8 by ERK will increase its stability (Herbert et al., 2013), while HDAC1 (histone deacetylase) will deacetylate it which will confer it a higher affinity for pri-miRNAs (Wada et al., 2012). The DEAD-box helicases DDX3X, p72 (DDX17) and p68 (DDX5) have been shown to be essential for the processing of certain subsets of miRNAs (Zhao et al., 2016; Remenyi et al., 2016; Salzman et al., 2007).

The SMAD proteins and p53 interact with p68 and hence regulate the microprocessor's activity (Davis et al., 2010; Garibaldi et al., 2016). ADAR and TAR-binding protein (TDP-43) were also reported to interact with the microprocessor complex and regulate its activity (Di Carlo et al., 2013; Bahn et al., 2015). Finally, other proteins will affect pri-miRNAs processing by Drosha and DGCR8 by binding to their terminal loop. For example, KSRP (KH-type splicing regulatory protein) and hnRNP A1 (heterogeneous nuclear ribonucleoprotein A1) will facilitate Drosha-mediated processing by binding to the loop of pri-let-7 and pri-mir-18a, respectively (Guil and Caceres, 2007; Trabucchi et al., 2009), while LIN28A will inhibit this processing by binding to pri-let-7 loop (Nam et al., 2012).

Interestingly, another class of miRNAs, which is not processed via the classic pathway, has been described: the mirtrons. Their promoter may be independent from the gene they are coded in (Monteys et al., 2010), and their pri-miRNA is encoded in introns and not processed by the microprocessor complex but needs pre-mRNA splicing, with the intervention of the debranching enzyme DBR1 (RNA lariat debranching enzyme) that linearises the intron (Ruby et al., 2007; Okamura et al., 2007). Several studies (Ladewig et al., 2012; Berezikov et al., 2007; Havens et al., 2012) have identified mirtrons in mammals and new ones are regularly discovered.

After having been generated by the microprocessor complex in the nucleus, the pre-miRNA is then exported by Exportin-5 (XPO-5) from the nucleus to the cytoplasm (Lund et al., 2004). This transport is dependent on the interaction of XPO-5 with RAN-GTP, a GTP-binding protein acting as a co-factor (Bohnsack et al., 2004). GTP is hydrolysed by RAN-GTP during the transport through the nuclear membrane which leads to the disassembly of the complex and the release of the pre-miRNA into the cytoplasm. The recognition of the pre-miRNA by XPO-5 is independent of its sequence but a double-stranded sequence of minimum 16 bp in length is required (Lund et al., 2004). Interestingly, XPO-5 knock-down was reported to induce a reduction of miRNA levels but no accumulation of pre-miRNA in the nucleus, suggesting that XPO-5 may also act as a stabiliser of the pre-miRNA (Yi et al., 2003; Iwasaki et al., 2013).

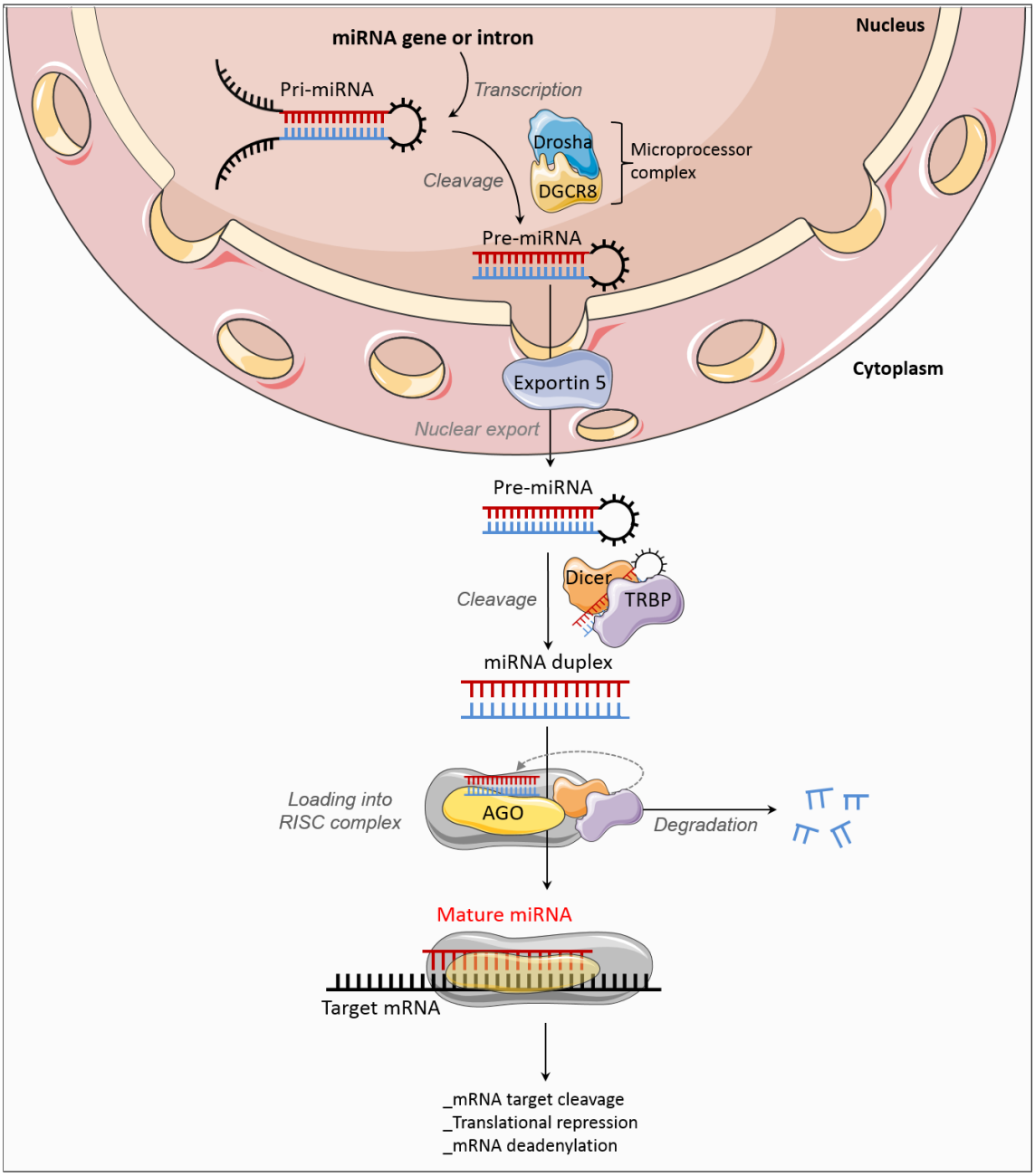

Figure 1.11: **Canonical pathway of miRNAs biogenesis in mammalian cells.**
The miRNA genes are transcribed into long dsRNA (pri-miRNAs), whose single strand ends will be cleaved by the microprocessor complex (Drosha and DGCR8 = Pasha, DiGeorge syndrome critical region gene 8) in the nucleus to give rise to pre-miRNAs. Exportin will mediate transport of pre-miRNA from the nucleus to the cytoplasm, where the Dicer/TRBP (HIV-1 TAR RNA binding protein) complex will cleave the terminal loop and load the miRNA/miRNA* duplex onto Argonaute proteins (Ago). The complex will then be unwound in this protein and, while the passenger strand will be degraded, the guide strand will remain bound to Ago which will recruit GW182 to form the mature miRISC complex in which the mature miRNA will exert its regulatory function on its target mRNA by binding to its seed sequence (classically in the mRNA's 3'UTR end).

In the cytoplasm, the RNase III enzyme Dicer and TRBP (TAR RNA-binding protein) process the pre-miRNA into a mature miRNA duplex of ≈20 nt (Zhang et al., 2004). TRBP affects the stability of Dicer, as a decrease in the former leads to the latter's destabilisation and defects in pre-miRNA processing (Chendrimada et al., 2005). Furthermore, the MAPK/ERK pathway can phosphorylate TRBP which leads to higher expression of some growth-stimulatory miRNAs and increased cell growth and proliferation (Paroo et al., 2009). Similarly to their role on pri-miRNAs cleavage by Drosha, KSRP and LIN28A can affect pre-miRNA processing by Dicer: KSRP interacts with their terminal loop and enhance their Dicer-mediated processing (Trabucchi et al., 2009), while LIN28A will block pre-let-7 cleavage by Dicer. Notably, let-7 itself targets *Dicer*'s mRNA which shows the existence of a feedback loop (Forman et al., 2008) and highlights the need for a tight regulation of the pre-miRNAs processing by Dicer/TRBP. Other proteins will affect pre-miRNA processing by Dicer by degrading some pre-miRNAs or making them too unstable to be able to undertake further processing steps. Among them, MCPIP1 (MCP-induced protein 1) was shown to cleave the terminal loop of some miRNAs (including let-7g, mir-146a and mir-135b) and block their processing by Dicer (Suzuki et al., 2011).

The preference of Dicer for some pre-miRNAs more than others or its efficiency depends on the presence of a two-nucleotide-long 3' overhang originally generated by the Drosha-mediated cleavage (Zhang et al., 2004). Dicer will typically cleave the pre-miRNA structure 21 to 25 nucleotides away from the 3' helical end of the dsRNA's terminus (Zhang et al., 2002; Vermeulen et al., 2005; MacRae et al., 2006; MacRae et al., 2007). Additionally, when the phosphorylated 5' end is thermodynamically unstable, Dicer cleaves the pre-miRNA 22 nucleotides away from it (Park et al., 2011). These two mechanisms lead to heterogeneous miRNAs isoforms, as they can impact the 3' or 5' end stability and thus determine which strand will be loaded into miRISC (Frank et al., 2010). Although most miRNAs genes will preferentially give birth to one mature miRNA strand more than the other, the integrity of the miRNAs processing factors may affect this ratio, for example depending on the developmental stage or tissue (Krol et al., 2004; Ro et al., 2007; Chiang et al., 2010), which highlights the major role of Drosha and Dicer in miRNAs biogenesis.

The small RNA duplex generated from Dicer/TRBP cleavage is then loaded from Dicer to Argonaute (Ago) via the RISC-loading complex (consisting of TRBP, Dicer and Argonaute) (Chendrimada et al., 2005). Although Dicer has now been shown to not be essential for the loading of the miRNA duplex onto Ago (Betancur and Tomari, 2012; Suzuki et al., 2015), *in vitro* and *in vivo* studies have confirmed the existence of Dicer-Ago-TRBP complexes (Wang et al., 2009a; Gregory et al., 2005; MacRae et al., 2008). Thus, the role of all the components of the RISC-loading complex is still not fully understood. In human, it is believed that the four different Argonaute proteins (Ago1-4) indifferently associate with miRNAs subsets (Meister et al., 2004; Azuma-Mukai et al., 2008; Su et al., 2009; Yoda et al., 2010; Dueck et al., 2012) and asymmetric miRNA/miRNA* duplexes with central mismatches or wobble pairs at positions 8-11 are privileged (Yoda et al., 2010; Betancur et al., 2012). The selection of the guide strand loaded onto and processed by the RISC complex is mostly dependent on the thermodynamic stability of the 5' end of the two strands. The most stable will usually be the passenger strand and cleaved, while the least stable will become the guide strand (future mature miRNA) (Schwarz et al., 2003; Khvorova et al., 2003). The loading of the miRNA duplex into the RISC complex is an active process requiring ATP (Nykänen et al., 2001; Pham et al., 2004; Yoda et al., 2010). It has been suggested that the need for the Argonaute proteins to change conformation in order to accommodate the duplex was the reason for this use of energy (Wang et al., 2008b, Elkayam et al., 2012, Schirle and MacRae, 2012). The Hsc70/Hsp90 (heat shock cognate 70/heat shock protein 90) chaperone machinery uses ATP and mediates this dynamic conformational change (Iwasaki et al., 2010; Iki et al., 2010).

Following its loading into Ago, the mRNA/miRNA duplex is unwound in either a splicing-dependent or splicing-independent process. In mammals, only AGO2 has slicing capacities (Rand et al., 2005; Leuschner et al., 2006; Diederichs and Haber, 2007), which suggests that the splicing-independent pathway, slower and relying a lot on mismatches in the duplex (Yoda et al., 2010; Gu et al., 2011), is more common. The splicing-dependent cleavage of the accessory strand mediated by AGO2, or the slower splicing-independent process mediated by the three other Ago proteins do not require energy or the chaperone machinery (Iwasaki et al., 2010; Yoda et al., 2010).

Many modifications can affect the Ago proteins. MAPKAPK2 (MAPK-activated protein kinase 2) and AKT3 have been shown to phosphorylate AGO2 at Ser387 (Zeng et al., 2008; Horman et al., 2013) while the EGFR (epidermal growth factor receptor)-mediated phosphorylation of this protein occurs at Tyr393 under hypoxia conditions (Shen et al., 2013). Recently, Golden et al. and Quévillon Huberdeau et al. identified clusters of highly conserved sites undertaking hyper-phosphorylation (such as S824–S834) and thus affecting Ago2 activity (Quévillon Huberdeau et al., 2017; Golden et al., 2017). Furthermore, 4PH (type I collagen prolyl 4-hydrogenase) was reported to mediate prolyl-4 hydroxylation of AGO2, leading to its stabilisation and increase of its localisation with processing bodies (Qi et al., 2008). Cellular stress has also been linked to AGO2 inhibition by poly(ADP-ribosyl)ation in order to reduce the generation of miRNA that repress genes expression (Leung et al., 2011), and autophagy or degradation mediated by proteasome were also suggested to regulate the Argonaute proteins expression levels and activity (Chen et al., 2012; Smibert et al., 2013).

Finally, Argonaute loaded with the guide strand associates with GW182 to form the mature RISC complex (RNA-Induced Silencing Complex), where the miRNA can enact its regulatory role on the target mRNA after binding to its complementary seed sequence classically located on the 3'UTR (Khvorova et al., 2003), either by leading to the mRNA degradation (Guo et al., 2010) or by repressing its translation (Chekulaeva and Filipowicz, 2009).

Mechanisms of miRNAs-mediated silencing of mRNA The degradation of miRNA targets has been reported to represent 66 to 90 % of all miRNAs-mediated silencing by several studies on mammalian cells (Hendrickson et al., 2009; Guo et al., 2010; Eichhorn et al., 2014). Multiple studies have described the mechanisms of miRNA targets degradation as involving multiple enzymes from the cellular 5'→3' mRNA decay pathway, such as GW182 and PABPC (poly(A)-binding protein) (Rehwinkel et al., 2005; Chen et al., 2009), the CCR4-NOT deadenylase complex (Behm-Ansmant et al., 2006), the DCP1:DCP2 (decapping protein) and EDC3/4 (enhancer of decapping) (Behm-Ansmant et al., 2006; Eulalio et al., 2007), the Argonaute proteins (Chen et al., 2009), the poly(A)-binding protein and CAF1 deadenylase (Fabian et al., 2009), the exonuclease complex

PAN2:PAN3 (Fabian et al., 2012; Christie et al., 2013) and the RNA helicase DDX6 (DEAD box protein) (Chen et al., 2014; Mathys et al., 2014).

Figure 1.12 (A1/A2) presents the degradation of mRNA mediated by miRNAs. The first step of the pathway involves binding of GW182 to the Argonaute protein recruited by the miRNA (miRISC complex) by its AGO-binding domain (ABD) and the subsequent interaction of the PAM2 (PABP-interacting motif 2) section of its silencing domain (SD) to PABPC (Fabian et al., 2012). The deadenylation of the mRNA targets will then be catalysed by the PAN2:PAN3 complex followed by the action of CCR4-NOT which will have the effect of shortening and removing the 3' poly(A) tail of these targets (Fabian et al., 2012; Christie et al., 2013; Wahle and Winkler, 2013). DCP2 will then decap the deadenylated mRNAs, associated with other cofactors required for its activity (Behm-Ansmant et al., 2006), such as DCP1, DDX6 and EDC3/4 (Jonas and Izaurralde, 2013). XRN1 (5'-3' exoribonuclease 1) will finally degrade these deadenylated and decapped mRNAs. The integrity of this mRNA degradation process is ensured by direct interactions between the enzymes mediating the different steps. For example, CCR4-NOT (deadenylation) will interact directly with DDX6 (decapping) which itself binds to other members of the decapping complex (Mathys et al., 2014; Chen et al., 2014). Similarly, EDC4 (decapping factor) directly interacts with XRN1 which will start the 5'-3' decay from the 5'UTR and thus ensure that no deadenylated/uncapped mRNA accumulates in the cells (Chang et al., 2014; Jonas and Izaurralde, 2015).

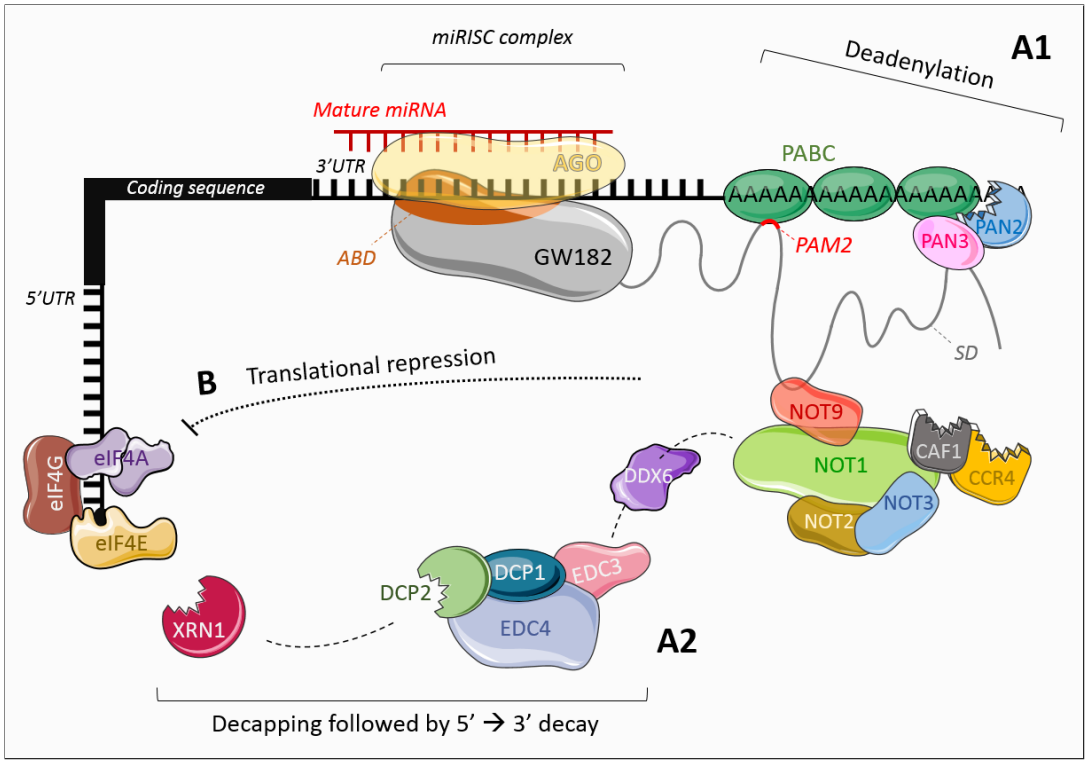

Figure 1.12: **Summary of the miRNAs-mediated gene silencing.** (**A1**) Argonaute transports the miRNA to its seed sequence on the mRNA 3'UTR and associates with GW182 via its Argonaute-binding domain (ABD) to form the RISC complex. GW182 then recruits poly(A) binding proteins (PABC) and interacts with the CCR4-NOT complex as well as poly(A) nucleases (PAN2/3) via its silencing domain (SD). These steps lead to the deadenylation and shortening of the mRNA. (**A2**) The CCR4-NOT complex will also interact with DDX6 (DEAD-box protein) which will itself bind to decapping factors DCP1/2 and EDC3/4. The latter will finally interact with XRN1 which will target the decapped 5'UTR and mediate its decay. (**B**) miRNA-mediated mRNA silencing is thought to be mediated via inhibition of the assembly of the eIF4 complex by CCR4-NOT.

The inhibition of mRNA translation mediated by the miRNAs (6 to 26 % of the miRNA-mediated repression, Eichhorn et al., 2014), also presented in Figure 1.12 (B), can be mediated by miRISC even without mRNA degradation (Humphreys et al., 2005; Iwasaki et al., 2009), and reversely mRNA degradation is able to take place even when translation is totally abolished because of its lack of cap structure or of open-reading frame preventing its reading by ribosomes (Eulalio et al., 2007; Meijer et al., 2013). However it has also been suggested that translation inhibition had to happen first before subsequent mRNA degradation could be triggered, suggesting the existence of intertwining dependent and independent mechanisms (Meijer et al., 2013; Barman and Bhattacharyya, 2015). miRNA-mediated inhibition of mRNA translation is still not completely explained, but the current consensus is that the former inhibits the capping-dependent translation of the

latter (Pillai et al., 2005; Mathonnet et al., 2007). The miRISC complex interferes with the action of the eIF4A helicases (enzymes that allow the pre-initiation complex to scan the 5'UTR towards the start codon and initiate translation, Jackson et al., 2010).
The way this repression mechanism by miRISC occurs is still controversial: Meijer et al. suggested that miRISC specifically recruits IF4A2 via interactions with the CCR4-NOT complex (Meijer et al., 2013). Another study suggested that both eIF4A1 and eIF4A2 were important targets for the translation inhibition mediated by miRISC (Fukao et al., 2014). However other studies cast doubt on the indispensability of the eIF4A enzymes by reporting that NOT1 directly binds to another helicase (DDX6) but not eIF4A2 (Rouya et al., 2014) or that the absence of eIF4A2 did not affect mRNA translation (Galicia-Vazquez et al., 2015). Similarly, although the GW182/CCR4-NOT complex is central to most of the miRNA-mediated inhibition of translation mechanisms previously suggested (Cooke et al., 2010), Ago1 has now also been suggested to inhibit mRNA translation independently of this complex (Barman and Bhattacharyya, 2015). All these studies and contradictory reports highlight that much remains to be understood about the repression of translation mediated by miRNAs.

Criteria for the binding of miRNAs to their mRNA targets and seed sequences predictions The presence of miRNAs seed sequences on their target mRNA depends on multiple factors. Although Watson-Crick complementarity is the first criteria (Grimson et al., 2007), numerous other elements have been characterised and need to be taken into consideration. Among them, the binding of miRNAs at their position 2-8 (Brennecke et al., 2005) and the proportion of G-C bases in the sequence (Wang, 2014) have been shown to be important to the formation of the miRNA/mRNA duplex, while the impact of the length of the seed sequence is still being debated (Ellwanger et al., 2011; Mullany et al., 2016). The thermodynamics and the free energy of the miRNA/mRNA duplex were also reported to play a role in its stability (Mathews et al., 1999; Hibio et al., 2012), and the evolutionary conservation of the target site suggests an importance of the region for miRNA binding (Friedman et al., 2009). Finally, structural considerations such as the accessibility of the target site or the presence of multiple binding sites may also be relevant criteria to be considered (Kertesz et al., 2007; Hon and Zhang, 2007).

Multiple bioinformatics tools have been developed to predict miRNAs seed sequences on mRNAs, each of them using an algorithm based on different criteria among the ones cited above. For example, the web interface microrna.org uses the miRanda algorithm based on free energy of the duplex and sequence complementarity (Betel et al., 2010). The miRDB database bases its predictions on support vector machines (SVM) learning and high-throughput datasets (Wang, 2016) and TargetScan, one of the most used and most robust tools currently available (Riffo-Campos et al., 2016), mainly considers conserved sites, expected number of seed sequences in the 3'UTR, perfect base pairing and predicted free energy of the duplex in order to predict miRNAs seed sequences (Agarwal et al., 2015). Other tools such as DIANA-microT or Rna22 have also been regularly updated and take many criteria into consideration for their predictions (Loher and Rigoutsos, 2012; Vlachos et al., 2014). The MiRTarBase database compiles information from experimentally validated miRNA/mRNA interactions (Chou et al., 2016). Furthermore, miRWalk is an online database regrouping the predictions from twelve databases in order to determine the most probable binding sequences for a set miRNA/mRNA duplex (Dweep and Gretz, 2015). However, from 2017 this multiple databases predictions tool will not be updated anymore and only available to download until 2019, and miRWalk will exclusively focus on a smaller subset (miRDB, TargetScan, MirTarBase) with a machine learning approach based on Ding et al.'s TarPmiR approach (Ding et al., 2016).

Non-classic miRNAs binding and function Although miRNAs typically bind to their target mRNA on their seed sequence located on the 3'UTR of the gene, which is what miRNA target prediction algorithms take into consideration, a few examples of other types of interactions have now been reported. Lee et al. studied the interaction of hsa-mir-34a with several genes using dual reporter luciferase assays and suggested that it binds to *AXIN2* through both 3'UTR and 5'UTR and to *WNT1* through its 5'UTR specifically (Lee et al., 2009). Another study reported that mir-134, mir-296 and mir-4708 can simultaneously bind to *Nanog*'s coding sequence and inhibit its translation (Tay et al., 2008). Furthermore, mir-423-5p mimic was shown to target the progesterone receptor and *IGSF1* promoter and hence induce transcriptional silencing of these genes (Younger and Corey, 2011a).

Finally, another study from the same author described an interaction between mir-193b mimic and progesterone receptor at a sequence downstream of the gene's termini (Younger and Corey, 2011b), suggesting other possible modes of action of the miRNAs. However, these studies are not recent and very little studies have since confirmed these observations.

Vasudevan et al. were the first to suggest that miRNAs can have the opposite effect as what they are known for, meaning they may have a role of activators of translation for some targets in some specific cell cycle conditions and cell types. Indeed, they showed that the TNFα UA-rich element (ARE), a sequence located in the 3'UTR that causes mRNA deadenylation and subsequent degradation, recruits mir-369-3p and thus mediates the up-regulation of translation. This process changes along with the cell cycle; it represses translation in proliferating cells while it mediates activation in the G_1/G_0 (Vasudevan et al., 2007). Several other examples of direct miRNAs-mediated up-regulations have now been reported. Mir-10a directly binds to the 5'UTR of ribosomal proteins and enhances their synthesis by reducing their translational repression following amino acids starvation (Orom et al., 2008). Mir-34a/b-5p binds to the longest β-actin transcript's 3'UTR, present in some tissues in particular, and up-regulates its expression (Ghosh et al., 2008). Mir-328 has been shown to have two different activities mediating myeloid cells differentiation and survival: it can decoy the repressive protein hnRNP E2 (RNA binding protein) but also up-regulate its transcription independently of its seed sequence (Eiring et al., 2010). Finally, among other examples, mir-744 and mir-1186 were reported to induce cyclin B1 expression in mouse embryonic fibroblasts cells, leading to enhanced cell proliferation in cases of short-term expression of the miRNA but to the inhibition of tumour progression in the long term (Huang et al., 2012).

The complexity of the miRNAs biogenesis and regulation machineries, added to their multiple roles on mRNA expression make them very interesting elements to study the mechanisms of multifactorial diseases such as cancer or ADPKD.

1.3.2 miRNAs in human diseases

miRNAs in non-kidney diseases As described above, miRNAs regulate gene expression. Many of them have been directly linked to diseases, and the increasing number of miRNA discoveries suggests that the targeted genes are much more numerous than previously thought. This could be either an advantage since it would widen the potential therapeutic targets in a disease, but could also be inconvenient because it becomes difficult to select the most relevant ones (60 % of all human mRNAs are estimated to be a miRNA target (Ha, 2011; Di Leva et al., 2014)). The effects of repression or induction of miRNA expression are various: DNA methylation and repair, cell growth, apoptosis or cell fate specification (Ha, 2011).

Some miRNAs have been linked to pulmonary diseases and asthma (mir-20 and mir-210 for example), probably because of their role in lung development and inflammatory response (Tomankova et al., 2010). Furthermore, mir-29 was shown to be down-regulated by TGFβ (Transforming growth factor) in human foetal lung fibroblast cells, which can lead to less repression of fibrosis-related genes and therefore the development of pulmonary fibrosis (Cushing et al., 2011).

Chen et al. studied the role of miRNAs in sickle-cell disease. They discovered that mir-320 down-regulates CD71 during the terminal differentiation of reticulocytes, which could partly explain the red blood cell phenotype in the patients (Chen et al., 2008a).

In liver diseases, they have been implicated in regulating infection by Hepatitis C Virus. Indeed, low levels of mir-122, the most expressed hepatic miRNA, have been linked to a reduced auto-replication of the virus genome (Jopling et al., 2005). Miravirsen, a mir-122 inhibitor, is currently being tested for the treatment of HCV infection (see below) (Janssen et al., 2013). Furthermore, the miRNA implication in cell differentiation, metabolism, or apoptosis could explain the consequences of their deregulation in the liver (Chen, 2009). Some studies have shown cooperation between miRNAs and the Interferon (IFN) signalling system to control viral infection (Pedersen et al., 2007). Contrarily, some viruses also encode miRNAs that interact with host cells. The role of miRNAs in infection is thus variable.

Some miRNAs such as mir-15a, mir-15b, mir-16, mir-195 or mir-124a2 have been linked to the development of diabetes by regulating the expression of several transcription factors in the pancreas (Joglekar et al., 2007; Baroukh et al., 2007). Furthermore, glucose concentration was shown to affect the expression levels of many miRNAs in pancreatic cells, for example mir-27a, mir-130a, mir-192, mir-200a, mir-320, mir-337, mir-369-5p, mir-379 and mir-532 (Hennessy et al., 2010), mir-296, mir-484 and mir-690 (Tang et al., 2009), or mir-375 (El Ouaamari et al., 2008). Mir-375 in particular has been largely studied in the pathogenesis of diabetes. The knock-down of this miRNA in zebrafish and mice models led to anomalies in pancreatic development and decreased β cells mass (Kloosterman et al., 2007; Poy et al., 2009) along with enhanced insulin secretion (Poy et al., 2004), whereas its over-expression reduced the insulin secretion induced by glucose in pancreatic cells (Xia et al., 2011). Generally, miRNAs have been shown to induce diabetes and microvascular (nephropathy) or macrovascular (atherosclerosis or cardiomyopathy) complications in various tissues such as liver, heart, brain and kidney (Moura et al., 2014; Simpson et al., 2016). Diabetic nephropathy was shown to be mediated by miRNAs such as mir-21, mir-216, mir-93 or the mir-29 family essentially through the aberrant expression of TGFβ regulating these miRNAs and the subsequent podocyte apoptosis, proteinuria and kidney dysfunction (Lin et al., 2014; Lan, 2012; Zhang et al., 2009; Long et al., 2010, 2011; Kato et al., 2009), and other miRNAs such as mir-377 or mir-192 have been shown to have a role in the fibrosis observed in this pathology (Krupa et al., 2010; Wang et al., 2008a).

Cardiomyopathies were linked to mir-1, mir-206, mir-548 and mir-320, targeting Hsp60, VEGF or IGF-1, for example (Shan et al., 2010; Gupta et al., 2013; Wang et al., 2009b), and atherosclerosis was suggested to result from dysregulation of mir-16 and mir-155 affecting COX-2 (inflammatory gene) and myosin light chain kinase, respectively (Shanmugam et al., 2008; Weber et al., 2014).

In vascular diseases, mir-143 and mir-145 were shown to be the most abundantly expressed miRNAs in the smooth muscle cells and that a down-regulation of these miRNAs affected angiotensin-converting enzyme (ACE) levels which led to the reduction of aorta's contractility and development (Dahan et al., 2014).

Mir-10a was reported to inhibit pro-inflammatory adhesion molecules and lead to endothelial cell dysfunction (Kumar et al., 2014; Fang et al., 2010), while mir-122 and mir-33 were shown to regulate lipids biogenesis and metabolism in hepatocytes and macrophages (Esau et al., 2006; Wen and Friedman, 2012; Horie et al., 2010). Romaine et al. published a review of all miRNAs involved in cardiovascular diseases (Romaine et al., 2015). For example, patients with heart failure show affected expression levels of a few miRNAs such as mir-122, mir-210, mir-499 and mir-622 in several studies, suggesting the dysregulation of major processes affecting cardiac function (Corsten et al., 2010; Endo et al., 2013; Vogel et al., 2013; Olivieri et al., 2013).

In cancer, miRNA regulation is similarly complex as in viral infections, with some functioning as oncogenes and others as tumour suppressors (Di Leva et al., 2014). They have been linked to numerous cancers such as colon (mir-15/16), ovarian (mir-34), prostate (mir-17$\sim$92) or breast (mir-200 family) cancer (Di Leva et al., 2014). The proteins from the miRNAs biogenesis machinery are often targeted: many studies have reported the down-regulation of Dicer and Drosha in several cancer types including lung cancer (Karube et al., 2005), breast cancer (Dedes et al., 2011), endometrial cancer (Torres et al., 2011), leukaemia (Allegra et al., 2014), colorectal cancer (Iliou et al., 2014), nasopharyngeal carcinoma (Guo et al., 2012) and ovarian cancer (Merritt et al., 2008) by very diverse mechanisms such as the loss of TAp63, a p53 family member normally inducing Dicer's transcription (Su et al., 2010), the dysregulation of epigenetic modifications of Dicer, for example methylation, under hypoxic conditions leading to the silencing of its promoter (Van Den Beucken et al., 2014), or the enrichment of miRNAs directly targeting Dicer such as let-7 (Tokumaru et al., 2008), mir-103/107 (Martello et al., 2010) or mir-630 (Rupaimoole et al., 2016). Mutations of Exportin 5 have also been reported to lead to pre-miRNAs accumulation in the nucleus of cancerous colorectal, gastric or endometrial cells (Melo et al., 2010). The dysregulation of Argonaute proteins can also be a cause for cancers; an increased expression of this protein was detected in gastric carcinoma (Zhang et al., 2013) and its phosphorylation by EGFR leading to its inhibition was linked to a poorer diagnosis in breast cancer patients (Shen et al., 2013).

Additionally to the direct dysregulation of the miRNAs machinery, mutations in miRNAs loci or genes of proteins affecting miRNAs can also lead to the development of cancer. Indeed, Zhang et al. used high-resolution array-based comparative genomics analysis in 227 human breast and ovarian cancers and melanoma and showed that a large proportion (72.8 %, 37.1 % and 85.9 %, respectively) of the miRNAs genes loci showed an alteration of copy numbers, 41 genes being common between the three cancer types (Zhang et al., 2006). This suggests that the altered expression of miRNAs found in cancer could partly be due to the deletion or amplification of genomic regions containing their coding sequence along with the deregulation of the miRNAs biogenesis enzymes. Another suggested cause for miRNAs dysregulation in cancer is the phosphorylation of KSRP (KH-type splicing regulatory protein) by the ATM kinase in response to DNA damage that leads to its binding to pri-miRNAs and their enhanced processing (Zhang et al., 2011b).

Epigenetic modulation is another way by which miRNAs expression may be affected in cancer. For example, AML1/ATO-mediated CpG methylation of mir-223 repressed its expression in haematopoietic stem cells, leading to leukaemia (Fazi et al., 2007). Furthermore, in pancreatic, brain and breast cancers, DNA hypermethylation is linked to the down-regulation of mir-124a, mir-145-5p and mir-125, respectively (Wang et al., 2014b; Chen and Xu, 2015; Donzelli et al., 2015).

Generally, a few miRNAs families have been shown by multiple studies to be major drivers for cancer development (tumour-suppressive miRNAs). The let-7 family, for example, includes 10 isoforms that target mRNAs encoding oncogenes such as *KRAS* (Roush and Slack, 2008). Let-7 knock down in cancer cells induces the dysregulation of signalling networks involving the RAS proteins resulting in tumour progression (Johnson et al., 2005; Yu et al., 2007). The mir-34 family has also been the focus of many cancer studies, as its three members mir-34a, 34b and 34c were found down-regulated in multiple cancers such as breast and lung cancer. Their transcription is regulated by the tumour suppressor p53, whose expression is altered in cancer cells (Tarasov et al., 2007; Chang et al., 2007; Raver-Shapira et al., 2007; Okada et al., 2014). Mir-34a regulates the expression of genes coding for proteins involved in the cell cycle such as CDK4 and

CDK6 (cyclin dependent kinases) (Guo et al., 2015; Sun et al., 2008), proteins linked to metastasis development such as MYC, AXL, Notch and MET (Bu et al., 2013; Yamamura et al., 2012; Maroni et al., 2017; Cho et al., 2016), and proteins preventing apoptosis such as BCL-2 and SIRT-1 (Li et al., 2013a). Another important miRNAs subset is the mir-200 family that regulates the expression of genes playing a role in the epithelial-mesenchymal transition (EMT). When cancer cells change from an epithelial to a mesenchymal phenotype they become more stable and invasive and the cancer progresses, therefore the regulation of EMT-related proteins is essential to the integrity of the tissue (Voulgari and Pintzas, 2009; Craene and Berx, 2013). As an example, mir-200 and ZEB1 (zinc-finger E-box-binding homeobox 1), a transcriptional repressor of CDH1 (E-cadherin, involved in cytoskeletal rearrangements), reciprocally regulate each other through a negative feedback loop (Korpal et al., 2008; Park et al., 2008; Gregory et al., 2008). Indeed, mir-200 down-regulates ZEB1, which in return binds to this miRNA's promoter and reduces its expression, thereby leading to EMT in cancer cells (Burk et al., 2008). Other families of miRNAs recurrently involved in cancer development as tumour suppressors are mir-15/16 and mir-520 (Aqeilan et al., 2010; Keklikoglou et al., 2012; Peng et al., 2016), whereas mir-10b, mir-17∼92, mir-21, mir-210, mir-221 and mir-155 have been reported to be oncogenes (Si et al., 2007; Ouyang et al., 2014; Mattiske et al., 2012; Sun et al., 2014b; Ren et al., 2017; Fuziwara and Kimura, 2015). Other examples are regularly being described, suggesting much is still left to discover about the mechanisms mediating miRNAs roles in cancer development and progression.

miRNAs in kidney diseases and ADPKD Several miRNAs have been involved in the development of kidney diseases. Defects of the miRNAs machinery enzymes themselves can impact the integrity of the organs. For example, knock-outs of Drosha in podocytes in mice result in a collapsing glomerulopathy (Zhdanova et al., 2011) and the silencing of DGCR8 in mice embryos lead to defects in kidney development, the development of kidney cysts and renal failure and eventually premature death of the animals (Bartram et al., 2015). Furthermore, the conditional deletion of Dicer results in apoptosis of nephron progenitor cells (Nagalakshmi et al., 2011; Ho et al., 2011).

Some miRNAs have been found differentially expressed between kidney regions: mir-192 and mir-194 are enriched in the cortex compared to the medulla of rats kidneys whereas mir-27b shows the opposite expression profile in the same model (Tian et al., 2008), and some others were found more expressed in the kidney compared to other organs: mir-215, mir-146a and mir-886 were exclusively enriched in the kidney while let-7a–g, mir-21, mir-192, mir-194, mir-200a and mir-204 were over-expressed in the kidney along with other organs (Landgraf et al., 2007; Sun et al., 2004; Baskerville and Bartel, 2005). However, these expression patterns differ depending on the developmental stage and age of the organ, adding complexity to the understanding of miRNAs dysregulation in renal diseases (Tang et al., 2011).

MiRNAs have been shown to regulate the kidney's water reabsorption as well as its homeostasis by acting on proteins involved in these mechanisms such as aquaporins and the renin-angiotensin-aldosterone system (Sepramaniam et al., 2010; Butterworth, 2015).

Kidney fibrosis mediated by TGFβ1 has been linked to the dysregulation of several miRNAs. Aberrant synthesis of TGFβ by infiltrating inflammatory cells participates in renal fibrosis as well as other pathological events such as tubules loss due to the accumulation of myofibroblasts, mesangial cells hypertrophy, induction of EMT and podocytes apoptosis (Boor and Floege, 2011; Zeisberg et al., 2003; López-Hernández and López-Novoa, 2012; Jiang et al., 2014). TGFβ has been shown to affect the expression levels of multiple miRNAs, and reversely some miRNAs can target TGFβ, suggesting the existence of a feedback loop between the two elements (Butz et al., 2012). This cytokine acts on the processing of some miRNAs, for example mir-21 and mir-29, through the intervention of the SMAD proteins and their cofactor p68 which bind to the terminal loop of pri-miRNAs to facilitate their recruitment by the microprocessor complex (see above). Interestingly, Smad3 has opposite effects on these two miRNAs: it promotes renal fibrosis by up-regulating mir-21 but inhibiting the expression of mir-29 (Zhong et al., 2011; Qin et al., 2011). Mir-21 has been linked to fibrosis in various other organs such as the heart or the lungs (Thum et al., 2008; Liu et al., 2010), and CKD patients showed high increases of mir-21 expression levels (Zawada et al., 2014; Szeto et al., 2012). This miRNA was shown to target PPARα (regulator of lipids metabolism) and Mpv171 (mitochondrial

protein involved in the metabolism of reactive oxygen species), hence leading to kidney fibrosis (Chau et al., 2012).

Furthermore, mir-192 has also been linked to the induction of TGFβ-mediated renal fibrosis as it was differentially expressed by this cytokine in different *in vitro* models (Wang et al., 2010a; Putta et al., 2012). However, *in vivo* models showed contradictory results as it was up-regulated in fibrotic kidneys of rodents after renal ablation but down-regulated in diabetic nephropathy models at late stages (Chung et al., 2010; Krupa et al., 2010; Kato et al., 2007; Wang et al., 2010a). Mir-192 was shown to target E-cadherin transcriptional repressors Zeb1 and Zeb2, hence its down-regulation by TGFβ results in decreased levels of E-cadherin and therefore phenotypical changes of epithelial cells (Krupa et al., 2010; Chau et al., 2012; Wang et al., 2010a).

Denby et al. studied the role of mir-214 in renal fibrosis. Their results showed that this miRNA promotes renal fibrosis by regulating the transcriptional response to injury. The authors suggested that inhibiting mir-214 could be a new antifibrotic treatment (Denby et al., 2014).

Renal cell carcinoma (RCC) and other renal cancer subtypes have been reported to be mediated by several miRNAs. Notably, the Cancer Genome Atlas Network performed a comprehensive analysis and suggested that some miRNAs such as mir-17-5p, mir-21, mir-34a, mir-200c and mir-215 correlated with RCC patients' survival (The Cancer Genome Atlas Network, 2013). These observations still need to be validated in *in vivo* models. Furthermore, mir-562 was reported to target *EYA1* and its reduced expression to be responsible for the development of the childhood renal cancer called Wilm's tumour (Drake et al., 2009), while mir-483-3p was found highly over-expressed in the same disease (Veronese et al., 2010). Finally, Saini et al. characterised mir-708 as a tumour suppressor in RCC and suggested it targets to be Zeb2 and BMI1, two regulators of E-cadherin (Saini et al., 2011).

Micro-RNAs have also been shown to play a role in immune diseases and infection of the kidney, notably through their regulation by IGFβ. For example, IgA nephropathy (IgAN) is known to be linked to C1GALT1-mediated glycosylation of IgA1, and C1GALT1 was suggested to be a target for mir-148b (Serino et al., 2012).

A down-regulation of mir-223, a miRNA known to cause glomerular endothelial proliferation characteristic of the disease, was also shown in glomerular and circulating endothelial cells of IgAN patients (Bao et al., 2013). Furthermore, biopsies from IgAN patients showed a correlation between aberrant levels of miRNAs linked to the immune response (mir-146a and mir-155) and to fibrosis (mir-192) and severity of the disease (Wang et al., 2010c, 2011a). Other miRNAs suggested to have a role in IgAN are mir-17, mir-29 and mir-93 (Trionfini et al., 2014).

Kidney biopsy samples of lupus nephritis patients, a renal autoimmune disorder, showed that 30 miRNAs were repressed in the disease (*e.g.* mir-296, mir-346, mir-615) whereas 36 were increased (*e.g.* mir-200c, mir-600, mir-30a-5p) (Dai et al., 2009), while mir-150 was also linked to the renal fibrosis observed in this disorder (Zhou et al., 2013).

Furthermore, some miRNAs were suggested to be predictive of graft rejection in kidney transplant patients. Indeed, miRNAs expressed by resident renal cells let-7c, mir-30a-3p and mir-10b were down-regulated in renal allograft biopsies, while mir-155, mir-142-5p and mir-223, surmised to originate from graft-infiltrating immune cells, were over-expressed in these tissues. These results were confirmed by measuring the miRNA levels in HREC (human renal epithelial cells) and PBMC (peripheral blood mononuclear cells) cells (Sui et al., 2008; Anglicheau et al., 2009).

Few miRNAs have been studied for the pathogenesis of polycystic kidney diseases. The best characterised subset in this disorder is the mir-17∼92 cluster that was reported to have an influence on ADPKD phenotype in different studies. The mir-17 family consists of 15 miRNAs grouped into three different clusters. The mir-17∼92 cluster is composed of mir-17, mir-18a, mir-19a, mir-20a, mir-19b-1 and mir-92-1 and located on chromosome 17 (Li, 2015). It is essential to the development of various organs and its deletion results in mice leads to kidney developmental defects among others (Ventura et al., 2008; Mendell, 2008). As mentioned above, its transcription can be increased by the binding of the C-MYC oncogenic transcription factor which links it to multiple cancers including kidney (The Cancer Genome Atlas Network, 2013; Lichner et al., 2015).

This family is over-expressed in the kidney of various PKD murine models in which it leads to the formation of cysts (Patel et al., 2013; Hajarnis et al., 2017), and its members were shown to directly target *PKD1* and *PKD2* for mir-17 (Tran et al., 2010; Patel et al., 2013; Sun et al., 2010), or *PKHD1* (fibrocystin, involved in the development of Autosomal Recessive Polycystic Kidney Disease ARPKD) for mir-92 (Hiesberger et al., 2004). Conversely, mice knocked-down for this cluster showed a reduced cysts epithelial cells proliferation, an improved renal function and an overall better survival (Patel et al., 2013; Hajarnis et al., 2017). The mechanisms explaining the role of mir-17∼92 in the pathogenesis of ADPKD are only starting to be understood. Apart from their direct targeting of the polycystins genes *PKD1* and *PKD2*, they have been shown to target mTOR and TGFβ (Patel et al., 2013), two factors involved in cysts growth (O Donnell et al., 2005; Mendell, 2008; Conkrite et al., 2011). Furthermore, a recent study suggested that this family of miRNAs modulates mitochondrial metabolism in *Pkd1* knock-out mice models by inhibiting Pparα. Indeed, deletion of mir-17∼92 induced the activation of gene networks controlled by this factor and its relative expression was inversely correlated to the expression levels of this cluster (Hajarnis et al., 2017).

Patel et al. studied the role of miRNAs on renal tubule maturation. They showed that the ablation of Dicer was linked to a down-regulation of mir-200. After the inhibition of this miRNA in epithelial cells, tubulogenesis was abnormal and interestingly, *PKD1* was over-expressed. Further bioinformatics analyses identified a putative binding site in the *PKD1* gene and the authors concluded that mir-200 could play an important role in ADPKD by regulating the dosage of *PKD1* (Patel et al., 2012). Furthermore, mir-200 is known to be a target for HNF1β, another gene involved in cystic kidney disease. Tubules-specific knock-down of *Hnf1*β in mice results in cysts formation and reduced levels of the mir-200 family (Hajarnis et al., 2015). The mechanisms of action of mir-200 may be linked to the induction of EMT, as this miRNA targets ZEB1 and ZEB2 and TGFβ, suggesting that in normal conditions mir-200 regulates the expression of genes involved in PKD and therefore maintains tubules homeostasis (Burk et al., 2008; Adam et al., 2009; Brabletz and Brabletz, 2010; Gregory et al., 2011; Xiong et al., 2012; Brabletz et al., 2011).

Furthermore, Lakhia et al. recently reported a higher mir-21 expression in cysts from ADPKD patients and in PKD mice models, and that cAMP signalling promotes mir-21 expression in mice cystic kidneys. Furthermore, deletion of this miRNA reduced disease progression in an orthologous mouse model and the authors hypothesised that it targets *Pdcd4*, a gene previously reported to be proapoptotic, and therefore mediates cysts growth (Lakhia et al., 2016). This hypothesis will need to be validated with further experiments.

Deletion of Bicc1 (Bicaudal C1), a post-transcriptional regulatory protein, in mice has also been shown to induce the formation of renal fluid-filled cysts and to modulates the expression of *Pkd2*. Furthermore, Bicc1 was reported to inhibit the repression of *Pkd2* by mir-17 and therefore lead to increased levels of polycystin 2 in the kidney (Tran et al., 2010; Piazzon et al., 2012). Bicc1 was also suggested to recruit mir-125 and mir-27a to mediate the silencing of AC6 (adenylate cyclase 6) and PKIα (protein kinase inhibitor), two enzymes essential to the conversion of cAMP and its function (Piazzon et al., 2012). cAMP accumulation being known to result in cysts formation, the relevance of Bicc1 and the miRNAs it targets may be of importance to understand the pathogenesis of ADPKD. Finally, microarray and systems biology approaches (network analyses) have been used to identify dysregulated miRNAs in ADPKD and try to identify some relevant candidates involved in the pathogenesis of the disease. Pandey et al. carried out microarrays in ADPKD kidney tissues and identified other miRNAs dysregulated in the disease, such as mir-196a and mir-31 (Pandey et al., 2008). Lee et al. also used microarrays to analyse the miRNA profiles of PKD-rat cholangiocytes and liver samples from ADPKD patients (Lee et al., 2008). The results showed a reduced expression of mir-15a in the livers of the patients and an up-regulation of its target Cdc25A (Lee et al., 2008). Dweep et al. performed a parallel mRNA/miRNA microarray on PKD rats kidneys and showed the dysregulation of mir-31, mir-34a, mir-132, mir-146b, mir-199a-5p and mir-214 (Dweep et al., 2013). These bioinformatics studies however require further validation in *in vitro* and *in vivo* models in order to confirm the role of these miRNAs. Network analyses consist in associating bioinformatics pre-studies, miRNA/mRNA microarrays, qPCR and/or immunohistochemistry to determine a link between miRNA levels, gene expression and phenotypic characteristics.

For example, Song et al. used gene set enrichment analyses to identify over-represented pathways in cysts compared to minimally cystic tissue of ADPKD patients at different stages, and found that genes exclusive to kidney epithelial cells were down-regulated in ADPKD and that major pathways such as Wnt/β-catenin, pleiotropic growth factors (EGFR) and G-coupled proteins receptors (PTGER2) were increased in the disease (Song et al., 2009). Several other studies have used this "systems biology" approach in different ADPKD models and their results revealed numerous new potential miRNAs or gene targets involved in ADPKD. These targets are genes implicated in various signalling pathways or cellular processes, such as Wnt, JAK/STAT, cell proliferation and differentiation, growth factor signalling and others (Menezes et al., 2012; Chen et al., 2008b; Lee et al., 2004a; Schieren et al., 2006; Dweep et al., 2013; Pandey et al., 2011; Husson et al., 2004).

Table 1.3: Examples of miRNAs suggested to be involved in human kidney diseases

Disorder	miRNA	Up-or down regulation	Reference(s)
Renal cell carcinoma	mir-17 / 21 / 34a / 200c / 215	U / U / D / D / D	The Cancer Genome Atlas Network (2013)
	mir-483	U	Veronese et al. (2010)
	mir-562	D	Drake et al. (2009)
	mir-708	D	Saini et al. (2011)
Lupus nephritis	mir-30 / mir-36	D / U	Dai et al. (2009)
	mir-150	U	Zhou et al. (2013)
IgA nephropathy	mir-146a / 155	U / U	Wang et al. (2011a)
	mir-200c / 141 / 205 / 192	D / U / U / U	Wang et al. (2010c)
	mir-200a / 200b / 429	D / D / D	Wang et al. (2010b)
Diabetic nephropathy	mir-21	U	Zhong et al. (2013), Zhang et al. (2009)
	mir-29a	D	Lin et al. (2014)
	mir-29c	U	Long et al. (2011)
	mir-93	D	Long et al. (2010)
	mir-192	D / U	Krupa et al. (2010), Wang et al. (2010a) / Kato et al. (2007), Chung et al. (2010), Deshpande et al. (2013)
	mir-216	U	Kato et al. (2009)
Kidney fibrosis	mir-21	U	Glowacki et al. (2013), Zhong et al. (2011) Chau et al. (2012)
	mir-29	D	Qin et al. (2011)
	mir-192	D / U	Krupa et al. (2010), Wang et al. (2010a) / Chung et al. (2010), Putta et al. (2012), Deshpande et al. (2013)
	mir-200a / 200b	D	Wang et al. (2011b)
	mir-433	U	Li et al. (2013b)
ADPKD	mir-21	U	Lakhia et al. (2016)
	mir-17∼92	U	Patel et al. (2013), Hajarnis et al. (2017)
	mir-200	U	Patel et al. (2012), Hajarnis et al. (2015)

miRNAs as disease biomarkers and therapeutic treatments Because miRNAs have been reported to intervene in many different pathologies and are detectable and stable in body fluids, they have been studied as biomarkers in order to improve non-invasive diagnosis techniques, get a more accurate prognosis and allow early treatments of the diseases. Next-generation sequencing (NGS) techniques have allowed to generated new miRNAs signatures from patients urine, blood or other fluids.

For example, Wang et al. analysed the miRNAs expression levels in pancreatic juice samples between pancreatic ductal carcinoma patients, chronic pancreatitis patients and healthy volunteers and identified some differentially expressed ones that could be potential markers of the disease (Wang et al., 2014a). Similarly, Roth et al. found that mir-10b, mir-141 and mir-155 were significantly enriched in lung cancer patients' serum compared to healthy controls and that their expression levels were correlated to other markers of the disease such as urokinase plasminogen activator levels or lymph node metastasis, suggesting they could be relevant biomarkers of the disease (Roth et al., 2011). Khalid et al. reported that the expression of mir-21, shown to be increased following kidney injury and fibrosis (Glowacki et al., 2013), in hypothermic machine perfusate, correlated with eGFR values 6 and 12 months after kidney transplantation (Khalid et al., 2016). As hypothermic machine perfusion is an efficient preservation method for kidneys intended to be transplanted, mir-21 could be a biomarker of organ quality in the context of pre-transplant organ assessment (Khalid et al., 2016; Ferraresso and Favi, 2016). Finally, Ben-Dov et al. measured miRNAs expression in sedimented urine and in cell-free ultrafiltration-retained urine (containing exosomes) samples from ADPKD patients and found that mir-1, mir-133, mir-223 and mir-199 were dysregulated in the disease, which was the first step to determine new miRNAs biomarkers for this pathology. More experiments are needed to confirm the potential of these miRNAs to be prognosis biomarkers (Ben-Dov et al., 2014). Exosomes are extracellular vesicles, generated by the endosomal pathway by the exocytosis of multivesicular bodies. They are 50-100 nm in diameter and their density ranges from 1.13 to 1.19 g/mL (Buzas et al., 2014; Livshts et al., 2015), and they contain specific elements such as heat shock proteins, major histocompatibility complex molecules, tetraspannins, cystoskeleton elements such as actin and tubulin, as well as mRNA and miRNAs (Akers et al., 2013; Avci and Balci-Peynircioglu, 2016). They originate from multiple cell types such as epithelial cells (Li and Wang, 2017), neuronal cells (Chivet et al., 2012), reticulocytes (Johnstone et al., 1987), B and T cells (Raposo et al., 1996), macrophages and fibroblasts (Hu et al., 2015), and are present in body fluids such as saliva (Ogawa et al., 2011), blood (Caby et al., 2005), semen (Kelly et al., 1991), amniotic fluid (Keller et al., 2007), cell lines medium (El Andaloussi et al., 2013) and urine (Pisitkun

et al., 2004). The fusion of the plasma membrane of a podocyte or the apical membrane of an epithelial cell with the outer membrane of the multivesicular bodies leads to the release of vesicles (*e.g.* exosomes) from these elements to the urinary space (Gonzales et al., 2010). They are classically isolated from urine by ultra-centrifugation and/or sucrose density gradient and the elements they carry, for example miRNAs and mRNAs, are parallel to what is found in kidney cells and can give information on dysregulated genes and processes in the organ (Gonzales et al., 2010). Optimising exosomes-isolation techniques and quantification or blotting of mRNA and miRNAs extracted from these structures is then an important field of research for the development of miRNAs as disease biomarkers in order to make these techniques less expensive and time-consuming and allow their use in routine clinical practice.

MiRNAs-based therapies are currently being investigated in multiple diseases and several techniques are being developed. These therapies are typically divided between anti-miRs (miRNA inhibitors) and miRNA mimics. They are usually associated with delivery systems designed in order to enhance their stability and the efficacy of their delivery to the targets (Rupaimoole and Slack, 2017). Some of these delivery enhancers are N-acetyl-D-galactosamine conjugation (GalNAc) that mediates the endocytosis of the miRNAs by clathrin (Nair et al., 2014), neutral lipids emulsions (NLE) (Trang et al., 2011), poly-L-lactic acid (PLLA) (Yu et al., 2015), TargomiRs (developed by EnGeneIC) that derive from bacteria and are conjugated with antibodies to specifically target disease sites (Taylor et al., 2015), and chitosan (Ragelle et al., 2013).

The LNA™ (locked nucleic acid, a class of nucleic acid analogues locked into the optimal N-conformation for binding to its complementary mRNA with a higher affinity, see Exiqon website; *http://www.exiqon.com/lna-technology*) miravirsen, developed by Hoffmann LaRoche and Santaris Pharma A/S, was the first miRNA-based therapy to enter a phase II clinical study (Janssen et al., 2013). This antisense RNA oligo inhibits the Dicer and Drosha-mediated processing of the mir-122 precursors by interacting with their stem-loop structure (Gebert et al., 2014), and the results in pre-clinical trials on rodents and non-human primates showed a reduction of HCV mRNA, an efficient delivery to the liver and a reduced accumulation of cholesterol (Elmen et al., 2008a,b).

As no adverse reaction was observed in healthy volunteers of the phase I study, the molecule entered phase II in 2009. The phase IIa study in HCV patients showed a prolonged reduction of HCV RNA, few cases of viral rebound and mostly grade 1 adverse effects (Janssen et al., 2013). Phase IIb trials are currently ongoing to confirm these promising results.

MRX34 is a mimic of mir-34 currently investigated as a treatment in cancer by Mirna Therapeutics. In rodents, MRX34 treatments resulted in a significant reduction of tumours along with an enrichment of mir-34 in these structures (Bader, 2012; Misso et al., 2014). Three patients from the phase I study showed a stabilisation of the disease and a reduction of mir-34 targets in white blood cells. However, as severe immune-related adverse events occurred in several patients, the development of this miRNA mimic was stopped at the phase I stage and the pre-clinical studies protocol will need to be redesigned in order to take immune-related events into consideration (Beg et al., 2017).

The company miRagen is currently undertaking phase I clinical trials for MRG-201 (mir-29 mimic) in patients with scleroderma, and MRG-106 (antimir-55) in patients with cutaneous T-cell lymphoma. The interim report presented in April 2017 reported that MRG-201 treatment is well tolerated by patients and more detailed results are expected soon for both studies (see miRagen website; *http://www.miragen.com/clinical-trials/*).

Another example of miRNA having entered phase I clinical trials is MesomiR-1 a mir-16 mimic developed by EnGeneIC and the Australian Asbestos Disease Research Institute for the treatment of malignant pleural mesothelioma and lung cancer. The first results suggest little adverse events of the treatment in the patients and an improvement of their quality of life parameters (Zandwijk et al., 2015).

Finally, RG-125 (AZD4076) is a molecule resulting from a collaboration between AstraZeneca and Regulus that has been tested in phase I studies since late 2015. This mir-103/107 inhibitor was tested as a treatment in non-alcoholic steatopheatitis (NASH), or fatty liver disease, but AstraZeneca recently announced the end of its clinical development (see Regulus website; *http://regulusrx.com/*).

At present, no miRNA is undergoing clinical studies on patients for the pathogenesis of Chronic Kidney Disease or Autosomal Dominant Polycystic Kidney Disease. A few pre-clinical trials have been undertaken suggesting that some miRNAs-based therapies (anti-miR or miRNA-mimic) could be potential drugs candidates in the future. Currently, the most advanced miRNA candidate for the treatment of ADPKD is an anti-mir-17 that had promising effects on cysts-originating cells and PKD mice and will soon be filed for an Investigational New Drug program by Regulus (Hajarnis et al., 2017 and see Regulus website; *http://regulusrx.com/*).
All the other potentially interesting miRNAs-based therapies in ADPKD (see previously cited miRNAs involved in the pathogenesis of ADPKD) are only in pre-clinical phases and still being characterised in animals before being able to progress to clinical studies.

1.4 Rationale and hypothesis

The kidney, a complex and essential organ, can be affected by various disorders leading to chronic kidney disease (CKD), a condition affecting around 10 % of the population and therefore a major public health issue. Among the pathologies resulting in CKD, Autosomal Dominant Polycystic Kidney Disease (ADPKD) is the most common inherited kidney disorder and its patients manifest severe phenotypes eventually leading to end-stage renal disease (ESRD) and the need for kidney transplantation for half of them.
The conditions for the development of ADPKD are a germline mutation in one or the two *PKD* genes, and a 'second hit' that needs to occur for the patient to manifest symptoms. This second hit is typically thought to be a somatic mutation or insufficient levels of polycystins expressed in the kidney. However, patients carrying the same *PKD1* or *PKD2* mutation will exhibit phenotypes of varying severity, suggesting that sporadic events or third hits are also influencing the patients outcome. These sporadic events can be of genetic (somatic mutation), environmental (kidney injury) or other (miRNAs) nature.
Micro-RNAs are small single-stranded nucleic acids known to regulate genes expression in the cells either by initiating their degradation or repressing their translation. Their biogenesis involves multiple steps mediated by different factors whose dysregulation can result in aberrant miRNAs expression and impairment of genes regulation.

miRNAs have been reported to play major roles in multiple diseases such as vascular pathologies and cancer, and a few of them have recently given promising results as disease biomarkers or potential future treatments.
However, their role in ADPKD is not well known. Only the mir-17∼92 cluster was consistently proven to play a direct role in the pathogenesis of the disease, while a few other miRNAs have been suggested to be relevant but more work needs to be done to fully demonstrate and understand their involvement in the disease. Bioinformatics studies listed many new potential candidates which need to be further validated experimentally.

We surmised that some miRNAs, in particular those we initially identified from a parallel mRNA/miRNA microarray performed on human ADPKD cells, are consistently dysregulated in ADPKD and influence its severity by affecting factors and pathways responsible for the cysts formation and aberrant cell proliferation and apoptosis observed in the disease. Generally, the aims of my project were to characterise new miRNAs involved in ADPKD, to identify targets of these nucleic acids directly influencing the disease phenotype by different approaches and to understand the mechanisms governing their dysregulation in this pathological context.

Chapter 2

Materials and Methods

2.1 Materials and Reagents

All chemicals were purchased from Sigma Aldrich (Saint Louis, USA) unless stated otherwise.

2.1.1 SDS-PAGE gels for Western blotting

Table 2.1: Composition of SDS-Page gels for Western blotting

	Separating gel (x4)			Stacking gel (x4)
Reagent	**7 %**	**12.5 %**	**15 %**	**4 %**
dH_2O	8 mL	6.3 mL	3.8 mL	3050 μL
1.5M Tris-HCl (pH 8.8)	4 mL	4 mL	4 mL	–
0.5M Tris-HCl (pH 6.8)	–	–	–	1250 μL
30 % Acrylamide-Bis Solution 37.5:1 *(BioRad)*	3.7 mL	5.4 mL	7.9 mL	670 μL
10 % SDS	160 μL	160 μL	160 μL	50 μL
10 % APS	160 μL	160 μL	160 μL	50 μL
TEMED *(Thermo Fisher)*	16 μL	16 μL	16 μL	10 μL

2.1.2 Buffers

Table 2.2: Composition of IP buffer used to resuspend proteins for Western blotting

Compound	Concentration
NaCl	150 mM
$NaPO_4$ (pH 7.0)	25 mM
Triton X-100	1 %
NP-40	0.5 %
Protease & Phosphatase Inhibitors Cocktails	1x

Table 2.3: Composition of PBS buffer

Compound	Concentration
NaH_2PO_4	4.6 mM
Na_2HPO_4	16 mM
NaCl	150 mM

Table 2.4: Composition of Tris-Buffered Saline 0.2 % Tween (TBST) buffer

Compound	Concentration
NaCl	136 mM
Tris	20 mM
Tween 20	0.2 % v/v

Table 2.5: Composition of Western blot running buffer

Compound	Concentration
Glycine	190 mM
Tris Base	25 mM
SDS	0.1 % v/v

Table 2.6: Composition of Western blot transfer buffer

Compound	Concentration
Glycine	192 mM
Tris Base	25 mM
Methanol	10 % v/v

Table 2.7: Composition of lysis buffer for genotyping

Compound	Concentration
NaCl	2 mM
EDTA	5 mM
Tris (pH 8.0)	100 mM

Table 2.8: Composition of TAE buffer for agarose gel electrophoresis

Compound	Concentration
Tris Base	40 mM
EDTA (pH 8.0)	1 mM
Glacial Acetic Acid	0.1 % v/v

2.1.3 Antibodies

Table 2.9: List of primary and secondary antibodies used for Western blotting and IHC

Target	Company	Reference	Species	Technique / Dilution
Anoctamin 1	Santa Cruz Biotechnology	9272	Monoclonal Mouse IgG2b	WB = 1/ 500
Calbindin D-28K	Cell Signaling Technology	13176	Monoclonal Rabbit IgG	WB = 1/ 1,000 IHC = 1/ 500
CLIC5A / CLIC5B	Abnova	H00053405-M03	Monoclonal Mouse IgG2a	WB = 1/ 2,000 IHC = 1/ 100
pAkt	Cell Signaling Technology	9271	Polyclonal Rabbit	WB = 1/ 1,000
Total Akt	Cell Signaling Technology	9272	Polyclonal Rabbit	WB = 1/ 2,000
pERK	Cell Signaling Technology	9101	Polyclonal Rabbit	WB = 1/ 2,000
Total ERK	Cell Signaling Technology	9102	Polyclonal Rabbit	WB = 1/ 2,000
PI3K-p85α	Sigma-Aldrich	HPA001216	Polyclonal Rabbit	WB = 1/ 2,000
PI3K-p110α	Cell Signaling Technology	4249	Monoclonal Rabbit IgG	WB = 1/ 1,000
TRBP	Proteintech	15753-1-AP	Monoclonal Rabbit IgG	WB = 1/ 500
β-actin	Abcam	ab6276	Monoclonal Mouse IgG1	WB = 1/ 15,000
Calnexin	Sigma-Aldrich	C4731	Polyclonal Rabbit	WB = 1/ 2,000
Mouse	Dako	P0447	Polyclonal Goat - HRP	WB = 1/ 5,000
Rabbit	Dako	P0448	Polyclonal Goat - HRP	WB = 1/ 5,000
Mouse	Vector Labs	MP-7402	Polyclonal Horse - HRP	IHC = Kit conc.
Rabbit	Vector Labs	MP-7401	Polyclonal Horse - HRP	IHC = Kit conc.

2.1.4 Plasmids

Table 2.10: List of plasmids generated for this project - native sequences
The positions numbers refer to the first and last bases cloned from the original 3'UTR sequence

Plasmid backbone	Insert	Position	Insert length	Cloning sites
pmirGLO vector	ANO1 3'UTR	1061-1504	443 bp	XbaI
pmirGLO vector	CALB1 3'UTR	128-472	344 bp	XbaI
pmirGLO vector	CELF2 3'UTR	4380-4874	494 bp	XbaI
pmirGLO vector	CLIC5 3'UTR	882-1312	924 bp	XbaI
pmirGLO vector	ERBB4 3'UTR	29-433	404 bp	SacI/XbaI
pmirGLO vector	IGFBP5 3'UTR	1769-2050	281 bp	XbaI
pmirGLO vector	IL1RAP 3'UTR	1002-1452	450 bp	SacI/XbaI
pmirGLO vector	PIK3R1 3'UTR	864-1305	441 bp	XbaI
pmirGLO vector	PKP2 3'UTR	542-957	416 bp	SacI/XbaI
pmirGLO vector	SYT1 3'UTR	21-457	436 bp	XbaI

Table 2.11: List of plasmids generated for this project - mutant sequences

Plasmid backbone	Mutated bases
pmirGLO-ANO1 3'UTR	$_{1402}$GT>CA
pmirGLO-CALB1 3'UTR	$_{221}$GGTC>CCAG
pmirGLO-CELF2 3'UTR	$_{4681}$CTGT>GACA
pmirGLO-CLIC5 3'UTR	$_{1131}$GA- - - -ACTG>CT- - - -TGAC
pmirGLO-ERBB4 3'UTR	$_{94}$CAG>GTC
pmirGLO-IGFBP5 3'UTR	$_{1944}$GCCA>CGGT
pmirGLO-IL1RAP 3'UTR	$_{1045}$ACTG>TGAC
pmirGLO-PIK3R1 3'UTR	$_{967}$CCAG>GGTC
pmirGLO-PKP2 3'UTR	$_{612}$CTGT>GACA
pmirGLO-SYT1 3'UTR	$_{2320}$CTGT>GACA

SV40 late poly(A) signal	106–327
SV40 early enhancer/promotor	426–844
hRluc-neo fusion protein coding region	889–2664
Synthetic polyadenylation signal	2728–2776
β-lactamase (Amp^r) coding region	3037–3897
Co/E1-derived plasmid origin of replication	4052–4088
Human phosphoglycerate kinase promoter	5094–5609
luc2 reporter gene	5645–7297
Multiple cloning site (MCS, Figure 1)	7306–7350

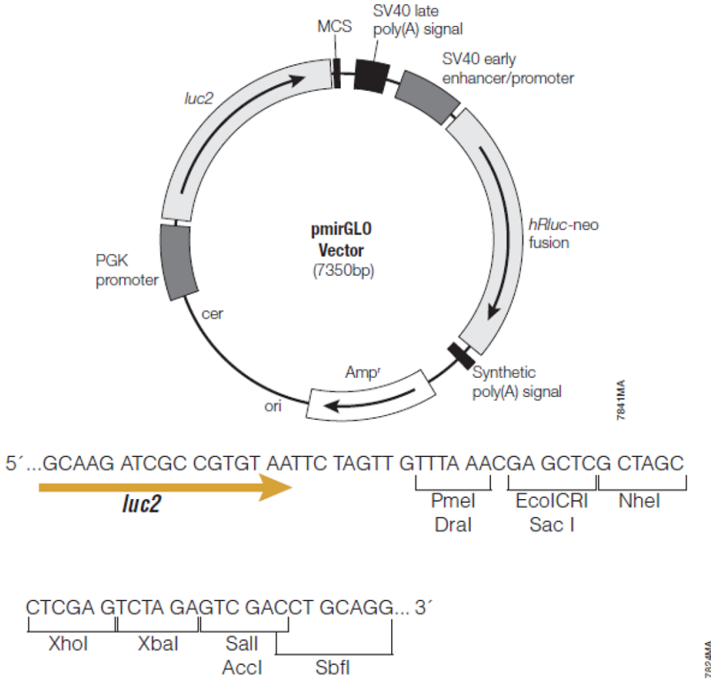

Figure 2.1: **Map of the pmirGLO vector used as a backbone for cloning and for the dual-reporter luciferase assays**

2.1.5 Primers

The coding sequences of the genes were taken from the NCBI database *(https://www.ncbi.nlm.nih.gov/gene/)* and the 3'UTR sequences from the USCS Genome Browser database *(http://genome.ucsc.edu/)*. The following primers were designed using the *Primer3* online tool *(http://bioinfo.ut.ee/primer3/)*, and then processed through the *PrimerBlast* software *(https://www.ncbi.nlm.nih.gov/tools/primer-blast/)* to get more confidence about their specificity. They were then ordered from MWG Operon and resuspended in Tris-EDTA buffer (TE = Tris 10 mM, EDTA 1 mM, pH 8.0).

Table 2.12: List of primers designed for PCR and cloning

Name	Sequence (5'⟶3')
ANO1 3'UTR F	TAGCCTCGAGTCTAGACAGGAATGTCACTGTTGGACA
ANO1 3'UTR R	GCAGGTCGACTCTAGAAATGTCCAGCCACAGTCCTC
CALB1 3'UTR F	TAGCCTCGAGTCTAGATGTGGCTCATTCTTTTCAGCT
CALB1 3'UTR R	GCAGGTCGACTCTAGATGGAAAAGCACATTCCTCCT
CELF2 3'UTR F	TAGCCTCGAGTCTAGACCTCAAAGGCGTAACGAGTT
CELF2 3'UTR R	GCAGGTCGACTCTAGACACCAGAGCAAGCCACAAAA
CLIC5 3'UTR F	TAGCCTCGAGTCTAGAAAAGTGGATGGGAGTGGGAG
CLIC5 3'UTR R	GCAGGTCGACTCTAGATTCACCTGGCAGTTGAGTCA
ERBB4 3'UTR F	GGTCGTGAGCTCCACACCTGCTCCAATTTCCCC
ERBB4 3'UTR R	CTCGTATCTAGAATGCACACATCAGTTCCTGC
IGFBP5 3'UTR F	TAGCCTCGAGTCTAGAGCCAGGGAAGGTGAGTAACT
IGFBP5 3'UTR R	GCAGGTCGACTCTAGAGAGTTTCGGAATCTGGCTGC
IL1RAP 3'UTR F	GGTCGTGAGCTCGCCTTGAGAGTTGCTTTTGG
IL1RAP 3'UTR R	CTCGTATCTAGATGGACAAGAGTTCCAGTGGTT
PIK3R1 3' UTR F	TAGCCTCGAGTCTAGAGCTTCCCCACCCCAGTTTT
PIK3R1 3'UTR R	GCAGGTCGACTCTAGACACCCCACTTGATACATCCCT
PKP2 3'UTR F	GGTCGTGAGCTCATCCCCTTGGGTTGTTTTTC
PKP2 3'UTR R	CTCGTATCTAGACCAGGCAGTCTGAGAGAAGG
SRY F	AGAGTGAAGCGACCCATGAA
SRY R	TGTTGTCCAGTTGCACTTCG
SYT1 3'UTR F	TAGCCTCGAGTCTAGACATTTGCCCATATAGTGCTC
SYT1 3'UTR R	GCAGGTCGACTCTAGAGCTGGAATGCAGACGATAC

Table 2.13: List of primers designed for site-directed mutagenesis

Name	Sequence
ANO1 Mut F	GTTTTGTATATAAATAGACAATTAAAAATTAGGC
ANO1 Mut R	GCCTAATTTTTAATTGTCTATTTATATACAAAAC
CALB1 Mut F	AAGAAGAAAGTCTATGCTTAGGGGTCTCAGTACACCCAATTTTAAAA
CALB1 Mut R	TTTTAAAATTGGGTGTACTGAGACCCCTAAGCATAGACTTTCTTCTT
CLIC5 Mut F	TCCAGCAGCTGCTCCTGCCTCTTTCATGACTAGCCTGTAATGGGTAAAAG
CLIC5 Mut R	CTTTTACCCATTACAGGCTAGTCATGAAAGAGGCAGGAGCAGCTGCTGGA
ERBB4 Mut F	CTTCCTTCTACCCCAAGGCGTCTCGTTTTGACACTTCCCAG
ERBB4 Mut R	CTGGGAAGTGTCAAAACGAGACGCCTTGGGGTAGAAGGAAG
IGFBP5 Mut F	CTTCCTCCATTCTGCGGTGTCCCTGCATCCTCC
IGFBP5 Mut R	GGAGGATGCAGGGACACCGCAGAATGGAGGAAG
IL1RAP 2 bases Mut F	ATTAATATTCTAAGAGAATTAACACTATTTCCTGTCACCTATTCACT
IL1RAP 2 bases Mut R	AGTGAATAGGTGACAGGAAATACACATAATTCTCTTAGAATATTAAT
IL1RAP 4 bases Mut F	ATTAATATTCTAAGAGAATTATGACTATTTCCTGTCACCTATTCACT
IL1RAP 4 bases Mut R	AGTGAATAGGTGACAGGAAATAGTCATAATTCTCTTAGAATATTAAT
PIK3R1 Mut F	TAAAAGTAAATGTACAGGATGGGTCTAAAAAAAAAAAATGGCTTCA
PIK3R1 Mut R	TGAAGCCATTTTTTTTTTTTAGACCCATCCTGTACATTTACTTTTA
PKP2 2 bases Mut F	TTAGATTACAGAGTATGCATGAGAGTAAGAAAAAGAAATTGAGAGGAA
PKP2 2 bases Mut R	TTCCTCTCAATTTCTTTTTCTTACTCTCATGCATACTCTGTAATCTAA
PKP2 4 bases Mut F	TTAGATTACAGAGTATGCATGAGACAAAGAAAAAGAAATTGAGAGGAA
PKP2 4 bases Mut R	TTCCTCTCAATTTCTTTTTCTTTGTCTCATGCATACTCTGTAATCTAA
SYT1 Mut F	CACAAATGACATTTAATTTCAGACAATTCAGCTTTAAGTTGTTCAC
SYT1 Mut R	GTGAACAACTTAAAGCTGAATTGTCTGAAATTAAATGTCATTTGTG

Table 2.14: List of primers designed for qPCR of human genes

Name	Forward Primer (5'⟶3')	Reverse Primer (5'⟶3')
AGO1	TGACAACCGTTTCACAGCAG	GAAGTACATGGTGCGCAGAG
AGO2	AGATCAACGTCAAGCTGGGA	CGCGTGGACTTGTAGAACTG
AGO3	ACCAGTGTATGCGGAAGTGA	GGCTTCTTTCCATCACCAGC
AGO4	CAGGGGATGGGAAGAAACCT	GGGTTTGAAGCGTGTGGATT
ANO1	ACGAGGAGTGTGTGAAGAGG	TGCATGGTCCCGTTCTTACT
AQP1	TTCCGTGCCCTCATGTACAT	CACCATCAGCCAGGTCATTG
AQP2	TTTGGCTTGGGTATTGGCAC	CTGAGAGCATTGACAGCCAG
AR	CCCACTTGTGTCAAAAGCGA	AATGGGCAAAACATGGTCCC
CALB1	TCATCCCTCATCACAGCCTC	CGGAAGAGCAGCAGGAAATT
CCNA1	GGGCTGGGGAGAAGAGTATC	GGAAGGCATTTTCTGATCCA
CDK1	TGGAGAAGGTACCTATGGAGTTG	GAAGAATCCATGTACTGACCA
CDKN1A	CCCAAGCTCTACCTTCCCAC	AGGCACAAGGGTACAAGACA
CELF2	GTCATGGTCGGAAAAGGAGC	CCACAGCGTTGGACTTTTCA
CLIC5	TCGGCAACTGTCCTTTCTCT	GAGCCTTGGTTAGGCCTCTT
CLIC5A	CAGGGACCCCGAGATCGA	TTTCAGGGGTCAAGGTCTCC
CLIC5B	GCCACTCAGCTGAATACCCA	GGCCTTACTGTGCTGAATGG
CMYC	AACACACAACGTCTTGGAGC	GCACAAGAGTTCCGTAGCTG
DICER1	TGGTCCACGAGTCACAATCA	CAGCCAATCGTACACAGCTC
DMD	AAGTGGAAATGTTGCCAAGG	GCAATGTGTCCTCAGCAGAA
DOCK4	AACAACTGGGACTGGACCTG	CCACAAAGAGGGAGCAATGT
ENPP4	ATCATGGGATGACCCAGTGT	AGCCTTTGTGAAATGCAGGT
ERBB4	GTACTTGGTCCCTCAGGCTT	TGGGTGCTACTGTCCTCTTG
ESR1	CAAGCCCGCTCATGATCAAA	TCAAATCCACAAAGCCTGGC
ESR2	TTAGTGGTCCATCGCCAGTT	TCCTTCACACGACCAGACTC
FLI1	AGGGGCACAAACGATCAGTA	GCCGTGCACTTTGGTCATAA
FOXO1	GCAGCCAGGCATCTCATAAC	CCATGTCACAGTCTAAGCGC
FRAS1	GCCGTTGCCATGGTGATATT	TCCTCCCCATCCTGAAACAC
FSTL1	AAGTGCCTCAACCCATCT	TGCTCACTCTCTTGGTCT
GAPDH	CCATCTTCCAGGAGCGAGAT	TGCTGATGATCTTGAGGCTG
GREM2	CACGTGAAGAAGGAGGAGGA	TTCTTGAGTCGGAAGGGTGG
ID4	AGTGCGATATGAACGACTGCT	CACAGAATGCTGTCGCCCT

Name	Forward Primer (5'⟶3')	Reverse Primer (5'⟶3')
IGFBP5	AGTGAAGAAGGACCGCAGAA	TCCTTTGCGGTCACAATTGG
IL1RAP	CTGTGCATCTTTGACCGAGA	ACCTGCCCTGTGGATACTTG
ITGB8	GGGCCAAGGTGAAGACAATA	TGTGCATTGATGCTGAGACA
JPH1	GTCCGAATCCAAGTCTTCCA	AGCCATATCCATGCCTCTTG
KIF22	CTGGGCAAAGTGGTAGATGC	CTCTCTTTGCCTCTGGTGGA
KRT19	CTTTGTGTCCTCGTCCTCCT	GTCGCGGATCTTCACCTCTA
LCN2	CAGGGGAAGTGGTATGTGGT	AGTCAGCTCCTTGGTTCTCC
MCM5	CAATCCACGAAGCCATGGAG	AGATGGTGGGCATGAAGTCA
MCM6	GTTTCAGAGCAGCGATGGAG	GCAGGTCTTGGAATGCAACA
MCM7	CATGCCTCTGATCATGTGCC	AGCACCGTGATACTACGAGG
MCPIP1	CCACCTCGAGAGTACTGGTC	GGAAACACACCACACAGCTT
MFI2	CCCAAGAACTACCCCTCCTC	GTGGTCGTCTCCAAACAGGT
MYCN	CCAAGGCTGTCACCACATTC	TCCTCCGAGTCAGAGTTTCG
MYO10	TCAAGCCAAACATGCAGAAG	CGTGCTAAGAAGCCCAAGAC
NPR3	ATGGAGATGGCTCATGGAAG	CGGCGATACCTTCAAATGTT
PIK3CA	GGAGCCCAAGAATGCACAAA	TTTGTTGTCCAGCCACCATG
PIK3CB	AGCTGGTTTGGATCTTCGGA	CAGGTCATCCCCAGAGTTGT
PIK3CD	GAGAAGGACCTGGTGTGGAA	GCTCATCGTCCGTCAGTTTC
PIK3R1	ATATACCCGCACATCCCAGG	TTTCATTGCCCAACCACTCG
PIK3R2	GGGGACATTTCAAGGGAGGA	CAGAAGTGAGTGGCTCTGA
PIK3R3	AGCCACCTAAGCCAATGACT	AAGAAGGTCCCATCTGGCAT
PKP2	ATCTTCACCGAACCAGCAGT	GGCTTCTCTGGCTGTACTGG
PLAU	TGAGGTGGAAAACCTCATCC	CACAGCATTTTGGTGGTGAC
PODXL	GGCGCTTCGGATGAGAAATT	ACCCCTGCCTCCTTTAGTTC
POLE	GCTGTGTGTGTGTGGTCAAT	TTCCAGGTAGCTGAACTGGG
PTGER2	GCTTTCGCCATGACCTTCTT	CCGAGACAATGAGAAGCAGC
PTGIS	GTATCCTTTGGCAAGCGGAG	AGCCGTTTCCCATCCTTGTA
RGCC	GCCACTTCCACTACGAGGAG	TTTTGTCAAGATCAGCAATGAA
RPS6KA2	ATCAAGCCACCGTTCAAACC	ACTCGGTGTCTGTGGCTTTA
SHROOM3	ACCCTGTCATCTTTCCCCTG	TAGCCCTGACCATTTGCTGA
SLC12A3	ACAGAGTCAAGTCCTTCGG	GTGAGCACGTTTTCCTGGTT

Name	Forward Primer (5'⟶3')	Reverse Primer (5'⟶3')
SLC22A10	CAGGTTTGGGCGAAGATTTA	AAAGGTACAGACGCCACCAC
SLCO2A1	TCTATCTTCCACCCGGTCTG	AGGAGTGGTCAATGGTGAGG
SOX5	CAATTTGCTCCAGCAACAGA	GCTTCCCTCCTGGAGATACC
SPOCK2	GTTGTACTGGGTGGGTCGG	CCGGCAATTTCATGGAGGAC
SSPN	CCACTATTCGCAGCTCACAC	TGAGGGAGCATATCCTGACA
SYK	AAAGTTCCTGATCCGAGCCA	GCAAGTTCTGGCTCATACGG
SYT1	TCTGCTTCTCCCTTCGCTAC	TACCACCACCTGCACTTTCT
TARBP2	CCAGAATAGGGAAGACGCCT	CTTTGAGGTGTTTGAGGGCC
TES	TGGCTGTGACGAGCTGATAT	CTTCTGGGTCGATGGCATTG
UMOD	AGACGAGGACTGCAAATCGA	TTGTCGAAGCCCAGACTCTT
Pre-mir-582	CTGTGCTCTTTGATTACAGTTGT	TGTTTCTACTTTGCACCCTTTG

Table 2.15: List of primers designed for qPCR of mouse genes

Name	Forward Primer (5'⟶3')	Reverse Primer (5'⟶3')
β-Actin Mouse	TGTTACCAACTGGGACGACA	TCTCAGCTGTGGTGGTGAAG
Ano1 Mouse	AGACCACAAAGAGGCTCTCC	TCCGTAACTTGCCCATTCCT
Calb1 Mouse	ATGCCAGCAACTGAAGTCCT	AGCAAAGCATCCAGCTCATT
Ccna1 Mouse	CCTGGCATTTGATCTGACCG	TGCAGGGGAAGAACTACAGG
Celf2 Mouse	CAGGCTTGACGAATGGTACG	CCGTTCATAGCCTGGATTGC
Clic5 Mouse	GCAAAACACCGGGAATCTAA	CCACAATCTTGACCACATGC
Fstl1 Mouse	GACGCCCTCATTGAACTGTC	TTGGTCTTTTCTGCTGTGCC
Igfbp5 Mouse	CGAGATGGCTGAAGAGACCT	GCCTTGTTCGGATTCCTGTC
Kif22 Mouse	TTCTCTGACTTCGAGCAGCA	TGCCCAGTACAAAGAGGGAG
Krt19 Mouse	ATTGAGGAGCTGAACACCCA	ATCTGTGACAGCTGGACTCC
Pik3r1 Mouse	ACCTGGACTTAGAGTGTGCC	GAGTGTAATCGCCGTGCATT
Plau Mouse	AACCCTACAATGCCCACAGA	TTCTGGTAGATGGCTGCGAA
Rps6ka2 Mouse	TGGATGAGTCTGGAAACCCC	GCCGATCCTAGCCAGAATCT
Shroom3 Mouse	CACAGTGCAGACTCCAGGTA	GCTTTTGGATCGTCGAGGTC
Slco2a1 Mouse	TGCTTTGTCATGGCCTCCTA	AGAGGTCGGTCTGAAAGTGG
Syt1 Mouse	CTTCTCCAAGCACGACATCA	CTCGAACGGAACTTCAAAGC

The following primers were not generated by myself but ordered from Thermo Fisher for TaqMan qPCR assays or Qiagen (Hilden, Germany) for SYBR Green pre-miRNA assays:

Table 2.16: List of primers purchased for TaqMan assays and SYBR Green pre-miRNA assays

Name	Supplier	Reference
U6 snRNA	Thermo Fisher	1006
Rnu 48	Thermo Fisher	1973
mmu-mir-193b	Thermo Fisher	2467
hsa-mir-193b	Thermo Fisher	2367
hsa-mir-193b*	Thermo Fisher	2366
mmu-mir-582-5p	Thermo Fisher	471065_mat
hsa-mir-582-5p	Thermo Fisher	1983
hsa-mir-582-3p	Thermo Fisher	2399
mmu-pri-mir-193b	Thermo Fisher	Mm03308440_pri
mmu-pri-mir-582	Thermo Fisher	Mm03308696_pri
hsa-pri-mir-582	Thermo Fisher	Hs03303897_pri
hsa-pri-mir-193b	Thermo Fisher	Hs03304420_pri
mmu-pre-mir-193b	Qiagen	MP00004704
mmu-pre-mir-582	Qiagen	MP00006195
hsa-pre-mir-193b	Qiagen	MP00001253

2.2 Preliminary work: constitution of a new database

The work presented in this section was performed by Dr Andrew Streets before the start of the present PhD project and served as the basis for this thesis.

2 normal (UCL93 and RFH) and 4 cystic (Ox161c1, SKI001, Ox938, SKI002) cell lines were previously established in our laboratory by immortalisation of healthy or cystic human kidneys cells (Streets et al., 2013; Parker et al., 2007). The cells were plated on 10 cm^2 Petri dishes and cultured in DMEM F-12 (Gibco, Carlsbad, USA) + 5 % Nu serum (Corning, Corning, USA) + 1 % L-Glutamine (Lonza, Basel, Switzerland) + 1 % Penicillin/Streptomycin (Lonza) at 33 °C, 5 % CO_2. When they reached around 70 % confluence, the cells were synchronised by serum-starvation for 24 hours followed by a 24-hours long

new incubation in serum-containing medium. Trizol reagent (Ambion, Carlsbad, USA) was used to extract the RNA following the manufacturer's instructions. One-Colour Agilent microarrays (Agilent, Santa Clara, USA) were performed at the Sheffield Institute for Translational Neuroscience (SiTRAN) to assess miRNA and mRNA expression and the data was analysed through GeneSpring GX software (Agilent). (semi-quantitative) real-time TaqMan qPCR (see general (sq) RT-PCR method below) was performed three times on three different RNA extractions to confirm the deregulation of the Top 5 miRNAs (Mir-582-5p, mir-335-5p, mir-660-5p, mir-181a-2-3p, mir-193b-3p). From these 5 miRNAs, mir-193b-3p was significantly down-regulated by 0.5-fold and mir-582-5p by 0.8-fold compared to normal. To determine a list of deregulated genes that could be potential targets of these two miRNAs, our miRNA and mRNA microarrays datasets were matched using the 'Protein Analysis Through Evolutionary Relationships' (PANTHER) classification system (available at www.pantherdb.org). 14 and 19 potential target genes were found up-regulated by at least 4-fold for mir-193b-3p and mir-582-5p, respectively.

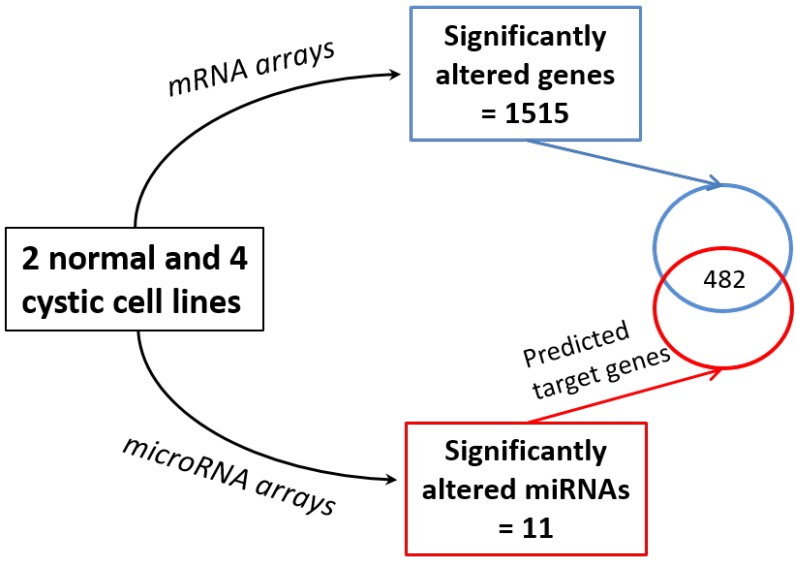

Figure 2.2: **Parallel mRNA/miRNA diagram.**
Diagram of the parallel mRNA/miRNA microarray. *Published in Streets et al., 2017.*

2.3 Selections of targets using bioinformatics analyses and comparisons of datasets

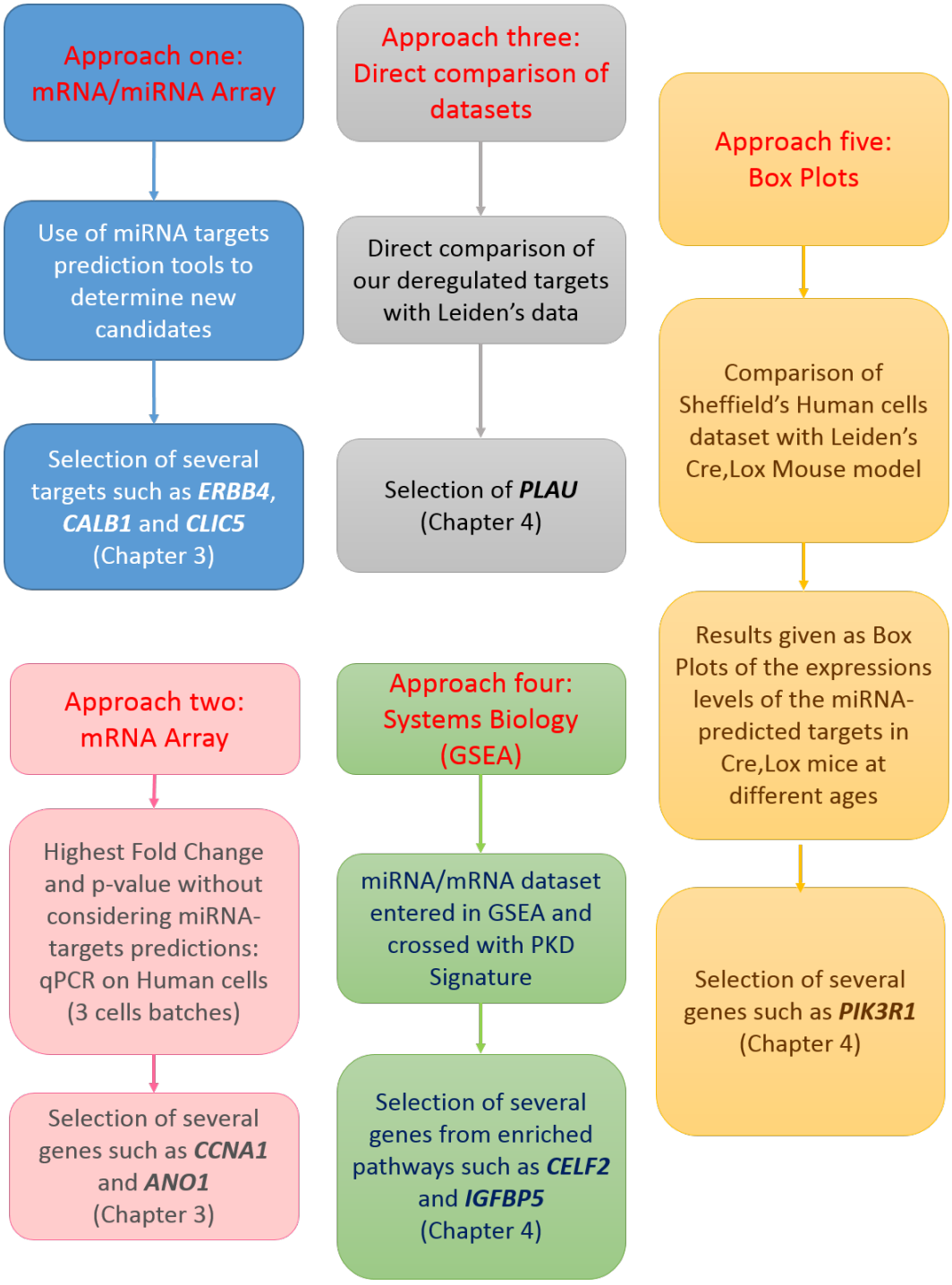

Figure 2.3: **Different methods used in this project to select interesting candidates**

As shown in Figure 2.3, I used several methods to select new targets based on bioinformatics and systems biology approaches.

The first approach presented in the first part of chapter 3 consisted in analysing our parallel mRNA/miRNA dataset using the PANTHER classification system and classifying the targets by biological processes. From this, the most relevant targets were selected and their deregulation was measured by (sq) RT-PCR in one batch of three normal and four cystic human cells. The genes found up-regulated in the cystic cells were validated in a second independent batch and the confirmed candidates were selected for further studies.

The second approach (shown in the second part of chapter 3) consisted in focusing only on the results of our mRNA microarray without taking the miRNA dataset into consideration. The dataset elements were ranked by highest fold change and highest significance and the most relevant targets were select based on their expression levels in the kidney and on what was known of their function from the literature. The selected targets' deregulation was then assessed by (sq) RT-PCR on several independent batches of cells, and the ones that were confirmed were kept for further experiments.

Chapter 4 regroups the results from the selection methods three, four and five. These have in common a collaboration with Dorien Peter's and Peter-Bram 't Hoen's teams in Leiden University Medical Center (LUMC, Netherlands), meaning they use different ways of comparing our dataset with their own dataset generated from *Pkd1*-conditional Cre,Lox mice at different ages and using their 'PKD Signature' algorithm.

Method three consisted in directly comparing the deregulated candidates that were also predicted targets for our two miRNAs from our dataset with the Leiden group's preliminary dataset as well as three other datasets using mouse (Menezes et al., 2012), rat (O' Meara et al., 2012) and human (Song et al., 2009) models and validate their deregulation by (sq) RT-qPCR. This preliminary dataset was obtained previously to the high-throughput RNA-seq dataset they generated in order to define their 'PKD Signature'.

The fourth approach was based on a functional enrichment analysis using Gene Set Enrichment Analysis (GSEA) (Subramanian et al., 2005) and the Leiden group's 'PKD Signature'. The Molecular Signatures Database (MSigDB) (Liberzon et al., 2011) is a tool that uses the GSEA to classify elements from a dataset and identify enriched pathways, oncogenic signatures, biological processes for example, compared to another condition (here we compared ADPKD and normal condition). Figure 2.4 summarises the different steps undertaken for this analysis. First of all, I entered either the list of all deregulated genes from our dataset, the list of all predicted targets for mir-193b-3p or mir-582-5p or the list for all predicted targets actually found deregulated in our dataset, in the GSEA MSigDB algorithm and queried for the 100 most enriched canonical pathways, biological processes and hallmark gene sets. We sent this list ranked by p-value to Leiden who after ranking the same elements by k/K ratio (enrichment) selected the top 20 of each and entered them in their 'PKD Signature'. The 'PKD Signature' was generated through a meta-analysis of PKD expression profiles from the Leiden group's own dataset and previously published datasets and contains 1,515 genes (see Malas et al., 2017). From this step was obtained a list of the most significantly enriched pathways, biological processes and hallmark gene sets as well as the deregulated genes in each of these categories found in at least one of the datasets (not necessarily ours). Finally, the most interesting candidates were selected based on literature information and potential connection to ADPKD, and their deregulation in the disease was validated through further experiments.

The fifth and final approach described in chapter 4 is based on a direct comparison with the Leiden group's dataset, again, but this time using box plots presenting the expression levels of the genes from our dataset measured in their inducible *Pkd1* deletion model at different time points. This gave a visual indication of the evolution of our candidates' expression over time in this ADPKD mouse model, hence suggesting that they were deregulated in at least two models of the disease. The ones with increasing expression over time and a potentially relevant role in ADPKD were selected, and (sq) RT-PCR were performed to validate their deregulation in our models.

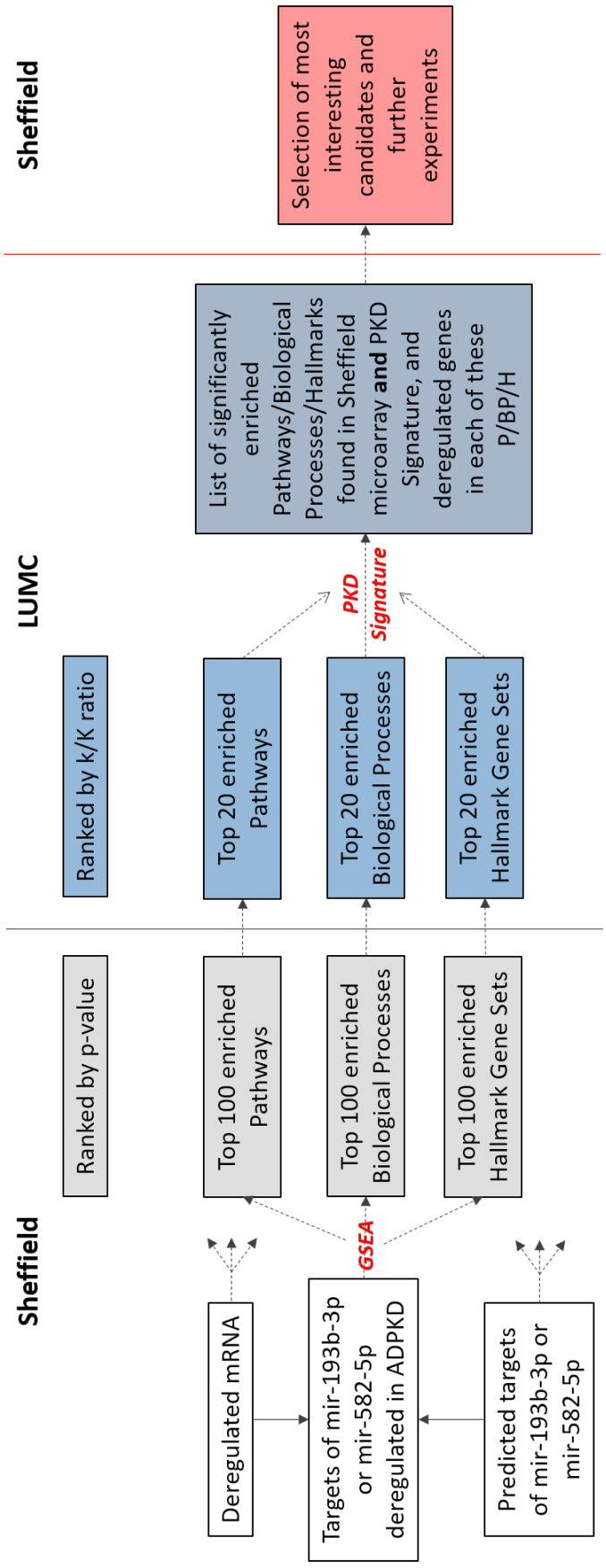

Figure 2.4: **Summary of the Gene Set Enrichment Analysis (GSEA) performed in collaboration with our partners in Leiden**

This list of bioinformatics analysis methods is not comprehensive and only presents the approaches that gave me interesting candidates to study further.

2.4 Mouse models

The *Pkd1*^{nl,nl} (NeoLox model) mice and tam-*KspCad*-Cre;*Pkd1*$^{\text{del2-11,lox}}$ (CreLox model) mice were bred as previously described (Lantinga-van Leeuwen et al., 2004, 2007; Malas et al., 2017). NeoLox mice at 2, 4 or 10 weeks of age were culled and weighed and their kidneys were then extracted, weighed and snap-frozen in liquid nitrogen. Ear clips were taken from the animals in order to determine their genotype.

2.5 Cell lines

Several murine and human cell lines were used in this project. Mouse F1 cells (F1/WT and F1/Cre) were generated by Lee et al. (2015) out of cells extracted from collecting ducts of wild-type or *Pkd1*$^{fl/fl}$ double KO mice. Mouse Embryonic Kidney cells (MEK$^{+/+}$ WT and MEK$^{-/-}$ Null) were generated by Nauli et al. (2003) and issued from collecting ducts of *Pkd1*$^{del34/del34}$ or wild-type E15.5 embryos, expressing a truncated PC-1 protein lacking most of its C-terminus. The human cell lines UCL93c3 and RFH (non cystic) and Ox161(c1), SKI001, Ox938 and SKI002 (cystic) were generated by immortalisation of epithelial tubular cells isolated from patients kidneys (normal or ADPKD) removed for clinical indications (described in Parker et al., 2007). The cystic cell lines all express a truncated version of PC-1 (see Table 2.17). CL5, CL8 and CL11 (normal) were issued from proximal tubules from a single patient and immortalised in Dr Racusen's laboratory (John Hopkins University, Baltimore, USA). Cells were not cultured beyond passage 30 except for the CL5, CL8, CL11 that were given as frozen vials of cells at passage 50. A "batch" of cells in the present thesis is defined as: all the cell lines were thawed at the same time, passaged the same number of times before being plated and synchronised and their RNA extracted, which implies they were cultured in the exact same conditions and any variability observed would not be due to a difference in incubation time or number of passages since thawing.

Table 2.17: List of germline and somatic mutation of the human ADPKD cell lines used in this project

Cell line	Type of mutation	Mutation
Ox161	Germline	4609G>T
Ox161c1	Somatic	12335_12350delCCTTGCGTGGAGAGCT
SKI001	Germline	IVS43-2A>G
	Somatic	3364delG
	Somatic	6549_6550insT
Ox938	Germline	7000_7001insGCTGGCG
SKI002	Germline	IVS25-3C>G
	Somatic	2312_2324delTGCTTGCAGCCAC

2.6 Cell culture

HEK293, CL5, CL8, CL11 (human) and F1/WT, F1/Cre (mouse) cells were cultured at 37 °C, 5 % CO_2 in DMEM F-12 + 10 % FBS + 1 % Penicillin-Streptomycin + 1 % L-Glutamine. RFH, UCL93, Ox161c1, SKI001, Ox938 and SKI002 cells were cultured at 33 °C, 5 % CO_2 in DMEM F-12 + 5 % Nu serum + 1 % L-Glutamine + 1 % P/S. MEK WT and $MEK^{-/-}$ Null (mouse) were cultured at 33 °C, 5 % CO_2 in DMEM F-12 + 5 % FBS + 1 % Penicillin-Streptomycin + 1 % L-Glutamine + 1 % Insulin-Transferrin-Selenite (Gibco) + 0.0004 % Hydro-Cortisone + 0.15 % Triiodothyronine. Passages were performed using 0.05 % Trypsin-EDTA (Gibco) after washings with PBS.

2.7 RNA extraction from mouse kidney and cultured cells

¼ of mouse kidney was cut and lysed in 500 μL of Trizol reagent using a BeadBug homogeniser and 0.3 mm zirconium beads-filled tubes. The lysate was then transferred to 1.5 mL eppendorf tubes and 200 μL of Trizol was added and mixed. The miRNAs were then extracted using the miRNEasy extraction kit from Qiagen and following the manufacturers instructions. RNA was extracted from the tissue lysates or the cells using a direct Trizol extraction according to the manufacturer's instructions. After a treatment with DNase (Thermo Fisher, Waltham, USA) in order to remove the genomic DNA residues, the RNA was either retro-transcribed into cDNA or stored at -80 °C for a few weeks.

2.8 RNA retrotranscription to cDNA and semi-quantitative real-time PCR

2.8.1 Genes and primary miRNAs

The high capacity RNA-to-cDNA kit (Applied Biosystems, Carlsbad, USA) was used to retro-transcribe typically 2 μg or 4 μg of RNA. The synthesized cDNA was diluted 1/20 in ddH_2O.

Table 2.18: Cycle for retro-transcription of RNA for genes and primary miRNAs

Temperature	Time
37 °C	60 min
95 °C	5 min
4 °C	∞

Genes The real-time PCR primers were designed for each gene using their coding sequence and the Primer3 software (see Tables 2.14 and 2.15 above), and ordered from MWG Operon. For one reaction, 3.5 μL of ddH_2O, 7.5 μL of SYBR Green PCR master mix (Thermo Fisher) and 1 μL of primers at 5 μM were mixed. These 12 μL of mix were added to 3 μL of diluted cDNA and loaded in a 384 well plate.

Primary miRNAs The TaqMan pri-miRNA assay primers were ordered from Thermo Fisher (see Tables 2.16 above). For one reaction, the mix was composed of: 1 μL 20x primers, 10 μL TaqMan qPCR master mix No Amp UNG (Thermo Fisher) and 5 μL ddH_2O. The 16 μL of this mix were added to 4 μL of diluted cDNA and loaded into a 384-well plate.

2.8.2 Precursor miRNAs

The precursor miRNAs were retro-transcribed using miScriptII RT kit from Qiagen. 500 ng of RNA were mixed with ddH_2O to get a total volume of 12.5 μL. These 12.5 μL were added to a mix composed of 4 μL of 5x miScript HiFlex buffer, 2 μL of 10x miScript nucleic mix, 1 μL miScript RT enzyme and ddH_2O qs 20 μL. Table 2.19 describes the cycle used in the thermocycler.

Table 2.19: Cycle for retro-transcription of RNA for precursor miRNAs

Temperature	Time
37 °C	60 min
95 °C	5 min
4 °C	∞

The 10x primers for human and mouse pre-mir-193b and mouse pre-mir-582 were purchased from Qiagen. The primers for human pre-mir-582 were designed based on the sequence given by mirBase and the Primer3 software and ordered from MWG Operon. The real-time PCR mix for one reaction was composed of: 5 μL of SYBR Green PCR master mix, 1 μL of 10x primers or 1 μL of forward and reverse primers at 5 μM, and 2 μL of ddH_2O. 1 μL of the previously retro-transcribed RNA was added to this mix in a 384-well plate.

2.8.3 Mature miRNAs

TaqMan miRNA assay primers were purchased from Thermo Fisher. The mature miRNAs were retro-transcribed specifically using this assay's 5x RT primers.
For one reaction 250 ng of RNA, or 5 μL in ddH_2O, were added to 7 μL of mix made of: 0.15 μL of dNTP mix, 1 μL of MultiScribe RT enzyme, 1.5 μL of 10x RT buffer, 0.19 μL of RNase inhibitor and 4.16 μL of ddH_2O. To these 12 μL were added 3 μL of 5x RT primers.

Table 2.20: Cycle for retro-transcription of RNA for mature miRNAs

Temperature	Time
16 °C	30 min
42 °C	30 min
85 °C	5 min
4 °C	∞

Mature miRNAs quantification was performed using the assay's 20x primers.
For one reaction, 1 μL of TaqMan small RNA assay primers were mixed with 1.4 μL of cDNA previously retro-transcribed, 10 μL of TaqMan reagent and 7.6 μL of ddH_2O. These 20 μL of mix were loaded into a 384-well plate.

2.8.4 Amplification cycles

Semi-quantitative real-time PCR were then performed using an ABI 7900 machine (Applied Biosystems).
The amplification cycle was the same for genes, pri-miRNAs, and mature miRNAs:

Table 2.21: Cycle for real-time PCR of mature and primary miRNAs and genes

Temperature	Time	Repeats
95 °C	10 min	
95 °C	15 sec	x40
60 °C	1 min	

It was slightly different for precursor miRNAs:

Table 2.22: Cycle for real-time PCR of precursor miRNAs

Temperature	Time	Repeats
95 °C	15 min	
94 °C	15 sec	x40
55 °C	30 sec	
70 °C	30 sec	

The specificity of the SYBR Green primers was assessed by adding an extra dissociation step at the end of the cycle and observing a single peak. *GAPDH* and β-*actin*, and Rnu48 and U6 snRNA were used as references for human and mouse genes, and human and mouse miRNAs respectively. The $2^{-\Delta\Delta C_T}$ method was used to calculate the relative changes in gene expression between conditions (fold changes) (Livak and Schmittgen, 2001).

2.9 Agarose gel electrophoresis

Agarose was diluted at 1 % in TAE buffer as well as 0.5 μg/mL of ethidium bromide. After the gel was cast and solidified, the samples were mixed with 6x blue loading dye (New England Biolabs, Ipswich, USA), and loaded in the wells along with a DNA ladder (NEB). The gel was then run at 100-120 V for about an hour, until the samples were

run well enough but not too far to exit the gel. Imaging was finally performed using a Chemidoc XRS device (BioRad, Hercules, USA).

2.10 PCR and cloning of 3'UTR of genes of interest into pmirGLO vectors

The pmirGLO vector commercialized by Promega (Madison, USA) contains a renilla reporter as well as a firefly luciferase reporter, surrounding the Multiple Cloning Site (MCS) where we inserted the 3'UTR sequence of our genes of interest. First of all, between 200 and 400 bases of the 3'UTR containing the predicted seed sequence of the miRNAs were amplified by qPCR using cDNA from a human cell line (typically HEK). The PCR mix was composed of 0.4 μL of dNTP at 10 mM, 100 ng of cDNA, 0.2 μL of Phusion enzyme (NEB), 4 μL of 5x buffer and ddH_2O *qs.* 20 μL. The amplification cycle was as presented on Table 2.23

Table 2.23: Cycle for polymerase chain reactions using Phusion enzyme

Temperature	Time	Repeats
98 °C	30 sec	
98 °C	30 sec	x35
50 °C to 65 °C	30 sec	
72 °C	30 sec	
72 °C	10 min	
4 °C	∞	

The PCR products were then run into a 1 % agarose gel to check that the amplification was efficient and the size was correct. The pmirGLO vector was digested with XbaI restriction enzyme: 1 μg of vector was mixed with 1 μL of Phusion enzyme, 2 μL of buffer D (Promega) and ddH_2O *qs.* 20 μL and the solution was incubated at 37 °C for 2 hours. The digested vector and PCR product were purified using the NucleoSpin Gel and PCR Clean-Up Kit (Clontech Takara, Kusatsu, Japan). Concentrations were measured using a Nanodrop 1000 spectrophotometer (Thermo Fisher) and the PCR product was then ligated into the digested vector using the 5x In-Fusion mix (Clontech) and 100 ng vector for 20 ng insert. After 15 min of incubation at 50 °C, the ligation product was transformed into JM109 competent bacteria, plated on ampicillin-LB-Agar plates and extracted using

the mini-prep kit from Omega (Norcross, USA) and following the manufacturer's instructions. The constructs were validated by sequencing.

2.11 Site-directed mutagenesis

To introduce 2, 4 or 6 mutations in the miRNA seed sequences from the 3'UTR sequences of our genes of interest, site-directed mutagenesis was performed using the pmirGLO-gene construct generated previously and used for dual-reporter luciferase assays. The primers were designed by centering their 30-bases-long sequence on the genes' target sequence and modifying 2, 4 or 6 bases of this section, and then ordered from MWG Operon. The reaction mix for one reaction was as follows: ddH_2O 37.5 μL, 5 μL of 10x Pfu Turbo buffer (Thermo Fisher), 1 μL of template vector at 50 ng/μL, 1 μL of each primer at 100 ng/ μL, 1 μL of dNTP Mix at 10 μM, 2.5 μL of DMSO and 1 μL of Pfu Turbo enzyme (Thermo Fisher) Table 2.24 indicates the incubation cycle that was followed:

Table 2.24: Cycle for site-directed mutagenesis

Temperature	Time	Repeats
95 °C	30 sec	
95 °C	30 sec	x16
50 °C to 68 °C	1 min	
68 °C	1 min /kb	
4 °C	∞	

Similarly to the regular PCR reaction and cloning protocol (see above), the samples were then digested with DpnI, transformed into bacteria and sent to sequencing to confirm the insertion of the mutant bases.

2.12 Dual-reporter luciferase assays

MirVana mir-193b-3p mimic, mir-582-5p mimic and Negative control were purchased from Thermo Fisher and resuspended at 20 μM in sterile ddH_2O. HEK293 cells were plated on a 96-wells plate at 25,000 cells/well the day before transfection. For 5 replicates, 0.5 µL of Lipofectamine 2000 reagent (Thermo Fisher) was mixed to 500 ng pmirGLO vector and 50 µL of OptiMEM medium.

Depending on the condition, Negative control miRNA or mir-193b mimic or mir-582 mimic was also added to the mix for a final concentration of 10 nM or 50 nM (e.g. 1.25 μL or 2.5 μL of 2 μM miRNA). After 15 min, 10 μL of the mix was loaded drop by drop on the cells confluent at 70 % with 90 μL of their usual culture medium without antibiotics. 24 hours after transfection, the cells were lysed using a passive lysis buffer, and luciferase/renilla signals ratios were measured using the dual-reporter luciferase assay reagents from Promega. 30 μL of passive lysis buffer was added directly into the wells to lyse the cells and 20 μL from each well were used for signal detection using a Varioskan Flash luminometer (Thermo Fisher).

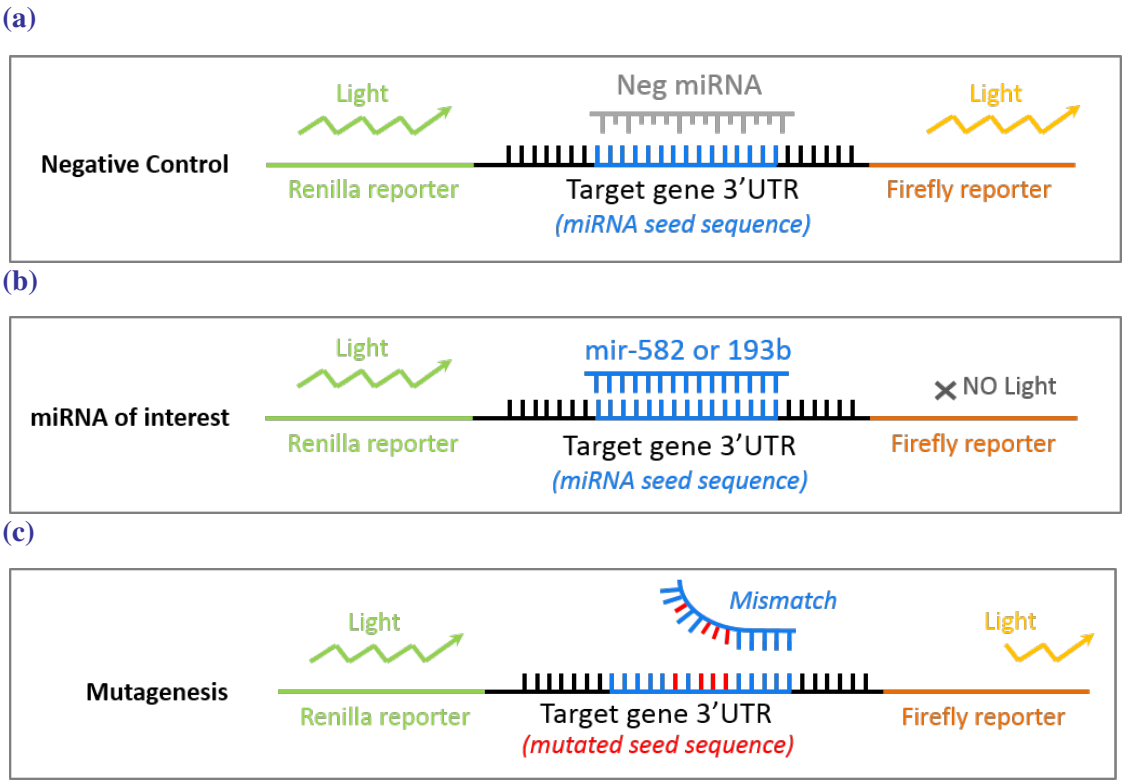

Figure 2.5: **Mechanism of the dual-reporter luciferase assay**
(a) When cells are transfected with a Negative control miRNA, it can not recognize the miRNA seed sequence so does not inhibit the expression of the firefly reporter. (b) When the cells are transfected with our miRNA of interested, its binding to its seed sequence will inhibit the firefly reporter activity and induce a drop in the fluorescence levels. (c) Mutating four or more bases of the 3'UTR predicted seed sequence induces a mismatch and an incomplete or absent binding of the miRNA to this seed sequence. The fluorescent signal then reaches back or gets close to its initial levels.

2.13 Transfection of cells with small RNAs (siRNAs and miRNAs)

MirVana mir-193b-3p inhibitor and mir-582-5p inhibitor were purchased from Thermo Fisher. ON-TARGETplus human *PIK3R1* siRNA SMARTPool and ON-TARGET plus Non-targeting siRNA were purchased from GE Dharmacon (Lafayette, USA) and reconstituted in ddH_2O. HEK293, UCL93, Ox161c1 and SKI001 cells were trypsinised after having reached confluence in a 75 cm^2 flask and resuspended in 15 mL of their respective culture medium. For each condition, 150 μL of OptiMEM were mixed with 7 μL of Lipofectamine RNAiMax reagent (Thermo Fisher) and 5 μL of miRNA or siRNA at 20 μM for 5 min. 2 mL of the resuspended cells per well were then added in 6-well plates and the OptiMEM + small RNA + RNAiMax mix added drop by drop directly on the cells. The medium was changed after 24 hours and the cells cultured for 72 hours before RNA or proteins extraction and further experiments.

2.14 MTS proliferation assay

Ox161 and UCL93 cells were plated at 10,000 cells/well in a 96-wells plate in their regular medium. They were transfected the day after with an RNAiMax + miRNA mix. For 5 wells, 50 µL of OptiMEM medium were mixed with 1.5 µL of RNAiMax reagent and 1.25 µL of Negative control miRNA, mir-193b mimic or mir-582 mimic miRNAs at 20 µM (50 nM final). After a 15 minutes incubation 10 µL of the mix was added to each well directly on the cells in 90 µL of regular medium without antibiotics. 48h after transfection, 20 µL/well of Solution Reagent from the "CellTiter96 Aqueous One Solution Cell Proliferation assay" kit (Promega) were added directly in the wells. After 3 hours of incubation the absorbance of the wells was measured at 492 nm.

2.15 Extraction of proteins from cells and BSA dosage

After removal of the culture medium, the cells were washed with 1 mL of PBS and recovered by pipetting up and down or scrapping. After centrifugation 2 min at 1,000 g, the cells were resuspended in 50 μL of protease inhibitor 1x (Sigma Aldrich) and phosphatase inhibitor (Roche, Basel, Switzerland) in IP buffer, left on ice for 30 min with vortexing every 10 min and finally spinned down for 5 min at 13,000g.

The proteins extracted from our cells were dosed using the DC Protein assay kit from BioRad. The standards were prepared as indicated in Table 2.25:

Table 2.25: Standards for dosage of proteins

Concentration (μg/mL)	**BSA (μL)**	**IP Buffer (μL)**
0	0	50
0.2	7.1	42.9
0.4	14.3	35.7
0.6	21.4	28.4
0.8	28.4	21.4
1.0	35.7	14.3
1.2	42.9	7.1
1.4	50	0

The A* reagent was prepared by mixing 1 mL of A reagent with 20 μL of S reagent. 5 μL of standard or sample were added to 25 μL of A* reagent and 200 μL B reagent. The absorbance was measured at 750 nm after 15 min at room temperature, and the samples concentrations were calculated from the standard curve.

2.16 Western blotting

After measuring the proteins concentrations in the samples, the proteins samples were mixed 1:1 with Laemmli buffer containing 10 % of β-mercaptoethanol and incubated for 30 min at 37 °C in order to lightly denaturate the proteins. Homogeneous amounts of proteins were loaded on sodium dodecyl sulfate – polyacrylamide 7 % to 15 % gels (composition indicated in Table 2.1). The samples were run for around 1h30 at 100-120 V in running buffer. The proteins were then transferred to PVDF membranes previously activated in methanol baths, using the wet transfer protocol and buffer for 1 hour at 100 V. Basically, the system was as follows:

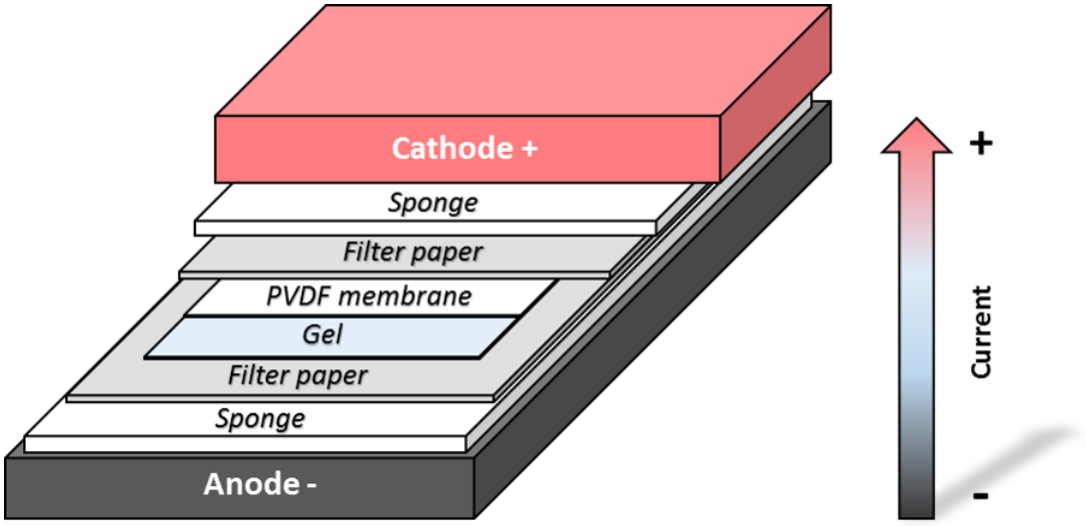

Figure 2.6: **Diagram of Western blot wet transfer**

After a 1 hour saturation step in milk 10 % or Bovine Serum Albumin 5 % in TBST, the membranes were incubated at 4 °C overnight with the primary antibodies listed in Table 2.9 at the indicated concentrations in milk 5 %-TBST or BSA 5 %-TBST. The membranes were washed three times 10 min with TBST and stained with species-specific secondary antibodies coupled with HRP. The proteins were revealed with ECL reagents (BioRad), read with a Chemidoc XRS device (BioRad) and analysed with the ImageLab 5.1 software (BioRad).

2.17 Bacteria transformation and plasmid amplification

JM109 competent bacteria (*E.coli*) stored at -80 °C were slowly thawed on ice. 50 μL were incubated at 4 °C for 30 min with 1.5-3 μL of the desired plasmid, then heat-shocked in a 42 °C water bath and kept on ice for 2-3 min in order to let the membrane close. 250 μL of SOC medium was added and the bacteria were incubated at 37 °C for 1h 30 under shaking and were plated on Luria agar – 100 μg/mL ampicillin Petri dishes. Some of the colonies present on the plate after an overnight incubation were inoculated in sterile LB broth – 100 mg/mL ampicillin and incubated overnight at 37 °C under shaking. The inoculated medium was centrifuged at 4,700 g for 10 min. The DNA was then extracted using the E.Z.N.A. Plasmid mini kit from Omega Bio-tek and the samples concentrations were measured using a Nanodrop spectrophotometer.

2.18 Extraction of genomic DNA and genotyping

2.18.1 Cultured human cells

The cells were scrapped and centrifuged at 1,500 g for 5 min. The medium was then removed and the cells incubated in 50 μL of lysis buffer for 10 min at 95 °C. The solution was left to cool down then proteinase K was added at 1 mg/mL final concentration and the mix was incubated at 56 °C for 30 min. The proteinase K was then inactivated by incubating the tube at 95 °C for 10 min.

2.18.2 Male and female control volunteers

Mouth swabs were taken from a male and a female adult volunteers by rubbing the swab for 15 sec on both inner cheeks. The swabs were then placed inside a 15 mL Falcon tube and incubated overnight at 56 °C in 1 mL of lysis buffer/proteinase K (1 mg/mL) mix. The swab was removed from the tube on the following day and proteinase K inactivated by incubating the solution for 20 min at 95 °C.

The concentrations of the samples from cells and volunteers were then measured using a Nanodrop and the PCR reaction mix was prepared as follows: 5 μL of 5x Green Taq buffer (Promega), 0.5 μL of PCR Nucleotide Mix (10 mM), 0.5 μL of each primer at 10 μM, 0.2 μL of GoTaq polymerase enzyme (Promega), 250 ng of gDNA and ddH_2O *qs.* 25 μL. Table 2.26 indicates the following amplification cycle:

Table 2.26: Cycle for genotyping from gDNA

Temperature	Time	Repeats
95 °C	2 min	
95 °C	30 sec	x38
55 °C	30 sec	
72 °C	1 min	
72 °C	2 min	
4 °C	∞	

2.19 3-Dimensional cyst assay

Depending on experimental conditions, Ox161c1 cells were either not transfected or transfected with Negative control siRNA or with *ANO1* siRNA or *PIK3R1* siRNA or mir-582-5p mimic at 50 nM in a 6-well plate the day before plating (see above). After trypsinisation and resuspension in their usual culture medium at $2.0.10^6$ cells/mL, 10 μL of cells were mixed to 90 μL of Matrigel Matrix (Corning) per well and plated in a 96-well plate. This reagent solidifying quickly at room temperature, all steps were carried out on ice and using cold material. As a result, 10,000 cells were plated per well. The culture medium was added 30 min after plating and changed every other day. For the inhibitor conditions, tannic acid (Sigma Aldrich), CaCCinh-A01 (A01, Sigma Aldrich) or LY294002 (Tocris, Bristol, UK) were added at 10 μM, 20 μM or 100 μM respectively on the first day of culture. DMSO was used at the same concentration as the highest DMSO-concentrated condition, *i.e.* 0.02 %. When needed, IGF-1 treatment was started 24 hrs after plating.

For the *ANO1* assay, the cells were cultured in medium containing forskolin at 50 μM to induce an enlargement of cysts important enough to be able to see a reduction in cysts area. Furthermore, as the cells for each condition (not transfected, Negative control, anti-*ANO1* siRNA, mir-582 mimic) were resuspended and plated independently, inducing an unavoidable variability in their seeding density, the cysts size was measured at three different time points and expressed as percentages of the areas at the first time point.

For the *PIK3R1* assay, for the same reasons mentioned above, the variability induced by seeding density was limited by adding a non-IGF-1-treatment control for each of the conditions in order to avoid seeing effects due to variability in the cells confluency.

Imaging was performed using an Olympus IX71 inverted microscope. Between 57 and 179 cysts were randomly taken in pictures across 1 well (optimisation experiment) or 3 wells in order to cover the widest variety of sizes and avoid bias. The area of each cyst was then measured using the Image J software.

2.20 Treatment of cells with steroids

To study the effects of phenol red present in the classic DMEM F-12 culture medium used for our human cell lines, RFH, UCL93, Ox161c1 and SKI001 were washed and cultured in phenol-red free medium for 10 days before being plated in 6-well plates and harvested for miRNA assays four days later. From then they were continuously kept in this phenol red-free medium all along the steroid treatments experiments.

Dihydrotestosterone (DHT) and β-estradiol (E2) were purchased from Sigma Aldrich and resuspended in DMSO at 10 mM. UCL93 and SKI001 were plated in 6-well plates at 250,000 cells/well and were treated with DHT or E2 at 20 nM or 100 nM for 4 days, with a medium change every day for 4 days. DMSO was diluted similarly to the most concentrated steroid and added to the cells as a control condition of the effects of this compound.

2.21 Activation of Akt/ERK pathways using IGF-1 treatment on cells

UCL93 and SKI001 were plated at 250,000 cells/well in 6-well plates, the SKI001 having been transfected or not with siRNAs depending on the experiment. 24 hrs after plating, the cells were starved for 48 hrs in a medium lacking Nu serum to achieve synchronisation between the wells. IGF-1, purchased from Abcam, was resuspended at 1 mg/mL in ddH_2O and stored at -20 °C. 3 days after plating and starving, IGF-1 was added to the well at 50 μg/mL at different time points: 1 hour, 30 min, 15 min, and 5 min (for the first experiment) or 15 min (for the experiment with anti-*PIK3R1* siRNA experiment). All the wells were harvested at the same time, followed by a proteins extraction, dosage and Western blotting.

2.22 Treatment of cells with actinomycin D

Actinomycin D was purchased from Sigma-Aldrich and resuspended at 4 mg/mL in DMSO. RFH and Ox161c1 were plated at 250,000 cells/well in 6-well plates and treated with actinomycin D at 5 ng/μL for 24 hrs, 12 hrs, 6 hrs, 3 hrs and 1 hr. All wells were harvested at the same time and miRNAs extracted for subsequent miRNAs qPCR.

2.23 Immunohistochemistry on human and mouse kidney tissues

The kidneys were fixed in paraffin and sectioned using a microtome. The slides with the kidney sections were stored at room temperature until use. After two dewaxing steps in xylene for 5 minutes each, they were rehydrated by series of 2 minutes-long ethanol baths at 99 % (twice), 95 % and 70 %, followed by a wash in dH_2O for 5 minutes. The endogenous peroxydase activity was then quenched using H_2O_2 3 % in methanol for 20 min, followed by a wash in dH_2O for 2 min. The antigen retrieval step was carried out next by bringing slides to the boil in 10 mM tri-sodium citrate (pH 6.0) and cooling them down in a bath of cold water or ice. After rinsing the slides in PBS or TBST, each section was blocked using horse serum (ImmPress Kit from Vector Labs, Burlingame, USA) 2.5 % or goat serum (Vector Labs) 5 % in PBS for 1 hour at room temperature. The primary antibody diluted in horse or goat serum at indicated concentrations (see Table 2.9 above) in PBS, as well as the control IgG of the relevant species diluted at the same concentration, were then applied on the sections and the slides were left for at least 1 hour at 4 °C in a humidified chamber. After three washes with PBS or TBST, the secondary antibodies were added to the slides for 30 min at room temperature. The slides were again washed three times with PBS or TBST and then stained with a few drops of DAB (Cell Signaling Technology, Danvers, USA) until colour developed to the desired intensity (typically 1 to 10 minutes). The colour development reaction was stopped by immersing the slides in dH_2O. Counter-staining was then performed using hematoxylin for 30 sec. The sections were then rinsed in dH_2O and placed in Scott's water to stabilize the colour. After another wash in dH_2O, the slides were dehydrated by 1 minute-long baths of ethanol at increasing concentrations (70 %, 95 % and two times 99 %) and xylene. Finally, the sections were mounted with coverslips using mounting medium (Consul Mount from Thermo Fisher) and let to set before imaging.

2.24 Statistical analyses

The *GraphPad Prism 7.0* software package was used for all statistical analyses. Variables were presented as mean +/- SEM and differences between groups calculated with unpaired Student's two-tailed t-test or with Mann-Whitney test with the relevant corrections if needed, $p<0.05$ being considered statistically significant.

2.25 Copyright

Figures 1.10, 1.11, 1.12, 3.35, 4.2, 4.3, 4.24, 5.14 and 5.15 were drawn using free-to-reuse individual elements from Servier Medical Art under Creative Common CC-BY 3.0 and CC-BY 4.0 licenses, in combination with components designed by me for the purpose of this thesis. Figures issued from published papers were reused with permission from the publisher, as indicated.

Chapter 3

Selection of new targets from a parallel miRNA/mRNA microarray

3.1 Introduction

The first goal of this project was to identify relevant targets for two miRNAs selected from a dataset generated from an earlier parallel mRNA/miRNA microarray performed in our laboratory on normal and cystic human kidney cell lines (Andrew Streets, University of Sheffield).

Microarrays, first introduced in the 1990s, are among the most widely used techniques to measure the abundance of transcripts in biological samples, alongside the more recently developed next generation RNA sequencing (RNA-seq). The principle of mRNA (or miRNA) arrays is as follows: total RNA (minimum 200 ng, Stefano (2014)) is isolated from biological samples, mRNA purified from other RNAs and reverse transcription performed for around 16 hours to generate complementary DNA (cDNA) (ThermoFisher, 2017). T7 RNA polymerase then amplifies cDNA via the intermediary of cRNA strands, and this cDNA is subsequently purified and labelled with a fluorescent probe (or, rarely, a radioactive probe), typically of two or more different colours to differentiate the reference from experimental samples (Nature Education, 2017; 't Hoen, 2003). The purification and labelling of the cDNA takes between 4 and 6 hours (ThermoFisher, 2017; Stefano, 2014). The labelled cDNA is then hybridized on a microchip formed of thousands of spots, each containing unique DNA sequences corresponding to a specific gene and will form hydrogen bonds with complementary bases on these sequences (University of Utah, 2017). After an overnight incubation, the non-specific bonds will be washed off using detergents and the chip scanned following excitation of the fluorescent dye by a laser.

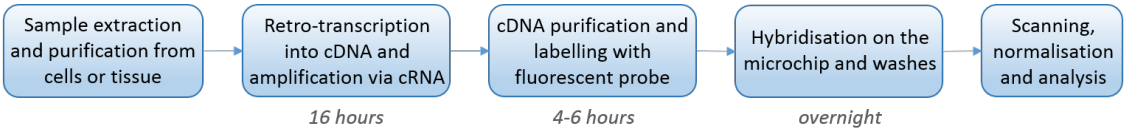

Figure 3.1: **Workflow of microarray experiments.**

The colour and the intensity of the fluorescence will give information on which DNA sequences were hybridised (hence which genes were expressed in the sample) and which sample expresses it the most. The statistical test used to analyse microarray data is a Student's t-test and it is estimated that microarrays are very accurate for fold changes above 2 (Marioni et al., 2008; Stefano, 2014).

Analysis of microarrays data is simple and does not require the support of a specialised bioinformatician, and a raw data file from a typical microarray takes little storage space (about 0.7 MB for an Agilent microarray file, (Stefano, 2014)).

Next-generation sequencing technologies were introduced about 10 years ago and have been constantly improved since. They allow the study of differential gene expression over a wider range than microarrays as they are not limited to the probes designed for the chip, and hence are able to discover new genes from incompletely or non-sequenced genomes. Moreover, they have the ability to identify alternative splice variations, single nucleotide polymorphisms (SNPs) and post-transcriptional modifications (Hurd and Nelson, 2009) and are more sensitive than microarrays as they require less sample and can detect low abundance transcripts (Marioni et al., 2008; Sîrbu et al., 2012).
The protocol for RNA sequencing varies across platforms but is generally as follows: RNA is extracted from tissues and purified using DNase digestion to remove traces of genomic DNA. Its purity and quantity are essential factors for the functioning of the sequencing and are checked by capillary and/or gel electrophoresis for the former and by UV absorbance or fluorometry for the latter (New England Biolabs, 2017; University of Oregon, 2017). As little as 10 pg of RNA sample can be sufficient to perform an RNA-seq experiment (Stefano, 2014). Additionally, mRNA is separated from other RNAs by hybridisation with poly(dT) oligomers via their poly(A) tail (New England Biolabs, 2017). In the specific case of miRNAs the selection is based on size via magnetic beads or separating gel and a 3' and 5' adapter ligation step occurs prior to retrotranscription (Eminaga et al., 2013). Fragmentation of the nucleic acids by sonication, enzymatic digestion or nebulisation will result in the production of fragments of appropriate size for sequencing (ranging from 40 to 400 bp depending on the platform, New England Biolabs, 2017; Syed et al., 2009) and is followed by a retrotranscription of the RNA into single strand cDNA and the production of double stranded cDNA using DNA polymerase (Zhu et al., 2001). Finally adaptor sequences, acting either as attachment or amplification elements, as sequencing priming sites or as 'barcodes' allowing multiplex sequencing, are ligated to the fragmented cDNA via RT-PCR or ligation which is then ready for sequencing (Head et al., 2014; University of Oregon, 2017).

All these steps of library construction take about 4 hours which is similar to the microarray protocol (Stefano, 2014).

(a)

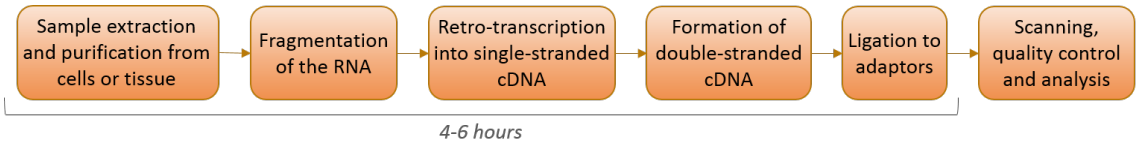

(b)

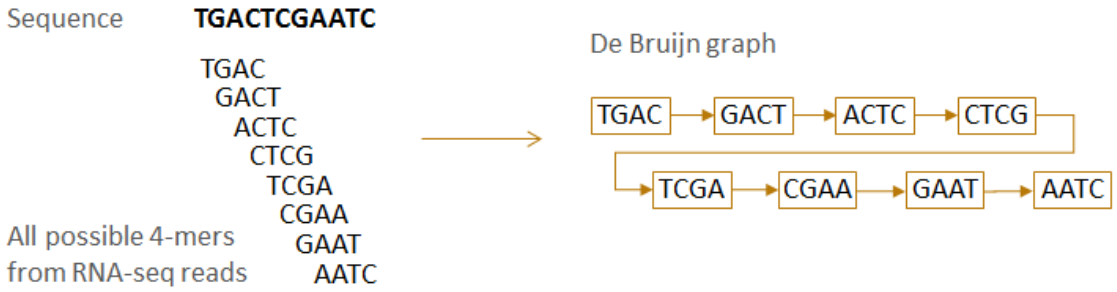

Figure 3.2: **Principle of RNA-seq experiments.**
(a) Workflow of RNA-seq experiments. (b) Simplified representation of the use of Bruijn graphs and k-mers for RNA-seq

The analysis of RNA-seq data is very complex and involves multiple steps that vary depending on the sequencing platform. These steps can be a grouping of the sequences according to their barcode, a removal of the adaptors, a selection of selecting reads free from sequencing errors and a normalisation of reads based on their k-mer coverage (k-mer are all the typical DNA substrings of length k often represented by *De Bruijn* graphs, see Figure 3.2b) (Brown et al., 2012; University of Oregon, 2017). Next-generation sequencing datasets allow to either align the reads to a reference genome in order to identify the genes expressed in the sample or to assemble a transcriptome *de novo* by aligning the common sequences of the fragmented cDNAs and building *de Bruijn* graphs (Chang et al., 2015; Compeau et al., 2011). RNA-seq is more sensitive than microarray as it can accurately detect fold changes of 1.25, and statistical analyses are typically performed using Fisher exact test (Stefano, 2014). However, the datasets it generates are heavy ($\sim$5 GB for an uncompressed raw file, Stefano, 2014) and the high complexity of their analysis requires specific training and the input of bioinformaticians knowledgeable in this particular field.

As a summary, while RNA-seq allows the generation of larger datasets thanks to a broader dynamic range and tends to be more accurate and sensitive than microarrays, the latter are still commonly used in practice as they are more straight forward to perform and analyse, remain more economic ($300 per sample vs. $1,000, Stefano (2014)) and their data is less challenging to store than the large RNA-seq datasets.

3.2 Preliminary work: constitution of a new database based on a parallel mRNA/miRNA array from human ADPKD cells

The results presented in this section were generated by Andrew J. Streets before the start of this project. This project is based on the data generated from an initial pilot study in our laboratory and aims at validating its results and taking it further. This preliminary work consisted in validating two dysregulated miRNAs from mRNA/miRNA microarrays and establishing a list of their predicted target genes that were enriched in ADPKD compared to normal. In order to constitute a new database of dysregulated miRNAs/mRNAs in ADPKD, 4 cystic (Ox161, Ox938, SKI001 and SKI002) and 2 normal (UCL93 and RFH) cell lines were cultured and synchronised in order to obtain mRNA and miRNAs and perform microarray analyses. Figure 3.3 summarises this experiment. 1,515 genes and 30 pathways were significantly dysregulated from the mRNA array and 11 miRNAs were significantly altered in the miRNA array. A list of 482 altered genes could be established by comparing the results of the mRNA and microRNA arrays.

(a)

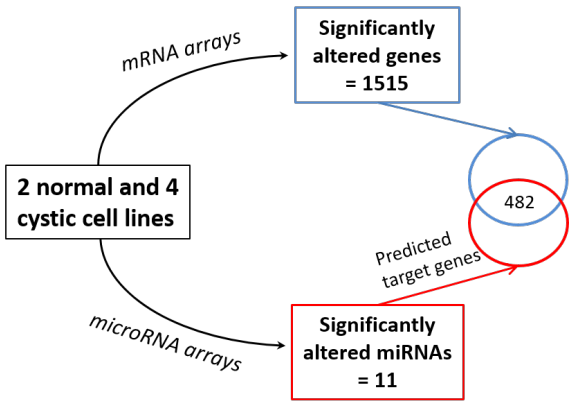

(b)

Analyzed List: Up-regulated genes > 2 fold		
PANTHER Pathways	**Fold Enrichment**	**P-value**
FGF signaling pathway (P00021)	4.17	1.67E-03
Gonadotropin releasing hormone receptor pathway (P06664)	2.93	4.17E-03
Alpha adrenergic receptor signaling pathway (P00002)	> 5	5.09E-03
Histamine H1 receptor mediated signaling pathway (P04385)	> 5	7.64E-03
EGF receptor signaling pathway (P00018)	3.38	9.46E-03
MYO_signaling_pathway (P06215)	> 5	1.36E-02
GBB_signaling_pathway (P06214)	> 5	1.36E-02
Activinbetasignaling_pathway (P06210)	> 5	1.36E-02
ALP23B_signaling_pathway (P06209)	> 5	1.36E-02
Angiogenesis (P00005)	2.86	2.01E-02
Apoptosis signaling pathway (P00006)	3.19	2.17E-02
Oxytocin receptor mediated signaling pathway (P04391)	5	2.30E-02
Thyrotropin-releasing hormone receptor signaling pathway (P04394)	4.78	2.58E-02
SCW_signaling_pathway (P06216)	> 5	2.69E-02
DPP_signaling_pathway (P06213)	> 5	2.69E-02
DPP-SCW_signaling_pathway (P06212)	> 5	2.69E-02
BMP_signaling_pathway-drosophila (P06211)	> 5	2.69E-02
Wnt signaling pathway (P00057)	2.13	2.75E-02
CCKR signaling map (P06959)	2.6	2.97E-02
5HT2 type receptor mediated signaling pathway (P04374)	4.31	3.34E-02
Thiamine metabolism (P02780)	> 5	4.01E-02
Toll receptor signaling pathway (P00054)	3.93	4.22E-02
Analyzed List: Down-regulated genes > 2 fold		
PANTHER Pathways	**Fold Enrichment**	**P-value**
Heterotrimeric G-protein signaling pathway-Gi alpha and Gs alpha mediated pathway (P00026)	2	9.84E-03
Heterotrimeric G-protein signaling pathway-Gq alpha and Go alpha mediated pathway (P00027)	2.11	1.07E-02
Ionotropic glutamate receptor pathway (P00037)	2.57	1.44E-02
Enkephalin release (P05913)	3.66	2.51E-02
Cadherin signaling pathway (P00012)	1.72	2.76E-02
Nicotine pharmacodynamics pathway (P06587)	2.77	3.65E-02
Metabotropic glutamate receptor group II pathway (P00040)	2.69	4.06E-02
Heterotrimeric G-protein signaling pathway-rod outer segment phototransduction (P00028)	2.69	4.06E-02

Figure 3.3: **Parallel mRNA/miRNA summary.**
(a) Diagram of the parallel mRNA/miRNA microarray. (b) PANTHER gene list analysis software (www.pantherdb.org) gave a list of enriched pathways from the 1,515 genes found up or down-regulated at least 2-fold in ADPKD cells compared to normal. *Published in Streets et al. (2017).*

As presented in Figure 3.4a, 11 miRNAs were down-regulated in ADPKD cells compared to normal, while 1 (mir-196a-5p) was found up-regulated from the microarray.

To validate these results, the expression levels of the 5 most dysregulated miRNAs (mir-582-5p, mir-335-5p, mir-660-5p, mir-181a-2-3p and mir-193b-3p) were assessed by TaqMan (sq) RT-PCR. Consistently with microarray results, two of these miRNAs were significantly decreased in cystic cell lines; mir-193b-5p with a 0.5 fold change and mir-582-5p with a 0.8 fold change (Figure 3.4b).

(a)

Systematic Name	p-value	Regulation (C/N)	Fold Change
hsa-mir-582-5p	1.59E-04	Down	51
hsa-mir-335-5p	0.016439	Down	50
hsa-mir-660-5p	6.42E-06	Down	14
hsa-mir-181a-2-3p	0.035598	Down	5
hsa-mir-193b-3p	0.041946	Down	3
hsa-mir-196a-5p	0.035520	Up	2
hsa-mir-210	0.035822	Down	1.8
hsa-mir-27a	0.012968	Down	1.5
hsa-mir-15b	0.018344	Down	1.5
hsa-mir-16	0.024463	Down	1.4
hsa-mir-30d	0.041664	Down	1.4

(b)

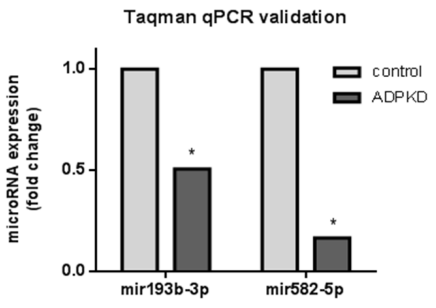

Figure 3.4: **MiRNAs identified by microarray.** (a) 10 miRNAs were found down-regulated and 1 up-regulated in cystic cells compared to normal. (yellow: miRNAs measured by TaqMan (sq) RT-PCR, red: miRNAs confirmed down-regulated in ADPKD cells) (b) mir193b-3p and mir-582-5p were confirmed down-regulated in ADPKD cells by TaqMan (sq) RT-PCR. Values presented as fold change of normal cells.
** 0.05 > p > 0.01 (Unpaired t-test)]*

The next step in the analysis of the microarray results was to establish a list of mir-193b and mir-582 predicted target genes dysregulated in ADPKD. This was done by matching the results of the mRNAs and miRNAs arrays and predicting target genes for these two miRNAs by TargetScan.

Figure 3.5 presents the predicted target genes of mir-193b-3p (Figure 3.5a) and mir-582-5p (Figure 3.5b) that were increased by a fold change of at least 4 in ADPKD cells compared to normal.

(a)

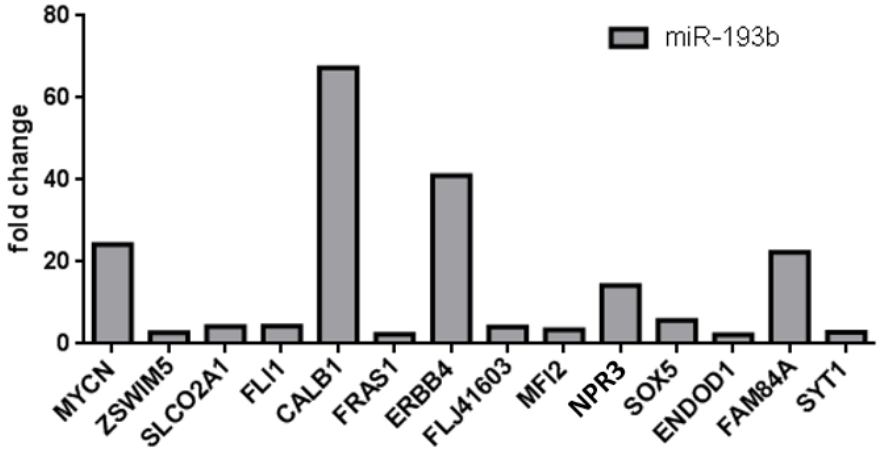

(b)

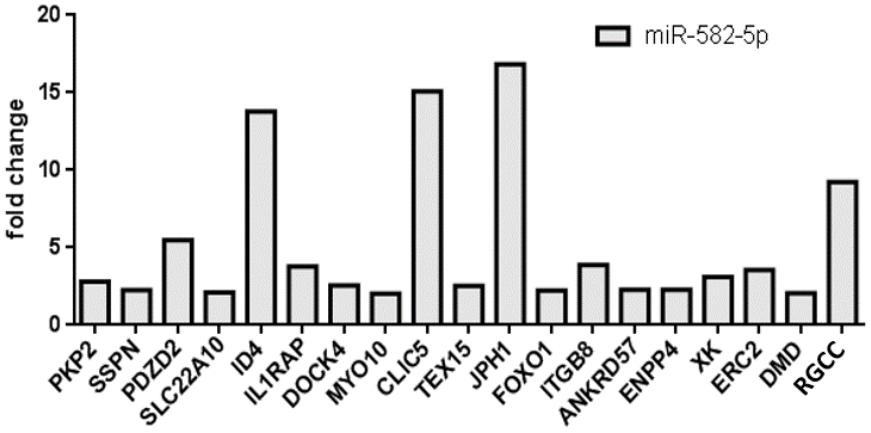

Figure 3.5: **Predicted target genes for mir-193b-3p and mir-582-5p also found up-regulated >4-fold in ADPKD cells.**
(a) mir-193b-3p and (b) mir-582-5p predicted and deregulated target genes were determined by matching the results of the mRNAs and miRNAs microarray with *in silico* predictions from TargetScan. Values are presented as fold change compared to normal cells.

For mir-193b-3p, 14 genes were significantly up-regulated at least 4 times in ADPKD compared to normal, the highest fold changes being *CALB1*, *ERBB4* and *MYCN* (67.3, 41.0 and 24.2 respectively). For mir-582-5p, 19 genes showed at least a 4-fold increase in cystic cells, the most up-regulated being *JPH1*, *CLIC5* and *ID4* with fold change values at 16.8, 15.1 and 13.8 respectively.

The following section describes work performed for the *ERBB4*-related paper published in AJP Renal Physiol in April 2017 and, unless stated otherwise, my contribution to this paper (Streets et al., 2017).

3.3 *ERBB4* is a determinant of cyst growth in ADPKD

ERBB4 (fold-change 41 in the microarray, potentially regulated by mir-193b-3p) was the first candidate selected from the list of genes established previously with parallel microarrays and qPCR validation because this gene was previously linked to the Jak/STAT pathway (Olayioye et al., 1999) and its over-expression was shown to cause increased proliferation and disruption of cell polarity in *in vitro* and *in vivo* kidney models (Veikkolainen et al., 2012).

First of all, the deregulation of *ERBB4* was validated in two independent batches of two normal (RFH and UCL93) and four cystic (Ox161, SKI001, Ox938 and SKI002) human kidney cells to confirm the results of the microarray (see Figure 3.6).

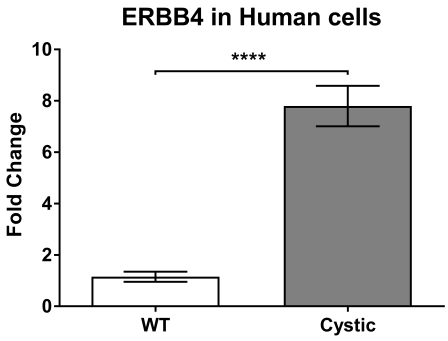

***Figure 3.6:* Real-time PCR for the relative expression of *ErbB4* in normal and ADPKD human cells.**
ErbB4 mRNA levels were measured in two independent batches of two normal (RFH, UCL93) and four cystic (Ox161, SKI001, Ox938, SKI002) ADPKD human cells.
The values are represented as fold changes compared to the two normal cell lines.
***** $p < 0.0001$ (Unpaired t-test with Welch's correction).*

NB: The figure presented here is different from its equivalent in the reference paper (Figure 3A) as the former was performed by me and the latter was performed by A. Streets. However, the results are similar i.e. they show a significant increase of ERBB4 expression in human ADPKD cells.

ErbB4 was significantly up-regulated in the cystic cells by a fold change of 7.8 compared to normal. This increase was consistent between batches and cystic cell lines. Because mir-193b-3p was found significantly down-regulated in the same cells (Figure 3.5a) and *ErbB4* is a predicted target for this miRNA, dual-reporter luciferase assays aimed at confirming this interaction.

One of the potential mir-193b seed sequences on *ErbB4* 3' UTR (see Figure 3.7b) was identified, amplified from HEK cells RNA and cloned into a pmirGLO vector containing a firefly luciferase and a renilla reporters (see Figure 2.1).

Figure 2.5 in the Materials and Methods chapter explains the principle of the dual-reporter luciferase reporter assay: when no miRNA is interacting with the *ErbB4* 3'UTR sequence either because of an absence of miRNA or the transfection of a Negative miRNA, the firefly luciferase reporter can be expressed which leads to the emission of a light signal. On the contrary, when the transfected miRNA can bind its seed sequence the firefly luciferase reporter is not expressed and no light signal can be measured. Renilla being coded upstream from the MCS, it will always be expressed and will be used as a control of the efficiency of transfection.

Figure 3.7 presents the seed sequence and results from algorithms predictions for the interaction between mir-193b-3p and *ErbB4*. Seven algorithms (mirRWalk, miRanda, miRDB, miRMap, Pictar2, RNAhybrid and TargetScan) predicted *ErbB4* as a target for mir-193b-3p (Figure 3.7a). From Figure 3.7c, we can see that transfecting HEK293 with the pmirGLO-ErbB4 vector and mir-193b-3p mimic at 20 nM and 50 nM induced a strong and significant reduction of fluorescent signal to levels below 50 % of the Negative miRNA-control condition. Inserting three mutations in the gene's 3'UTR sequence induced an inhibition of this effect to get back to normal levels of fluorescence, suggesting that the reduction of fluorescent signal was specifically due to an interaction between mir-193b-3p and *ErbB4*. This was the first evidence that mir-193b-3p targets this gene's mRNA.

(a)

			MiRNA binding sites prediction Algorithms											
Gene	EntrezID	miRNA	miRWalk	microT4	miRanda	mirbridge	miRDB	miRMap	miRNAMap	Pictar2	PITA	RNA22	RNAhybrid	Targetscan	SUM
ErbB4 (Human)	2066	hsa-miR-193b-3p	1	0	1	0	1	1	0	1	0	0	1	1	7

(b)

```
    3' ucgcccugaaacUCCCGGUCAa 5' hsa-miR-193b
                    | |||||||
77:5' uccuucuacccc AAGGCCAGUa 3' ERBB4
```

(c)

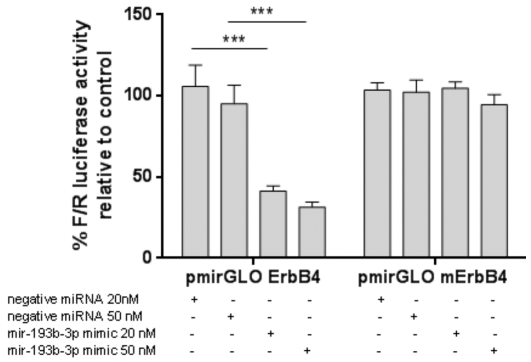

***Figure 3.7: ErbB4*/mir-193b-3p interaction.**
(a) Results from mirWalk 2.0 multiple databases prediction for mir-193b-3p/*ErbB4* interaction in human and mouse. (b) Predicted seed sequence of mir-193b-3p on *ErbB4* 3'UTR (source: www.microrna.org). Yellow: seed sequence of mir-193b-3p on *ErbB4* 3' UTR sequence. Red: three mutated bases for dual-reporter luciferase assay with mutants. (c) Dual-reporter luciferase assays (n=3) intensity of fluorescence values represented as percentage of control condition (Negative miRNA-transfected cells) with WT (left) and mutant (right) *PIK3R1* 3'UTR sequence at 20 and 50 nM miRNA concentration (*Published as figure 3D in Streets et al. (2017)*).

A. Streets then performed immunohistochemistry and immunoblots stainings in human cells and two models of ADPKD mice and confirmed that the ErbB4 protein is over-expressed in ADPKD kidneys in these models. T. Magayr performed immunoblotting and (sq) RT-PCR on urine samples from healthy volunteers and ADPKD patients and also showed an increased expression of ErbB4 in ADPKD patients, significantly correlating with the decline in eGFR. Finally, A. Streets demonstrated that ErbB4 is involved in ADPKD cells proliferation using 3D cysts assays and BrdU proliferation assays and gave evidences that its action is mediated by its ligands NRG-1 (Neuregulin 1) and EGF (Epidermal Growth Factor). Indeed, inhibition of ErbB4 with a molecule inhibitor or an antibody led to a significantly reduced proliferation of cystic cells.

Furthermore, treatment of normal and cystic cells with NRG-1 or EGF induced a higher phosphorylation of ErbB4 in Ox161c1 (cystic) than in UCL93 (normal) and led to a significantly higher cyst growth of Ox161c1 in Matrigel compared to the untreated condition (Streets et al., 2017).

Our ErbB4-centered paper presented a successful example of a candidate identified and selected from the parallel mRNA/miRNA microarray. The aim of the following experiments was to find one or several other candidates and understand their link to miRNAs and their role in ADPKD pathogenesis. All the experiments presented in the rest of this PhD thesis were performed by myself.

3.4 Identification of new candidates from the parallel mRNA/miRNA microarray

3.4.1 Selection, screening and validation of the most consistently enriched targets in ADPKD cells and their interaction with our miRNAs of interest

PANTHER classification system analysis To discover new targets of the two validated miRNAs (mir-193b-3p and mir-582-5p), it was decided to go for a pathways/network analysis approach that classified the candidates by biological process. An *in silico* analysis using the PANTHER programme (available at www.pantherdb.org) was performed to determine common biological processes between the genes that were previously found significantly enriched at least 4-fold in ADPKD (see Figure 3.5).

(a) mir-193b-3p targets

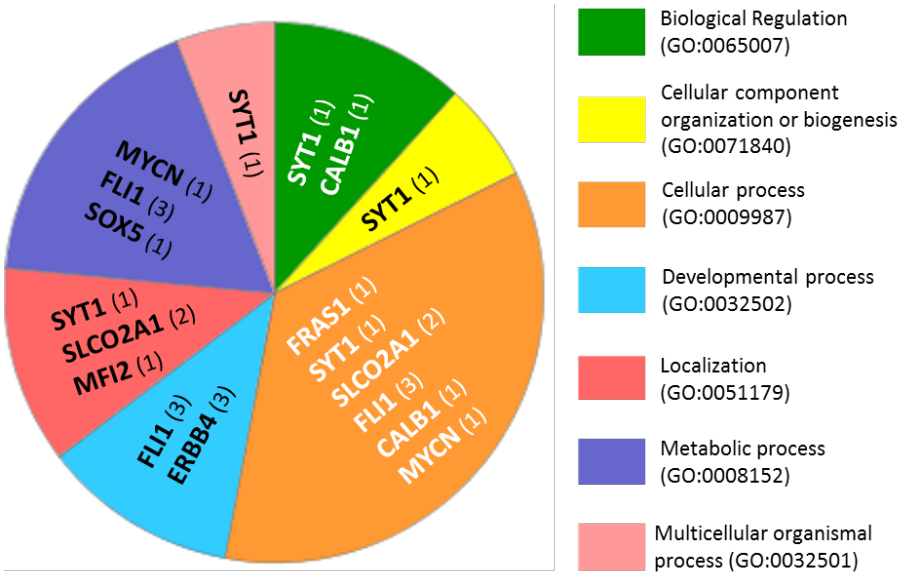

(b) mir-582-5p targets

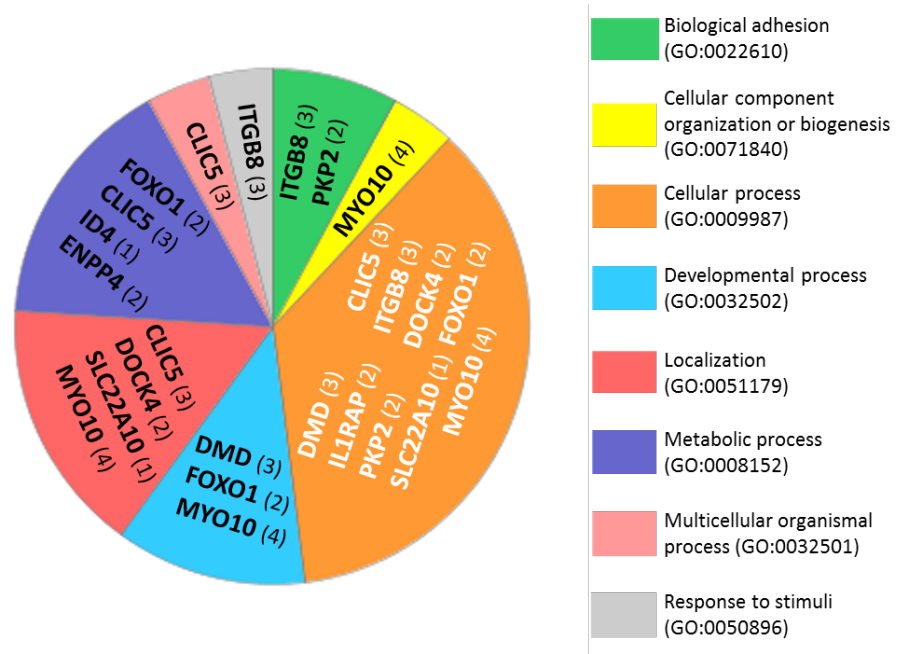

Figure 3.8: **PANTHER enrichment analysis results for mir-193b-3p and mir-582-5p up-regulated targets.**
Gene Ontology Biological Processes that could be affected by the predicted targets for mir-193b-3p and mir-582-5p and found enriched >4-fold in human ADPKD cells from the microarray. The list of genes was entered into the PANTHER classification system (www.pantherdb.org) and a grouping by GO biological processes was requested. The genes involved in each category are displayed on the chart along with the number of potential seed sequences for (a) mir-193b-3p or (b) mir-582-5p (in brackets).

The results of the PANTHER software analysis presented in Figure 3.8 show that a decreased level of mir-193b-3p or mir-582-5p leading to an enrichment of their potential genes targets could affect 7 and 8 Gene Ontology Biological Processes, respectively. In particular, “cellular process” (orange section) is described by Gene Ontology as including cell communication, cell cycle and cell proliferation, processes of major importance in cell physiology and important factors of cysts progression in ADPKD. This process being the most highly represented in the analysis results (six genes for mir-193b-3p and nine for mir-582-5p), these candidates were the first to be selected for (sq) RT-PCR validation in our human cell lines. Some of the targets involved in this process were also found in other enriched processes. For example, *CALB1* and *SYT1* for mir-193b-3p (Figure 3.8a) were members of the biological regulation process and *CLIC5* for mir-582-5p (Figure 3.8b) was involved in the metabolic process. This was interesting as it suggested that if these targets were to be confirmed enriched in ADPKD, they would give insights into the dysregulation of several pathways or processes in the disease. Other processes identified in ADPKD were the ”metabolic process”, ”localization” or ”adhesion”, for example.

SYBR Green (sq) RT-PCR screen of selected candidates Following this study, twenty-two candidates were selected; nineteen that were mentioned in the enriched processes shown in Figure 3.8 (7 for mir-193b-3p and 12 for mir-582-5p) and three (*JPH1*, *NPR3* and *RGCC*) that, although not part of the enriched processes listed by PANTHER, showed a high fold change in human ADPKD cells in the mRNA microarray so were deemed interesting to validate. The expression levels of these 22 genes’ mRNA were measured in two normal and four cystic human ADPKD cell lines by SYBR Green (sq) RT-PCR. Out of these candidates, nine (*CALB1*, *CLIC5*, *PKP2*, *IL1RAP*, *SYT1*, *JPH1*, *ENPP4*, *DOCK4*, *ITGB8*) showed an increase in ADPKD cells and were selected to be validated in a second independent batch of cells. For more clarity, I am only presenting the results of the two (sq) RT-PCR for these nine gene’s expression levels in human cells (the other genes not taken through are listed in the summary Table 3.2).

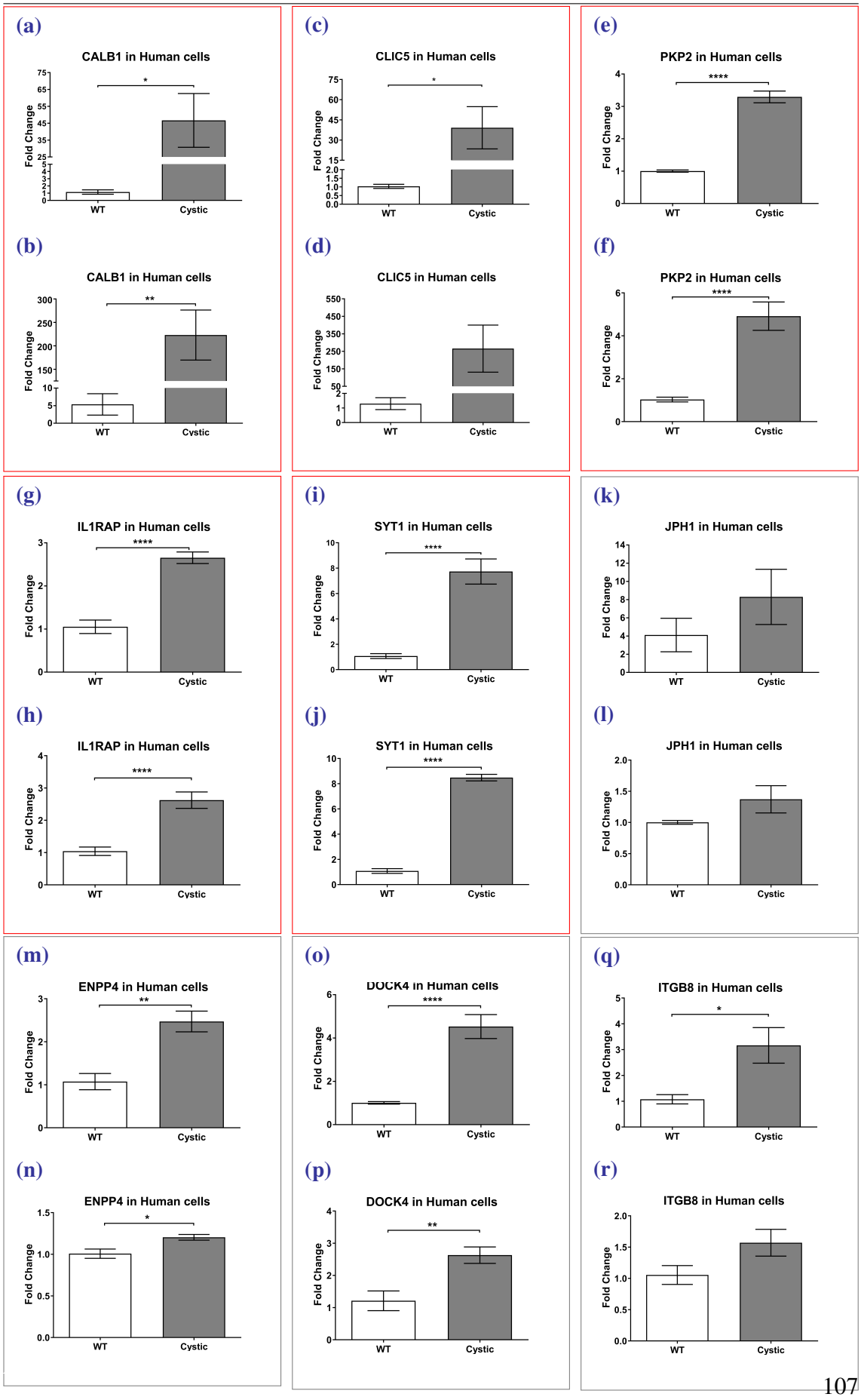
(a)
CALB1 in Human cells
Fold Change
WT
Cystic
(b)
CALB1 in Human cells
Fold Change
WT
Cystic
(c)
CLIC5 in Human cells
Fold Change
WT
Cystic
(d)
CLIC5 in Human cells
Fold Change
WT
Cystic
(e)
PKP2 in Human cells
Fold Change
WT
Cystic
(f)
PKP2 in Human cells
Fold Change
WT
Cystic
(g)
IL1RAP in Human cells
Fold Change
WT
Cystic
(h)
IL1RAP in Human cells
Fold Change
WT
Cystic
(i)
SYT1 in Human cells
Fold Change
WT
Cystic
(j)
SYT1 in Human cells
Fold Change
WT
Cystic
(k)
JPH1 in Human cells
Fold Change
WT
Cystic
(l)
JPH1 in Human cells
Fold Change
WT
Cystic
(m)
ENPP4 in Human cells
Fold Change
WT
Cystic
(n)
ENPP4 in Human cells
Fold Change
WT
Cystic
(o)
DOCK4 in Human cells
Fold Change
WT
Cystic
(p)
DOCK4 in Human cells
Fold Change
WT
Cystic
(q)
ITGB8 in Human cells
Fold Change
WT
Cystic
(r)
ITGB8 in Human cells
Fold Change
WT
Cystic

←—***Figure 3.9*: (sq) RT-PCR for the relative expression of nine candidates selected from the parallel miRNA/mRNA microarray between normal and cystic ADPKD human cells.**
Values are expressed as fold change of the levels in normal cells (UCL93 and RFH). Nine genes out of twenty-two were selected from the first (sq) RT-PCR screen on two normal (RFH, UCL93) and four cystic (Ox161, SKI001, Ox938 and SKI002) human cell lines because they were up-regulated in ADPKD compared to normal (Top panels: a, c, e, g, i, k, m, o, q). A second (sq) RT-PCR was performed on another independent batch of cells to confirm their deregulation in ADPKD (Bottom panels: b, d, f, h, j, l, n, p, r). Red: Genes taken further after the two (sq) RT-PCR screens.
** 0.05>p>0.01 ** 0.01>p>0.001 *** 0.001>p>0.0001 **** p<0.0001 (Unpaired t-test with Welch's correction)*

Out of the 22 candidates, the nine that were selected showed a significant and/or high increase in ADPKD cells compared to normal. In particular, *CALB1*'s mRNA levels were increased 47.7-fold in the cystic cells (Figure 3.9a). Although the four ADPKD cell lines showed an over-expression of *CALB1*, the significance was low because there was a variability between these cells: the range of increase went from 5.1-fold in Ox938 and 8.5-fold in SKI002 to 28.6-fold in Ox161 and 118-fold in SKI001. Similarly, *CLIC5* (Figure 3.9c) was highly up-regulated in ADPKD cells by a fold change of 39.1 compared to normal, but the significance was low because of a variability between the cells (7.6-fold increase in SKI002 and 129-fold increase in Ox161). The other candidates showed a lower but highly significant up-regulation in ADPKD cells compared to normal, such as *PKP2* (Figure 3.9e), *IL1RAP* (Figure 3.9g) and *SYT1* (Figure 3.9i) where the mRNA's expression levels were 3.3, 2.6 and 7.7-fold increased in ADPKD cells, respectively. A second (sq) RT-PCR on these nine genes gave confirmation of the up-regulation of five of them in the cystic cells. These five genes (*CALB1*, *CLIC5*, *PKP2*, *IL1RAP* and *SYT1*, red boxes in Figure 3.9) showed either a highly significant up-regulation (*PKP2*: Figure 3.9f, *IL1RAP*: Figure 3.9h and *SYT1*: Figure 3.9j), either a very high fold change value (fold change of 223 for *CALB1*: Figure 3.9b and 266 for *CLIC5*: Figure 3.9d). The results for the other genes were not as convincing, some of them not showing any significant or high over-expression in ADPKD (*JPH1*: Figure 3.9l or *ITGB8*: Figure 3.9r).

From the enrichment analysis and the (sq) RT-PCR screen five up-regulated genes in ADPKD from two different types of experiments were selected out of the 33 candidates found enriched at least 4-fold in the microarray (Figure 3.5). The next steps consisted in proving the interaction between these genes and their predicted miRNA target using dual-reporter luciferase assays.

Dual-reporter luciferase assays to confirm the miRNA/mRNA interactions

Dual-reporter luciferase assays are the method of choice to study the interaction between a miRNA and its predicted gene target. Plasmids containing part of the 3'UTR sequence of the five selected candidates containing (one of) the seed sequence(s) for mir-193b-3p or mir-582-5p accordingly (Figures 3.10a, 3.10b, 3.10c, 3.10d and 3.10e) between the control Renilla luciferase (hRluc-neo) reporter and the Firefly luciferase (luc2) reporter were generated. *CALB1* was a predicted target for mir-193b-3p while mir-582-5p was predicted to target the four other genes' mRNA *CLIC5*, *PKP2*, *IL1RAP* and *SYT1*. Co-expressing the miRNAs mimics and the 3'UTR-coding plasmid induced a significant reduction of the fluorescent signal for all the targets. pmirGLO-*CALB1*'s expression levels (Figure 3.10f) were reduced to 71 % of the negative control condition with 10 nM of mir-193b-3p mimic and to 57 % with mir-193b-3p mimic at 50 nM. Similarly, *CLIC5*'s fluorescence levels were at 71 % of control at 10 nM and 54 % at 50 nM with p-values highly significant. The three other genes *PKP2*, *IL1RAP* and *SYT1* showed lower reduction levels with fluorescence intensities around 70 % of the control at 50 nM. Co-transfections of mir-582-5p mimic at 10 nM also led to less significant fluorescent signal reduction for *PKP2* (Figure 3.10h) and *IL1RAP* (Figure 3.10i).

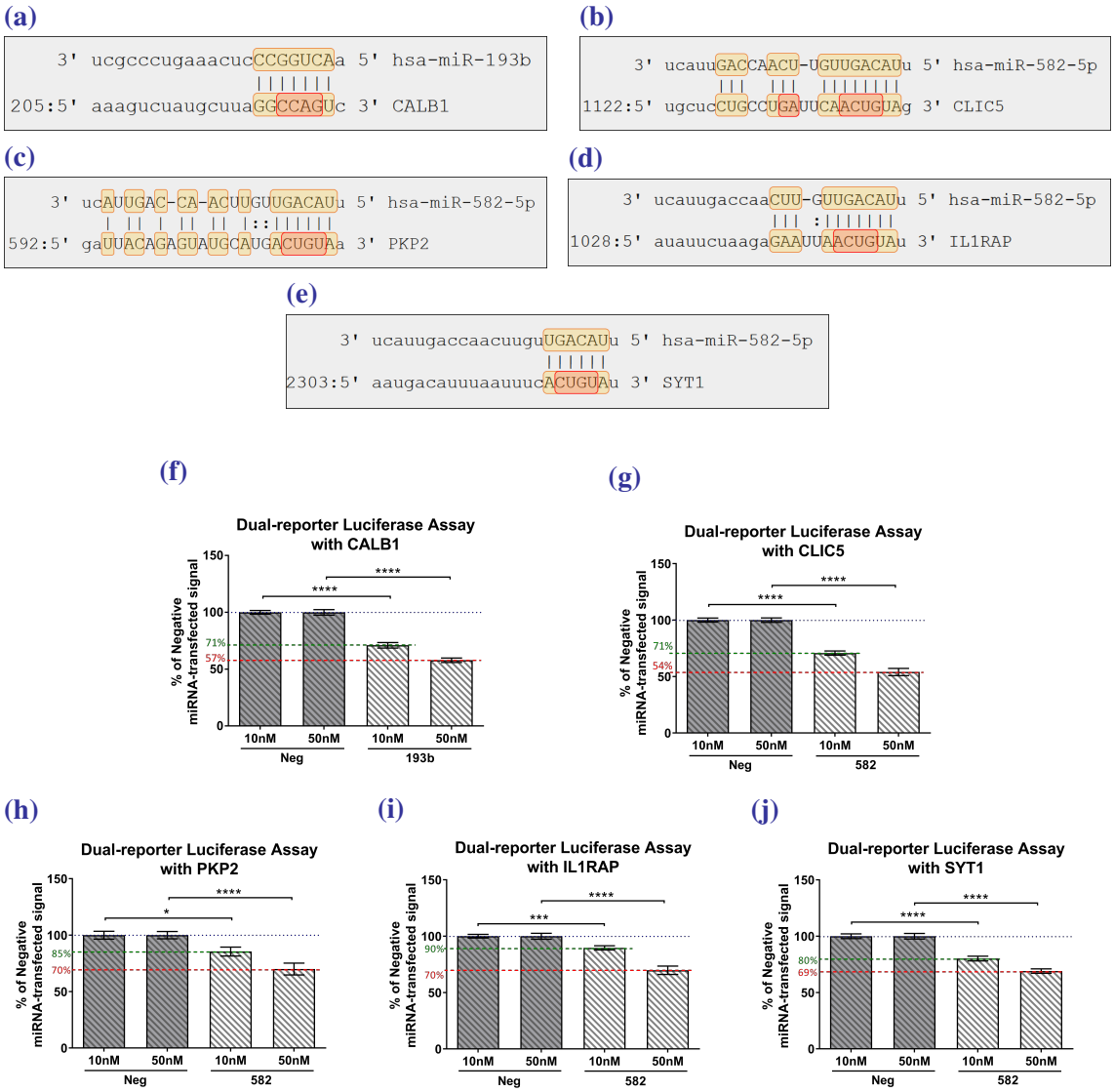

Figure 3.10: **Dual-reporter luciferase assays for miRNA/mRNA interaction study.**
(a, b, c, d, e) Predicted seed sequences of mir-193b-3p on *CALB1* 3'UTR or of mir-582-5p on *CLIC5*, *PKP2*, *IL1RAP* and *SYT1* (source: www.microrna.org). Yellow: seed sequences of the miRNA on the 3' UTR sequence. Red: four to six mutated bases for dual-reporter luciferase assay with mutants. (f, g, h, i, j) Dual-reporter luciferase assays (n=3) showing the Negative-miRNA-transfected condition (control) as a reference and the reduction of fluorescent signal compared to the control in mir-193b (labelled "193b") or mir-582-mimic ("582") -transfected conditions at 10 and 50 nM miRNA concentration.
** p=0.01 *** p=0.0002 **** p<0.0001 (Unpaired t-test).*

The luciferase assays with the WT 3'UTR sequences suggesting that all the candidates could be targets for their predicted miRNA, albeit to a lesser extent for *PKP2*, *IL1RAP* and *SYT1* than for *CALB1* and *CLIC5*, mutant 3'UTR sequences-coding plasmids were generated in order to see a reversion of the inhibition of signal.

When four bases of the mir-193b-3p seed sequence were mutated in *CALB1* 3'UTR, the inhibition of the fluorescent signal observed with WT sequence was almost totally reversed (Figure 3.11a) at 10 nM and 50 nM of mir-193b-3p mimic concentration, suggesting that this effect of mir-193b-3p on the WT sequence was due to an interaction between this miRNA and its seed sequence on *CALB1* 3'UTR and that inserting mutations in this seed sequence led to a mismatch between the two thus preventing their interaction and the inhibition of firefly luciferase signal.

The first experiments on *CLIC5* were performed with four mutations (ACUG bases, see seed sequence in Figure 3.10b), results presented in Figure 3.11b. Similarly to *CALB1*, mutating mir-582-5p seed sequence on the gene's 3'UTR induced a significant reversion of signal from 67.8 % to 85.4 % of the Negative control with mir-582-5p mimic at 10 nM and from 62.5 % to 78.6 % of control at 50 nM. However, this reversion not being total, an hypothesis was that this could be due to the complexity and length of the predicted seed sequence of mir-582-5p on *CLIC5*'s 3'UTR and two more mutations were introduced in this sequence as indicated in Figure 3.10b. The luciferase assays with the six mutations gave very similar results to those with four mutations and did not improve the reversion of fluorescent signal, suggesting there were other reasons for the only partial effect of the mutations on mir-582-5p seed sequence. It was still concluded that there was an interaction between mir-582-5p and *CLIC5* and further studies on this gene were carried out.

Mutations in the 3'UTR sequences of the three other genes *PKP2*, *IL1RAP* and *SYT1* (Figures 3.11c, 3.11d and 3.11e) did not induce any significant or high restoration of the fluorescent signal. Co-expression of mir-582-5p at 50 nM and mutant *PKP2* led to a significant reduction but low and not total, and did not show any change at 10 nM.

Similarly, the higher fluorescence level observed with mir-582-5p at 10 nM for *SYT1* was not strongly significant and no change was visible at 50 nM (Figure 3.11e). Hence, it was concluded that there was not enough evidence to demonstrate the interaction between mir-582-5p and *PKP2*, *IL1RAP* or *SYT1* and they were therefore excluded from the study.

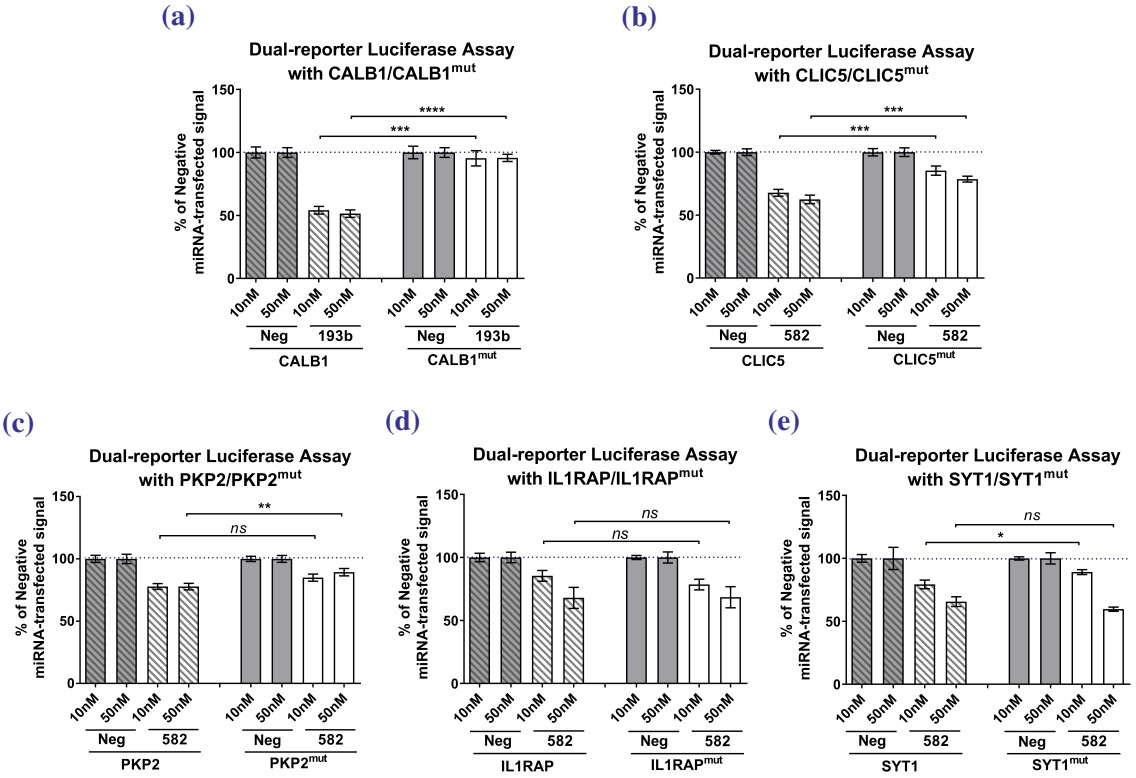

***Figure 3.11:* Dual-reporter luciferase assays with mutant mir-193b-3p or mir-582-5p predicted seed sequences.**
Dual-reporter luciferase assays (n=3) intensity of fluorescence values represented as percentage of control condition (Negative miRNA-transfected cells) with WT (left) and mutant (right) genes' 3'UTR sequences at 10 and 50 nM miRNA concentration.
** p=0.035 ** p=0.006 *** 0.001>p>0.0001 **** p<0.0001 (Unpaired t-test).*

The luciferase assays were useful to select two targets from the initial microarray thanks to their highly probable interaction with my two miRNAs of interest mir-193b-3p or mir-582-5p: *CALB1* and *CLIC5*. The next steps of the study consisted in validating this deregulation at the protein level and in other models *i.e. Pkd1*$^{-/-}$ mice cells and kidney tissues.

3.4.2 Calbindin-1 is a target for mir-193b-3p deregulated in ADPKD

The first target selected from the parallel mRNA/miRNA microarray, the enrichment pathway analysis and the (sq) RT-PCR screen and that was shown for the first time to be interacting with mir-193b-3p was *CALB1*, coding for the Calbindin (or Calbindin D-28K) protein. Calbindin is known to act as a Ca^{2+} sensor and transporter in several different organs including the kidney (Schmidt, 2012). Its function in ADPKD is unknown but as

the PC1/PC2 complex has been suggested to influence calcium signalling and the loss of these proteins' function directly or indirectly leads to the formation of cysts, the influence of a calcium sensor/receptor protein could make sense in the pathogenesis of ADPKD (Mangolini et al., 2016).

Confirmation of the *CALB1*/mir-193b-3p interaction Transfecting normal (UCL93) cells with mir-193b-3p inhibitor and cystic (Ox161c1) cells with mir-193b-3p mimic and analysing the evolution of *CALB1*'s mRNA levels were done to confirm the luciferase assays results i.e. the interaction between mir-193b-3p and *CALB1*.

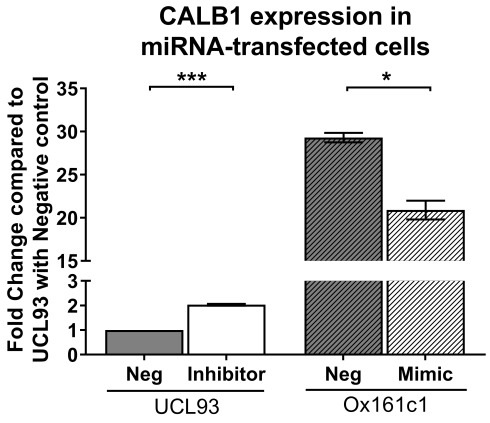

***Figure 3.12:* RT-PCR for the relative expression of *CALB1* in human kidney cells transfected with mir-193b-3p inhibitor or mimic.** The levels of expression of *CALB1* in UCL93 transfected with mir-193b-3p inhibitor and Ox161c1 transfected with mir-193b-3p mimic are expressed as a fold change of the control condition (UCL93 with Negative miRNA). *n=3, * p=0.02 *** p=0.0001 (Unpaired t-test)*

The first observation that could be done from the results presented in Figure 3.12 is that the Ox161c1 cells over-expressed *CALB1* by 29-fold compared to the UCL93 (normal) cells, confirming that this gene is enriched in our model of human ADPKD cells compared to normal.

Transfecting normal cells with a miRNA inhibitor and cystic cells with a miRNA mimic should theoretically lead to an increased and decreased expression of the target gene, respectively. This is in line with what was found with the mir-193b-3p/*CALB1* couple. Indeed, the transfection of normal cells (UCL93) with mir-193b-3p inhibitor led to a significant 2.0-fold increase in *CALB1* expression while transfecting cystic cells (Ox161c1) with mir-193b-3p mimic led to a decrease to 0.7-fold level compared to Negative miRNA-transfected Ox161c1.

Added to the results of the luciferase assays, several evidences were shown that *CALB1* is a target for mir-193b-3p.

The next steps of the analysis were to confirm the deregulation of calbindin D-28K at the protein level in our model of human cells and in human kidney.

Expression levels of calbindin D-28K in human ADPKD cells Western blotting of calbindin was performed in two normal (UCL93 and RFH) and four cystic (Ox161c1, SKI001, Ox938 and SKI002) human cell lines to show an increased expression of the protein in ADPKD.

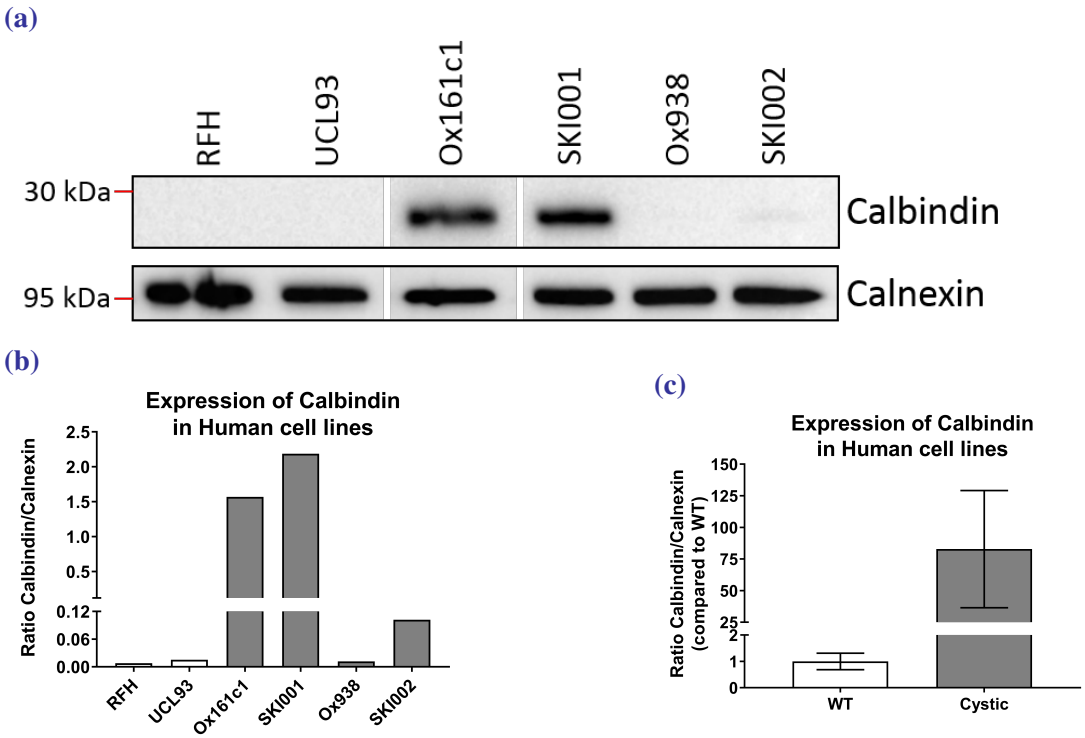

Figure 3.13: **Western blotting of calbindin in normal and cystic human kidney cells.** (a) Calbindin was stained in proteins extracted from two normal (RFH and UCL93) and four cystic (Ox161c1, SKI001, Ox938 and SKI002) human ADPKD cells. Calnexin was used as a loading control. (b) The calbindin/calnexin ratio was measured for each cell line to quantify their expression levels. (c) The expression levels of calbindin were expressed as fold change in cystic cells (grey bars) compared to normal cells (white bars).

As shown in Figure 3.13, calbindin levels in the two normal cells, as well as in the Ox938 (cystic) were barely detectable (ratios around 0.01). In the other cystic cells, however, the band corresponding to the correct protein size was detectable and highly enriched in Ox161c1 and SKI001 (ratios at 1.57 and 2.18 respectively, corresponding to increases of 134 and 187-fold compared to the two normal cell lines). The band was faint in SKI002 but still detectable (ratio of 0.1 or enrichment by 8.7-fold). In the previous (sq) RT-PCR experiments (Figures 3.9a and 3.9b), the relative levels of expression of *CALB1* were similar: Ox938 showed the lowest up-regulation of the mRNA levels while Ox161 and SKI001 were the most enriched cell lines, suggesting that the protein levels are proportional to the mRNA levels.
In order to confirm the enrichment of calbindin D-28K in another model, immunohistochemistry (IHC) was performed on healthy and cystic human kidney tissue.

Immunohistochemistry on human kidney for calbindin D-28K Healthy sections of an adult human kidney and an adult ADPKD patient's kidney were stained for calbindin D-28K and the images from these stainings are presented in Figure 3.14.
The healthy kidney section showed a well structured kidney presenting all the cortex and medulla structures such as glomeruli, distal and proximal tubules. A strong and specific staining was visible in some tubules (Figures 3.14a, b, c), but there was no staining of the glomeruli (Figure 3.14a). The ADPKD kidney, however, was more disorganised with few clear structures identifiable and very little staining (Figures 3.14d, e, f), even in the areas not immediately close to a cyst. The very few stained structures such as the one seen in Figure 3.14e are likely to be tubules. No positive cysts were found in the kidneys examined (data not shown). The staining intensity, however, was equivalent to the one in the healthy kidney section.

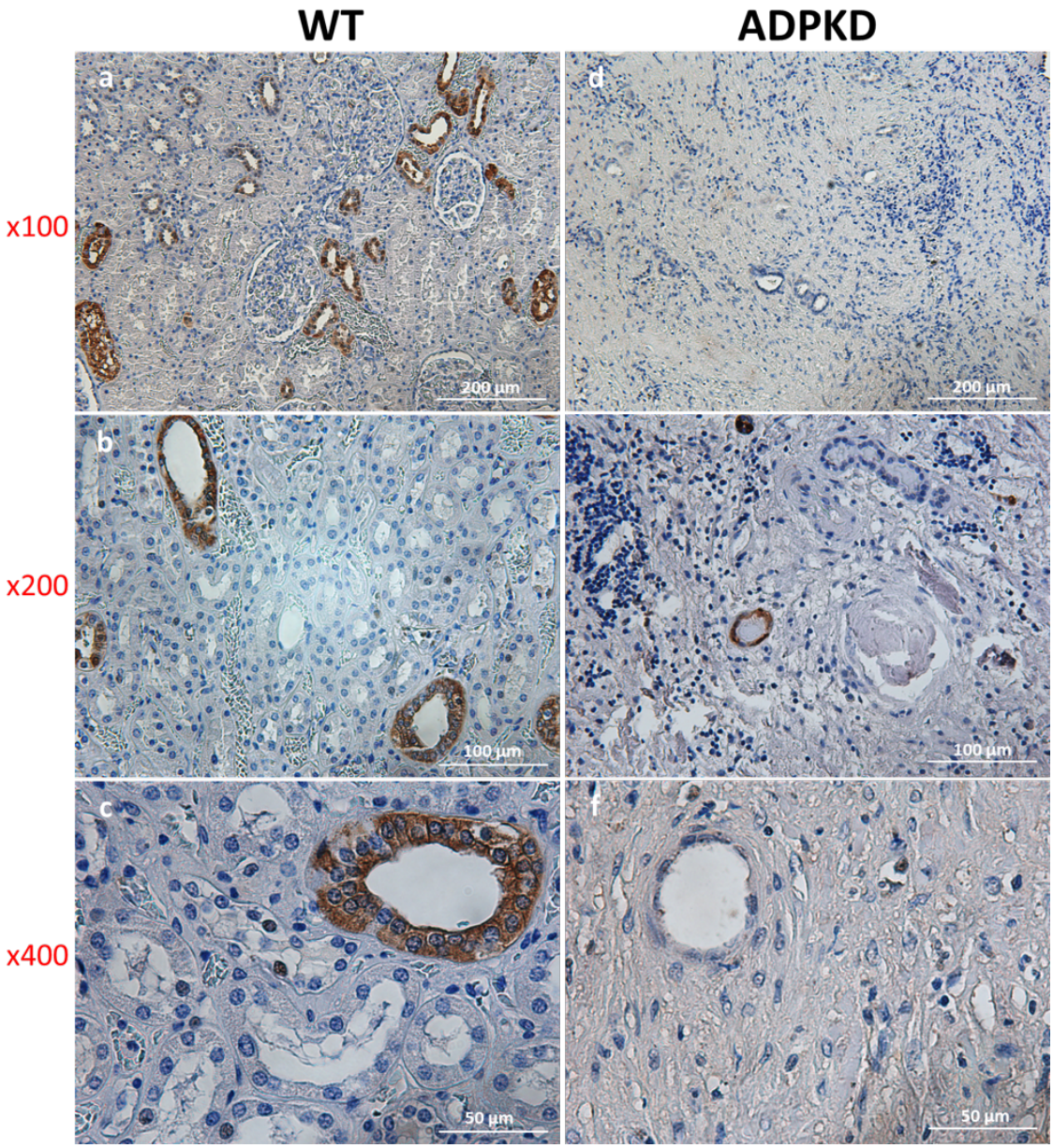

Figure 3.14: **Immunohistochemistry of calbindin D-28K in healthy and ADPKD human kidney.**
Healthy (left) and ADPKD (right) human kidney sections were stained for calbindin and imaged at magnifications 100 (a, d), 200 (b, e) and 400 (c, f). The legend is indicated on the bottom right corner of the different images.

Staining was repeated on a different patient's kidney in order to confirm this observation (Figure 3.15). Similarly, no staining could be observed on this section, whether it was on the cyst's area (Figure 3.15a) or in the rest of the kidney (Figure 3.15b).

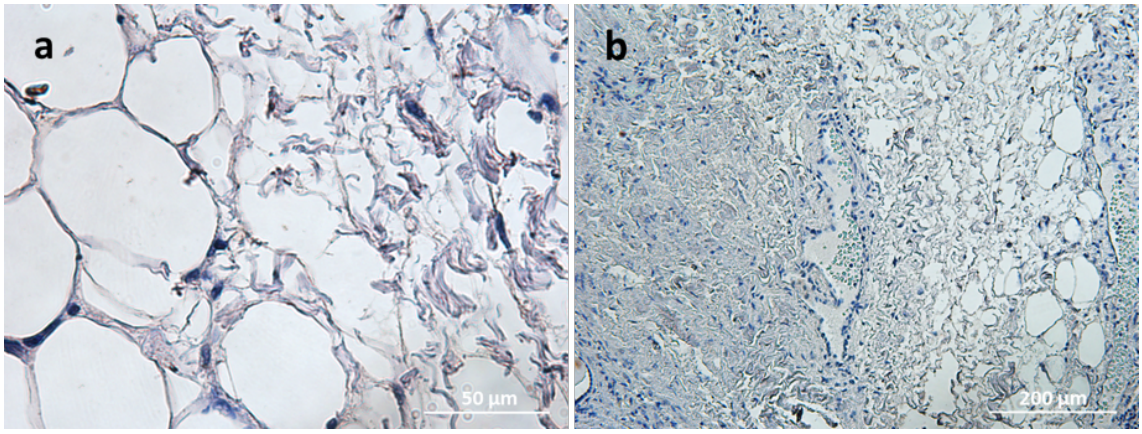

Figure 3.15: **Immunohistochemistry of calbindin D-28K in a different ADPKD human kidney.**
A different ADPKD patient's kidney section was stained for calbindin and imaged at magnifications 400 (a) or 100 (b). The legend is indicated on the bottom right corner of the different images.

The immunohistochemistry stainings showed contradictory results to the previous human cells-based experiments, *i.e.* it showed less or no expression of calbindin in ADPKD compared to a strong expression in healthy kidney. In order to understand whether this was due to a variability between human cells and human kidney, the expression of calbindin was studied in several different mice models.

Expression of calbindin in several mouse models The relative expression levels of *Calb1* were measured by (sq) RT-PCR in four different models of ADPKD mice: two cell lines called Mouse Embryonic Kidney (MEK) cells and F1 cells, and two *in vivo* models: *Pkd1*^{nl,nl} (NeoLox) at 4 and 10 weeks of age and tam-*KspCad*-Cre;*Pkd1*$^{\text{del2-11,lox}}$ (CreLox) at 4 months of age (see Materials and Methods chapter for more details).

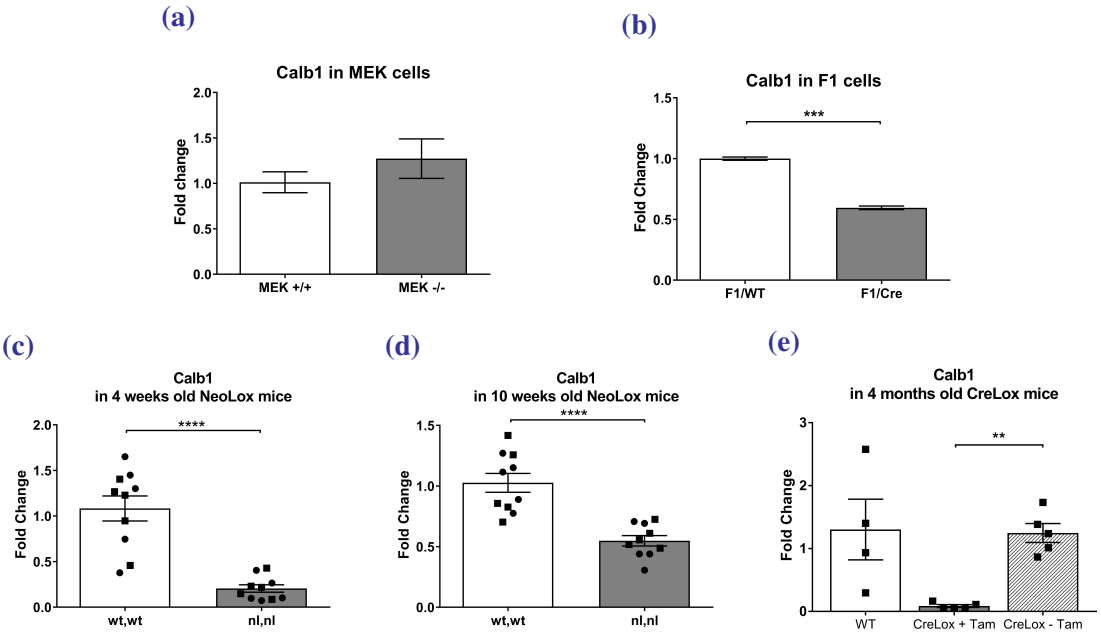

Figure 3.16: **(sq) RT-PCR for the relative expression of *Calb1* in four different mouse models of ADPKD.**
(sq) RT-PCR was performed in (a) MEK cells, (b) F1 cells, (c, d) five females and five males WT and five females and five males NeoLox mouse kidneys at 4 and 10 weeks and (e) four WT, five CreLox+Tamoxifen and five CreLox-Tamoxifen kidneys at 4 months. The CreLox model is a conditional model that presents an ADPKD phenotype after injection of tamoxifen (grey bar). The values are expressed as a fold change compared to WT conditions (white bar). Males are symbolised as squares and females as circles.
** p=0.001 *** p=0.003 **** p<0.0001 (Unpaired t-test with Welch's correction).*

While *Calb1* expression was unchanged in MEK (Figure 3.16a), it was significantly down-regulated in all the other models. Indeed, *Calb1* was significantly under-expressed in F1/Cre cells at levels of 0.59-fold of F1/WT (Figure 3.16b) and significantly down-regulated to levels at 0.20 and 0.55 of the WT mice in the NeoLox model at 4 and 10 weeks of age, respectively (Figures 3.16c and 3.16d). The down-regulation of *Calb1* in CreLox mice treated with tamoxifen reached a 0.08-fold value compared to the WT mice (Figure 3.16e). The untreated CreLox mice showed a relative expression level around the value of the WT and a significant difference with the ADPKD condition.
All these taken together, *Calb1* was strongly down-regulated in the mouse model at the mRNA level.
Immunohistochemistry was performed next on NeoLox mice kidneys to confirm this observation at the protein level.

Expression of calbindin D-28K in 2 and 4 weeks old NeoLox mice kidney tissue

Pkd1^{nl,nl} mouse kidneys paraffin-embedded sections were processed for detection of calbindin by immuno-histochemistry. Calbindin D-28K was detectable in two week (Figure 3.17) and four week (Figure 3.18) WT and ADPKD (NeoLox) mice kidneys.

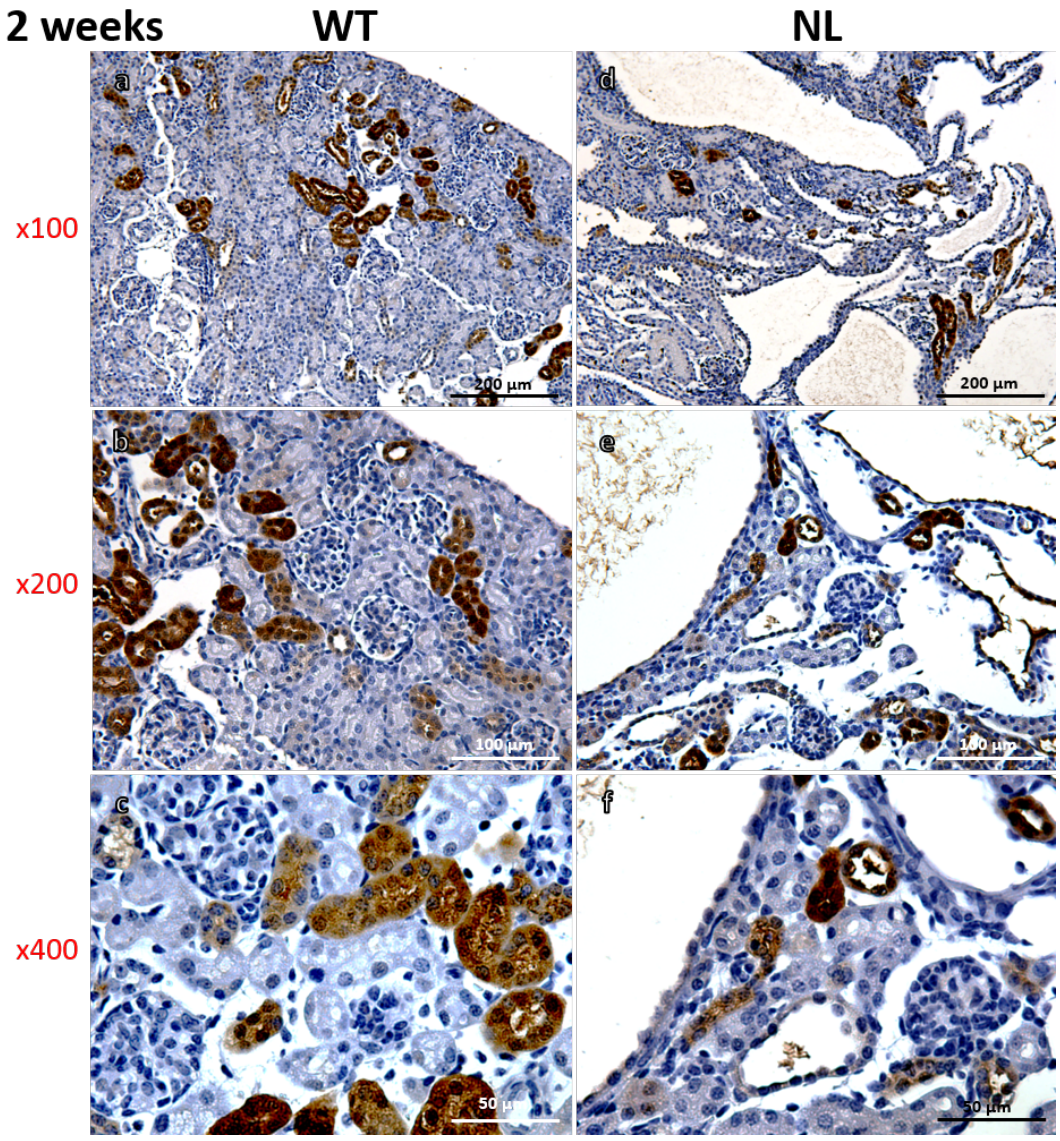

Figure 3.17: **Immunohistochemistry of calbindin D-28K in 2 weeks old NeoLox mice kidneys.** Healthy (left) and NeoLox (right) mice kidney sections were stained for calbindin and imaged at magnifications 100 (a, d), 200 (b, e) and 400 (c, f). The legend is indicated on the bottom right corner of the different images.

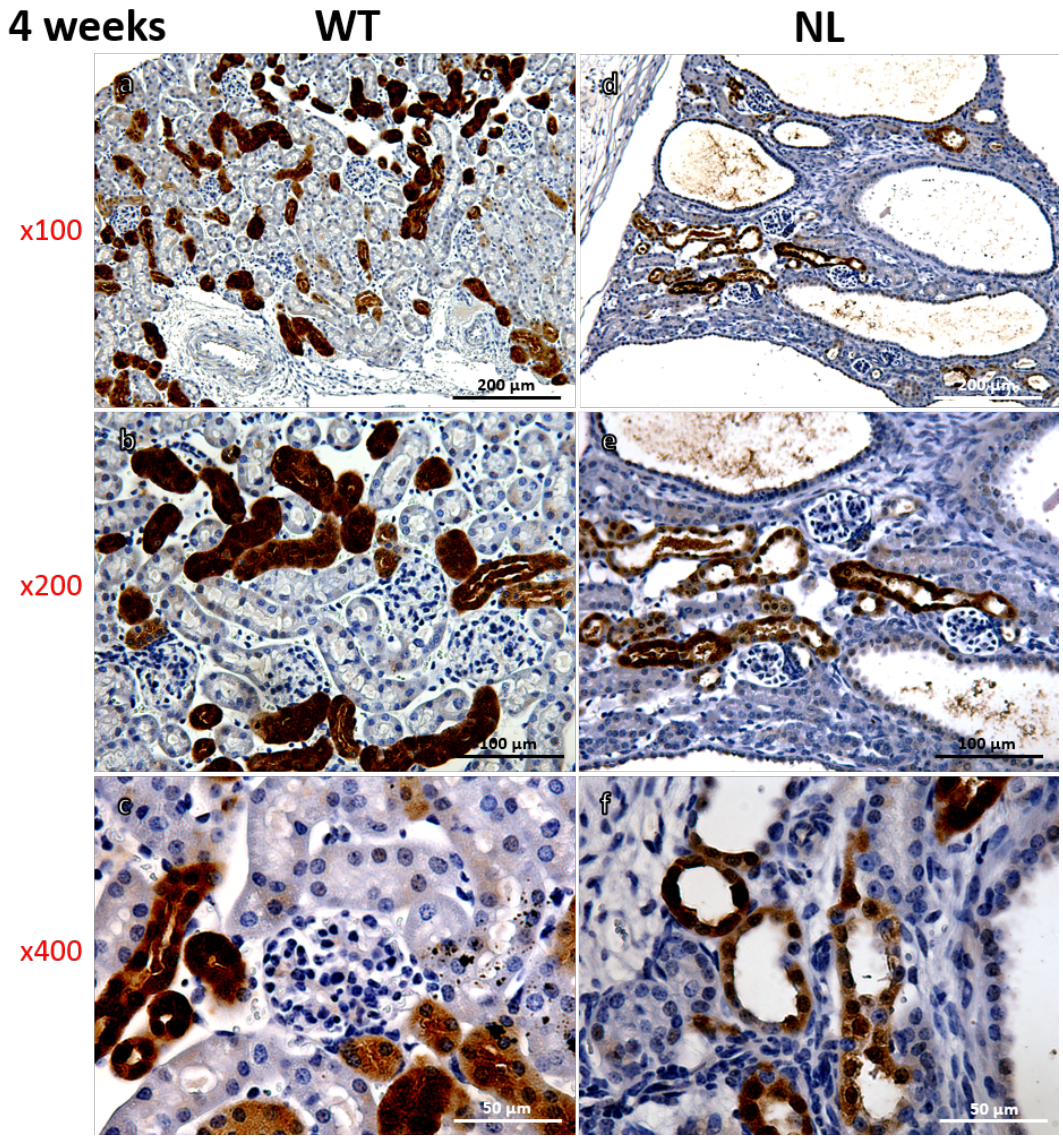

Figure 3.18: **Immunohistochemistry of calbindin D-28K in 4 weeks old NeoLox mice kidneys.** Healthy (left) and NeoLox (right) mice kidney sections were stained for calbindin and imaged at magnifications 100 (a, d), 200 (b, e) and 400 (c, f). The legend is indicated on the bottom right corner of the different images.

Pkd1^{nl,nl} mice kidneys at 2 weeks already presented large cysts while 4 weeks old mice kidney were almost totally composed of cysts and had few medullary and cortical structures left. At both time points a strong, specific and localised tubular staining was detectable in both WT and ADPKD conditions. Similarly to what was observed in human kidneys (Figure 3.14), some tubules were stained while some others and the glomeruli were not.

The intensity of staining was similar between WT and ADPKD kidneys, but the loss of tubules in the NeoLox condition suggests a global defect in the calbindin protein in the disease compared to healthy kidneys.

As a summary, the expression of calbindin and its deregulation in ADPKD was contradictory between our model of human cells and human kidney tissues and multiple mice models. However, I showed multiple evidences that *CALB1* is a target for mir-193b-3p, which could be of interest in future therapeutics approach in diseases where this protein is confirmed to be dysregulated.

3.4.3 Chloride intracellular channel 5 (CLIC5) is a potential target for mir-582-5p and is deregulated in ADPKD

CLIC5 was strongly enriched in human ADPKD cells (see Figure 3.9) and belongs to a family of six putative ion channels structurally related to glutathione-S-transferases (GST) proteins (Singh et al., 2007). The CLICs have been reported to have various activities not exclusively related to chloride channel; Clic5 interacts with ezrin and podocalyxin, members of the actin cytoskeleton and hence has a role on podocyte integrity (Pierchala, 2010), and may also act as an enzyme due to its homology with the GST proteins (Littler et al., 2010). As it is highly expressed in the kidney (http://biogps.org database, see Wu et al. (2016)) and based on my initial results for this gene/protein, this candidate was deemed a potentially relevant target for ADPKD and selected for further studies.

Interaction between *CLIC5* and mir-582-5p UCL93 (normal) and Ox161c1 (cystic) cells were transfected with mir-582-5p inhibitor or mir-582-5p mimic, respectively, and the relative expression levels of *CLIC5* measured by (sq) RT-PCR in these cells. The results are presented in Figure 3.19.

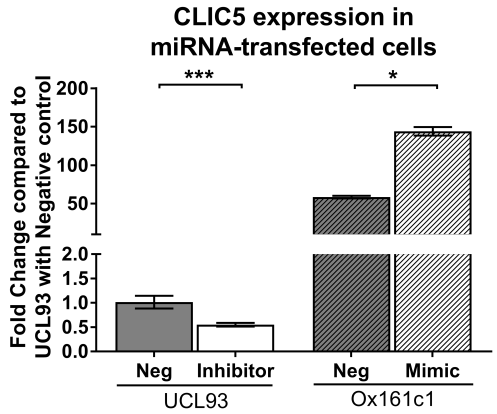

Figure 3.19: **RT-PCR for the relative expression of *CLIC5* in human kidney cells transfected with mir-582-5p inhibitor or mimic.**
The levels of expression of *CLIC5* in UCL93 transfected with mir-582-5p inhibitor and Ox161c1 transfected with mir-582-5p mimic are expressed as a fold change of the control condition (UCL93 with Negative miRNA).
*n=3, * p=0.02 *** p=0.0001 (Unpaired t-test)*

As mentioned previously, transfection with mir-582-5p inhibitor should theoretically induce an increase in *CLIC5* expression while transfecting cystic (Ox161c1) cells with mir-582-5p mimic should lead to decreased *CLIC5* levels relative to the control condition. First of all, the levels of *CLIC5* were 58-fold higher in the cystic cells compared to normal, which is in line with the previous (sq) RT-PCR results in human cells.
Unexpectedly, transfection of the cells with mir-582-5p inhibitor or mimic induced opposite effects than expected. Indeed, the expression of mir-582-5p inhibitor in UCL93 led to a 0.5-fold reduction of *CLIC5*'s levels compared to the negative control condition, while the transfection of Ox161c1 with mir-582-5p mimic led to an increase of this gene's mRNA level by 2.5-fold compared to the negative control condition in Ox161c1.

Because *CLIC5* codes for two isoforms: CLIC5A (isoform 1) and CLIC5B (isoform 2), the first one missing the first 159 amino-acids and having different amino acids at positions 160-180 compared to the canonical sequence isoform 2 (www.uniprot.org, see Figure 3.20a), it was suggested that the two isoforms or mRNA coding for these isoforms may react differently to the co-expression of mir-582-5p. The expression levels of *CLIC5A* and *CLIC5B* were measured individually in two batches of six human cell lines to check which isoform is deregulated in ADPKD.

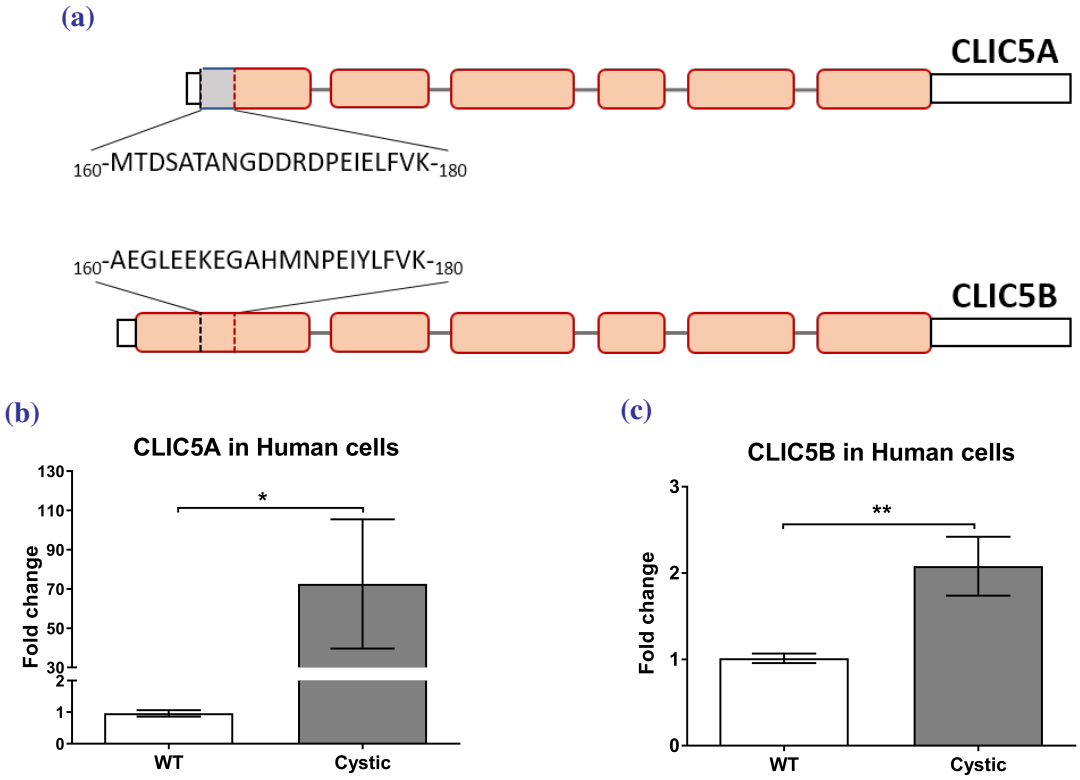

Figure 3.20: **Real-time PCR to measure the relative expression of *CLIC5A* and *CLIC5B* in 6 human cell lines.**
(a) The human CLIC5A isoform differs from CLIC5B by the missing amino-acids 1-159 and a different sequence between positions 160-180 where the specific primers were designed. (b) *CLIC5A* and (c) *CLIC5B* expression was measured in two independent batches of 2 normal (white bar) and 4 cystic (grey bar) cell lines. The values are represented as fold change compared to both normal cell lines (RFH and UCL93).
** p=0.04 ** p=0.006 (t-test with Welch's correction)*

CLIC5A was more highly up-regulated in ADPKD cells than *CLIC5B*. *CLIC5A*'s relative expression levels reached 72.5-fold compared to normal cells, with however a large standard error of the mean value due to a wider range of expression between cell lines (Ox161c1 and SKI001 over-expressed *CLIC5A* by 485-fold and 78-fold in one of the batches compared to 5.2 and 2.2-fold for Ox938 and SKI002, respectively) and between batches (Figure 3.20b). *CLIC5B* up-regulation (2.1-fold compared to normal), was more consistent between cell lines and cells batches (Figure 3.20c).

Expression levels of CLIC5 in human ADPKD cells To confirm the results of the qPCR, Western blotting of CLIC5 was performed in human cells. Because the antibody used for this experiment showed several bands around the expected size of CLIC5A (the

band for CLIC5B was more clear), an optimisation step was necessary preliminarily to the blotting in all cells. HEK cells were either not transfected, or transfected with a plasmid coding for CLIC5A-GFP or a plasmid coding for CLIC5A-RFP. This allowed me to blot either GFP either CLIC5 to study the specificity of the anti-CLIC5 antibody.

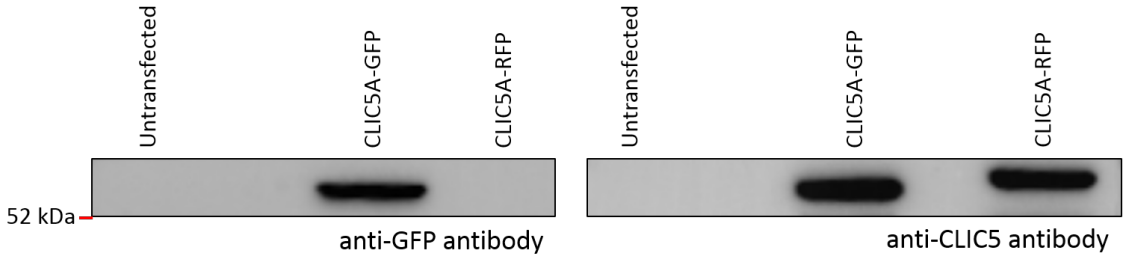

Figure 3.21: **Western blotting of GFP or CLIC5 in CLIC5A-GFP or CLIC5A-RFP transfected cells.**
HEK293 were not transfected or transfected with a CLIC5A-GFP or a CLIC5A-RFP plasmid and their proteins stained for GFP (left) or CLIC5 (right). Expected sizes: CLIC5A = 32 kDa, GFP = 27 kDa, RFP = 27 kDa.

As seen in Figure 3.21, after transfecting HEK cells with a CLIC5A-GFP-coding plasmid the anti-GFP antibody was able to specifically detect a band at the expected size (32+27=59 kDa). The untransfected and the CLIC5A-RFP-transfected cells did not show any band confirming the specificity of the anti-GFP antibody. When the staining was done with the CLIC5 antibody, both transfected conditions showed a strong band around the expected size, the CLIC5A-RFP band being slightly higher than the CLIC5A-GFP. The band for the CLIC5A-GFP condition having been detected at the exact same size with both antibodies, the anti-CLIC5 antibody was confirmed able to stain CLIC5A and at the expected size. Western blotting of CLIC5A and CLIC5B was then carried out on six human cell lines: two normal (RFH and UCL93) and four cystic (Ox161c1, SKI001, Ox938 and SKI002). The expression of CLIC5B was increased in SKI001 and Ox938, mostly, compared to the two WT cell lines RFH and UCL93 (Figures 3.22a and 3.22c), and the global levels of the protein were increased by 1.4-fold compared to normal (Figure 3.22e). CLIC5A was over-expressed in all the cystic cells compared to normal, SKI001 and Ox938 cells showing the highest levels of expression (Figures 3.22a and 3.22b). Global expression levels of CLIC5A were 2.4 times higher in cystic cells than in WT (Figure 3.22d) and this increase was significant.

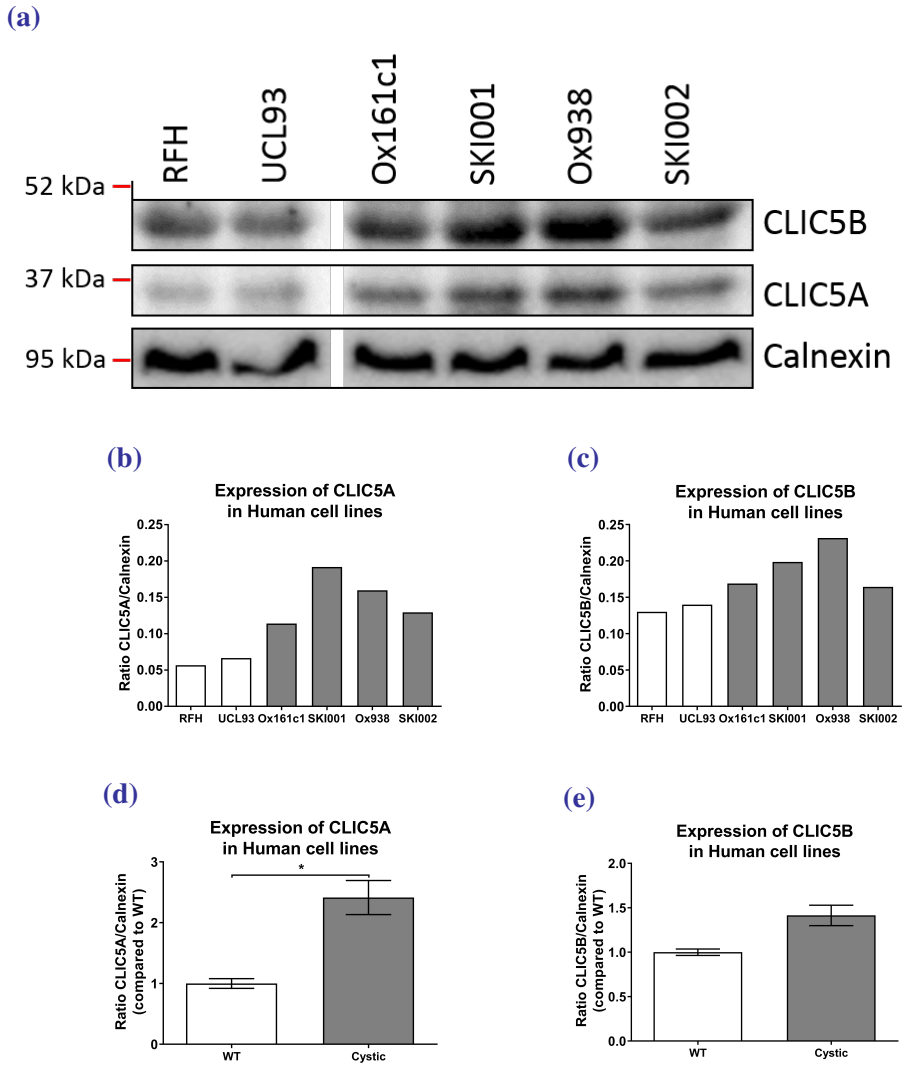

Figure 3.22: **Western blotting of chloride intracellular channels 5a and 5b in normal and cystic human kidney cells.**
(a) CLIC5A and CLIC5B were stained in proteins extracted from two normal (RFH and UCL93) and four cystic (Ox161c1, SKI001, Ox938 and SKI002) human ADPKD cells. Calnexin was used as a loading control. (b, c) The CLIC5A or CLIC5B/calnexin ratio was measured for each cell line to quantify their expression levels. (d, e) The expression levels of CLIC5A and CLIC5B were expressed as fold change in cystic cells (grey bars) compared to normal cells (white bars).
** p=0.029 (Unpaired t-test).*

CLIC5A was more increased in the cystic cells than CLIC5B, which, although not as importantly, is similar to what was found at the mRNA level by (sq) RT-PCR (see Figure 3.20).

In order to confirm this increase of CLIC5 in another human model, immunohistochemistry was performed on healthy and cystic human kidney tissue.

Immunohistochemistry on human kidney for CLIC5

IHC was performed on a healthy and an ADPKD kidney sections to stain CLIC5. Figure 3.23 presents the results of this staining: in both WT and ADPKD tissue, no staining was detected in the tubules or what is left of the medullary and cortical structures. Only the glomeruli showed a specific staining in both conditions. The intensity of staining was slightly higher in WT, but the main difference laid in the number of these structures detectable in the sections. Indeed, while multiple glomeruli were detectable in the WT kidney as its integrity was perfect (Figure 3.23a), only one was present in the whole ADPKD kidney section (Figure 3.23e).

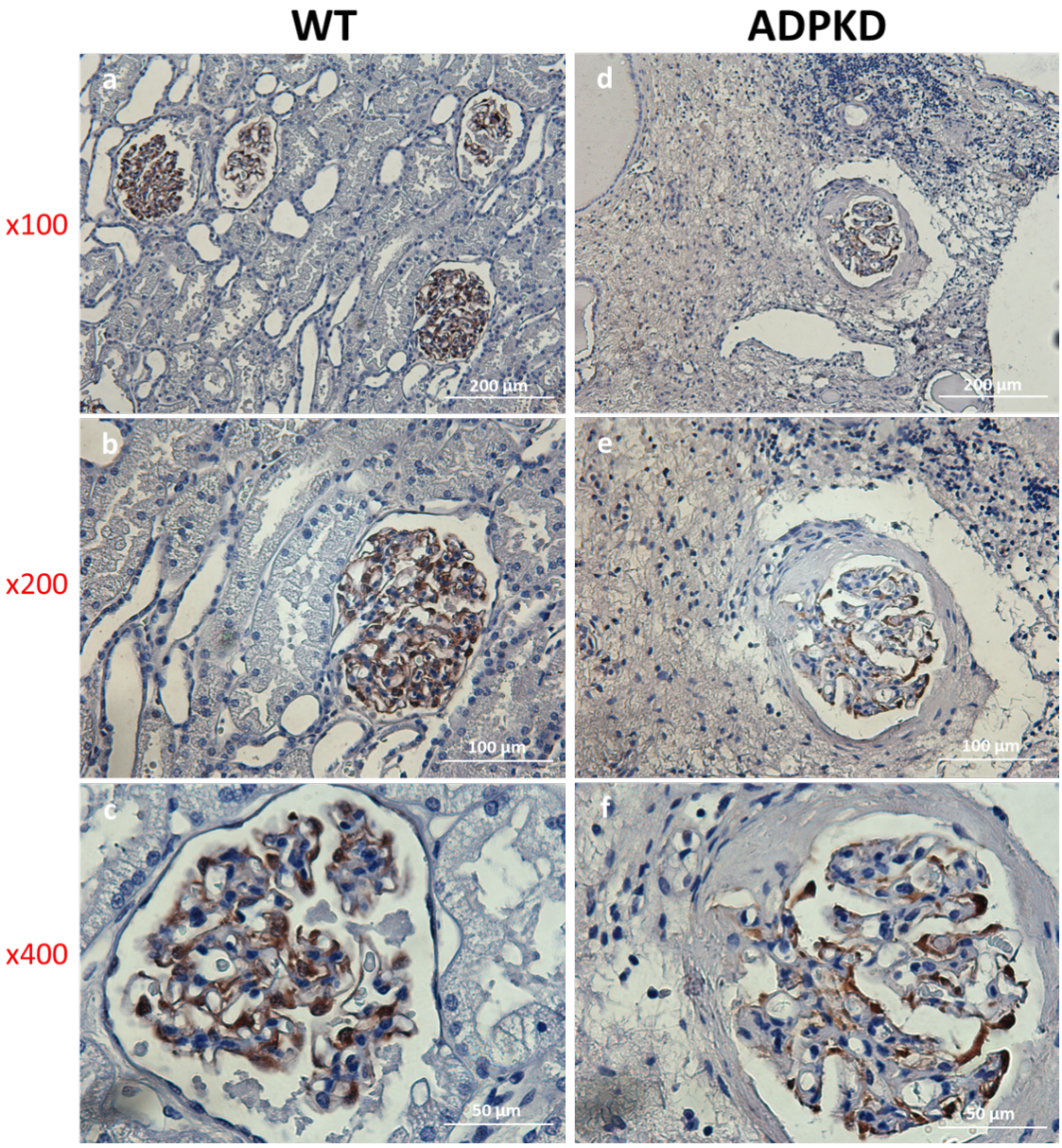

Figure 3.23: **Immunohistochemistry of CLIC5 in healthy and ADPKD human kidney.** Healthy (left) and ADPKD (right) human kidney sections were stained for CLIC5 and imaged at magnifications 100 (a, d), 200 (b, e) and 400 (c, f). The legend is indicated on the bottom right corner of the different images.

These observations suggest that, similarly to what was seen for calbindin D-28K, there is a difference between human cells and other models. To confirm this hypothesis, the expression levels of CLIC5 were measured in several models of ADPKD mice.

Expression of Clic5 in several ADPKD mice models In *Mus musculus*, *Clic5* is predicted to code for only one isoform of the Clic5 protein, making it impossible to make the distinction between Clic5a and Clic5b like in human. The relative expression levels of *Clic5* were measured in the same mice models as previously used for *Calb1*.

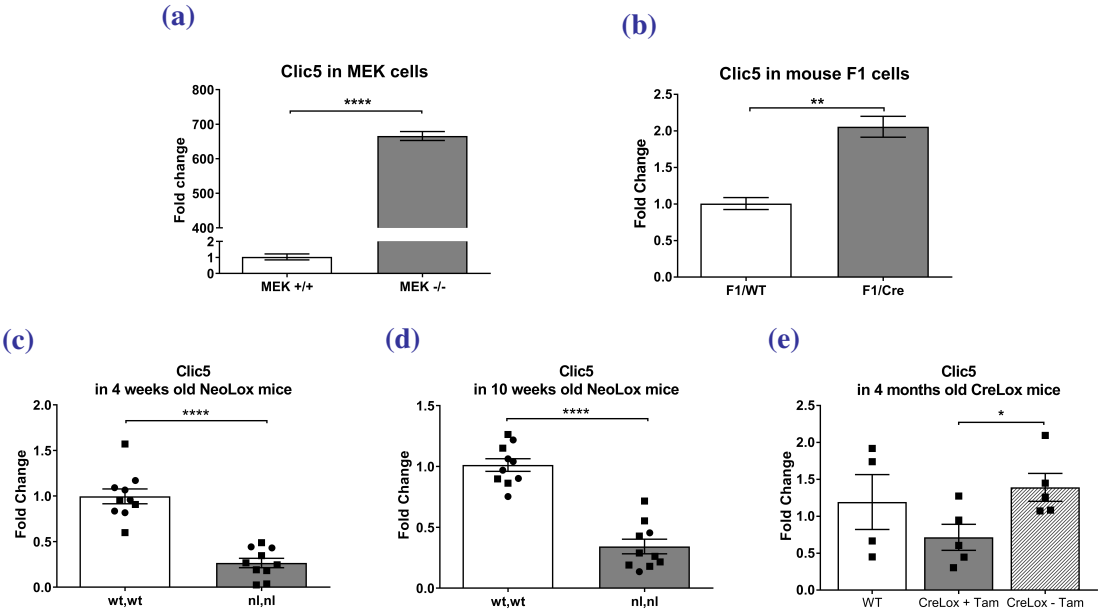

***Figure 3.24:* (sq) RT-PCR for the relative expression of *Clic5* in four different models of ADPKD mouse.**
(sq) RT-PCR was performed in (a) MEK cells, (b) F1 cells, (c, d) five females and five males WT and five females and five males NeoLox mouse kidneys at 4 and 10 weeks and (e) four WT, five CreLox+Tamoxifen and five CreLox-Tamoxifen kidneys at 4 months. The CreLox model is a conditional model that presents an ADPKD phenotype after injection of tamoxifen (grey bar). The values are expressed as a fold change compared to WT conditions (white bar). Males are symbolised as squares and females as circles.
*** p=0.006 **** p<0.0001 (Unpaired t-test with Welch's correction).*

Similarly to the results in human cells (Figure 3.9), *Clic5* was significantly enriched in both mouse cells models. Indeed, its expression levels were increased 665-fold in MEK (Figure 3.24a) and 2-fold in F1 cells (Figure 3.24b). In the $Pkd1^{nl,nl}$ mouse model (NeoLox), however, this gene was significantly down-regulated at 4 and 10 weeks (Figures 3.24c and 3.24d). The expression levels decreased to values 0.27 and 0.34-fold the ones in the WT conditions at these time points, respectively. No difference could be detected in the conditional CreLox model between the tamoxifen-induced ADPKD condition and the WT condition, but a significant 0.3 point reduction was observed between the tamoxifen positive and the tamoxifen negative conditions (Figure 3.24e).

As a summary, *Clic5* was over-expressed in all the cell models we tested (four human and two mouse cell lines), but was down-regulated in human and mice kidneys. The last experiment I performed on this candidate was an immunohistochemistry on NeoLox mice kidneys in order to study Clic5's deregulation in a mouse model at the protein level.

Expression of Clic5 in NeoLox mice kidneys at 2 and 4 weeks *Pkd1*^{nl,nl} hypomorph mice were sacrificed at 2 and 4 weeks and their kidneys fixed in paraffin for future immunohistochemistry. Staining of Clic5 in these mice is presented in Figures 3.25 (2 weeks) and 3.26 (4 weeks).

Background staining was visible in some tubules in WT and in the remnants of the medulla and cortex in ADPKD at 2 and 4 weeks. Similarly to human kidney, the glomeruli showed a very strong staining in WT and ADPKD at both ages, at equivalent intensity between the healthy and diseased kidney. The difference between the two conditions resided in the number of glomeruli present in the section: WT kidneys presented visibly more glomeruli than ADPKD kidneys, suggesting a global loss of expression of the Clic5 expressed in these structures.

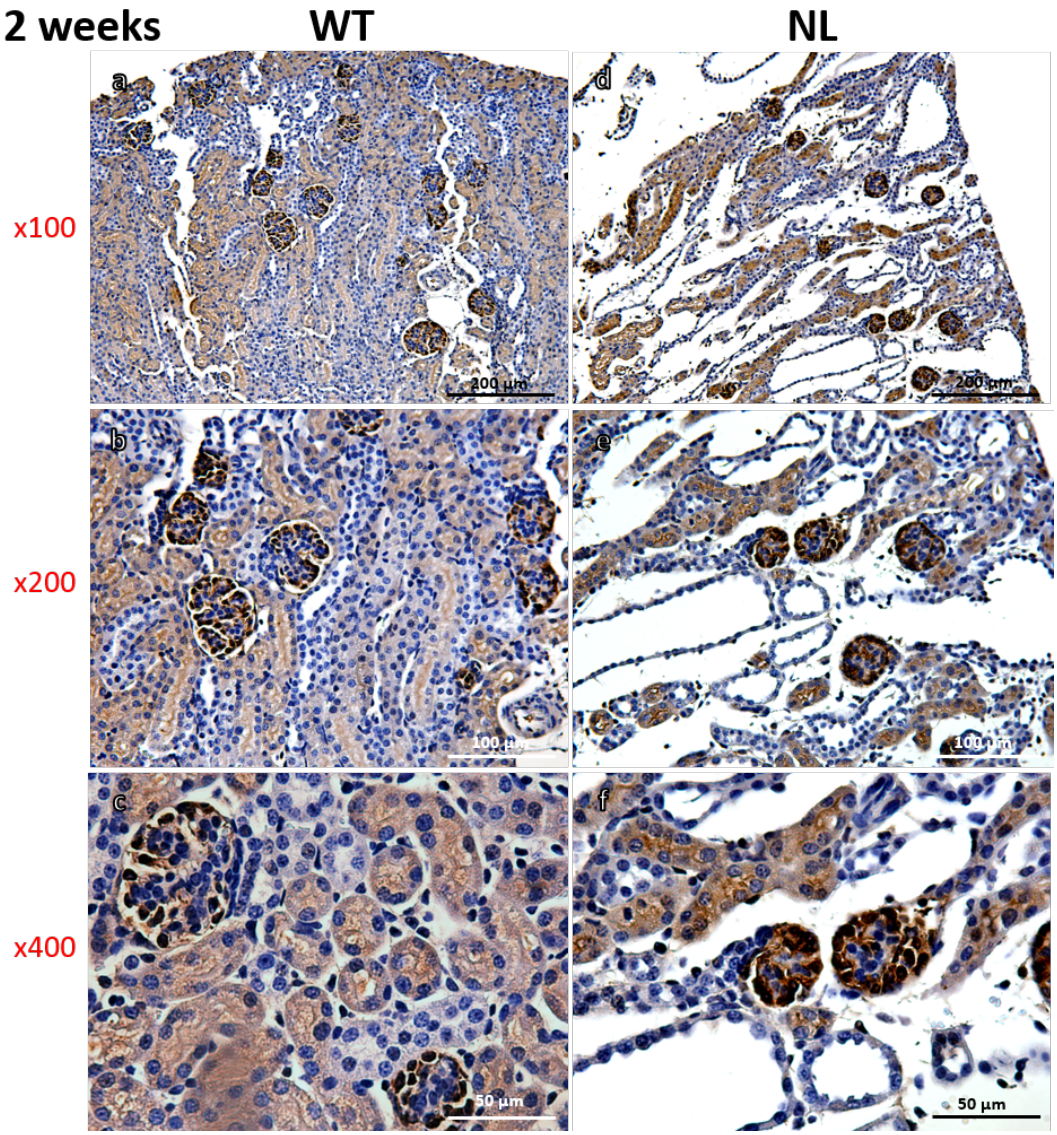

Figure 3.25: **Immunohistochemistry of chloride intracellular channel 5 (Clic5) in 2 weeks old NeoLox mice kidneys.**
Healthy (left) and NeoLox (right) mice kidney sections were stained for Clic5 and imaged at magnifications 100 (a, d), 200 (b, e) and 400 (c, f). The legend is indicated on the bottom right corner of the different images.

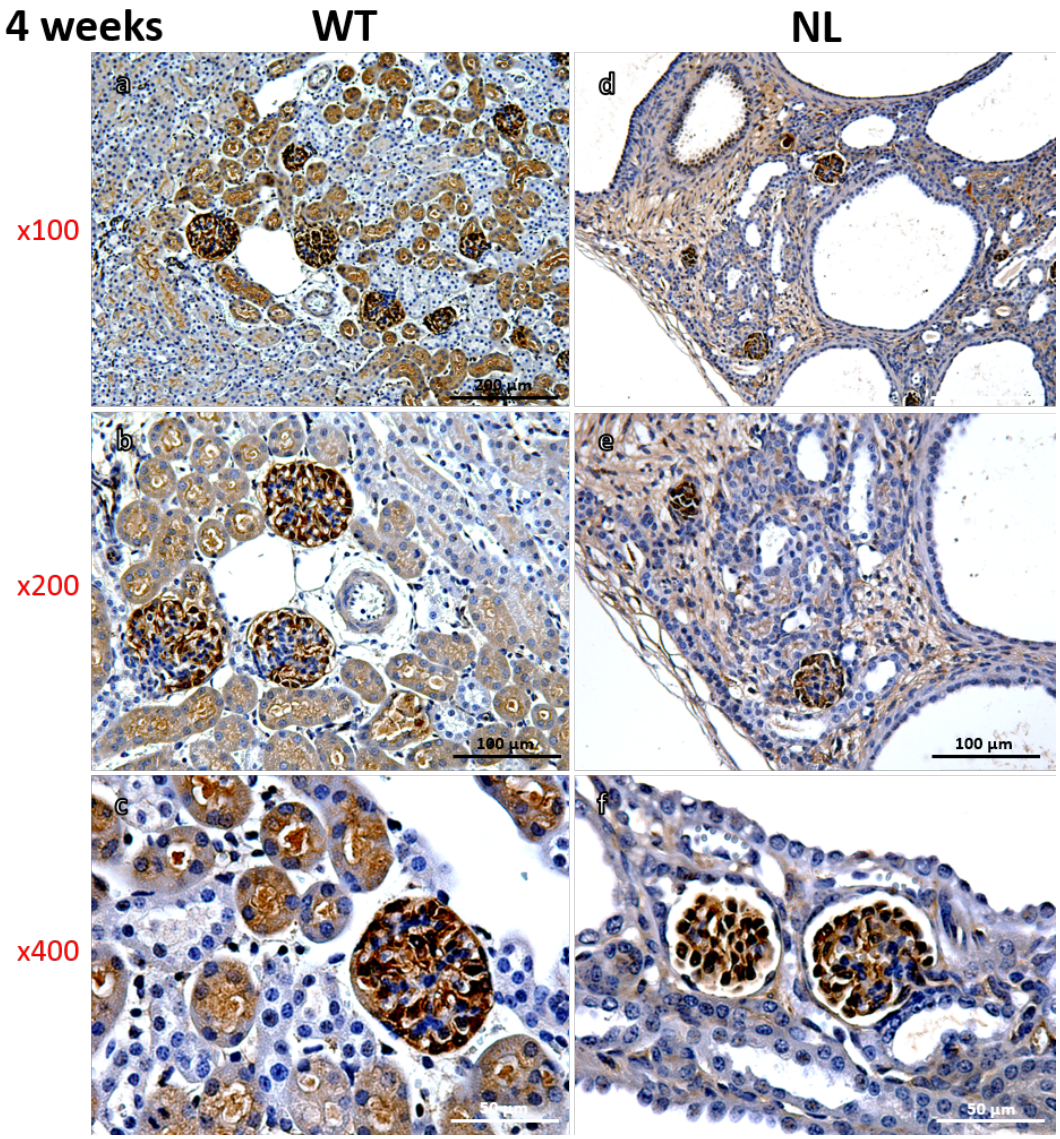

Figure 3.26: **Immunohistochemistry of chloride intracellular channel 5 (Clic5) in 4 weeks old NeoLox mice kidneys.**
Healthy (left) and NeoLox (right) mice kidney sections were stained for Clic5 and imaged at magnifications 100 (a, d), 200 (b, e) and 400 (c, f). The legend is indicated on the bottom right corner of the different images.

Taken together, the data on *CLIC5* was different between models. Human and mouse cell lines suggested an increase of this gene's expression and the protein in ADPKD, while *in vivo* models such as human and mice kidneys showed a global down-regulation of *CLIC5* and its protein. This underlined the importance of validating the dysregulation of a candidate in different models before performing further experiments in order to work on a consistently enriched gene across models.

3.5 Selection of new candidates from our mRNA microarray

Following this, the second approach was decided (described in Figure 2.3 in the Materials and Methods chapter). Rather than basing my selection on the list of predicted targets for mir-193b-3p and mir-582-5p, I ranked the most enriched mRNA from the initial microarray by p-value and fold change and focused on the potentially most relevant candidates for ADPKD based on their function. Eight genes were selected from this approach and are presented in Table 3.1.

Table 3.1: Genes selected from our mRNA microarray based on their fold change, p-value and function

p-value	FC Absolute	Gene Symbol	Name
0.003	84.20	**SPOCK2**	SPARC/Osteonectin Cwcv And Kazal Like Domains Proteoglycan 2
0.019	56.88	**ANO1**	Anoctamin 1 calcium activated chloride channel
7.37E-05	26.09	**RPS6KA2**	Ribosomal protein S6 kinase 90 kDa polypeptide 2
3.91E-04	18.51	**PTGIS**	Prostaglandin I2 (prostacyclin) synthase
8.63E-04	12.35	**CCNA1**	Cyclin A1
0.003	8.73	**GREM2**	Gremlin 2 DAN family BMP antagonist
4.82E-04	8.50	**SYK**	Spleen tyrosine kinase
0.007	7.30	**LCN2**	Lipocalin 2

Among the genes selected for further (sq) RT-PCR validation steps, *SPOCK2* and *ANO1* were the ones presenting the highest fold changes with increases of 84.20-fold and 56.88-fold compared to normal cells. The three following, namely *RPS6KA2*, *PTGIS* and *CCNA1* were short-listed because of their rather high increase (between 12.35 and 26.09) and their high p-value ($p<0.0008$). The last three candidates were interesting because of their function or fold change and p-value. As said above, (sq) RT-PCR were carried out in three independent batches of normal and cystic human cells. For more clarity, only the three consistently deregulated genes (*RPS6KA2*, *ANO1* and *CCNA1*) are presented in the following Figure 3.27. The summary of all genes tested can be found in Table 3.2.

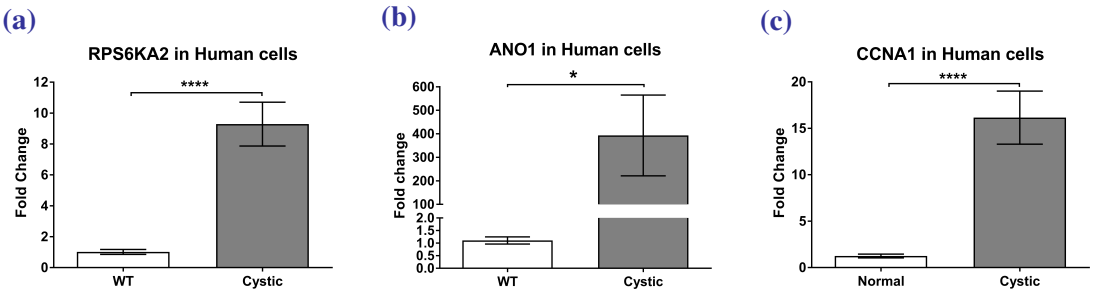

***Figure 3.27:* (sq) RT-PCR for the relative expression of *RPS6KA2*, *ANO1* and *CCNA1* in two normal and four cystic human cells.**
(sq) RT-PCR was carried out for eight candidates selected from the mRNA microarray in three independent batches of two normal (RFH and UCL93) and four cystic (Ox161c1, SKI001, Ox938, SKI002) cell lines. (a) *RPS6KA2*, (b) *ANO1* and (c) *CCNA1* were significantly down-regulated in cystic cells compared to normal. Values are expressed as fold change of the levels in normal cells (white bar).
** p=0.04 ** p=0.001 **** p<0.0001 (Unpaired t-test with Welch's correction).*

RPS6KA2 (Figure 3.27a) was significantly enriched by 9.3-fold in cystic cells compared to normal, while *CCNA1* (Figure 3.27c) expression was significantly increased by 16.1-fold in ADPKD cells and *ANO1* (Figure 3.27b) was over-expressed 393-fold in the disease conditions.

Because of the possible inconsistency between models found in the previously mentioned work on *CALB1* and *CLIC5*, the next steps consisted in validating the deregulation of these three targets in three different mice models: two mice cell lines MEK and F1, and one *in vivo* mouse model $Pkd1^{nl,nl}$ hypomorph at 4 and 10 weeks (Figure 3.28).

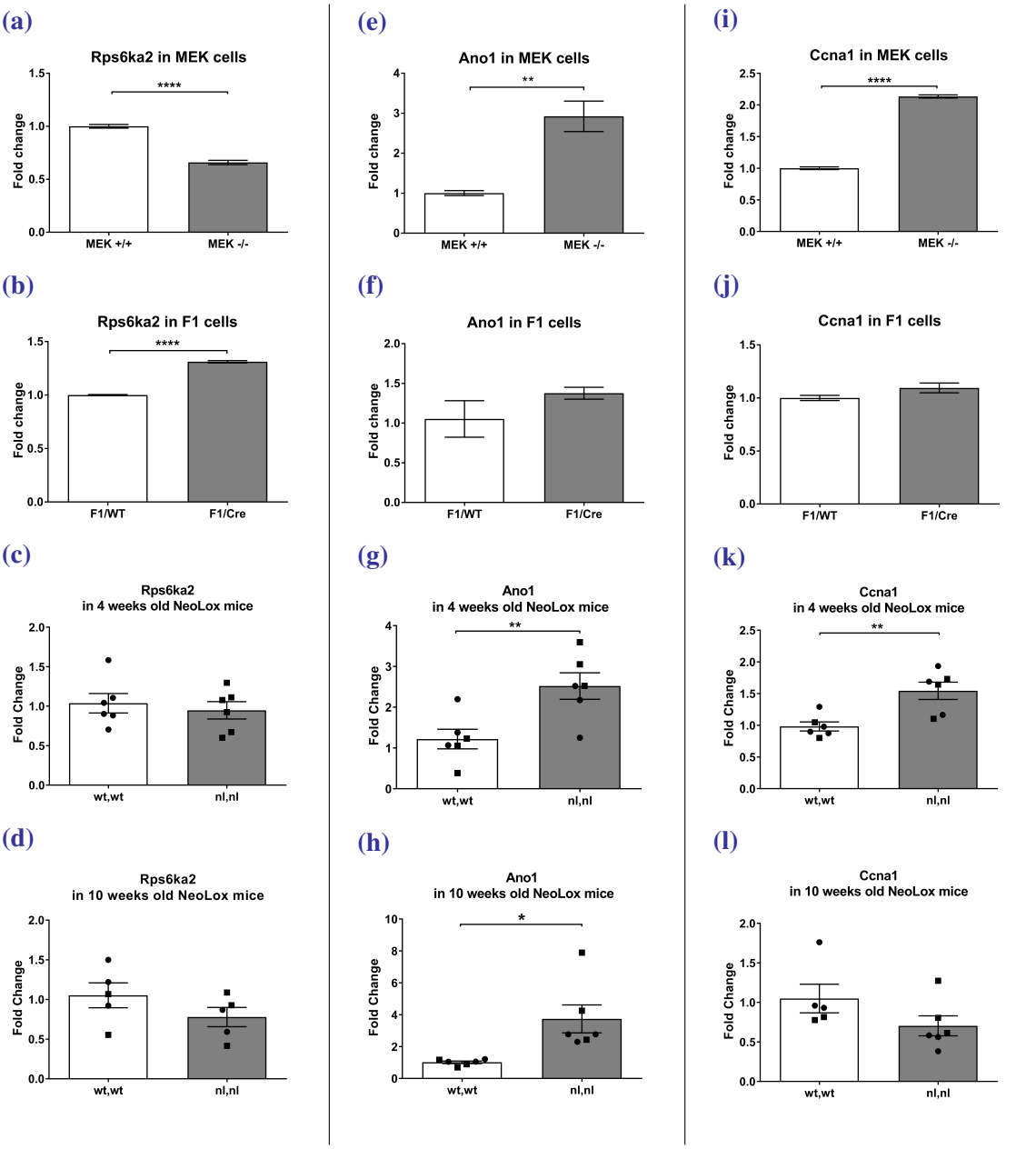

Figure 3.28: **(sq) RT-PCR for the relative expression of *Rps6ka2*, *Ano1* and *Ccna1* in two ADPKD mouse cell lines and one *in vivo* mouse model.**
(sq) RT-PCR was carried out for (left panel) *Rps6ka2*, (central panel) *Ano1* and (right panel) *Ccna1* in (a, e, i) MEK cells (n=3), (b, f, j) F1 cells (n=3) and NeoLox mice at (c, g, k) 4 weeks (three males and three females of each phenotype) and (d, h, l) 10 weeks (three males and three females of each phenotype). Values are expressed as fold change of the levels in normal conditions (white bars) and ADPKD conditions are shown in grey bars. Males are symbolised as squares and females as circles.
** p=0.027 ** 0.009>p>0.001 **** p<0.0001 (Unpaired t-test).*

Rps6ka2 showed contradictory data between models. Indeed, while it was significantly down-regulated to 0.7 fold in MEK Null compared to MEK WT (Figure 3.28a), it was very slightly but significantly increased 1.3-fold in F1/Cre compared to F1/WT (see Figure 3.28b), and showed no change in expression in the $Pkd1^{nl,nl}$ hypomorph mouse model at both time points (Figures 3.28c and 3.28d).
Ano1, on the contrary, presented a consistent up-regulation in MEK and NeoLox mice at both time points. Indeed, its expression was significantly increased by 2.9-fold in MEK (Figure 3.28e) and by 2.5 and 3.8-fold in the hypomorph model at 4 and 10 weeks respectively (Figures 3.28g and 3.28h). No change was visible in the F1 cells (Figure 3.28f).
Finally, *Ccna1* was significantly enriched in half of the models: 2.1-fold increase in MEK and 1.5-fold increase in 4 weeks old NeoLox mice (Figures 3.28i and 3.28k). No change in this mRNA's expression levels was detectable in either the F1 cells or the 10 weeks old mice kidneys (Figures 3.28j and 3.28l).

Out of the eight genes identified by analysing solely the results of the mRNA microarray, *ANO1* appeared to be the most promising candidates as its increase was strong in the initial microarray and conserved across almost all other models. As the microrna.org database predicted it could be a target for mir-582-5p, the interaction between these two element was assessed using dual-reporter luciferase assays.

Interaction between *ANO1* and mir-582-5p Part of *ANO1*'s 3'UTR sequence containing the predicted seed sequence of mir-582-5p was cloned into a pmirGLO vector as previously and dual-reporter luciferase assays were performed with the WT and the mutant sequence in which two bases were mutated.

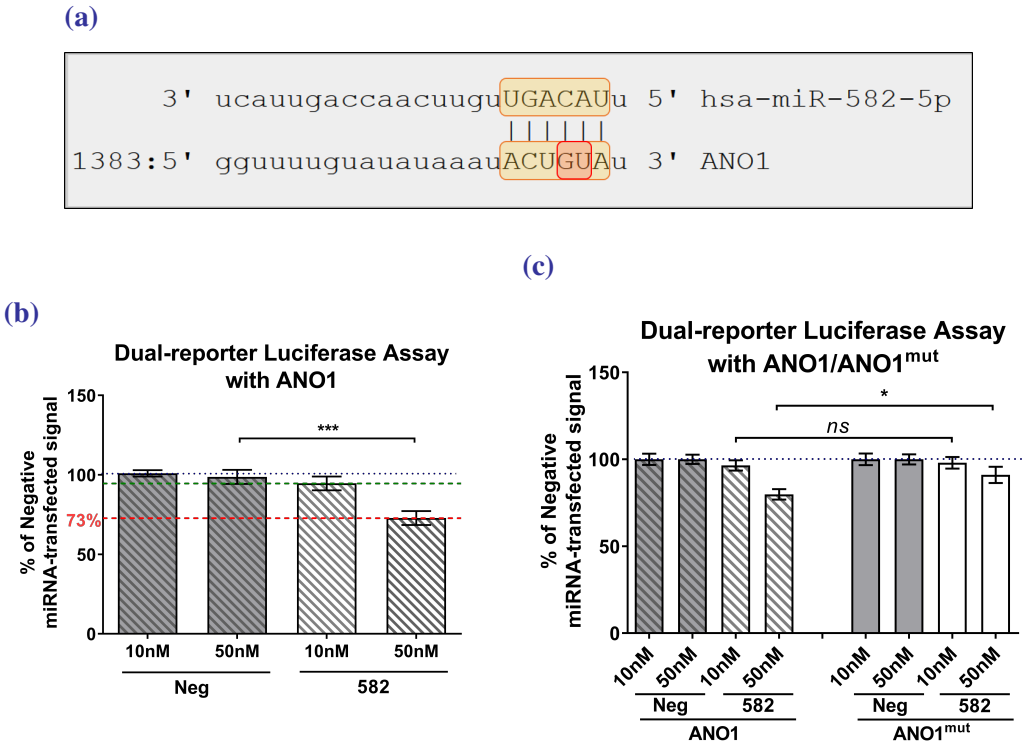

Figure 3.29: **Interaction between mir-582-5p and *ANO1*.**
(a) Predicted seed sequence of mir-582-5p on *ANO1* (source: www.microrna.org). Yellow: seed sequence of the miRNA on the 3'UTR sequence. Red: two mutated bases for dual-reporter luciferase assay with mutant. (b) Dual-reporter luciferase assay (n=3) showing the Negative-miRNA-transfected condition (control) as a reference and the reduction of fluorescent signal compared to the control in mir-582-mimic ("582")-transfected condition at 10 and 50 nM miRNA concentration. (c) Dual-reporter luciferase assays (n=3) intensity of fluorescence values represented as percentage of control condition (Negative miRNA-transfected cells) with WT (left) and mutant (right) *ANO1* 3'UTR sequence at 10 and 50 nM miRNA concentration.
** p=0.048 *** p=0.0003 (Unpaired t-test).*

As seen in Figure 3.29b, co-expressing *ANO1* and mir-582-5p mimic at 50 nM led to a significant reduction of fluorescent signal to 73 % of the negative miRNA-transfected condition. No effect could be seen with the miRNA mimic at 10 nM. When two mutations were inserted in the 3'UTR sequence, the fluorescent signal was significantly restored to 91% of the negative control in the 50 nM miRNA condition (no effect was seen at 10 nM, see Figure 3.29c). These results suggested an interaction, albeit weak, exists between *ANO1* and mir-582-5p.

Similarly to what was done previously with *CALB1* and *CLIC5*, UCL93 (normal) and Ox161c1 (cystic) cells were transfected with mir-582-5p inhibitor or mir-582-5p mimic, respectively, and the expression levels of *ANO1* measured in the cells.

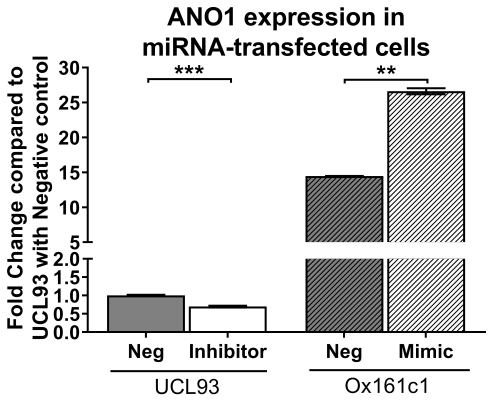

***Figure 3.30:* RT-PCR for the relative expression of *ANO1* in human kidney cells transfected with mir-582-5p inhibitor or mimic.**
The levels of expression of *ANO1* in UCL93 transfected with mir-582-5p inhibitor and Ox161c1 transfected with mir-582-5p mimic are expressed as a fold change of the control condition (UCL93 with Negative miRNA).
*n=3, * p=0.01 *** p=0.0007 (Unpaired t-test)*

The expected results, if *ANO1* was a target for mir-582-5p, were an increase of mRNA levels with the miRNA inhibitor and a decrease with the miRNA mimic. The results presented in Figure 3.30, however, show the opposite. Indeed, transfection with the inhibitor led to a 0.3 point reduction of *ANO1* mRNA levels in UCL93 and transfecting Ox161c1 with the mimic induced a 1.84-fold increase of *ANO1* expression levels. The basal levels of *ANO1* were 14.5-fold higher in the cystic cells compared to normal, which is in line with what what found previously.

Expression levels of anoctamin in human ADPKD cells The first step consisted in validating the anti-anoctamin antibody as the band detected by Western blotting appeared at a lower size than expected (≈75 kDa instead of 114 kDa), although the datasheet from the supplier suggested a band at that size (75 kDa). Ox161c1 cells were transfected with a negative control or anti-*ANO1* siRNA and their proteins run in Western blot.

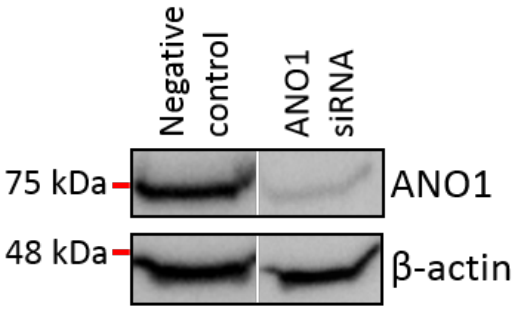

***Figure 3.31:* Western blotting of anoctamin in negative control or anti-*ANO1*-transfected Ox161c1 cells.**
Ox161c1 were transfected with a negative control siRNA or an anti-*ANO1* siRNA and their proteins stained for anoctamin and β-actin.
Expected sizes: ANO1 = 114kDa (calculated) / 75 kDa (expected from datasheet), β-actin = 42 kDa.

As shown in Figure 3.31, transfecting Ox161c1 with an anti-*ANO1* siRNA led to a strong decrease of intensity of the unique band at ≈75 kDa. This proved the efficiency of the siRNA and supported the idea that the observed band may be specific of this protein, albeit lower than anoctamin's calculated size.

Next, proteins from two independent batches of two normal and four cystic human cell lines were run in an SDS-PAGE gel and stained for anoctamin and β-actin (Figure 3.32)

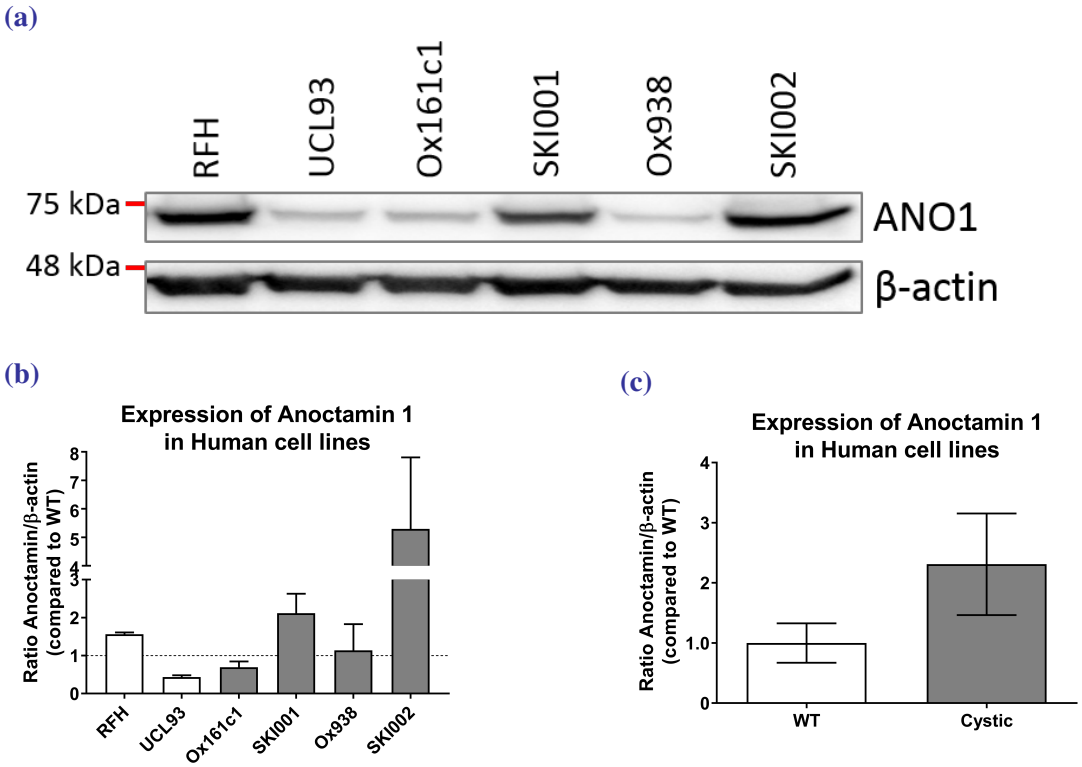

Figure 3.32: **Western blotting of anoctamin in normal and cystic human kidney cells.** (a) Anoctamin (expected size: 75 kDa) was stained in proteins extracted from two independent batches of two normal (RFH and UCL93) and four cystic (Ox161c1, SKI001, Ox938 and SKI002) human ADPKD cells. β-actin (expected size: 42 kDa) was used as a loading control. (b) The anoctamin/β-actin ratio was measured for each cell line and reported to the average value of the two normal cell lines (RFH and UCL93, white bars). (c) The expression levels of anoctamin were expressed as fold change in cystic cells (grey bars) compared to normal cells (white bars).

The expression levels of the protein stained at 75 kDa, deemed to be anoctamin, were higher in SKI001 and SKI002 (ratios at 2.1 and 5.3, respectively) than in the two normal cell lines RFH (1.56) and UCL93 (0.44). The ratio anoctamin/calnexin in Ox938 (1.3) was equivalent to the one in RFH but higher than UCL93. Only Ox161c1 expressed anoctamin at lower levels than the average of the two normal cell lines (0.7), although it was higher than in the UCL93. Globally, anoctamin was over-expressed about 2.3-fold in cystic cells compared to normal although this was not significant because of the variability between cell lines.

ANO1 having been found up-regulated in ADPKD at the mRNA and protein levels in various models, and an interaction with mir-582-5p being suggested, the next experiment of this study consisted in performing a 3-Dimensional cyst assay to study effects of its knock-down on cysts proliferation.

Role of *ANO1* on cysts proliferation Human cystic cells (Ox161c1) were either not transfected or transfected with a non-targeting siRNA, an anti-*ANO1* siRNA or a mir-582-5p mimic, and treated with forskolin in order to induce cysts growth. Untransfected cysts were in parallel treated with an inhibitor of anoctamin: CaCCinh-A01 (specific to anoctamin) or tannic acid (more wide). The cysts were imaged at 7, 12 and 19 days and the results are presented in Figure 3.33.

The forskolin control condition had the expected effect on the cells and induced a strong cysts growth at 7, 12 and 19 days (Figures 3.33a, 3.33b and 3.33c), with average areas reaching 1,080, 1,812 and 2,777 μm^2, respectively, and cysts looking round and large under the microscope (Figure 3.33i1). Tannic acid induced a strong and significant inhibition of cysts progression at 7 days (379 μm^2 vs. 1,080 μm^2, see Figure 3.33a), but seemed to have toxic effects on the cysts from 12 days of culture, as they were very small and the medium got more yellow in colour suggesting an acidification of its pH. Hence, no data for this inhibitor is presented at 12 or 19 days.

Treatment with the specific inhibitor of anoctamin CaCCInh-A01 led to an inhibition of cysts size at 7 days (475 μm^2 on average, Figure 3.33a), 12 days (462 μm^2, Figure 3.33b) and 19 days (401 μm^2, Figure 3.33c), without seeming to affect the cells integrity (Figure 3.33i2). Over time, as the cysts in the control condition continuously grew and the ones in the A01 condition got significantly smaller, the relative size of the latter compared to the former decreased from 44 % to 14.5 % (Figure 3.33g), suggesting a strong and prolonged impact of the inhibition of anoctamin on cysts growth.

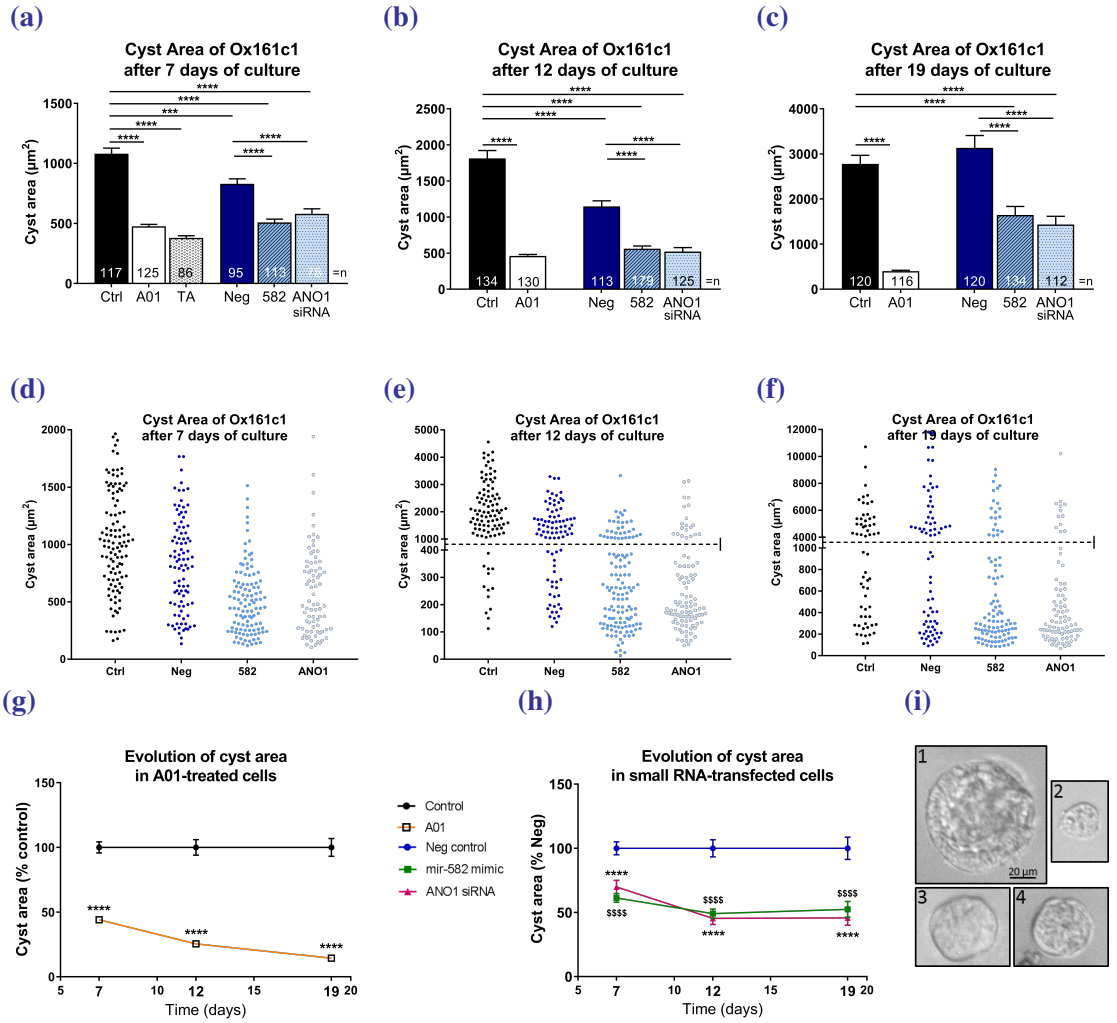

Figure 3.33: **3D-cyst Assay of Ox161c1 transfected or not with Negative control, or mir-582-5p mimic or anti-*ANO1* siRNA or treated with anoctamin inhibitors.**
Ox161c1 were either not transfected and treated with DMSO (Ctrl, black bar), CaCCInh-A01 (A01, white) or tannic acid (TA, grey), or transfected with Negative control siRNA (Neg, dark blue) or mir-582-5p mimic (582, blue) or anti-*ANO1* siRNA (ANO1 siRNA, light blue) and cultured for (a) 7, (b) 12 and (c) 19 days. n: number of cysts measured for each condition. (d), (e), (f) Dot-plot graph representing the distribution of the cysts sizes in the DMSO (Ctrl, black), negative control (Neg, dark blue), mir-582 mimic (582, blue) or anti-*ANO1* siRNA (ANO1, grey). The y axis of (e) and (f) were cut in order to focus on the small and large cysts. Evolution of cyst areas presented as percentages of control conditions (no treatment control or negative small RNA control) in (g) A01-treated cells or (h) siRNA/miRNA-transfected cells. (i) Example of representative cysts after 19 days of culture after (1) control condition, (2) A01 treatment, (3) mir-582 mimic transfection and (4) anti-*ANO1* siRNA transfection. Magnification x100.
**** p=0.0005 ****/$$$$ p<0.0001 (Mann-Whitney test)*

Transfecting cells with a negative control small RNA led to a significant decrease in cysts size compared to control condition at 7 and 12 days but, surprisingly, not at 19 days.

Looking at the global aspect of the cells in the three small RNA-transfected conditions, as presented in Figures 3.33d, 3.33e and 3.33f, there were a few very large cysts and many little or very little ones, only visible from a x100 magnification. The large cysts were of equivalent sizes in the negative control and mir-582 mimic or anti-*ANO1* siRNA, but the little cysts were smaller in the two latter compared to their control, in particular at 7 and 12 days (the cysts presented in Figures 3.33i3 and 4 are representative of the average cysts size in these conditions), leading to average sizes significantly lower in these two conditions compared to the negative small RNA control condition at the three time points. The average size of the cysts in the negative control condition increased moderately between 7 and 12 days (from 829.5 μm^2 to 1,148 μm^2, Figures 3.33a and 3.33b), but increased more strongly between 12 and 19 days (from 1,148 μm^2 to 3,135 μm^2, Figure 3.33c). A similar observation could be made for the mir-582 mimic condition (508.7 μm^2 at 7 days, 561.1 μm^2 at 12 days, 1,645 μm^2 at 19 days) and for the anti-*ANO1* siRNA condition (579.6 μm^2 at 7 days, 522 μm^2 at 12 days and 1435.5 μm^2 at 19 days), where the cysts size were rather stable between 7 and 12 days but highly increased between 12 and 19 days. Furthermore, the average cysts size between these two conditions remained equivalent at all the time points studied. over time, the relative expression levels of these two conditions compared to the negative control were very similar between each other: they decreased between days 7 and 12 and were stable afterwards (Figure 3.33h, for the mir-582 mimic and the anti-*ANO1* siRNA respectively: 61 % and 69 % at 7 days, 49 % and 45 % at 12 days, 52 % and 46 % at 19 days), while always being highly significantly lower than the negative reference condition. This suggested that both the mimic and the siRNA affected the cysts formation and progression at the earlier time points.

Effects of glucose deprivation on *ANO1* expression UCL93 (normal) and Ox161c1 (cystic) cells were cultured for two weeks in normal DMEM F-12, containing glucose at 3,151 mg/L, or in a 1:5 mix of normal DMEM and glucose-free DMEM (final glucose concentration at 630 mg/mL. The cells did not survive in full glucose-free medium). Their RNA was extracted and (sq) RT-PCR was performed to measure the relative expression of *ANO1* in the different conditions. The results are presented in the following Figure 3.34.

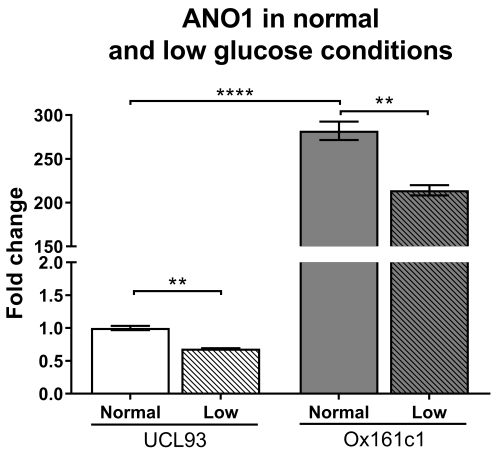

Figure 3.34: **RT-PCR for the relative expression of *ANO1* in human kidney cells cultured in normal or low glucose conditions.**
The levels of expression of *ANO1* in UCL93 (normal, white bars) or Ox161c1 (cystic, grey bars) cultured in normal (3,151 mg/L) or low (630 mg/mL) glucose concentration medium are expressed as a fold change of the control condition (UCL93 in normal glucose concentration). *n=3, ** 0.0083>p>0.0048 **** p<0.0001 (Unpaired t-test)*

First of all, in normal conditions *ANO1* was highly and significantly over-expressed in the cystic cells compared to normal (fold change 282), which confirms again the results of the previous (sq) RT-PCR validation experiments. Furthermore, for both cell lines culturing the cells in a low glucose medium for two weeks led to a significantly decreased expression of *ANO1*. In UCL93, *ANO1* expression level was reduced by 0.3 points, while it was 0.24 points lower in the cystic cells Ox161c1. Overall, lower glucose concentrations directly led to a decreased expression of *ANO1*.

As a summary, *ANO1* was found over-expressed in various models of ADPKD at the mRNA and protein levels, was suggested to be a target for a miRNA found highly down-regulated in our microarray, mir-582-5p, and its chemical inhibition or genetic knock-down led to significant decreases in cysts growth.

Table 3.2: Summary of all genes selected for analysis from miRNA array and/or mRNA array

Gene	Name	Selected from	Fold change microarray	FC human cells	FC mouse cells	FC mouse tissue	Luciferase Assay	Western Blotting	Reason for not taking further	miRNA
ANO1	Anoctamin 1 / TMEM16	mRNA array: highest fold changes	56	393 (*)	FC = 2.9 (MEK). Non significant increase in F1 cells	Up-regulation (FC = 2.52 & 3.7) in NeoLox at 4 and 10 weeks	Significant reduction of signal partially inhibited after mutagenesis	Over-expression in SKI001 and SKI002	–	mir-582
CALB1	Calbindin 1, 28 kDa	mRNA / miRNA array	70	46.7 (*)	FC = 0.6 in F1/Cre (***). No deregulation in MEK	Strong down-regulation in NeoLox (FC = 0.2) and trend to down-regulation in CreLox (not significant)	Significant reduction of signal to 57 %, totally reversed after mutagenesis	Over-expression in Ox161c1 and SKI001 cells	Contradictory data between models	mir-193b
CLIC5	Chloride Intracellular Channel 5	mRNA / miRNA array	15	CLIC5 = 39 $\longrightarrow$ CLIC5A = 143 (****), CLIC5B = 1.1	Up-regulation in F1/Cre (FC = 2) and MEK (FC = 665)	Strong down-regulation in NeoLox at 4 and 10 weeks (FC = 0.26 & 0.34)	Significant reduction of signal to 54 %, partially inhibited after mutagenesis	Over-expression of CLIC5A, less of CLIC5B	Contradictory data between models	mir-582
ERBB4	Erb-B2 Receptor Tyrosine Kinase 4	mRNA / miRNA microarray	37.2	7.8 (****)	–	Up-regulation in NeoLox (FC = 3.0868) and CreLox (FC = 2.6306)	Significant reduction of signal to 31.5 %, totally reversed after mutagenesis	Strong over-expression in human ADPKD cells	Published in AJP Renal (April 17)	mir-193b

Summary of all genes selected for analysis from miRNA array and/or mRNA array (continued)

Gene	Name	Selected from	Fold change microarray	FC human cells	FC mouse cells	FC mouse tissue	Luciferase Assay	Reason for not taking further	miRNA
SYT1	Synaptotagmin 1	mRNA/miRNA array	4	7.7 (****)	Up-regulation in F1 (FC = 2.1)	No difference between NeoLox or CreLox and ADPKD	Significant reduction of signal, but not affected by mutagenesis	No interaction with mir-582-5p	mir-193b
PKP2	Plakophilin 2	mRNA/miRNA array	3	3.3 (****)	–	Significant reduction of signal, but not affected by mutagenesis	–	No interaction with mir-582-5p	mir-582
IL1RAP	Interleukin 1 Receptor Accessory Protein	mRNA/miRNA array	4	2.6 (****)	–	Significant reduction of signal, but not affected by mutagenesis	–	No interaction with mir-582-5p	mir-582
RPS6KA2	Ribosomal Protein S6 Kinase A2	mRNA array: highest fold changes	2.6	9.3 (****)	Down regulation (FC = 0.6) in MEK Up-regulation in F1 (FC = 1.3)	No change at 4 or 10 weeks	–	Contradictory data between models	–
CCNA1	Cyclin A1	mRNA array: highest fold changes	12	16.1 (****)	Up-regulation in MEK (FC = 2). No change in F1	Up-regulation (FC = 1.49) in NeoLox at 4 weeks, no change at 10 weeks	–	Not entirely consistent across models. Not predicted to be a target for our miRNAs	–

Summary of all genes selected for analysis from miRNA array and/or mRNA array (end)

Gene	Name	FC Ox161	FC SKI001	FC Ox938	FC SKI002	Reason for not taking further
DMD	Dystrophin	0.07	0.7	15.4	45	No consistent up-regulation
DOCK4	Dedicator of Cytokinesis 4	3.1	7.5	3.06	4.5	Not validated on a second batch
ENPP4	Ectonucleotide Pyrophosphatase/Phosphodiesterase 4	4	2.4	1.5	2.4	Not validated on a second batch
FLI1	Friend Leukaemia Integration 1	0.82	5.2	1.4	2.28	No consistent up-regulation
FOXO1	Forkhead box protein O1	1.7	3.2	1.7	2.6	No high up-regulation
FRAS1	Fraser Extracellular Matrix Complex Subunit 1	2.4	1.4	2.4	0.2	No consistent up-regulation
GREM2	Gremlin 2	12.2	1.97	1.46	0.29	No consistent up-regulation
ITGB8	Integrin Subunit Beta 8	6.8	2	0.8	3	Not validated on a second batch
JPH1	Junctophilin 1	0.3	0.2	8	24.7	Not validated on a second batch
LCN2	Lipocalin 2	1.35	0.77	1.2	0.8	No up-regulation
MFI2	Melanotransferrin 2	2.8	0.5	0.8	0.4	No up-regulation
MYCN	N-Myc proto-oncogene	1.07	2.1	1.8	0.95	No high up-regulation
MYO10	Myosin X	1.7	1.9	0.5	0.1	No consistent up-regulation
NPR3	Natriuretic Peptide Receptor 3	0.3	3.2	4	0.6	No consistent up-regulation
PTGIS	Prostaglandin I2 Synthase	1.2	4.7	2.9	1.3	No consistent up-regulation
RGCC	Regulator of Cell Cycle	2	1	0.39	1.06	No consistent up-regulation
SLC22A10	Solute Carrier family 22 member 10	0.17	0.05	10.3	35.9	No consistent up-regulation
SOX5	SRY-related HMG box	2.1	1.9	0.96	0.09	No consistent up-regulation
SPOCK2	SPARC/Osteonectin Proteoglycan 2	0.77	1.07	0.43	0.64	No up-regulation
SSPN	Sarcospan	0.18	0.06	7.5	19.8	No consistent up-regulation
SYK	Spleen Associated Tyrosine Kinase	5.56	2.9	1.26	0.92	No consistent up-regulation

3.6 Discussion

This part of the project was based on the data from a parallel mRNA/miRNA array performed before the start of my PhD. This array allowed us to identify and characterise a new candidate involved in ADPKD's cyst progression, *ERBB4*, as well as to link it to a miRNA found down-regulated in ADPKD from this same microarray, mir-193b-3p. This was the first evidence of an interaction between these two genes and of their role in the pathogenesis of ADPKD, and we successfully published this data in *AJP Renal* in 2017. Because many other candidates identified from this microarray were still to be studied, the first aim of my PhD project was to narrow down their number, select and characterise new genes involved in the pathogenesis of ADPKD using different approaches.

3.6.1 Selection of new candidates from the parallel mRNA/miRNA microarray

The PANTHER enrichment analysis allowed me to classify the potential candidates according to the biological processes enriched in ADPKD. Indeed, this pathways/network approach gave a wider angle to the selection process as it led to characterise whole processes deregulated in the disease and the genes related to these rather than individual targets for each miRNA. The 4-fold value was a subjective choice that appeared to restrict the list of candidates to a reasonable number for further (sq) RT-PCR validations. The same process could however be applied to all the enriched targets in order to broaden their number but it would also probably involve selecting some less relevant elements. Finding the "cellular process" as the most enriched process was expected as it regroups major and fundamental actors of cell physiology such as cell cycle and proliferation. As cell proliferation is known to be a major factor of cysts progression in ADPKD (Welling, 1990), the genes identified as part of this process were selected for further analysis. Furthermore, processes such as "localisation" (regrouping transport and retention of cellular entities and proteins to various places of the cell) and "metabolic process" (regrouping, among others, DNA repair and replication, and protein synthesis and degradation) were also considered important in ADPKD pathogenesis, therefore the targets involved in these processes were also selected for further validation experiments.

Finally, three genes not part of the significantly enriched pathways (*JPH1*, *NPR3*, *RGCC*) were also added to the list of targets to validate as their expression levels were high in the initial microarray. This led to the selection of twenty-two candidates out of the thirty-two originally found up-regulated at least 4-fold, hence to the dismissal of ten potential targets that may be interesting to get back to in further studies.

Nine genes were over-expressed in human ADPKD cells compared to control, and five out of them were confirmed deregulated in another independent batch of cells. The variability between cell lines being large for *CALB1* and *CLIC5*, although all the cells over-expressed these genes, highlights the importance of using several cell lines for the validation experiments as the expression levels of some candidates can vary between batches and cells origin.

The luciferase assays were useful to determine the potential interaction between the five validated targets and the two miRNAs found down-regulated in the microarray. Only *CALB1* and *CLIC5* showed convincing results suggesting an interaction with mir-193b-3p and mir-582-5p, respectively. Indeed, while a co-expression of the genes' 3'UTR and their relevant miRNA mimic led to a significant and strong reduction of the signal, inserting mutations in the 3'UTR induced a total reversion of this signal reduction for *CALB1* and a partial reversion for *CLIC5*. My first hypothesis for this non total reversion was that the predicted seed sequence of mir-582-5p on *CLIC5* 3'UTR is quite long, hence mutating only four bases would not allow a total inhibition of the interaction between the two elements. However, the insertion of two more mutations in this 3'UTR sequence did not have any different effect on the fluorescent signal. Another potential explanation is that mir-582-5p has several predicted and non predicted seed sequences on *CLIC5* 3'UTR. No other predicted sequence was part of the 3'UTR section cloned the plasmid, but it did contain a sequence complementary to the miRNA's. Although a bases complementarity is not sufficient to predict miRNA seed sequence and multiple other factors are to be taken into consideration (Cloonan, 2015), this hints that a weak or non-specific interaction could occur in the transfected cells, hence maintaining an inhibition of the signal.

3.6.2 *CALB1*, a calcium channel deregulated in ADPKD

CALB1 codes for calbindin D-28K, a Ca^{2+} channel sensor and transporter, and its dysregulation in ADPKD could have made sense in the pathogenesis of the disease, although usually this ion's effects on cystogenesis were characterised in knock-down conditions and not over-expression as it was found in our human cells.

Transfection of cells with mir-193b-3p mimic and inhibitors induced expected effects on *CALB1* expression, giving another evidence that this gene is a target for this miRNA. Taken together, I reported for the first time that mir-193b-3p targets *CALB1 in vitro*.

Calbindin D-28K blotting in our human cells showed results in line with the (sq) RT-PCR, confirming the up-regulation of calbindin in most cystic cell lines (though not in Ox938). However, immunohistochemistry stainings on human tissue hinted that this dysregulation may not be consistent across models. Indeed, while the staining intensity in the marked structures (assumed to be distal tubules from their shape and because calbindin is classically used as a marker of these structures (Taylor et al., 1982)) was equivalent between the two conditions, there were much less tubules visible in the ADPKD kidneys. As the tissue was very disorganised, very little structures were identifiable. This suggested that the global expression of calbindin was decreased in ADPKD compared to normal, which is contrary to what was found in our cells.

This observation was confirmed in three different murine models (F1 cells, NeoLox at 4 and 10 weeks and CreLox). Only the MEK cells showed no difference in the expression levels of *Calb1*, which could be due to a difference in developmental stage of the mice from which the cell lines originated in the original model or to the difference between the mice genotypes themselves. Immunohistochemistry of $Pkd1^{nl,nl}$ mice tissues at 2 and 4 weeks confirmed that the expression levels of calbindin in the tubules were not changed *per se* but that there were less tubules in the ADPKD kidneys, thus less global expression of the protein in the disease condition.

An explanation as to why some of our human cells (namely Ox161c1 and SKI001) highly over-expressed the protein by (sq) RT-PCR and Western blotting could be a difference of renal segment origin between these cells and the others, in particular these cells would be originating from distal tubules while the other would be originating from other segments.

Unfortunately, Western blotting, immunofluorescence and (sq) RT-PCR were performed on these cells to detect specific segments markers such as aquaporin-1 (proximal tubules), aquaporin 2 (distal tubules) and Tamm-Horsfall protein (loop of Henle) but did not detect any specific signal, suggesting the cells have lost their markers and making it difficult to determine their origin (data not shown). We also hypothesised that mir-193b-3p may be differentially expressed between kidney segments, explaining *CALB1*'s difference of expression between these segments. Interestingly, this miRNA was reported to be enriched in the thick ascending loop of Henle compared to all other segments in an unpublished dataset we had access to (kindly shared by Prof Olivier Devuyst, University of Zurich, Switzerland), in which miRNAs expression patterns were measured in healthy 10 weeks old mice kidney segments. Moreover, the cell lines that expressed mir-193b-3p the least in the TaqMan (sq) RT-PCR validation experiment (Ox161 and SKI001, see Figure 3.4b) were the ones over-expressing *CALB1* the most, giving more evidence of an interaction between the two elements and suggesting these two cell lines may originate from a region at the junction between the thick ascending loop of Henle and the distal tubule. No segment-specific enrichment could be seen for mir-582-5p.

3.6.3 *CLIC5* was up-regulated in several models, but not all, of ADPKD

CLIC5 codes for the chloride intracellular channel 5 protein, predominantly expressed in the ear and kidney (Seco et al., 2015). It has not been linked to ADPKD before but its recently suggested interaction with $PI(4,5)P_2$ which has itself been shown to regulate the PI3K/Akt pathway known to be of major importance in ADPKD (Ye et al., 2013) (see chapter 4), and reports of mild renal dysfunction in *CLIC5* KO mice (Seco et al., 2015) suggested an effect of an over-expression of this gene in the pathogenesis of ADPKD.
Transfection of normal and cystic cells with mir-582-5p inhibitor or mimic gave unexpected results. Indeed, although the up-regulation of the gene in cystic cells was confirmed again, the relative expression levels of *CLIC5* showed the opposite of what was expected: an increased expression in inhibitor-transfected normal cells, and a decreased expression in the mimic-transfected cystic cells.

Several hypotheses can be made to try and explain this observation. First of all, the interaction between mir-582-5p and *CLIC5* might be weak, which would explain the non-total reversion of signal observed in luciferase assays, and a protein regulating *CLIC5* expression could be a stronger target for mir-582-5p, leading to a lower expression of this protein hence more expression of *CLIC5*. The identity of this protein remains to be determined as not much is known about *CLIC5* regulation. A suggestion could be the ezrin or gamma actin proteins which have been shown to regulate Clic5 activity in a feedback loop (Singh et al., 2007) and predicted to be potential targets for mir-582-5p by a few algorithms (MicroT4, RNAhybrid and RNA22). Whether this would also have an effect at the mRNA level still remains to be proved. Another hypothesis is a difference between *CLIC5A* and *CLIC5B*'s sensitivity to mir-582-5p transfection. Indeed, although these are two isoforms coded from the same gene, it is known that alternative polyadenylation can generate isoforms differing in their 3'UTR (Elkon et al., 2013), hence with missing or additional predicted seed sequences for miRNAs. This suggests that Clic5a and Clic5b may have a different sensitivity to mir-582-5p (or other miRNAs) and that transfecting this miRNA into cells may affect the two isoforms differently, either by not targeting them as much either by targeting other genes regulating these isoforms differentially. It would therefore be useful to perform sequencing of the 3'UTR of the two isoforms to confirm that this sequence is different between the two.

(sq) RT-PCR of *CLIC5A* and *CLIC5B* independently hinted a difference between the two isoforms, both of them being significantly increased in ADPKD human cells but *CLIC5A* to a larger extent than *CLIC5B*. The deregulation of *CLIC5B* was constant between cell lines and batches while *CLIC5A* was mostly increased in two cell lines Ox161c1 and SKI001, and different between the two batches measured. Western blotting showed similar data although the increase of Clic5a was less important than at the mRNA level, which could be explained by the variability between batches observed by (sq) RT-PCR.

Similarly to the calbindin results, immunohistochemistry of Clic5 in human kidney tissue did not show any difference in intensity between normal and ADPKD glomeruli but a global loss of these structures in the cystic kidney.

Indeed, the staining seemed specific to the glomeruli, which is where Clic5a is predominantly expressed, and very little glomeruli (only one in the presented section) were visible in ADPKD kidney. The reason why no staining was visible in the other structures such as the tubules, thus of Clic5b, may be due to the antibody itself not being sensitive to this isoform in IHC and another antibody might show a stronger staining. Nevertheless, these results suggested a global down-regulation of Clic5a in ADPKD which was opposite to what was found in human cells.

(sq) RT-PCR validation experiments in four different mice models and immunohistochemistry on NeoLox (*Pkd1* hypomorph) mice did not allow me to conclude on the deregulation of *CLIC5* in ADPKD. Indeed, while this gene was significantly down-regulated in NeoLox at the mRNA and protein level and in CreLox mice at the mRNA level, it was significantly and highly over-expressed in the two mice cell lines studied (MEK and F1). Only one isoform is known for *Mus musculus* so it was not possible to perform differential (sq) RT-PCR in the mice models to get more insight into what causes the difference between these models. A suggestion would be that because total ADPKD kidneys RNA and tissues were less rich in glomeruli (as it can be seen in the kidney sections), and Clic5 is largely expressed in these structures (also visible in the sections), their disruption largely influenced the mRNA quantification even if there was an increase in some other structures. Since both mice cell lines originate from collecting ducts, glomerular specific expression cannot explain these findings, hence showing an up-regulation of this gene by (sq) RT-PCR.

As a summary, although *CLIC5* cannot be totally dismissed from further ADPKD studies as it was found up-regulated in three human and two murine cell lines, the lack of consistency with the relative expression levels in total kidney tissues highlights the limits of my first approach and suggests that a validation across these models should be the first steps to undertake in order to select new candidates.

3.6.4 *ANO1* expression is increased in most models of ADPKD and may play a role in cysts progression

Because the first approach taken previously limited the candidates selection to the ones predicted to interact with the two down-regulated miRNAs by only one algorithm (TargetScan) and dismissed some strongly enriched targets, I decided to first focus on selecting genes based on their deregulation in multiple models and then characterise their interaction with the miRNAs. The eight most significantly and highly enriched genes were selected and their relative expression in ADPKD was measured by (sq) RT-PCR in three batches of normal and ADPKD human cells, which allowed us to short-list our selection to three genes to validate in the mouse model. The lower p-value for *ANO1* is explained by a variability in this mRNA's enrichment levels between cell lines but its average fold change value was still very high which incited us to select it for further experiments.
The CreLox model could not be used in the following experiments for practical reasons as the RNA samples were kindly offered by D. Peters and had run out after the previous experiments. While *RPS6KA2* was very variable between models, only the F1 cells supporting the human cells results, making it easy to dismiss, *CCNA1* was more difficult to conclude on as it was slightly up-regulated in two models (MEK and 4 weeks old NeoLox mice) but not changed in two others (F1 cells and 10 weeks old NeoLox mice).

ANO1 was chosen as an interesting target to study as it was significantly up-regulated in three out of the four models studied and showed a slight trend to an up-regulation in F1 cells, making it consistent across models and suggesting that it is well enriched in ADPKD with fold changes ranging from 1.5-fold in 4 weeks old $Pkd1^{nl,nl}$ mice to 393-fold in human cells.
ANO1 codes for anoctamin, a protein that was reported to induce cysts progression in a canine kidney cell model (MDCKII) (Buchholz et al., 2013) and linked to cAMP and calcium signalling (Tanaka and Nangaku, 2014). Although Buchholz et al. previously reported that anoctamin is expressed in the cyst-lining epithelium of many cysts in human ADPKD tissue and forskolin-stimulated MDCK, I am showing for the first time that *ANO1* is over-expressed in the disease compared to normal condition in human ADPKD cells, embryonic mouse kidney cells and a *Pkd1* hypomorph mouse model at two ages.

The following step consisted in validating its interaction with one of our significantly down-regulated miRNAs, mir-582-5p, for which the microrna.org database predicted one seed sequence on *ANO1*'s 3'UTR. I successfully generated a pmirGLO plasmid coding for part of the 3'UTR sequence of *ANO1* containing the predicted mir-582-5p seed sequence and used it to perform dual-reporter luciferase assays. There was a hint that the two elements could interact *in vitro* as the co-expression of the miRNA mimic at 50 nM led to a, albeit low, significant reduction of fluorescent signal. Despite multiple protocols and use of several couple of primers, it was not possible to insert more than two mutations in the *ANO1* sequence which limited the possible inhibition of the miRNA-mRNA interaction. However, an significant reversion of the fluorescent signal decrease could be observed, although not total as it was expected with only two mutated bases. The transfection of normal and cystic cells, similarly to what was observed with *CLIC5* previously, gave opposite results to what was expected. Mir-582-5p may target a protein negatively regulating *ANO1* more strongly than *ANO1* itself, hence its increase when mir-582-5p is artificially over-expressed. The identity of this protein remains to be determined. Taken together, the interaction between mir-582-5p and *ANO1*, if it exists, appeared weak and suggests that this gene may be regulated by other miRNAs in ADPKD. Interestingly, mir-194-5p, which we later found significantly down-regulated in human ADPKD urinary exosomes and mice kidneys (see chapter 5 of this thesis), was predicted to target this gene by nine algorithms (miRWalk, MicroT4, miRanda, miRDB, miRMap, PITA, RNA22, RNAhybrid, TargetScan). This strongly suggests that *ANO1* could be, more than mir-582-5p, a target for mir-194-5p which would explain its enrichment in ADPKD. This interaction between the two elements would be very interesting to validate in further experiments.

Western blotting of anoctamin in the human cells showed that two cell lines in particular (SKI001 and SKI002) are enriched in this protein compared to the average amounts in the two normal cell lines. The variability between cells could be explained by a difference between batches (cells more confluent for example) or a segment-specificity which, again, could not be proved because of a probable loss of tubules markers from the cells.

Moreover, the fact that Ox161c1 was the most *ANO1*-enriched cell line in all repeats of (sq) RT-PCR but the one expressing anoctamin 1 the least by Western blotting, added to the fact the band appears at 75 kDa instead of 114 kDa, casts a doubt on whether the protein stained is indeed anoctamin 1, although the anti-*ANO1* siRNA seemed to knock the signal down. Immunohistochemistry was attempted on human and mouse tissues to confirm the enrichment of anoctamin at the protein level but the antibody did not detect any signal (data not shown). Performing this experiment with another antibody may be interesting, although very few specific and IHC-compatible antibodies are available to purchase and most papers' authors used a home-made antibody.

Buchholz et al. performed 3D cysts assays of canine cells and organ culture of mice metanephric kidneys and reported that anoctamin is involved in cysts growth. Although these results seem convincing, the experiments were not performed on a human ADPKD model. Therefore, I decided to confirm these results in one of our human cells models of ADPKD (Ox161c1), expressing a truncated form of PC1 and known to form cysts in Matrigel, and see if the effects of knocking down anoctamin would not be hidden by the deficiency in PC1 and how they would maintain over time. Tannic acid is a strong inhibitor of the Calcium-activated Chloride Channels (CaCC) TMEM16A and TMEM16B with IC_{50} of 5.9 μM (Namkung et al., 2010) while CaCCInh-A01 (A01) is more specific of ANO1 (TMEM16A) and has an IC_{50} of 6.4 μM (He et al., 2011b). The concentrations chosen were the same as in Buchholz's paper: tannic acid at 20 μM and A01 at 10 μM. The first observation made was that tannic acid, at 20 μM, did induce a strong and significant reduction of cysts area after 7 days, but after 12 days and even more at 19 days the cysts' integrity looked compromised under the microscope and the gel and medium had changed colour, suggesting an over-acidification and off-target effects on the cells. Hence, the tannic acid condition was not analysed after day 7. Buchholz et al. only measured cysts areas after 5 days of treatment which can explain that this observation was not made in their study.

A01 led to a constant strong and significant inhibition of cysts growth over time. Indeed, while cysts in the control condition more than doubled in size between days 7 and 19, the average area of those under A01 treatment was consistently lower at the three

time points and constant over time (no significant difference in size between the time points). This meant that the relative area of the A01 condition cysts compared to the control condition strongly decreased between days 7 and 19. These results suggested that the chemical inhibition of anoctamin 1 led to a prolonged inhibition of cysts growth in a human model of ADPKD. The use of forskolin could be discussed as it artificially enhanced the cysts growth in the Matrigel by increasing cAMP levels thus making the conditions less physiological, but as Ox161c1 grow small cysts without this compound (see Figure 4.18a in chapter 4 of this thesis), the very little cysts caused by the A01 treatment would not have been visible or measurable and the analysis would have ended up biased. Furthermore, cAMP increases have been reported to directly enhance anoctamin 1-mediated chloride transport (Edlund et al., 2014), hence the effects of forskolin on cysts growth involve this channel and its inhibition blocks the chloride secretion mediated by cAMP and indirectly by forskolin.

The transfection of Ox161c1 with a negative control small RNA induced a significant off-target effect on the cysts growth at 7 and 12 days but not at 19 days. Similarly, the average cysts areas in the miRNA mimic and anti-*ANO1* siRNA conditions ('tests' conditions) was significantly lower than the negative control at all time points but significantly increased between days 12 and 19. The most probable theory is that the siRNA and miRNA mimics had a limited effect in time, which is supported by the manufacturer's documentation. The difference in average cysts area between negative control and siRNA or miRNA mimic, and the fact that the little cysts were smaller in these two test conditions at 7 days suggests that they had an impact on cyst formation. The significant decrease in relative size between 7 and 12 days also supported the theory that the siRNA and miRNA mimics prevented cyst growth as it means the negative control condition cysts grew faster than the two other conditions. Between days 12 and 19, however, the negative control, miRNA and siRNA may have lost their effect hence all the cysts suddenly grew back at normal rates, maybe explaining in part why the negative control condition values got back to normal levels at that time point. The significant difference between control and tests conditions at day 19 would then only be a reflection of the delay in cysts growth caused by the miRNA mimic or the siRNA until day 12 and that they could not compensate for.

Taken together, we showed that a genetic knock-down of *ANO1* had the same effects as the chemical inhibition of its protein, namely the inhibition of cysts growth over time. The less strong effect of the siRNA mimic is suggested to be due to the non-total transfection of the cells - which is also illustrated by the presence of a few large cysts. These larger cysts would skew the average area towards higher values and partially mask the effects of the siRNA on the cysts where it was efficiently transfected. My data is in line with the findings from Buchholz, and shows for the first time the role of anoctamin 1 in a human model of ADPKD, which is important because is suggests that inhibiting anoctamin could be sufficient to compensate the cysts growth induced by PC1 deficiency. I also suggest that this effect of anoctamin is conserved over time, which makes it potentially possible to use in longer term treatments in *in vivo* mice models and, eventually, human.
An increase of mir-582-5p amounts by transfection of a mimic also preventing cysts growth, added to the fact that mimicking this miRNA in the same cell line led to reduced cell proliferation (data not shown) suggest that this miRNA is an important factor of cysts progression in ADPKD. Whether the effects of anoctamin and mir-582-5p are linked or independent still needs to be determined as the interaction between the two elements was not totally convincing.

Finally, because anoctamin was suggested to be dependent on glucose concentrations by several studies in mouse intestines and kidneys (Yin et al., 2014; Kraus et al., 2016), the last experiment presented consisted in confirming this observation in the Ox161c1 in order to give a hint on the effect of anoctamin 1 over-expression on the phenotype of ADPKD in this model and support Kraus et al.'s hypothesis on the potentially affected pathways. Glucose concentrations were directly linked to *ANO1*'s expression levels, the more glucose the more expression of this gene. This goes along the previous findings that high glucose leads to high expression levels of anoctamin hence potentially a higher chloride secretion in pIMDCK cells and embryonic kidney cysts (Kraus et al., 2016).

However, as the normal cells are also sensitive to the change in glucose concentration, it is difficult to conclude that this factor is solely responsible for the enrichment of anoctamin in the cystic cells. Indeed, although it has been reported that the glucose metabolism is defective (enhanced glycolysis) in *in vivo* models of ADPKD (Rowe et al., 2013), the facts that even if they were capable of less glycolysis (which needs to be proved) the normal cells are also affected by the reduction of glucose concentration and that the relative expression of *ANO1* remains highly superior in the cystic cells even at low glucose concentrations suggest that, in this *in vitro* model (thus potentially in other models), the glucose concentration is not the only factor affecting *ANO1* expression.

Although the fact that Ca^{2+} is decreased in ADPKD could suggest a lower activation of the Ca^{+}-activated chloride channel anoctamin 1, it has been shown that over-expressed anoctamins present a lower threshold for their activation by this ion, suggesting that lower Ca^{2+} concentrations may have limited effects on their levels of activation as they need much less Ca^{2+} for their activation (Kunzelmann et al., 2011). Moreover, this threshold was also demonstrated to be lowered in hypoxia conditions, and hypoxia-inducible factors have been shown to be involved in the fibrosis observed in ADPKD, supporting the possibility for anoctamins to be activated under lower calcium concentrations in this disease (Wu et al., 2014; Norman, 2011). Additionally cAMP, known to be increased in ADPKD, is an activator of the CFTR channel that was itself suggested to activate anoctamin 1, giving another potential explanation for the over-activation of the already over-expressed anoctamin 1 in the disease (Kunzelmann et al., 2012; Edlund et al., 2014; Ousingsawat et al., 2011).

As a summary (see Figure 3.35), I propose that there are several factors influencing *ANO1* enrichment in ADPKD, including miRNAs, glucose metabolism and cAMP. The deregulation of these factors would lead to an increased expression of *ANO1* in ADPKD, resulting in more chloride secretion and cysts formation, growth and as it was suggested before, proliferation, notably by the activation of the MAPK pathway (described in the following chapter) (Duvvuri et al., 2012; Buchholz et al., 2013; Oh and Jung, 2016).

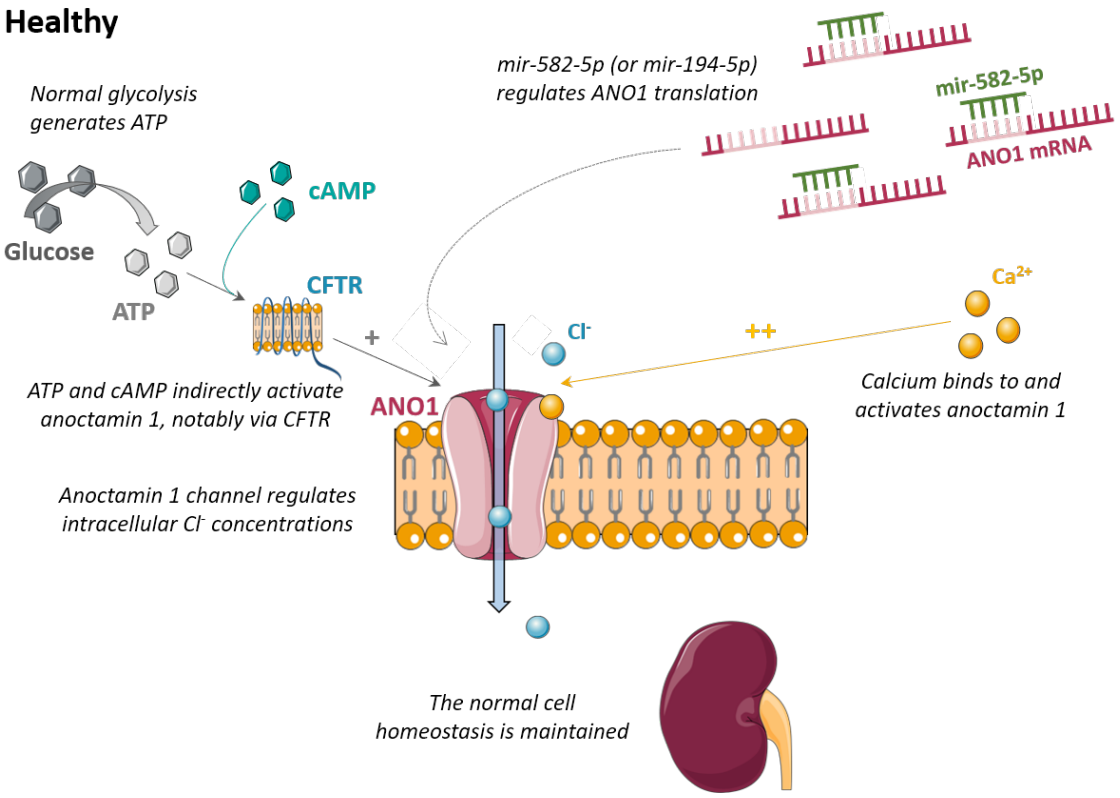
Healthy
Normal glycolysis generates ATP
Glucose
ATP
cAMP
CFTR
+
ATP and cAMP indirectly activate anoctamin 1, notably via CFTR
Anoctamin 1 channel regulates intracellular Cl- concentrations
mir-582-5p (or mir-194-5p) regulates ANO1 translation
mir-582-5p
ANO1 mRNA
Cl-
ANO1
++
Ca2+
Calcium binds to and activates anoctamin 1
The normal cell homeostasis is maintained

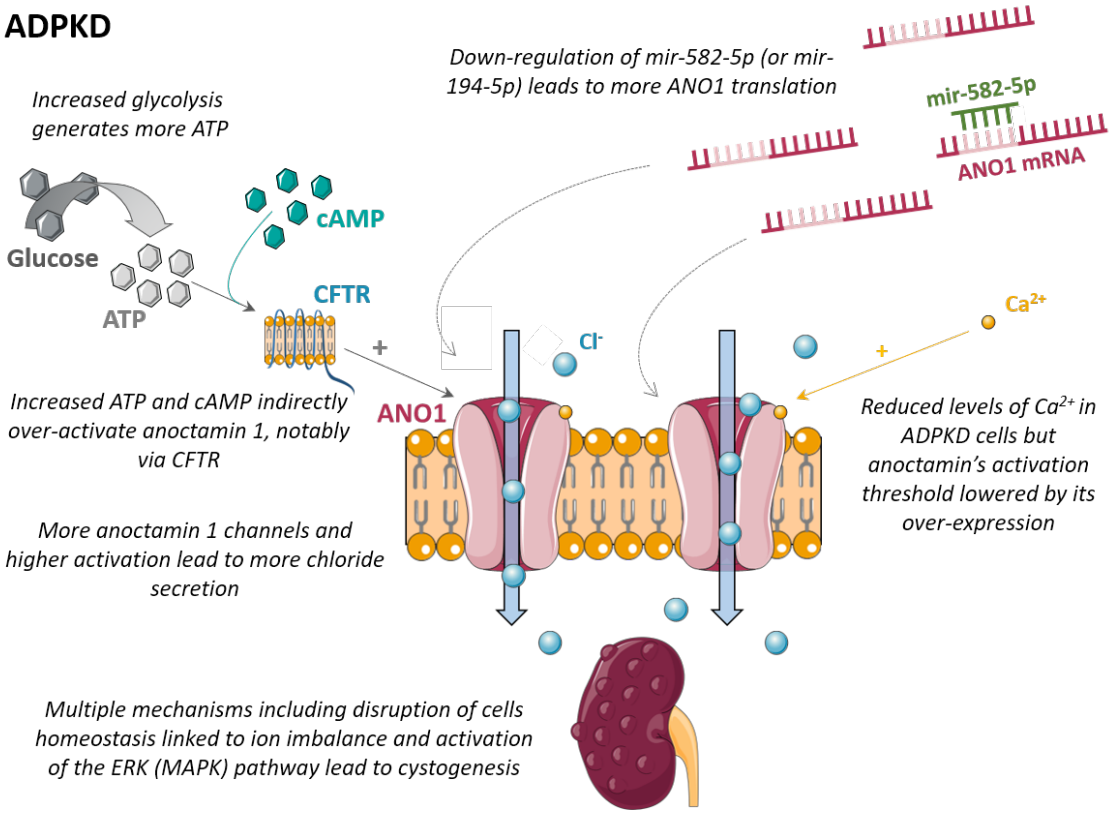
ADPKD
Increased glycolysis generates more ATP
Glucose
ATP
cAMP
CFTR
+
Increased ATP and cAMP indirectly over-activate anoctamin 1, notably via CFTR
More anoctamin 1 channels and higher activation lead to more chloride secretion
Down-regulation of mir-582-5p (or mir-194-5p) leads to more ANO1 translation
mir-582-5p
ANO1 mRNA
Cl-
ANO1
+
Ca2+
Reduced levels of Ca2+ in ADPKD cells but anoctamin's activation threshold lowered by its over-expression
Multiple mechanisms including disruption of cells homeostasis linked to ion imbalance and activation of the ERK (MAPK) pathway lead to cystogenesis

⟵ ***Figure 3.35*: Summary and hypotheses on the role of miRNAs and anoctamin-1 in the pathogenesis of ADPKD.**
In the healthy kidney (top panel), the normal expression levels of mir-582-5p (or any miRNA targeting *ANO1*) lead to normal translation levels of this gene and normal production of anoctamin channel. When glycolysis takes place, it generates ATP which along with cAMP at normal levels indirectly activates anoctamin 1, notably via the activation of the CFTR channel. Normal Ca^{2+} levels will also activate the channel after binding to the calmodulin binding domain. The protein can then exert its chloride channel action which helps maintain homeostasis in the cells.
In ADPKD (bottom panel), mir-582-5p (or mir-194-5p) is down-regulated (an hypothesis on what could explain miRNAs down-regulation in ADPKD is proposed in chapter 5) which leads to less negative regulation of *ANO1* expression and thus the translation of more anoctamin 1 than in the healthy kidney. Because glycolysis has been reported to be increased in ADPKD, it suggests that more ATP is produced which leads to more activation of the already more numerous anoctamin 1 channels, added to the increased cAMP levels that may result in more activated CFTR channels and the subsequent additional activation of anoctamin 1 channels. Although Ca^{2+} levels are known to be reduced in ADPKD, some studies suggested that an over-activation of anoctamin leads to a lowering of its activation threshold. Therefore, anoctamin may be equivalently activated by calcium in ADPKD as it needs less Ca^{2+} to be activated and it is over-expressed. Consequently to this over-expression and increased activation of anoctamin 1, more Cl^- will be secreted by the cells and their homeostasis will be disrupted, which associated to other mechanisms such as activation of the ERK (MAPK) pathway participates in the formation of cysts.

Chapter 4

Selection of new targets using bioinformatics analyses and comparisons with other databases

4.1 Introduction

The aim of the work presented in this chapter was to identify new targets of mir-193b-3p and mir-582-5p dysregulated in ADPKD using bioinformatics analyses.
The most promising candidate selected from these analyses was *PIK3R1*, coding for the p85α regulatory subunit of the phosphatidylinositol-4,5-bisphosphate 3-kinase (PI3-K). PI3-K is an essential enzyme involved in the PI3-K/Akt/mTOR pathway.

4.1.1 The PI3-K/Akt/mTOR and MEK/ERK (MAPK) pathways: brief summary

The PI3-K/Akt/mTOR pathway The PI3-K/Akt/mTOR pathway is a key mechanism regulating fundamental aspects of cellular function such as transcription and translation of genes, as well as cell cycle and cell survival. It is a highly complex pathway involving two main enzymes: PI3-K and Akt (also known as PKB), targeting multiple substrates and regulated by many other mechanisms. A simplified summary of this pathway is presented in Figure 4.2 below.
It typically gets activated when growth factors such as EGF (epidermal growth factor), IGF (insulin-like growth factor) or insulin bind to their receptor (Mendoza et al., 2011). The regulatory subunit of the PI3-Kinase will then either be directly recruited to the receptor or indirectly via the intervention of adaptor proteins called GRB2 or IRS1. The PI3-K enzymes form a family of eight different proteins grouped into three classes (Vanhaesebroeck et al., 2010) based on their lipid substrate preferences and structure. *PIK3R1*, my gene of interest, codes for three regulatory subunits belonging to the class I_A PI3-K.

As shown in Figure 4.1, the class I_A of PI3-K is composed of three different catalytic subunits and five different regulatory subunits. The catalytic subunits are called p110-α, p110-β and p110-δ, coded by *PIK3CA*, *PIK3CB* and *PIK3CD*, respectively. They bind to the so-called "p85" regulatory subunits encoded by *PIK3R1* (p85-α and its two shorter isoforms p55-α and p50-α), *PIK3R2* (p85-β) and *PIK3R3* (p55-γ) via their p85 binding domain (Engelman et al., 2006). The regulatory subunits contain two SH2 (Src homology 2) domains that bind to phospho-tyrosine residues on activated receptors or adaptor molecules such as GRB2 or IRS1 (Zhou et al., 1993), inducing the reversion of the basal inhibition of the associated p110 catalytic subunit and to the recruitment

of PI3-K substrate PIP_2 (Yu et al., 1998). The two longer isoforms (p85-α and p85-β) additionally present an SH3 and a BCR homology domains (BHD) which was suggested to mediate Rab family members activation through addition of GTP or interact with small GTPases such as Cdc42 or Rac (Fruman, 1998; Chamberlain et al., 2008). The catalytic subunits are composed of a catalytic domain, a helical domain, a C2 domain, and a Ras binding domain that binds to Ras and mediates p85 activation (Mandelker et al., 2009). Mutations causing an increased PI3-K in cancer are most frequently found in *PIK3R1*, *PIK3R2* and *PIK3CA* (Jaiswal et al., 2009; Cheung et al., 2011; Samuels and Ericson, 2006).

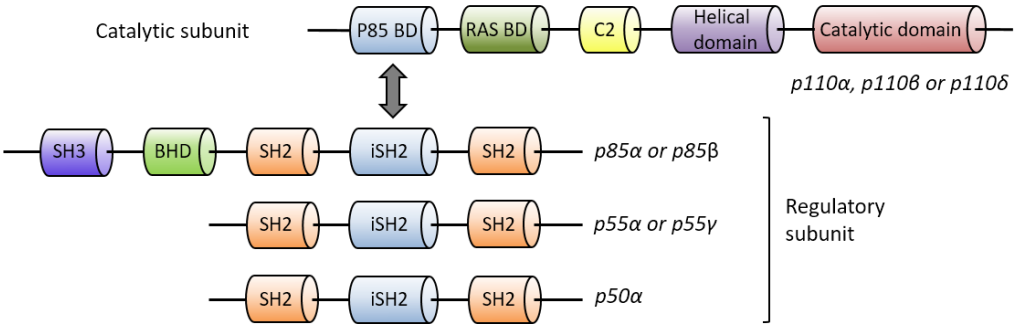

Figure 4.1: **Class I_A PI3-Kinase subunits.**
The PI3-K class I_A family is composed of three catalytic subunits p110-α, p110-β and p110-δ encoded by three different genes; *PIK3CA*, *PIK3CB* and *PIK3CD*, respectively. They bind to the regulatory subunits by their p85 binding domain (p85 BD). The regulatory subunits are five isoforms encoded by three different genes: *PIK3R1* codes for p85-α and two shorter isoforms p55-α and p50-α, *PIK3R2* codes for p85-β and *PIK3R3* codes for p55-γ.
RAS BD: Ras-binding domain / BHD: BCR homology domain / SH2/3: Src-homology 2/3 domain.

Class I_A PI3-K generate the PIP_3 lipid from PIP_2 (Vanhaesebroeck et al., 2001), which will activate multiple downstream components including Akt (Klippel et al., 1997; Franke et al., 1997). The PI3-K are also thought to regulate small GTPases such as members of the Ras, Rac and Arf families, that will themselves regulate other pathways such as the MEK/ERK pathway (Welch et al., 2003; Castellano and Downward, 2011; Krugmann et al., 2002; Eblen et al., 2002).

After being recruited by PIP_3, Akt undergoes phosphorylation by PDK1 (3-phosphoinositide-dependent kinase), leading to its full activation (Mora et al., 2004). pAkt can activate or inhibit many substrates involved in major pathways such as mTOR, NF-κB, CREB (cAMP/PKA), GSK3β (Wnt/TCF), caspase 9 or FOXO3 (Zhang et al., 2011a; Du and Montminy, 1998; Cohen and Frame, 2001; Delcommenne et al., 1998; Bai et al., 2009; Cardone et al., 1998; Laplante and Sabatini, 2012), leading to increased cell survival, reduced apoptosis, increased cell growth and cell cycle activation. In particular, pAkt inhibits the TSC1/2 (tuberous sclerosis) tumour suppressor thereby activating the mTORC1 complex (composed of mTOR, raptor (regulatory associated protein of mTOR) and GβL (mammalian lethal with SEC13 protein 8) (Inoki et al., 2002; Dunlop and Tee, 2009). The latter will then activate the S6K kinase and inhibit the translational inhibitor 4EBP, hence promoting protein synthesis and cell growth (Ma and Blenis, 2009; Hay, 2004; Gingras et al., 1999). mTOR can also associate with GβL, SIN-1 (stress-activated protein kinase-interacting protein 1) and rictor (rapamycin-independent companion of mTOR) to form the mTORC2 complex, which has been reported to have an activating effect on Akt (Sarbassov et al., 2005).

New substrates of Akt are still being discovered, making this pathway increasingly complex. Indeed, Ersahin et al. recently compiled data from 498 published studies on the PI3-K/Akt/mTOR pathway and referenced 254 components linked 478 times, showing that it regulates or is itself regulated by multiple pathways and thus collaborates with many of them including the Ras/MEK/ERK pathway described hereafter (Ersahin et al., 2015).

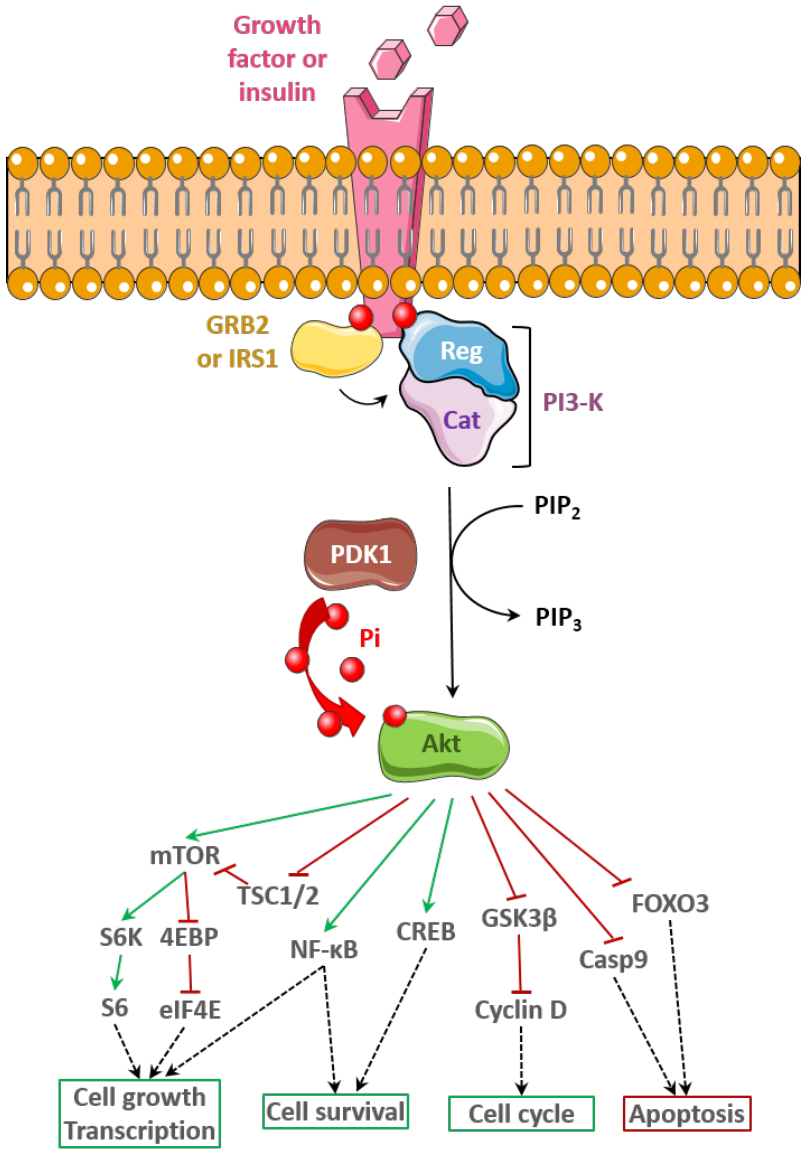

Figure 4.2: **Simplified PI3-K/Akt pathway.**
Growth factors or insulin activate PI3-K either directly either through docking protein such as GRB2 or IRS1. The regulatory subunit of PI3-K then recruits a catalytic subunit which form the active PI3-K. This enzyme will then generate phosphatidylinositol 3,4,5 triphosphate (PIP_3) from PIP_2 which will recruit Akt, itself phosphorylated and activated by PDK1. PTEN can inhibit the pathway by reversing the conversion of PIP_3 to PIP_2. p-Akt will then mediate the activation or repression of multiple cellular mechanisms by phosphorylation of proteins such as mTOR, NF-κB, CREB, GSK3β, Caspase 9 or FOXO3, for example. Green: activation / Red: inhibition
Casp9: caspase 9 / Cat: catalytic subunit / CREB: cAMP response element-binding protein / FOXO3: Forkhead box O3 / GRB2: Growth factor bound protein 2 / GSK3β: Glycogen synthase kinase 3 β / IRS1: Insulin receptor substrate 1 / mTOR: mechanistic target of rapamycin / NF-κB: nuclear factor kappa-light-chain-enhancer of activated B cells / PDK1: 3-phosphoinositide-dependent kinase 1 / Reg: regulatory subunit / TSC1/2: Tuberous sclerosis 1/2.

The Ras/MEK/ERK pathway (MAPK pathway) A second major pathway regulating cell proliferation and apoptosis is the MAPK pathway, also called Ras/MEK/ERK pathway. Ras is an oncoprotein typically activated by the binding of growth factors such as EGF, insulin or PDGF (platelet-derived growth factor) to their tyrosine kinase receptor. The phosphorylation of SH2 residues on the activated receptor mediates the binding of Grb2 which will then catalyse the exchange of Ras/GDP to Ras/GTP (Margolis and Skolnik, 1994).

Ras then recruits Raf (Rapidly accelerated fibrosarcoma), a serine/threonine protein kinase (MAPKKK), which will undergo several phosphorylation steps at the $S^{338\text{-}339}$, $Y^{340\text{-}341}$, S^{494} and S^{621} sites, and a dephosphorylation of the S^{259} site, resulting in its activation (Pumiglia et al., 1995; Kriegsheim et al., 2006; Fabian et al., 1993; Morrison et al., 1993; Dhillon et al., 2002a; Diaz et al., 1997; Marais et al., 1995). Ras has also been reported to activate PI3-K via its Ras-binding domain in the catalytic subunit (Rodriguez-Viciana et al., 1996; Pacold et al., 2000), whereas Akt was shown to inhibit Raf by phosphorylating its S^{259} site (Zimmermann and Moelling, 1999; Reusch et al., 2001) meaning the two pathways can co-activate or co-repress each other depending on factors such as cell type, developmental stage, intensity of signal or disease state (Mendoza et al., 2011). Following its activation, Raf will phosphorylate MEK1/2 (MAPK/ERK kinase or MAPKK) at the S^{218} and S^{222} sites, leading to its activation (Shapiro and Ahn, 1998; Lavoie and Therrien, 2015). Interestingly, PI3-K and Akt were shown to activate the Rac/GTP and PAK proteins, themselves mediating the phosphorylation and activation of the MEK1/2 and ERK1/2 members of the MAPK pathway, highlighting another relationship between these two pathways (Welch et al., 2003; Chan et al., 2008; Eblen et al., 2002; Rul et al., 2002).

Activated MEK1/2 will phosphorylate ERK1/2 (extracellular signal regulated kinase), a MAPK with over 150 substrates involved in major cellular functions such as cell proliferation and survival (McCain, 2013; Lake et al., 2016). For example, pERK1/2 was shown to positively regulate Myc, a protein involved in cell growth and differentiation (Sears et al., 2000; Grandori et al., 2000), as well as RSK (p90 ribosomal S6 kinase) and Elk-1 which will themselves activate the transcription factors CREB, c-Jun and c-fos, hence increasing cell proliferation and survival (Whitmarsh et al., 1995; Murphy et al., 2002; Marais et al., 1993; Anjum and Blenis, 2008; Leppä et al., 1998; Choi et al., 2011). Moreover, it negatively regulates the tumour suppressor FOXO3 (Yang et al., 2008b) and GSK3β that is itself a repressor of cyclin D (Ding et al., 2005; Takahashi-Yanaga and Sasaguri, 2008), hence inhibiting apoptosis and promoting cell cycle progression. Similarly to Akt, ERK1/2 has also been shown to inhibit TSC1/2 which therefore also promotes the activation of mTORC1 and the inhibition of its substrate 4EBP hence increases the transcriptional activity of the cell (Herbert et al., 2002; Ma et al., 2005). RSK was also suggested to activate S6 kinase adding to the increased cell growth and transcription (Roux et al., 2004). Figure 4.3 presents a simplified summary of the Ras/MEK/ERK pathway.

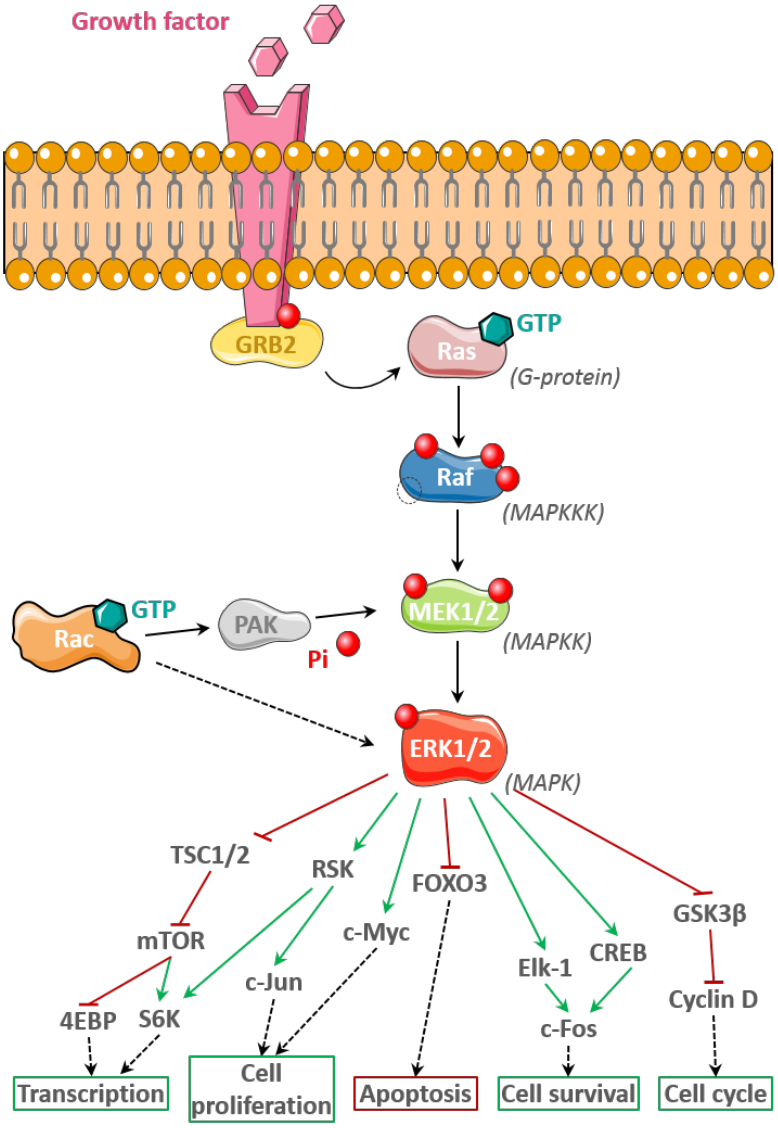

***Figure 4.3*: Simplified Ras/MEK/ERK (MAPK) pathway.**
The binding of growth factors to tyrosine kinase receptors induces the activation of Ras by exchange of a GDP group with a GTP by the accessory protein GRB2. Activated Ras mediates activating phosphorylation and dephosphorylation of Raf (MAPKKK), which will itself phosphorylate and activate MEK1/2 (MAPKK). pMEK1/2 will then activate ERK1/2, a MAPK responsible for the phosphorylation of over 150 different substrates including TSC1/2, c-Myc, RSK, Elk-1, FOXO3 and GSK3β, and therefore promoting cell proliferation, survival and cell cycle progression and repressing apoptosis. The Rac/GTP protein has been shown to be activated by Akt and PI3-K and to itself positively regulate PAK, MEK1/2 and ERK1/2. Green: activation / Red: inhibition.
CREB: cAMP response element-binding protein / ERK1/2: extracellular signal-regulated kinases / FOXO3: Forkhead box O3 / GRB2: Growth factor bound protein 2 / GSK3β: Glycogen synthase kinase 3 β / MEK1/2: MAPK/ERK Kinase 1 / PAK: p21 (RAC1) activated kinase 1 / RSK: ribosomal S6 kinase / Rac: Ras-related C3 botulinum toxin substrate / Raf: Rapidly accelerated fibrosarcoma / Ras: Rat sarcoma.

The Akt and ERK pathways in cancer and ADPKD Dysregulation of the PI3-K/Akt/mTOR and the Ras/MEK/ERK pathways have mostly been reported in cancer, and several clinical trials are currently being undertaken to develop inhibitors of PI3-K, Akt and/or mTOR as drugs against cancers (Https://clinicaltrials.gov/, 2017). Among the mutations leading to this pathway's over-activation in cancer, the loss of the PTEN tumour suppressor acting as an inhibitor of the PI3-K pathway has been characterised in several mice models of intestinal, mammary and endometrial cancers (Podsypanina et al., 1999). Activating mutations of the p110-α subunit encoded by *PIK3CA* have also been reported in up to 30 % of cancers such as colorectal, endometrial, breast and prostate (Engelman, 2009) cancers, as well as mutations in the p85-α regulatory subunit encoded by *PIK3R1* reported in human glioblastoma and ovarian cancer (McLendon et al., 2008; Philp et al., 2001). Furthermore, the oncogenic E17K somatic activating mutation of Akt has also been discovered in colorectal, lung, ovarian and breast cancers (Carpten et al., 2007; Malanga et al., 2008; Kim et al., 2008). Asati et al. listed over 50 active or completed clinical trials for PI3-K/Akt/mTOR drugs development in cancer, illustrating the promising effect of these treatments for the disease (Asati et al., 2016). As the MEK/ERK pathway has also been shown to promote cell proliferation and survival, two main factors of cancer development, notably by the activation of mTORC1, inhibitors of this pathway are also considered as potential anti-cancer drugs (around 20 referenced clinical trials in 2016, see Asati et al., 2016). Finally, because the two pathways are known to be tightly interlinked, dual PI3-K/ERK inhibitors are also being developed, for example the combination of PF-04691502 and PD-0325901 led to inhibition of cells growth in ovarian cancer (Sheppard et al., 2013) and 3-(2-aminoethyl)-5-(3-phenyl-propylidene)-thiazolidine-2,4-dione inhibited human leukaemia U937 cells proliferation and limited cell cycle progression in this model (Li et al., 2010).

In ADPKD, the mTOR pathway has been shown to be over-activated in the cystic cells and its inhibition to reverse cysts progression. Indeed, phospho-mTOR (activated form of mTOR) as well as its substrate phospho-S6K were strongly expressed in cysts lining epithelial cells of kidneys from ADPKD patients and at higher levels than epithelial cells of healthy kidneys (Shillingford et al., 2006).

Moreover, in the same study these findings were confirmed in mouse models presenting a cystic phenotype and the use of rapamycin, an mTOR inhibitor, reduced cystic disease and promoted apoptosis of cystic epithelial cells (Shillingford et al., 2006). Polycystin 1 was suggested to interact with TSC2, as *PKD1* deletion induced an increased expression of ERK hence indirectly mediated the repression of TSC1/2 and the activation of mTOR (Shillingford et al., 2006; Distefano et al., 2009). Additionally, Boehlke et al. suggested that cilia are also important for the regulation of mTOR implying that this underlies its dysregulation in ciliopathies such as ADPKD (Boehlke et al., 2010). All these studies support the idea of developing mTOR pathway inhibitors as drugs against ADPKD pathogenesis. Two molecules, Sirolimus (commercialised by Pfizer) and Everolimus (commercialised by Novartis), already used, *inter alia*, to prevent organ transplant rejection, were the subject of clinical trials for ADPKD until recently. However, the results of these trials were not encouraging and they were subsequently stopped. Indeed, no improvement of renal function could be detected in the treated group of patients after 18 months to 2 years, and adverse effects such as thrombocytopenia, leucopenia, peripheral oedema and hyperlipidaemia were observed in patients from the Everolimus study (Serra et al., 2010; Walz et al., 2010).

Among the explanations given to understand these clinical trial failures, the duration of treatments was suggested to be too short, the dose of Sirolimus used (calculated in order to limit side effects and drop-outs) may have been suboptimal to sufficiently inhibit renal mTOR and the high drop-out rate (due to adverse effects of Everolimus treatment) may have affected the power of the trials (Novalic et al., 2012; Serra et al., 2010; Walz et al., 2010; Braun, 2011). Despite these negative outcomes, several studies are still aiming to develop inhibitors of mTOR as ADPKD treatments. Two clinical trials are currently recruiting volunteers, and will involve less patients selected under stricter criteria than previously. The first one consists in administrating one oral dose of 3 mg Sirolimus once a week to avoid the loss of effect of this compound that could be seen with continuous exposure (Riegersperger et al., 2015), and the second aims to investigate the effects of Everolimus on the reduction of native kidney volume in ADPKD patients who have received a transplant (Assistance Publique - Hôpitaux de Paris, 2017).

Finally, combined inhibition of mTORC1 and mTORC2 or of mTORC1 and cAMP have recently been suggested to be more efficient for reducing cysts growth in ADPKD based on *in vitro* experiments on MDCK cells and *in vivo* trials in mice models of ADPKD (Ravichandran et al., 2014; Stephanis et al., 2017).

Taken all together, the PI3-K/Akt/mTOR and the Ras/MEK/Erk pathways are major regulators of cell proliferation, cell survival and cell growth through complex mechanisms involving reciprocal co-activation and co-repression, and have been linked to the pathogenesis of ADPKD. Characterising the processes by which these two pathways induce ADPKD would be important for the development of new treatments for this disease.

4.1.2 Bioinformatics and datasets comparisons for the identification of new miRNAs targets dysregulated in ADPKD

Following the previous approaches, it was decided that validating the deregulation of the selected candidates in more than one model was essential to increase the chances to get consistent results across models and avoid segment-specific or model-specific bias. As part of a Marie Curie Training Network, I had the opportunity to collaborate with Dorien Peters' and Peter-Bram 't Hoen teams in Leiden. D. Peters' team uses an inducible *Pkd1* knock-out mouse model and performed a high throughput RNA-sequencing to obtain the expression levels of a large number of genes, 2,376 of which were considered differentially regulated between the PKD model and normal (Malas et al., 2017). They also generated a 'PKD Signature' database of genes consistently dysregulated in PKD based on five studies using mice (Menezes et al., 2012 and Malas et al., 2017), human (Song et al., 2009) and rat models (O' Meara et al., 2012).

First of all I decided to directly compare our miRNA/mRNA array results with the Leiden group's microarray dataset (generated before their RNA-seq dataset mentioned later in this chapter) and the three others cited above to find mir-193b-3p or mir-582-5p targets common between two or more studies.

4.2 Direct comparison of five datasets and selection of *PLAU*

4.2.1 Selection of targets using direct comparisons and MirTarBase database

Only the mir-193b-3p and mir-582-5p predicted targets found to be deregulated in our array were compared to the other datasets. Tables 4.1a and 4.1b present the results of this datasets comparison. A list of 73 down-regulated and 82 up-regulated candidates was entered for mir-193b-3p and 119 and 174 up and down-regulated genes for mir-582-5p.

Table 4.1: Mir-193b-3p and mir-582-5p targets deregulated in ours and at least two other datasets.

(a) Mir-193b-3p targets

Gene	Other datasets	Deregulation
PLAU	LUMC (Mouse) / Menezes (Mouse) / O'Meara (Rat)	Up-regulated
SLC25A45	O'Meara (Rat) / Song (Human)	Down-regulated
RIMBP2	O'Meara (Rat) / Song (Human)	Down-regulated

(b) Mir-582-5p targets

Gene	Other datasets	Deregulation
SLC16A1	O'Meara (Rat) / LUMC (Mouse)	Up-regulated
RNF145	O'Meara (Rat) / Song (Human)	Up-regulated
BNIP2	Menezes (Mouse) / O'Meara (Rat)	Up-regulated
TFEC	O'Meara (Rat) / Song (Human)	Down-regulated
SLC16A10	O'Meara (Rat) / Song (Human)	Down-regulated
RIMBP2	O'Meara (Rat) / Song (Human)	Down-regulated

As my miRNAs of interest were found to be down-regulated in our model, I focused on their over-expressed targets. One and three up-regulated mRNA targets were found to be common to our dataset and at least two others for mir-193b-3p (Table 4.1a) and mir-582-5p (Table 4.1b), respectively. In order to shorten this list the MirTarBase (*http://mirtarbase.mbc.nctu.edu.tw/*) database that lists experimentally validated miRNA-target interactions was then consulted.

As none of the mir-582-5p targets had been validated and only one of the predicted mir-193b-3p targets came out of this analysis, namely *PLAU*, also found in the two other mouse studies and the rat study, this particular gene was chosen as a candidate for further experiments.

4.2.2 Measure of *PLAU* deregulation by (sq) RT-PCR in human cells

First of all, the expression of *PLAU* was measured in three independent batches of 2 normal and 4 cystic cell lines to see if there was a consistent up-regulation of this mRNA in ADPKD compared to normal.

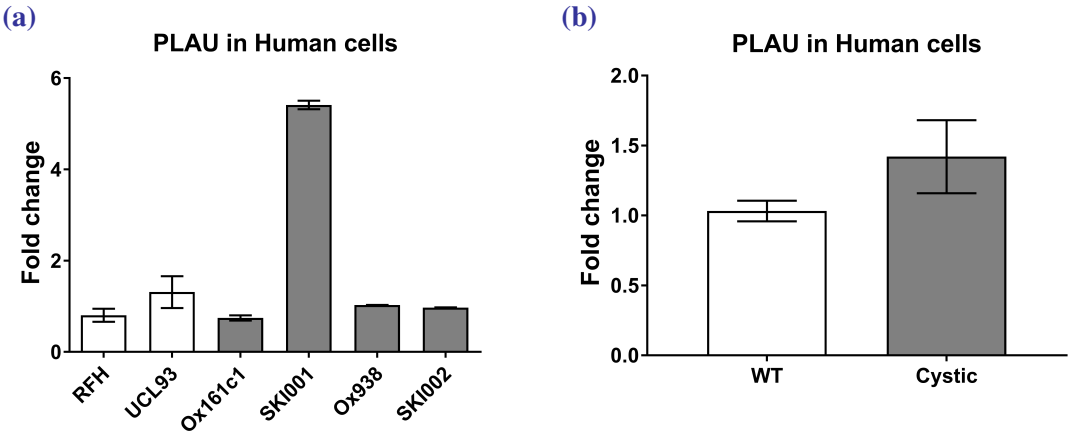

Figure 4.4: **Real-time PCR to measure the relative expression of *PLAU* in 6 human cell lines.** (a) Representative example of the three repeats: *PLAU* expression was measured in 2 normal (white bars) and 4 cystic (grey bars) cell lines. The values are represented as fold change compared to both normal cell lines (RFH and UCL93). (b) Combined data from three repeat experiments (n=3) grouping WT cells (white bar) and ADPKD cells (grey bar).

As shown in Figure 4.4a, representative example of the three repeats, only one cell line (SKI001) consistently over-expressed *PLAU* between batches. As a result, there was no significant increase in ADPKD compared to normal in our human cells models (Figure 4.4b). Because SKI001, a human ADPKD cell model, showed a rather high increase and *PLAU* was found over-expressed in three other studies, it was still decided to study its dysregulation in the mouse model.

4.2.3 Expression of *Plau* in mouse cells and kidney tissue

The expression of *Plau* was measured in two mouse cell lines (F1 and MEK) as well as mouse kidney tissue at 4 weeks of age.

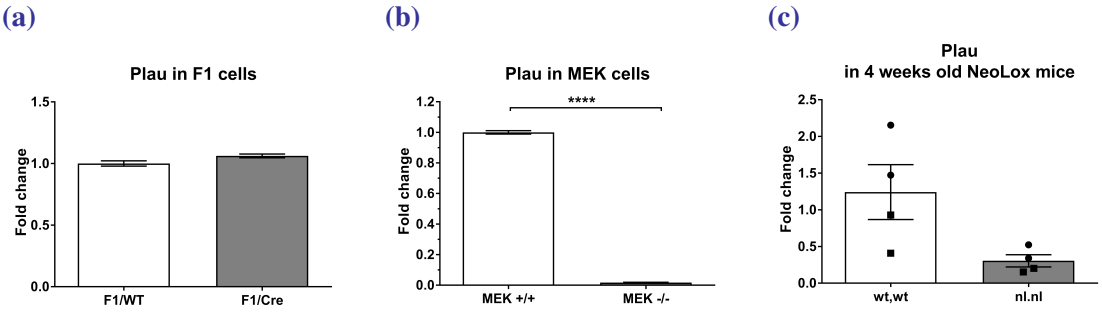

Figure 4.5: **Real-time PCR to measure the relative expression of *PLAU* in 2 different mouse cell lines and 4 weeks old NeoLox mice kidneys.**
(a) *PLAU* expression was measured in F1/WT (white bars) and F1/Cre (grey bars) cells (n=3), as well as (b) in MEK WT (white bars) and Null (grey bars) (n=3). The values are represented as fold change compared to normal cells (c) Expression of *PLAU* in 2 males and 2 females wt,wt and 2 males and 2 females nl,nl of 4 weeks of age.
***** $p<0.0001$ (Unpaired t-test)*

To observe a consistent result between human and mouse models, an over-expression of *Plau* would be expected in the F1 cells, MEK cells and/or kidney tissues. However, the F1 cells showed no change in *Plau* expression level (Figure 4.5a) and showed a strong down-regulation in MEK (Figure 4.5b) and kidneys (Figure 4.5c). As a result, although this gene was selected because found up-regulated in several studies and models, *Plau* was not selected for further experiments as no similar results could be replicated in the various models tested.

Consequently, as our partners in Leiden had since generated a new dataset from an RNA-seq experiment and created a 'PKD Signature' database, we collaborated to perform a Gene Set Enrichment Analysis to identify not only genes but also pathways that were enriched in ADPKD. This more complete systems biology approach aimed to widen the range of discoveries and at the same time find links between candidates.

4.3 Gene Set Enrichment Analysis and selection of new targets

4.3.1 GSEA results

To prepare the lists of genes to enter into the MSigDB software, all deregulated mRNAs from our study were combined to the Leiden group's dataset as well as the three other datasets previously cited. This gave me a list of all deregulated genes in at least one model of ADPKD. The TargetScan and MirTarBase prediction tools were then used to generate the list of predicted and validated targets for mir-193b-3p or mir-582-5p and the results were crossed with our list of all genes deregulated in at least one ADPKD model. Next, these lists were entered into MSigDB which gave an overview of the Top 100 most enriched pathways, gene sets and biological processes. These results were then sent to the Leiden group who crossed them with their 'PKD Signature' to find the most relevant connections and then sent back a list of the most significantly and strongly enriched pathways etc. as well as genes from these categories that were found in at least two datasets. The results at the end of the process are presented in Table 4.2 below. I also generated similar tables for the two miRNAs predicted targets but not necessarily dysregulated in ADPKD models (not shown). These were less informative as they gave much wider results and only an indication of the influence of the under-expression of my two miRNAs. Indeed, the non-restrictive list processed 931 genes for mir-193b-3p and 663 for mir-582-5p, compared to 305 and 246 genes when it was restricted to targets deregulated in ADPKD. Hence, I only worked on the latter for further exploratory experiments.

Table 4.2: GSEA results for mir-193b-3p (top) and mir-582-5p (bottom) targets found up-regulated in at least two datasets.

ADPKD Targets (mir-193b-3p)	p-value (Cells)	p-value (PKD Signature)						
EPITHELIAL_MESENCHYMAL_TRANSITION	8.83E-006	4.89E-026	MCM7	LOXL1	LAMC2	FLNA		
DNA_REPLICATION	3.96E-010	4.58E-005	MCM5	MCM6	MCM7	POLE		
UV_RESPONSE	0.0377	7.94E-008	IGFBP5					
ESTROGEN_RESPONSE_EARLY	0.000315	8.06E-011	KRT19					
PEROXISOME	4.63E-005	1.34E-013	SLC23A2					
MCM_PATHWAY	4.41E-006	0.00104	MCM7	MCM6	MCM5	CDT1		
XENOBIOTIC_METABOLISM	0.00185	3.49E-021						
FATTY_ACID_METABOLISM	0.015	1.92E-020						
IL6_JAK_STAT3_SIGNALING	0.0463	5.54E-009						
MISMATCH_REPAIR	1.44E-005	0.0233	MSH6					
MITOTIC_SPINDLE	9.20E-011	6.11E-008	CDK1	FLNA	KNTC1	KIF22		
ACTIVATION_OF_THE_PRE_REPLICATIVE_COMPLEX	9.50E-008	4.42E-006	MCM7	MCM6	MCM5	CDT1	POLE	
DNA_REPLICATION	8.14E-010	3.64E-007	CDT1	MCM5	MSH6	MCM7	POLE	RAD51
MYC_TARGETS_V1	2.64E-020	1.35E-006	MCM7	MCM6	MCM5			
ESTROGEN_RESPONSE_LATE	0.000315	4.88E-010	LAMC2	KRT19				
ADIPOGENESIS	0.0277	4.95E-014	ESYT1					
ANDROGEN_RESPONSE	0.0156	9.94E-006	KRT19	SLC38A2				
UNWINDING_OF_DNA	0.000998	0.00071	MCM7	MCM6	MCM5			

ADPKD Targets (mir-582-5p)	p-value (Cells)	p-value (PKD Signature)					
EPITHELIAL_MESENCHYMAL_TRANSITION	0.0121	4.89E-026	GJA1	FBN1	FSTL1		
ESTROGEN_RESPONSE_EARLY	0.000786	8.06E-011	SLC16A1	GJA1			
HYPOXIA	0.0121	1.16E-015	CDKN1A	TES			
UV_RESPONSE	6.09E-011	7.94E-008	GJA1	LPAR1	CELF2		
WNT_BETA_CATENIN_SIGNALING	0.00621	0.00194	AXIN2				
PROTEIN_SECRETION	0.00696	0.0162					
MITOTIC_SPINDLE	2.47E-006	6.11E-008	MYO9B				
ANGIOGENESIS	0.0363	9.94E-006	FSTL1				
ESTROGEN_RESPONSE_LATE	0.000786	4.88E-010	SLC16A1				
P53_PATHWAY	0.0035	2.99E-013	CDKN2B	CDKN1A	ZMAT3	CSRNP2	
ANDROGEN_RESPONSE	1.62E-005	9.94E-006	SLC38A2				
CELLULAR_RESPONSE_TO_EXTRACELLULAR_STIMULUS	0.0267	2.08E-005	CDKN2B	CDKN1A			

⟵ The enriched pathways, biological processes and gene sets are indicated with the significance value of their deregulation in our dataset ("Cells") and Leiden's PKD Signature. The genes involved in these processes and found up-regulated in at least two studies are indicated.
Genes in blue boxes were selected for further validation experiments.

18 and 12 processes were identified for mir-193b-3p and mir-582-5p, respectively. For both miRNAs, the most enriched element was the epithelial/mesenchymal transition, from which I selected *MCM7* (mir-193b-3p) and *FSTL1* (mir-582-5p). Other interesting pathways or gene sets identified were the responses mechanisms to hypoxia (*CDKN1A*, *TES*), UV (*IGFBP5*, *CELF2*) or oestrogens/androgens (*KRT19*), for example. Pathways more or less directly linked to cancer such as *MYC* (*MCM5, MCM6, MCM7*) and p53 (*CDKN1A*) were also significantly enriched in ADPKD models. Literature search was performed to find information about all the previously indicated targets and pathways and to identify the potentially most relevant for ADPKD pathogenesis (blue boxes in Table 4.2). This led to the selection of 8 genes involved in 12 enriched pathways for mir-193b-3p and 4 genes from 6 pathways for mir-582-5p.

4.3.2 Validation of targets selected from GSEA/MSigDB analysis

(sq) RT-PCR were performed on three different batches of three normal (CL11, RFH and UCL93) and four cystic (Ox161c1, SKI001, Ox938 and SKI002) human kidney cell lines to validate the over-expression of my previously selected targets. The combined results of these measurements are presented in Figure 4.6. The details of the fold change values in the various tested models can be found in the summary Table 4.3 at the end of this chapter.

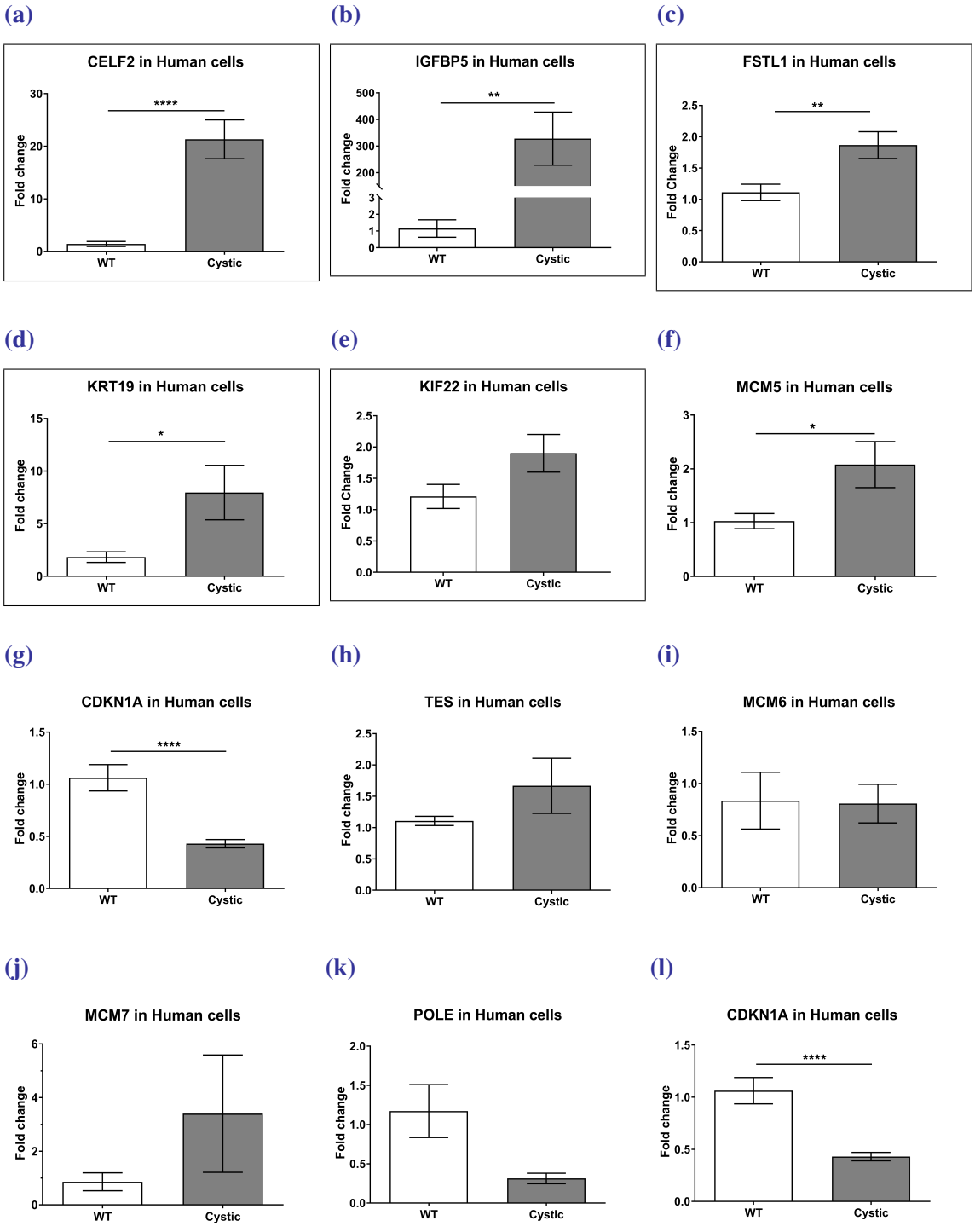

Figure 4.6: **Real-time PCR to measure the relative expression of targets selected from GSEA analysis in 9 human cell lines.**

The mRNA expression levels were measured in 3 normal (white bars) and 4 cystic (grey bars) cell lines in three independent batches of cells (n=3). The values are represented as fold change compared to normal cell lines (CL11, RFH and UCL93). The squares signal the genes selected for the next experiments.

** 0.05>p>0.01 ** 0.01>p>0.005 *** 0.005>p>0.0001 **** p<0.0001 (t-test with Welch's correction)*

Out of the 13 genes selected, five were found significantly (*CELF2* at 21.3-fold, *IGFBP5* at 328-fold, *FSTL1* at 1.87-fold, *KRT19* at 7.96-fold) or trending towards (*KIF22* at 1.9-fold) an up-regulation in ADPKD compared to Normal and thus selected for validation in the mouse model. *MCM5* and *CDK1* were also found over-expressed in ADPKD but not consistently enough between cell lines so were not taken through for further experiments. The other genes (*TES*, *MCM6*, *MCM7*, *POLE*, *CDKN1A*) did not show any up-regulation in ADPKD, two of them (*POLE* and *CDKN1A*) were even under-expressed in cystic cells which was opposite to what was expected. The five genes selected were then measured in mice models.

4.3.3 Validation of GSEA candidates in mouse cells and kidneys

(sq) RT-PCR were performed in three different mouse models: MEK WT/Null cells, F1/WT / F1/Cre cells and 4 or 10 weeks old NeoLox mice kidneys. For more clarity, only the results from the two genes that were the most interesting from these experiments (Figure 4.7), *CELF2* and *IGFBP5*, are presented. The results for the three other genes are indicated in the summary Table 4.3.

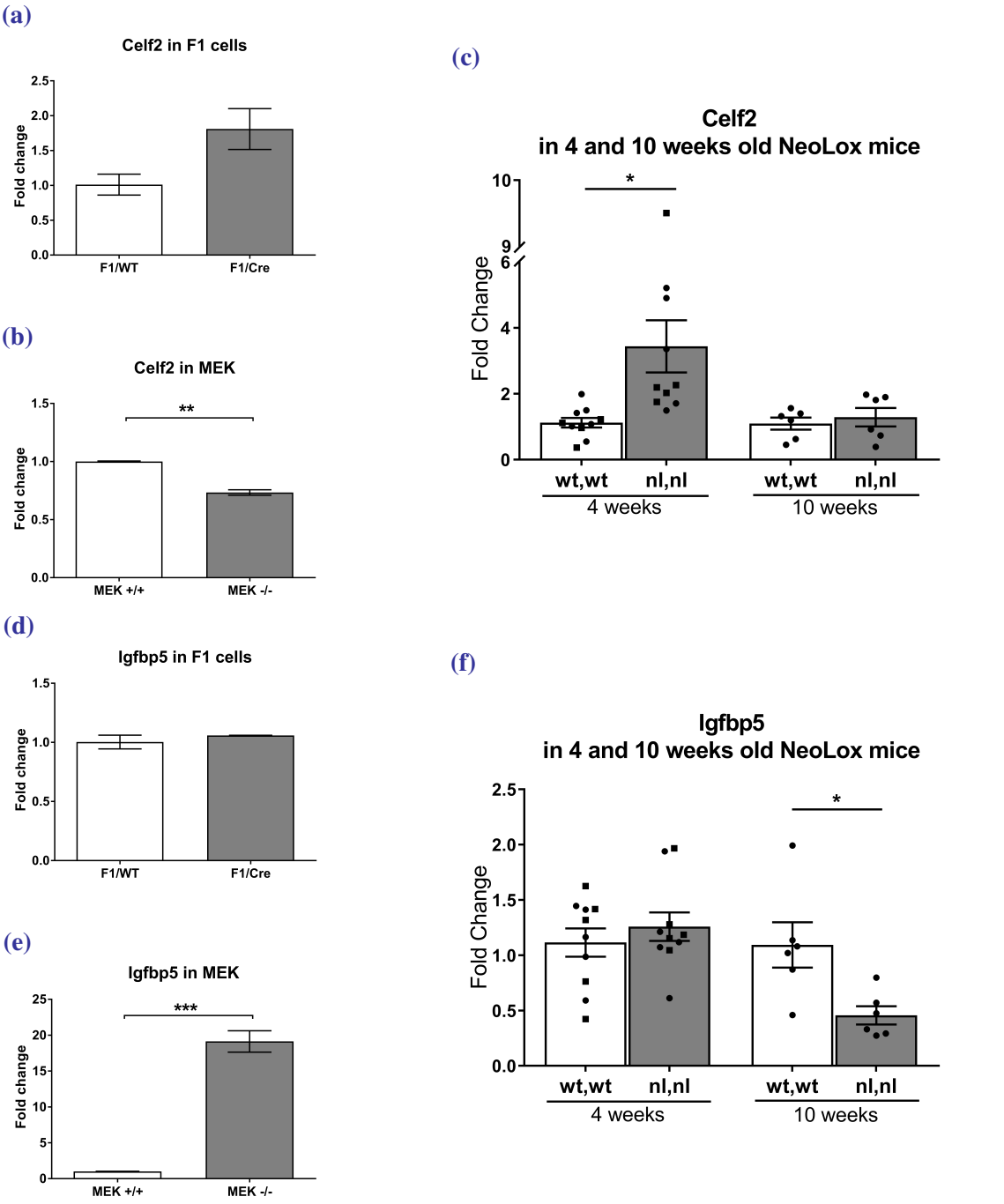

Figure 4.7: **Real-time PCR to measure the relative expression of *Celf2* and *Igfbp5* in three different models of mouse.**
The mRNA expression levels were measured in (a), (d) F1/WT and F1/Cre (n=3), (b), (e) MEK WT and MEK Null (n=3), (c) and (f) 5 males and 5 females WT and 5 males and 5 females NeoLox at 4 weeks and 3 males and 3 females WT and 3 males and 3 females NeoLox at 10 weeks. The values are expressed as fold change compared to WT (white bars) for each time point and the NeoLox (ADPKD) represented by the grey bars. Males are materialised as squares and females as circles.
** p=0.016 and p=0.011 (Unpaired t-test)*

Celf2 showed opposite results between the different mouse models used. It was up-regulated 3.4-fold in 4 weeks old NeoLox mice kidneys (Figure 4.7c), showed a non significant trend to an up-regulation in F1/Cre cells (Figure 4.7a), was unchanged in 10 weeks old NeoLox mice kidneys (Figure 4.7c) and was down-regulated in MEK Null cells (Figure 4.7b). *Igfbp5* was significantly up-regulated 20-fold in MEK Null compared to WT (Figure 4.7e), showed no change in F1 cells or 4 weeks old mouse kidneys (Figures 4.7d and 4.7f) and was significantly reduced in 10 weeks old mouse kidneys (Figure 4.7f). Globally, although these genes' over-expression was not consistent between all models, they were the two most promising ones out of the five previously mentioned and I went on with their characterisation by cloning part of their 3'UTR sequence and performing dual-reporter luciferase assays to study their interaction with mir-193b-3p and mir-582-5p.

4.3.4 Characterisation of selected GSEA genes interaction with my two miRNAs of interest

CELF2 and *IGFBP5* are predicted targets for mir-582-5p and mir-193b-3p, respectively. The potential seed sequences for both of these couples that were cloned and inserted into a pmirGLO vector are indicated in Figures 4.8a and 4.8b. Dual-reporter luciferase assays were performed to evaluate and validate the interaction between the genes of interest and their respective miRNAs. After many attempts, the insertion of mutations in the *CELF2* 3'UTR sequence was unsuccessful, leading me to stop working further on this gene. Mutagenesis of *IGFBP5*, however, was successful and the effect of inserting four mutations in the mir-193b-3p seed sequence on the fluorescent signal (Figure 4.8e) could be analysed.

(a)

hsa-miR-582-5p/CELF2 Alignment

```
    3' ucauugaccaacuuguUGACAUu 5' hsa-miR-582-5p
                       ||||||
748:5' guacaggagaaagguuACUGUAa 3' CELF2
```

mirSVR score: -0.0077
PhastCons score: 0.7820

(b)

hsa-miR-193b/IGFBP5 Alignment

```
    3' ucGCCCUG-AAACUCCCGGUCAa 5' hsa-miR-193b
         | | |: | | | |||||||
2471:5' uuCUGUAUGUCUUA-GGCCAGUa 3' IGFBP5
```

mirSVR score: -0.3649
PhastCons score: 0.5900

(c)

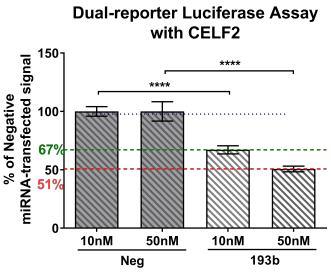

(d)

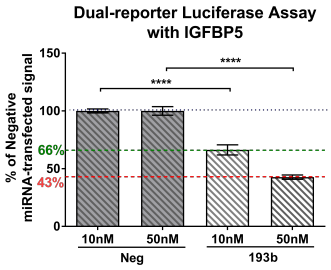

(e)

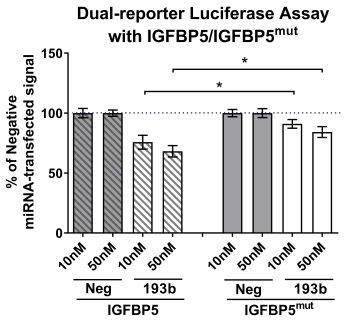

Figure 4.8: **Interaction between mir-582-5p and *CELF2* and mir-193b-3p and *IGFBP5*.** Predicted seed sequence of (a) mir-582-5p in *CELF2* 3'UTR and (b) mir-193b-3p in *IGFBP5* 3'UTR (source: www.microrna.org). mirSVR score: see Betel et al. Genome Biology, 2010 and PhastCons score: see http://compgen.cshl.edu/phast/. (c), (d) Dual-reporter luciferase assays (n=3) showing the Negative-miRNA-transfected condition (control) as a reference and the reduction of fluorescent signal compared to the control in (c) mir-582-mimic-transfected conditions at 10 and 50 nM miRNA concentration (*CELF2*) or (d) mir-193b-mimic-transfected conditions at 10 and 50 nM miRNA concentration (*IGFBP5*). (e) Dual-reporter luciferase assays (n=4). Intensity of fluorescence represented as percentage of control condition (Negative miRNA-transfected cells) with WT (left) and mutant (right) *IGFBP5* 3'UTR sequence (miRNA at 10 and 50 nM).
**** *$p<0.0001$ (Unpaired t-test)*

As shown in Figure 4.8, transfection of cells with mir-582-5p mimic and mir-193b-3p mimic induced a strong and significant reduction of the fluorescent signal from the pmirGLO vectors containing *CELF2* 3'UTR (Figure 4.8c) or *IGFBP5* 3'UTR (Figure 4.8d), respectively. This reduction was dose-dependent: at 10 nM the signal is reduced by 33 % (*CELF2*) and 34 % (*IGFBP5*), and reduced by 49 % and 57 % at 50 nM of miRNA mimic. Mutating four bases of the *IGFBP5* 3'UTR induced a significant but

low restoration of the signal (from 68 % reduction to 84 % at 50 nM), suggesting that the couple mir-193b-3p/*IGFBP5* may interact weakly *in vitro* at the level of the seed sequence cloned into the pmirGLO vector.

The next experiment presented in Figure 4.9 consisted in transfecting UCL93 cells with mir-193b mimic or mir-582 mimic or Ox161c1 with mir-193b inhibitor or mir-582 inhibitor and measure the mRNA levels of *IGFBP5* and *CELF2* in these cells 72 hours after transfection. Transfections are expected to induce an increased expression with the inhibitors and a decrease with the mimics.

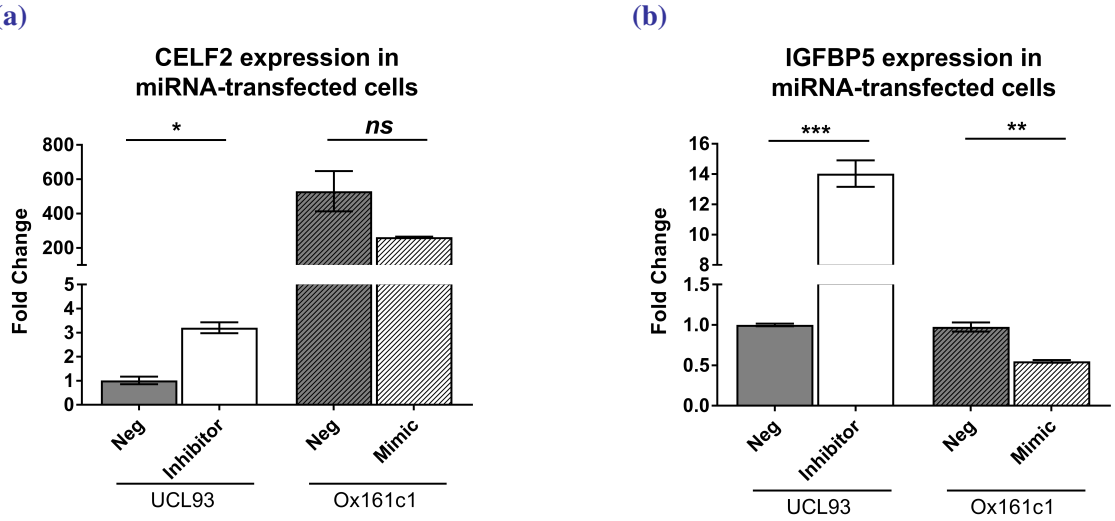

***Figure 4.9: CELF2* and *IGFBP5* expression in miRNA-transfected cells.**
Real-time PCR quantifying the levels of expression of (a) *CELF2* in UCL93 transfected with mir-582 inhibitor and Ox161c1 transfected with mir-582 mimic and in (b) *IGFBP5* in UCL93 transfected with mir-193b inhibitor and Ox161c1 transfected with mir-193b mimic. The values are expressed as fold change compared to UCL93 transfected with Negative control miRNA (control condition).
*n=3, ** p<0.002 *** p=0.001 (Unpaired t-test)*

CELF2 was increased 529-fold in Ox161c1 (cystic) compared to UCL93 (normal), confirming that this gene is consistently up-regulated in our ADPKD cells across batches. This was not visible for *IGFBP5*, as there was no significant difference between the two cell lines. Transfecting cells with the genes' relevant miRNA mimic induced an increased expression for both of them. This increase was much less important or significant for *CELF2* than *IGFBP5*, with a fold change of 3.2 for the former (Figure 4.9a) compared to 14 for the latter (4.9b). Transfection of cystic cells with miRNAs mimics, however, had a limited effect on their respective targets' expression.

The reduction of *CELF2* expression was not significant and the levels of *IGFBP5* were reduced to about half of the basal levels.

Because I did not manage to obtain a mutant sequence of the mir-582-5p seed sequence on the *CELF2* 3'UTR, and the transfection with miRNAs was not entirely convincing, the relevance of this candidate for a miRNA-associated work was difficult to prove. Furthermore, the variability between models for both *CELF2* and *IGFBP5* incited me to stop working on these targets and focus on the candidate identified and mentioned in the following section, *PIK3R1*, as it seemed more promising.

Indeed, in parallel of the validation experiments for the GSEA-selected targets, I had access to the data from the Leiden group's high throughput RNA-seq experiment on a conditional *Pkd1* knock-out mice model. They measured the expression of thousands of genes in mice at different ages and plotted the values for each one to represent a virtual over time expression level evolution.

4.4 Box plots: comparison of common genes with Leiden's RNA seq dataset and selection of *PIK3R1*

4.4.1 Box plots obtained from Leiden after sending the list of my genes of interest

Dorien Peters' team in Leiden kindly provided me with the values of expression levels of my genes of interest in their conditional *Pkd1* knock-out model, generated from an RNA-seq analysis (published since as Malas et al., 2017). Their mice were part of three different groups: the first group was given Tamoxifen at 3 months of age and sacrificed 1, 2 or 5 weeks after this stage ("Mild" group, boxes 2, 3 and 4 in Figure 4.10). The second group was given Tamoxifen at 40 or 38 days of age and sacrificed 86 or 88 days later, i.e. around 12 weeks ("Moderate" group, boxes 5 in Figure 4.10). Finally, the last group ("Severe" group, box 6 in Figure 4.10) was given Tamoxifen at 38 days and sacrificed 109 days later, i.e. around 15 weeks.

I sent my list of predicted targets for both miRNAs to the Leiden group, for which they sent me back the box plots in all mice groups. Most of the genes coming out of this analysis did not show any increase over time and a rather large proportion of them were even down-regulated in ADPKD mice compared to control.

Out of the 62 candidates for mir-193b-3p and 102 candidates for mir-582-5p, three appeared as interesting candidates based on their progressive increase in mRNA levels with ADPKD stages but also on their function and pathway from literature-based search. These three genes, also found up-regulated in our initial parallel mRNA/miRNA microarray, were *Pik3r1*, *Slco2a1* and *Shroom3*. *Pik3r1* and *Slco2a1* are predicted targets for mir-193b-3p and *Shroom3* for mir-582-5p.

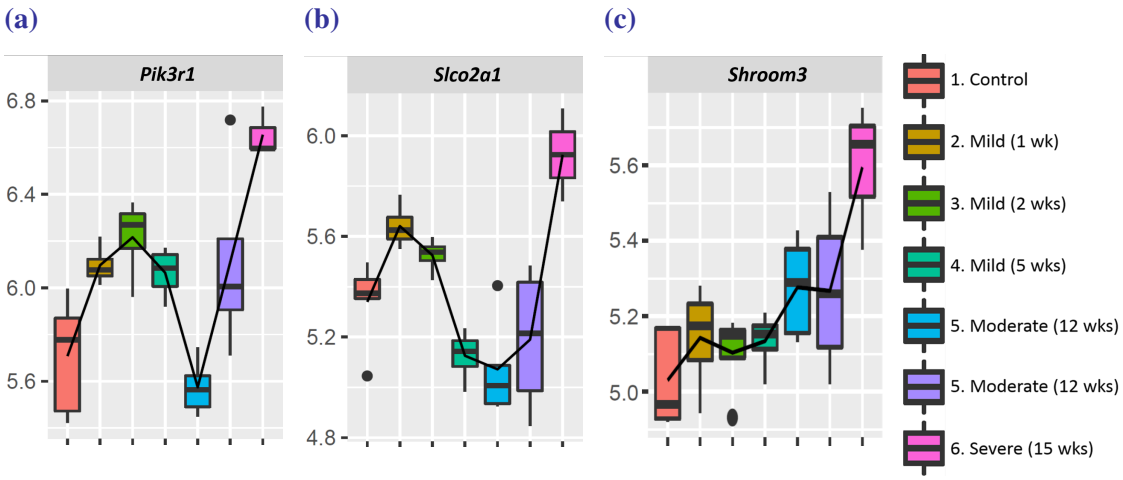

Figure 4.10: **Box Plots representing the expression of *Pik3r1*, *Slco2a1* and *Shroom3* in CreLox *Pkd1*$^{-/-}$ mice at different ages.**
Expression levels are expressed as log2 of cpm (count per million) for each group of mice for (a) *PIK3R1*, (b) *Slco2a1* and (c) *Shroom3*. The seven groups are, from left to right, control mice (orange box), Mild ADPKD mice (yellow, light green and dark green boxes), Moderate ADPKD mice (blue and purple boxes) and Severe ADPKD (pink boxes). Single dots represent outliers in the group plotted on the same vertical line.

These three genes showed a global increase in expression over time. Although only *Shroom3* was constantly increased between mild, moderate and severe ADPKD, *Pik3r1* expression was increased in the mild groups, one of the two moderate groups and the severe groups, which means that it was over-expressed compared to control mice at every time point, with a strong increase in the severe stage mice. *Slco2a1* expression was the most variable, with an up-regulation in the first two groups of mice, followed by a decrease to levels below the control in the next three time points, and then a strong increase again in the severe stage mice. Because these genes were the candidates with the most interesting potential function in ADPKD and the most visible increase over time, I then aimed to validate their deregulation in our human cells.

4.4.2 Expression of *PIK3R1*, *SLCO2A1* and *SHROOM3* in three different batches of normal and cystic human cells

Semi-quantitative real-time PCR were performed to validate the deregulation of the genes selected from the dot plots in our human cell lines (Figure 4.11). It was decided to perform this experiment in three independent batches of 6 cell lines to be able to observe a consistent deregulation rather than a batch-dependent non relevant up-regulation in ADPKD.

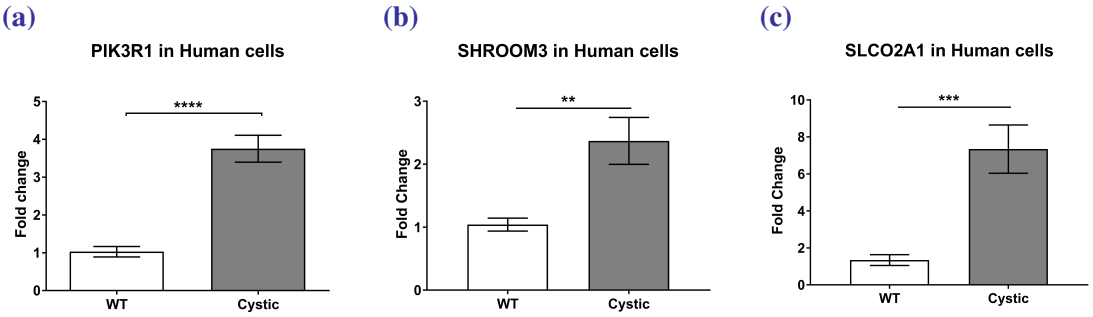

***Figure 4.11:* Real-time PCR to measure the relative expression of *PIK3R1*, *SHROOM3* and *SLCO2A1* in 6 human cell lines.**
(a) *PIK3R1*, (b) *SHROOM3* and (c) *SLCO2A1* expression was measured in three independent batches (n=3) of 2 normal (white bars) and 4 cystic (grey bars) cell lines. The values are represented as fold change compared to both normal cell lines (RFH and UCL93).
*** p=0.0018 *** p=0.0001 **** p<0.0001 (t-test with Welch's correction)*

As shown in Figure 4.11a, *PIK3R1* was consistently over-expressed in the cystic cells compared to normal by a fold change of 3.75, which supports the data from our microarray as well as what was observed by Dorien Peters' team and shown above as dot plots graphs. Ox161c1 and SKI001 were the most consistent cell lines in this gene's up regulation, while SKI002 showed an increase of *PIK3R1* mRNA expression in two out of three batches (data not shown). The global up-regulation of *SHROOM3* and *SLCO2A1* (Figures 4.11b and 4.11c), although significant, hides the fact that only one of the cell lines (SKI001 for *SHROOM3* and Ox161c1 for *SLCO2A1*) was consistently over-expressing these genes' mRNA. These genes' expression was then measured in two different models of mouse cells in order to avoid a bias in the deregulation of the gene due to the human cells model as was previously shown with *CALB1* and *CLIC5*. As no up-regulation could be seen for *Shroom3* and *Slco2a1* (data not shown, see summary in Table 4.3), I decided to focus on *Pik3r1* and the following data will be related exclusively to this candidate.

4.4.3 Expression of *Pik3r1* in two different models of mouse cells

In order to confirm what was observed in the human cells in the mouse model, *Pik3r1* expression was compared between WT and ADPKD in MEK and F1 cells.

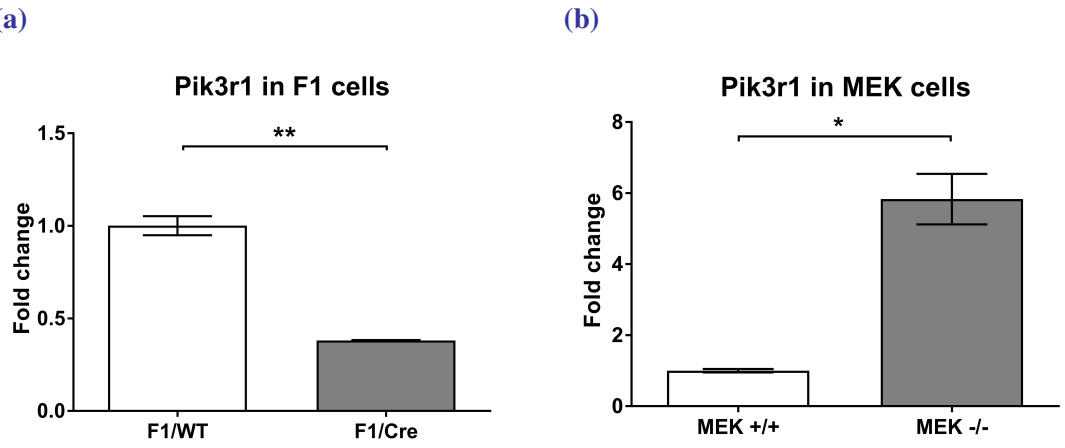

Figure 4.12: **Real-time PCR measuring the expression of *Pik3r1* in (a) F1/Cre and (b) MEK cells.**
The values are expressed as a fold change in Cystic cells (grey bars) compared to Normal (white bars).
** p=0.04 ** p=0.006 (Unpaired t-test)*

Although the F1 model showed a down-regulation in ADPKD (F1/Cre) compared to WT (Figure 4.12a), in the MEK model (Figure 4.12b), *Pik3r1* was highly and significantly up-regulated in ADPKD ($MEK^{-/-}$) compared to Normal (MEK WT). This is similar to what was found in the human cells, with an expression increased by 5.8-fold. The following step was to measure the expression of this gene in mouse kidneys at 4 and 10 weeks of age, in order to get the most thorough and accurate overview of its deregulation in ADPKD.

4.4.4 Expression of *Pik3r1* in NeoLox mouse kidneys at 4 and 10 weeks

The comparative expression of the gene of interest *Pik3r1* was measured in an orthologous *Pkd1*^{nl,nl} mouse model, in which the expression of *Pkd1* is reduced, and that reaches its maximum kidney-to-body-weight ratio (2KW/BW) at 4 weeks of age. Figure 3 presents the changes of expression of this gene measured by (sq) RT-PCR in the disease model nl,nl compared to WT at 4 and 10 weeks of age.

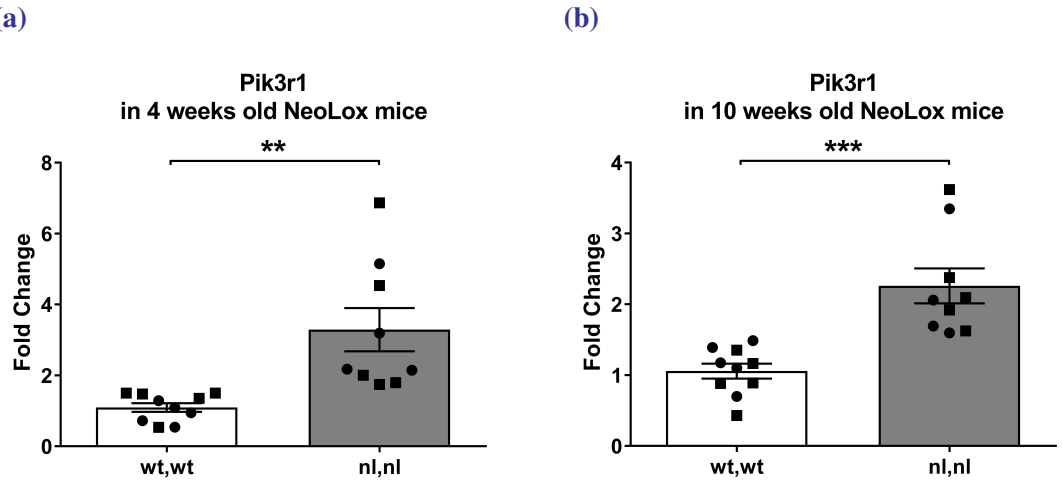

Figure 4.13: **Differential expression of *Pik3r1* in the kidney of 4 weeks old and 10 weeks old NeoLox mice.**
The values are represented as fold changes compared to all WT mice. Kidneys were extracted from five males and five females wt,wt as well as five males and four females nl,nl mice of (a) 4 weeks and five males and five females of (b) 10 weeks of age. Males are symbolised as squares and females as circles.
*** p=0.006 *** p=0.001 (Unpaired t-test with Welch's correction)*

Pik3r1 was significantly over-expressed in ADPKD compared to WT in the NeoLox mouse model at 4 and 10 weeks, with fold change values of 3.71 at 4 weeks and 2.3 at 10 weeks. In Figure 4.14 (sq) RT-PCR was used to compare the changes in expression of *Pik3r1* between males WT and NeoLox and between females WT and NeoLox, to study any effect of gender on the deregulation of the gene.

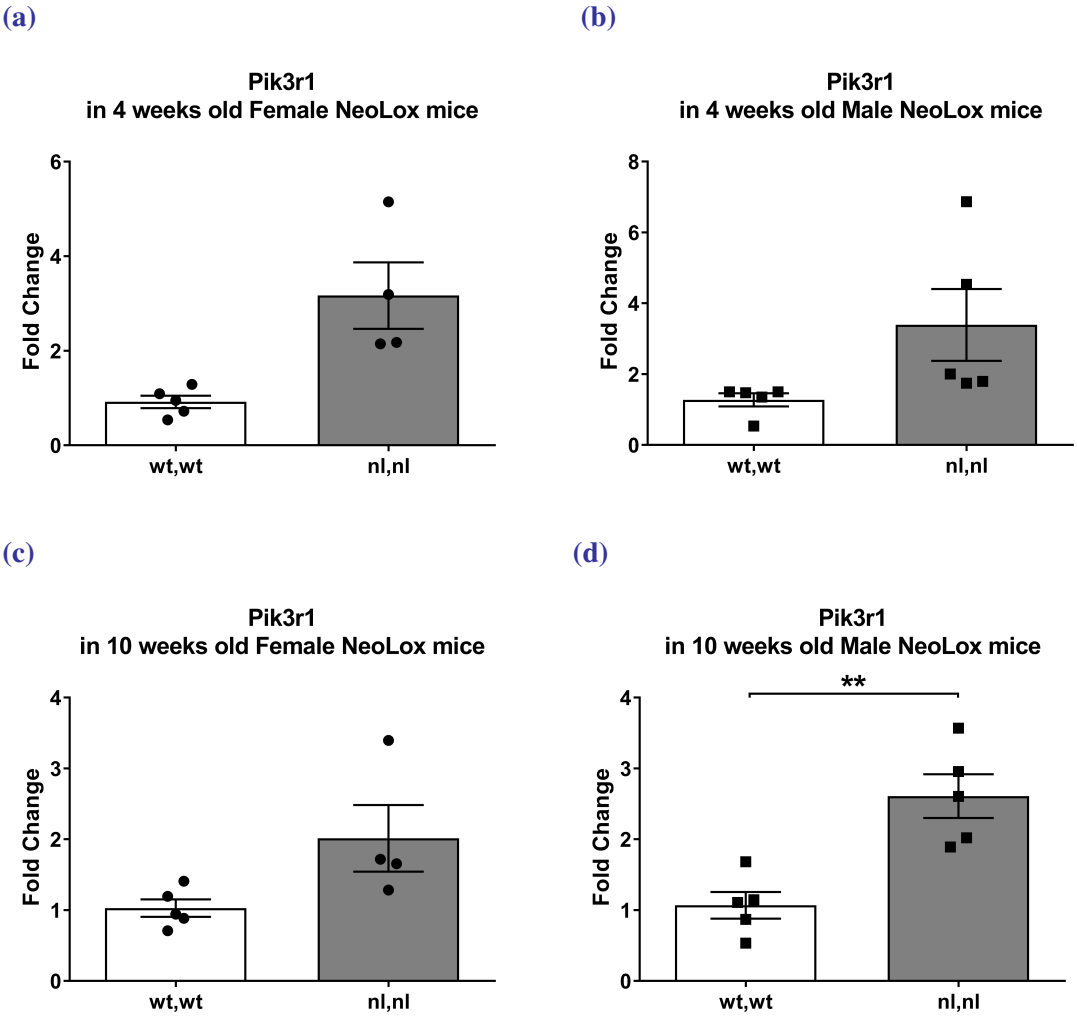

Figure 4.14: **Differential expression of *Pik3r1* in the kidney of 4 weeks and 10 weeks old female or male NeoLox mice.**
The values are represented as fold changes compared to WT mice of the indicated gender. (a),(c) female NeoLox (b),(d) male NeoLox.
*** p=0.0027 (Unpaired t-test)*

Although no difference between genders can be seen at 4 weeks, *Pik3r1* was significantly up-regulated in male but not in female mice at 10 weeks. Although there was a trend to an up-regulation in females (Figure 4.14c), this was not significant and seemed due to the presence of an outlier in the NeoLox mice that skewed the results towards an over-expression. The males however, all showed an increase of *Pik3r1* expression in ADPKD which resulted in a significant 2.6-fold increase compared to their WT counterparts (Figure 4.14d). At 10 weeks, the male-to-female ratio went from 1.04 to 1.3, supporting an enrichment of *PIK3R1* in the former and not in the latter.

4.4.5 Expression of the PI3K-p85α protein in normal and cystic human cell lines

This study's gene of interest *PIK3R1* codes for the most common regulatory subunit of the PI3-K enzyme, p85α. The proteins from five normal and four cystic renal human cell lines were extracted and a Western blot was run for PI3K-p85α. Indeed, as *PIK3R1* is over-expressed by 2-fold in these cells, the aim was to see whether the deregulation that was observed at the mRNA level could be confirmed and detectable at the protein level. As shown in Figures 4.15a and 4.15b, the anti-PI3K-p85α antibody detects a specific band of the predicted molecular weight (85 kDa). Indeed, after efficiently transfecting cells with an anti-*PIK3R1* siRNA, with a 70 % reduction of the mRNA expression, the band corresponding to the correct size of the protein disappears.

Following this, a Western blotting of PI3K-p85α was performed in all our cell lines. The results of this experiment are presented in Figure 4.15c. PI3K-p85α was strongly up-regulated in the cystic cells (Ox161c1, SKI001, Ox938 and SKI002) by 5.7-fold compared to normal. Figure 4.15d shows the expression of PI3K-p85α corrected for the β-actin loading control. Ox161c1 and SKI001 showed the highest PI3K-p85α increase and SKI002 the lowest.

(a) qPCR on siRNA-transfected cells **(b)** Immunoblotting on siRNA-transfected cells

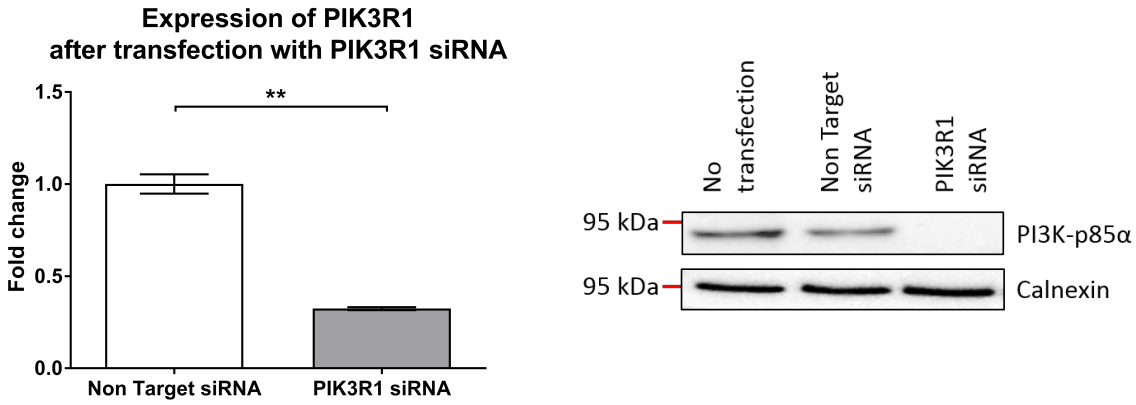

(c) Expression of PI3K-p85α in five normal and four cystic human kidney cell lines

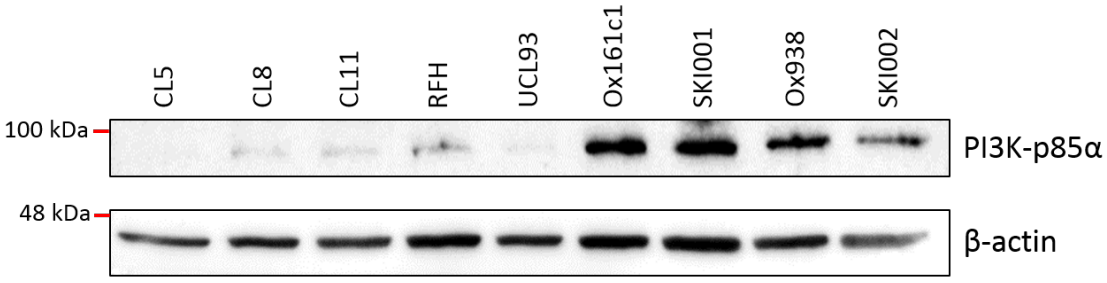

(d)

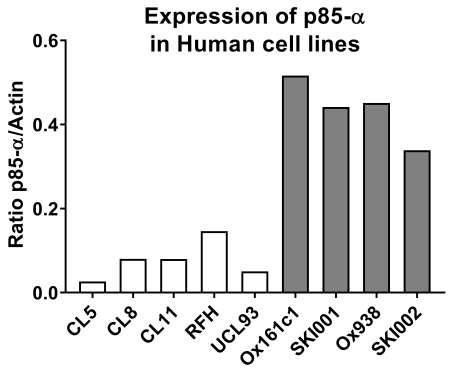

(e)

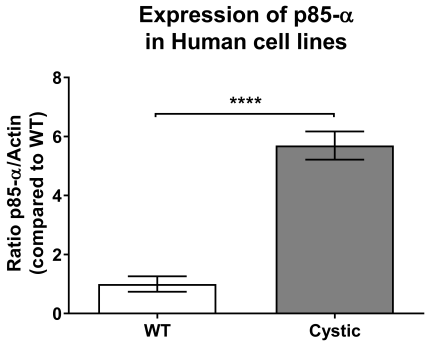

Figure 4.15: **Validation of anti-PI3K-p85α antibody by siRNA transfection and Western blotting and expression of p85-α in nine human cell lines.**
The specificity of the PI3K-p85α antibody was first validated by knocking-down *PIK3R1* expression using siRNA, (a) checking its efficiency by qPCR and (b) blotting the corresponding protein. (c) 20 μg of protein from each cell line (five normal cells: CL5, CL8, CL11, RFH and UCL93 (white bars) and four cystic cells: Ox161c1, SKI001, Ox938, SKI002 (grey bars)) were run in a 10 % SDS-PAGE gel and marked for β-actin (loading control, 42 kDa) or PI3K-p85α (85 kDa). (d) The p85-α/β-actin ratio was calculated for each cell line. (e) The p85-α/β-actin ratio was expressed as fold changes compared to the average value in WT cells.
*** p=0.006 **** p<0.0001 (Unpaired t-test)*

The up-regulation of *Pik3r1* having been proved in several models and at both the mRNA and protein level, the focus was then put on its interaction with his predicted partner mir-193b-3p that was up-regulated in our microarray (see above).

4.4.6 Prediction and demonstration of the interaction between mir-193b-3p and *PIK3R1* using dual-reporter luciferase assays and transfection of normal and cystic human cells

First of all, the probability of *PIK3R1* to be a target for my miRNA of interest mir-193b-3p was assessed. Using the miRWalk multiple databases prediction tool, all the available databases were selected to identify how many of them predicted an interaction between *PIK3R1* and mir-193b-3p (Figure 4.16a).
Out of twelve algorithms, six (MicroT4, miRMap, MiRNAMap, RNA22, RNAhybrid, TargetScan) predicted mir-193-3p to target *PIK3R1*. For the mouse orthologs, four algorithms predicted this interaction. This ranked mir-193b-3p in the top 7 % and 33 % of all miRNAs predicted to interact with *PIK3R1* by at least one algorithm in human and mouse, respectively. Mir-582-5p was not predicted to be a target for this gene in mouse (not shown). I considered this was enough information to support the probability of an interaction between *PIK3R1* and mir-193b-3p, so went on to carry out dual-reporter luciferase assays to validate this hypothesis.

Part of the human *PIK3R1* 3'UTR sequence was cloned into a pmirGLO vector coding for an upstream renilla reporter and a downstream firefly reporter. This insert contains the predicted seed sequence for mir-193b-3p on *PIK3R1* (Figure 4.16b). Similarly to what was done in the previous chapter (Figure 3.10), the fluorescent signal is at its maximum when no element can prevent the transcription of the firefly luciferase reporter, while a miRNA targeting the seed sequence coded upstream of this reporter would prevent or limit its transcription and consequently reduce the fluorescent signal recorded.

(a) MiRWalk multiple databases prediction results in human and mouse

			MiRNA binding sites prediction Algorithms											
Gene	EntrezID	miRNA	miRWalk	Microt4	miRanda	mirbridge	miRDB	miRMap	miRNAMap	Pictar2	PITA	RNA22	RNAhybrid	Targetscan	SUM
PIK3R1 (Human)	5295	hsa-miR-193b-3p	0	1	0	0	0	1	1	0	0	1	1	1	6
Pik3r1 (Mouse)	18708	mmu-miR-193b-3p	0	1	0	0	0	1	0	0	0	1	1	0	4

(b)

hsa-miR-193b/PIK3R1 Alignment

```
    3' ucgcccugaaacuccCGGUCAa 5' hsa-miR-193b
                      ||||||
950:5' guaaauguacaggauGCCAGUa 3' PIK3R1
```

mirSVR score: -0.0212
PhastCons score: 0.5498

(c)

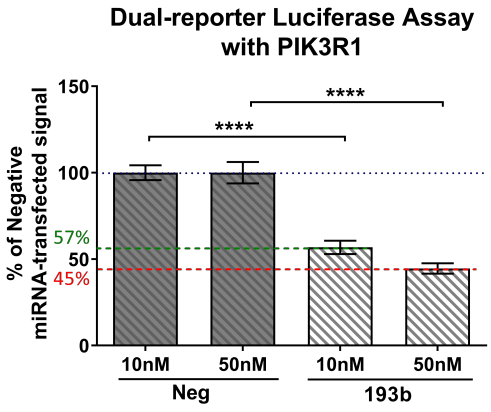

(d)

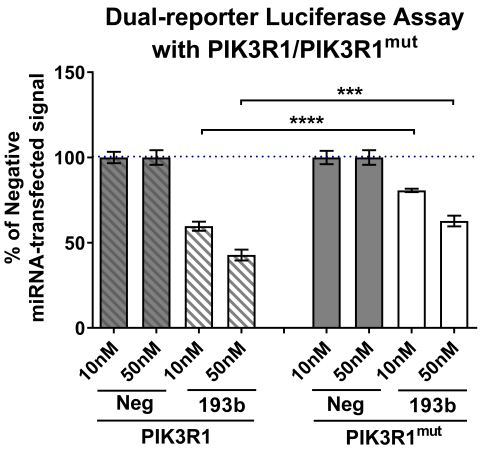

***Figure 4.16: PIK3R1*/mir-193b-3p interaction.**
(a) Results from mirWalk 2.0 multiple databases prediction for mir-193b-3p/*Pik3r1* interaction in human and mouse. (b) Predicted seed sequence of mir-193b-3p on *PIK3R1* 3'UTR (source: www.microrna.org). mirSVR score: see Betel et al. Genome Biology, 2010 and PhastCons score: see http://compgen.cshl.edu/phast/. (c) Dual-reporter luciferase assays (n=3) showing the Negative-miRNA-transfected condition (control) as a reference and the reduction of fluorescent signal compared to the control in mir-193b-mimic-transfected conditions at 10 and 50 nM miRNA concentration. (d) Dual-reporter luciferase assays (n=3) intensity of fluorescence values represented as percentage of control condition (Negative miRNA-transfected cells) with WT (left) and mutant (right) *PIK3R1* 3'UTR sequence at 10 and 50 nM miRNA concentration.
**** p=0.0003 **** p<0.0001 (Unpaired t-test)*

As shown in Figure 4.16c, transfection of HEK cells with mir-193b-3p mimic induced a significant reduction of fluorescent signal at 10 nM (43 % reduction) and 50 nM (54 %). This suggests an interaction between the *PIK3R1* 3'UTR cloned sequence and mir-193b-3p mimic. When 4 mutations were introduced in the seed sequence for this miRNA, the signal was partially but significantly restored to 80 % of control (20 % reduction) at 10 nM and 62 % of control (38 % reduction) at 50 nM (Figure 4.16d). It was concluded that mir-193b-3p does at least in part interact with *PIK3R1* 3'UTR at the selected seed sequence.

The next analyses aimed at proving the *PIK3R1*/mir-193b-3p interaction in a more physiological context, namely normal and cystic human kidney cell lines. In Figure 4.17, UCL93 (normal) and Ox161c1 (cystic) were transfected with Negative control or mir-193b inhibitor or mir-193b mimic, respectively. The expression of the gene of interest was then measured in the different conditions using real-time PCR (Figure 4.17a). First of all, the expression of *PIK3R1* at the basal level was increased by 2.8-fold in cystic cells compared to normal, confirming results shown previously in previous batches and the relevance of this particular batch of cells for my study. Transfecting UCL93 with mir-193b inhibitor induced an increase of *PIK3R1* expression by 1.7-fold while transfection of Ox161c1 with mir-193b inhibitor had the opposite effect which was a strong reduction of *PIK3R1* expression by 8.4-fold. This was expected as inducing a reduction of miRNA levels should lead to less down-regulation of its target gene, and the opposite effect should be seen when miRNA levels increase.

Similar transfections were performed on another batch of UCL93 and Ox161c1 and Western blotting of PI3K-85α and β-actin control was carried out, and the intensity of the bands as well as the ratios PI3K-85α/β-actin were measured (Figures 4.17b and 4.17c). Similarly to what was found by (sq) RT-PCR on another batch of cells, the basal difference of expression could be seen between normal and cystic cells and transfections with mir-193b inhibitor or mir-193b mimic induced an increased or reduced level of PI3K-85α in two repeats of the experiment.

(a) qPCR results

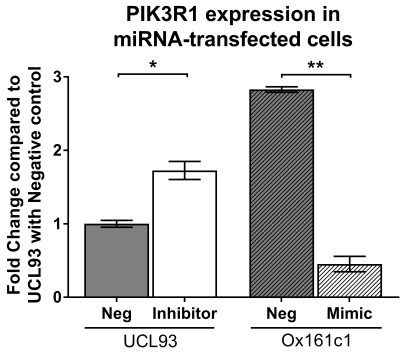

(b) Western blotting in miRNA-transfected cells

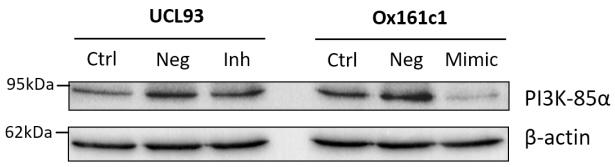

(c) Western blot quantification (n=2)

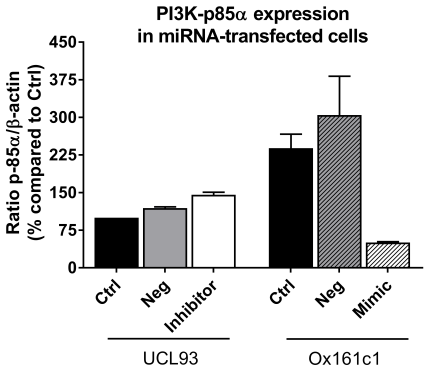

***Figure 4.17: PIK3R1*/mir-193b-3p interaction in human kidney cells.**
(a) Real-time PCR quantifying the levels of expression of *PIK3R1* in UCL93 transfected with mir-193b inhibitor and Ox161c1 transfected with mir-193b mimic. The values are expressed as a fold change of the control condition (UCL93 with Negative miRNA). (b) Western blotting of PI3K-p85α in UCL93 untransfected (Ctrl) or transfected with Negative control (Neg) or mir-193b inhibitor (Inh) and Ox161c1 untransfected or transfected with Negative control or mir-193b mimic. (c) Quantification of bands intensity from 2 repeats of Western blotting. Represented as PI3K-p85α/β-actin control ratio and as percentage of value in no miRNA control condition in UCL93.
** p=0.03 ** p=0.0022 (Unpaired t-test)*

All added together, I proved by different techniques that *PIK3R1* is increased in ADPKD and is a target for mir-193b-3p.

The next steps of my analysis were to prove that *PIK3R1* is involved in the development of cysts and ADPKD.

4.4.7 3-Dimensional cyst assays and role of *PIK3R1* in cyst development

3D cysts assays are useful to study the development of cysts in culture, as the cells grow in a 3 dimension matrix and can form cysts more or less large depending on the medium and culture conditions. I first decided to test different conditions to optimise the assay for my particular study, since IGF-1 acts on a similar pathway as insulin added as a supplement of insulin-transferrin-selenium (ITS), usually added to culture media for epithelial cells. Therefore two different medium conditions were chosen; a “full” medium containing all the usual chemicals (Nu Serum, ITS, Hydrocortisone (HC) and Epidermal Growth Factor (EGF)) and another ”poor” one containing Nu serum only. The effect of IGF-1 were also compared at 50 ng/mL and 100 ng/mL. Figure 4.18a shows the difference of cyst area between cells cultured in “full” medium containing ITS, EGF and HC and either not treated with any extra compound, or treated with DMSO, with IGF-1 at 50 ng/mL or 100 ng/mL or with forskolin, while Figure 4.18b presents the cyst areas of cells under the same various conditions but cultured in a “poor” medium containing none of the extra-compounds. First of all, the cells in the “poor” medium did not look healthy after 10 days of culture and the cysts areas were globally lower than cells cultured in the “classic” medium. In both conditions it was observed that DMSO at 0.02 % had no effect on the cysts size, and as expected the positive control forskolin induced a significant increase in cyst area. Finally, treatments with IGF-1 at 50 ng/mL and 100 ng/mL induced a significant increase in the cysts area correlated to the IGF-1 concentration.

In Figure 4.18c the cysts areas in both media are expressed as percentage of their respective DMSO conditions. This allows to compare the difference between the “poor” and “full” medium. Globally, in all conditions the presence of compounds did not mask the effects of IGF-1 as there was no significant difference in the increase in cysts areas between the two media.

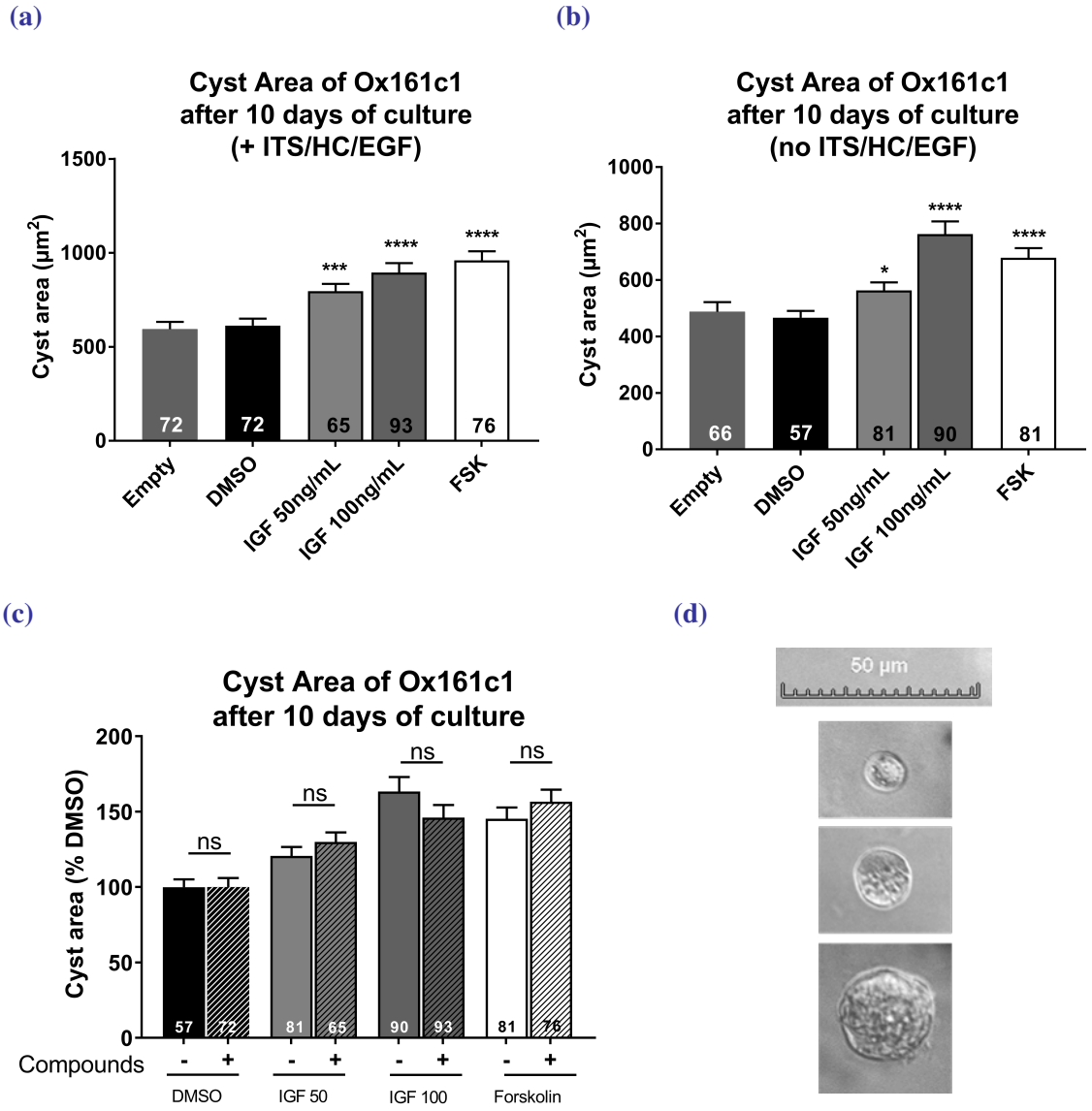

Figure 4.18: **3D-cyst Assay of Ox161c1 cultured in different conditions.**
Ox161c1 were cultured for 10 days with (a) or without (b) extra-ITS, HC and EGF, and with or without IGF-1 at 50 or 100 ng/mL. Forskolin (FSK) was used as a positive control of cyst growth. (c) combined data from (a) and (b) represented as percentage of DMSO condition in order to directly compare the two conditions. n: number of cysts measured for each condition. (d) Representative images of cysts of different sizes (small, medium and large) at magnification x200 with scale indicated on top.
** p=0.03 *** p=0.0005 **** p<0.0001 (Mann-Whitney test)*

It was therefore decided to perform the next experiment under the following conditions: medium containing EGF and HC (called ”ITS-depleted medium”) and IGF-1 used at 200 ng/mL in order to see a bigger effect of this compound.

Ox161c1 cells were transfected with a Negative control siRNA or an anti-*PIK3R1* siRNA and the effect of *PIK3R1* knock-down on the capacity of cells to respond to IGF-1 treatment was studied. Figure 4.19 presents the cysts areas in the different conditions at 7 and 12 days of incubation.

(a) **(b)**

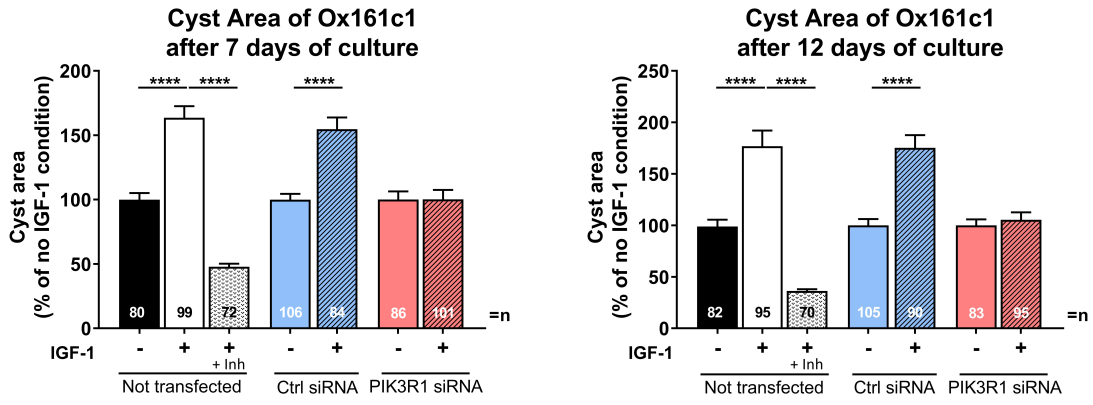

Figure 4.19: **3D-cyst Assay of Ox161c1 transfected or not with control or anti-*PIK3R1* siRNAs.**
Ox161c1 were either not transfected or transfected with Negative control siRNA or anti-*PIK3R1* siRNA and cultured for 7 and 12 days. Results are presented as percentage of control condition (no transfection and no IGF-1 treatment). n: number of cysts measured for each condition.
** p=0.03 *** p=0.0005 **** p<0.0001 (Mann-Whitney test)*

The results are similar at 7 and 12 days, the only difference being that, as expected, cysts were globally larger at the later time point (593 cm^2 vs. 658 cm^2, not shown).
Treatment with IGF-1 led to a significant increase in cyst area in untransfected cells or those transfected with a Negative control siRNA, hinting that the transfection procedure itself did not induce any significant off-target effect in the response to IGF-1 pathway activation. This activation was higher than in the preliminary experiment (146 % at 10 days with "full" medium and IGF-1 at 100 ng/mL (preliminary experiment) vs. 163 % and 176 % with "ITS-depleted" medium and IGF-1 at 200 ng/mL for the control condition).
Transfecting Ox161c1 with *PIK3R1*-targeted siRNA induced a total inhibition of the cyst growth induced by IGF-1 at 7 (Figure 4.19a) and 12 days (Figure 4.19b) of incubation.

The number and size of the cysts in the siRNA-transfected condition were similar to the untransfected condition, supporting the idea that the inhibition of growth was due to the blocking of the pathway rather than of an effect of the *PIK3R1*-targeting siRNA on the cysts integrity.

Culturing untransfected Ox161c1 with the *PIK3R1* inhibitor led to not only an inhibition of cysts growth but also to a reduction of their size compared to the untreated condition.

Globally, these results suggest that *PIK3R1* is an essential element involved in cyst growth in Ox161c1 and that its over-expression could be partly responsible for cysts growth in ADPKD. To study how the over-expression or inhibition of *PIK3R1* influences the regulation of the Akt/ERK pathway and its activation by IGF-1, Western blotting of the proteins involved in this pathway and of their phosphorylated forms were then performed.

4.4.8 Comparison of the activation of the Akt and ERK pathways in UCL93 and SKI001

SKI001 cells were chosen because they were the ones over-expressing *PIK3R1* the most, hence allowing me to better see the difference in the two cell lines mechanisms. UCL93 (normal) and SKI001 (cystic) cells were cultured in their regular medium then synchronised for 48 hours by serum starvation, before being treated with IGF-1 for 5, 15, 30 or 60 minutes. The activation of the Akt and ERK pathways was then assessed by blotting the phosphorylated (activated) forms of these two proteins and measuring their expression compared to the total amount of protein. Figure 4.20 shows a representative blot in UCL93 and SKI001 and the percentages of activation of Akt and ERK overtime from three different repeats of the experiment.

(a) Activation of the Akt and ERK pathways in UCL93

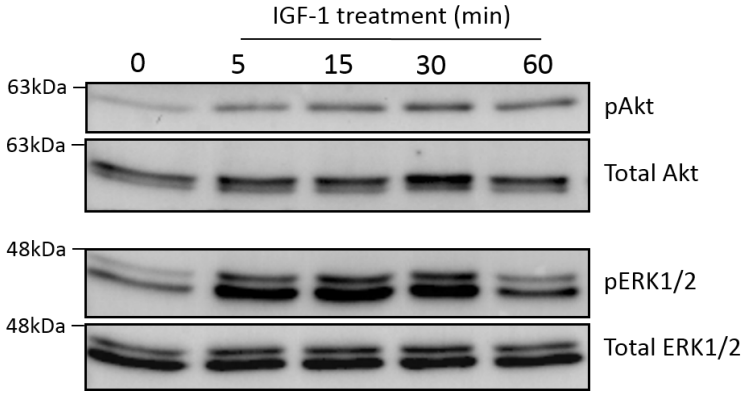

(b) Activation of the Akt and ERK pathways in SKI001

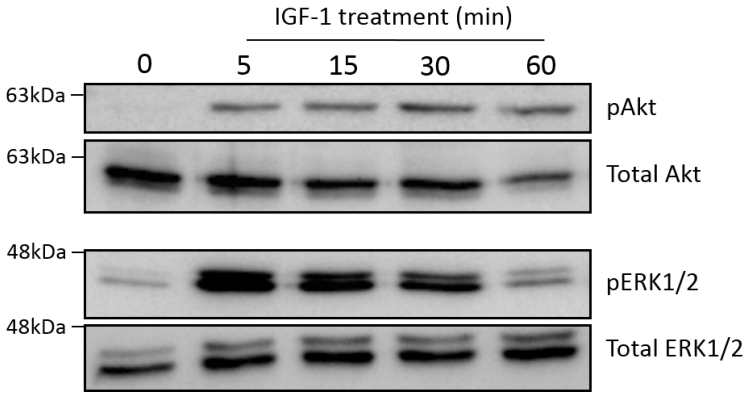

(c)

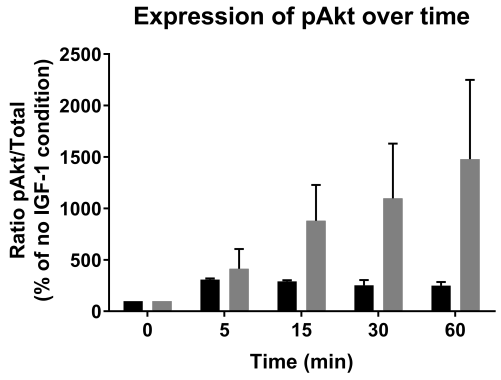

(d)

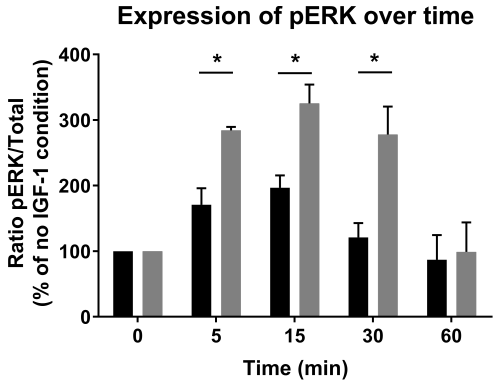

Figure 4.20: **Western blotting of Akt/pAkt and ERK/pERK in UCL93 and SKI001 after activation by IGF-1**.
(a), (b) UCL93 and SKI001 were synchronised and treated with IGF-1 for 5, 15, 30 or 60 min and Western blotting was performed on pAkt, total Akt, pERK1/2 and total ERK1/2. The phosphorylated forms mean an activation of the pathway. The ratios pAkt/Total Akt (c) and pERK/Total ERK (d) were calculated in three different repeats (n=3) of the experiment and represented as a percentage of the condition without IGF-1 (inactivated pathway) for both cell lines. UCL93 is represented as black bars and SKI001 as grey bars. ** 0.04>p>0.03 (Unpaired t-test)*

Figures 4.20a and 4.20b show a representative experiment. For both proteins Akt and ERK, the basal phosphorylation (activation) levels were higher in UCL93 (normal cells) than SKI001 (cystic cells), a finding consistent in all three experiments.
The activation of Akt appeared constant and progressive with the duration of IGF-1 treatment in SKI001, reaching a peak of 1,479 fold change compared to the inactivated control, but not in UCL93 where it remained almost constant throughout with a peak of 305 fold change at 5 minutes. ERK was activated quickly after the start of the IGF-1 treatment, reaching its peak at 15 minutes (325-fold increase compared to inactivated control in SKI001 and 197-fold increase in UCL93), and then decreased over time to go back to basal levels after an hour. Globally, the activation of both proteins was stronger in SKI001 (Figures 4.20c and 4.20d) than UCL93, although this difference was not significant for Akt because of variability between batches.
Because I showed that *PIK3R1* knock-down inhibits cysts progression and the Akt and ERK pathways are over-activated in cystic cells, I then studied the effect of *PIK3R1* knock-down on this pathways' sensitivity to IGF-1 in cystic cells.

4.4.9 Activation of Akt and ERK after *PIK3R1* KO

SKI001 (cystic) cells were plated on 6-well plates and two wells of each condition were either not transfected, transfected with a negative control siRNA or transfected with an anti-*PIK3R1* siRNA for 72 hours, and synchronised for 48 hours. For each condition, one well out of the two was treated with IGF-1 at 50 μg/mL for 15 min. The proteins were stained for PI3K-p85α, calnexin (loading control), phospho-Akt, total Akt, phospho-ERK or total ERK as seen in Figure 4.21.

(a) Expression of PI3K-p85α in five normal and four cystic human kidney cell lines

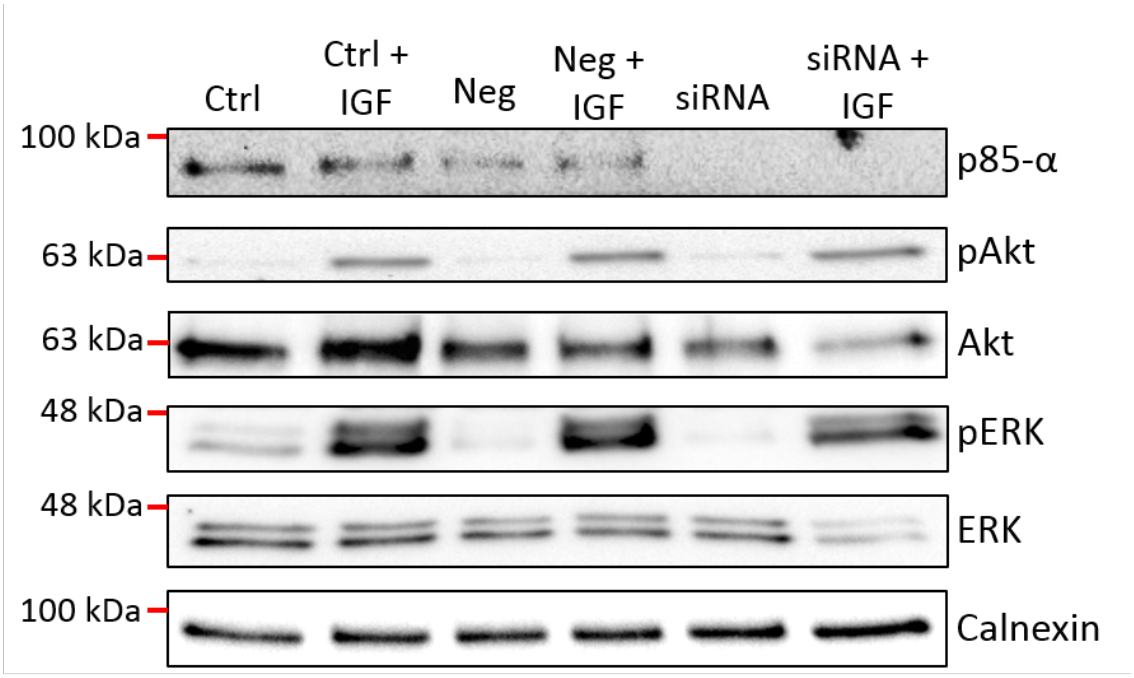

(b)

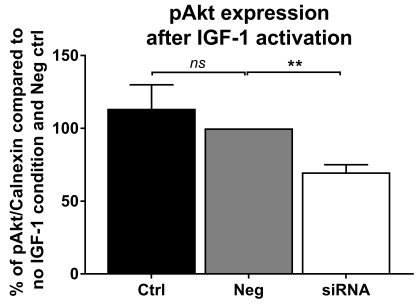

(c)

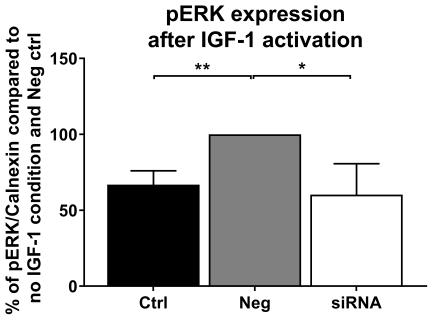

Figure 4.21: **Activation of the Akt and ERK pathways by IGF-1 treatment in SKI001 cells transfected or not with anti-*PIK3R1* siRNA.**
SKI001 were plated in 6-well plates and either not transfected (”Ctrl”, black bars) or transfected with a negative control (”Neg”, grey bars) or anti-*PIK3R1* siRNA (”siRNA”, white bars). One well of each condition was treated with IGF-1 at 50 μg/mL for 15 minutes, and the proteins from all wells were then extracted and run in 10 % SDS-PAGE gels. (a) The membranes were blotted for PI3K-p85α, calnexin (loading control), phospho-Akt, total Akt, phospho-ERK or total ERK. (b) The pAkt and (c) pERK ratios to the calnexin control (*i. e.* the activation levels after IGF-1 treatment) were calculated for each of the three conditions in four repeats of the experiment (n=4), and reported to the siRNA-transfected negative control value.
** p=0.01 ** 0.006>p>0.001 (Unpaired t-test)*

The blotting of PI3K-p85α confirmed the knock-down of this protein by transfection of the anti-*PIK3R1* siRNA (Figure 4.21a). In the Western blot example presented here, while the calnexin loading control showed an equivalent loading between the wells, the levels of total Akt and total ERK were more variable. The activation of the Akt pathway (Figure 4.21b) and the ERK pathway (Figure 4.21c) was measured by calculating the difference of pAkt or pERK quantification levels between the untreated and the IGF-1-treated conditions. The values are presented as ratios compared to the negative siRNA (negative control)-transfected condition in four repeats of the experiment. Transfection with the negative control siRNA did not induce a significant change of the pAkt amount compared to the untransfected condition but led to a significant increase of pERK by 1.5-fold. Transfection with the anti-*PIK3R1* siRNA resulted in a significant reduction of pAkt by 30.3 % on average compared to the negative siRNA control condition, and a significant reduction of pERK by 39 % on average.

4.4.10 Expression of *PIK3R1*-related genes in normal and ADPKD cells

PIK3R1 codes for one of the regulatory subunits of the PI3-K proteins, p85-α, and its rare splice variants p55-α and p50-α. This protein belongs to the Class I_A of PI3-Kinases that regroups two other less common regulatory subunits, p85-β and p55-γ coded by *PIK3R2* and *PIK3R3*, respectively, as well as three catalytic subunits coded by *PIK3CA*; p110-α, *PIK3CB*; p110-β and *PIK3CD*; p110-δ . I decided to measure the expression of the other PI3-K regulatory subunits as well as of the PI3-K catalytic subunits, to determine whether PI3K-p85α is the only protein subunit whose deregulation leads to ADPKD or whether this is a more global phenomenon for all the existing PI3-K enzymes variants.

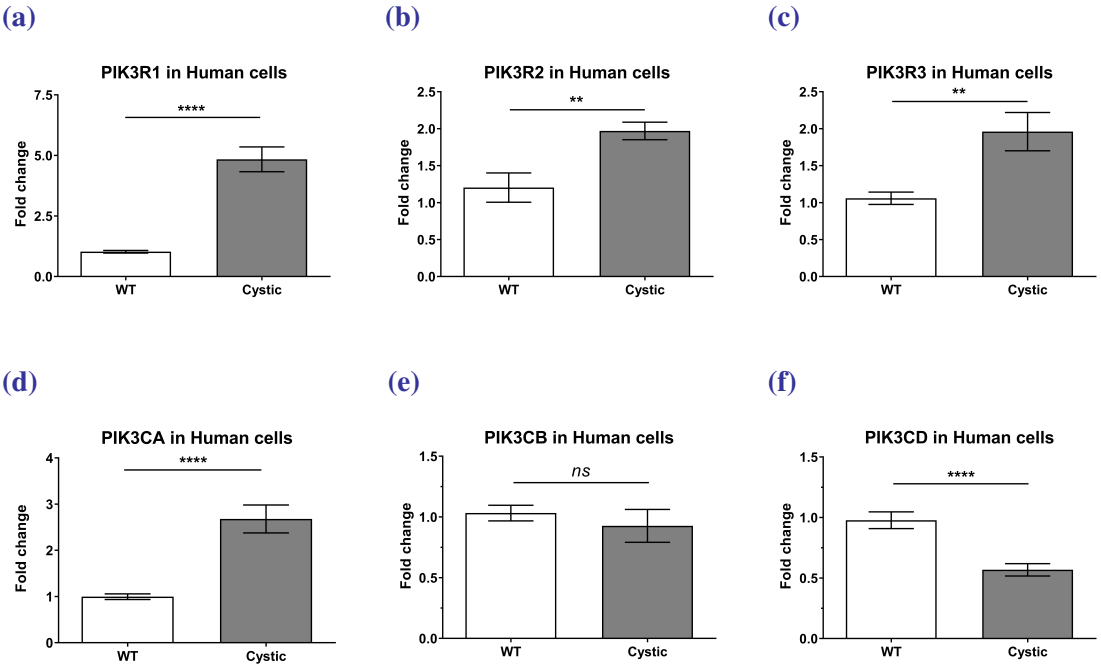

***Figure 4.22:* Expression of *PIK3R1*-related genes in normal and cystic cells.**
The expression of these genes was measured in two batches of five normal and four cystic cells. (a) *PIK3R1* was used as a positive control of the batch and technique. (b), (c) The expression of the genes coding for the other class IA regulatory subunits *PIK3R2* and *PIK3R3* was measured in the same batches. (d), (e), (f) The expression of the genes coding for the three class IA catalytic subunits *PIK3CA*, *PIK3CB* and *PIK3CD* was measured in the same batches
*** 0.003>p>0.0015 **** p<0.0001 (Unpaired t-test with Welch's correction)*

PIK3R1 was used as a positive control. As seen in Figures 4.22b and 4.22c, the genes coding for *PIK3R2* and *PIK3R3*, were also up-regulated although with a lower fold change than *PIK3R1*: 1.97 and 1.96 fold change for the former compared to 4.84 fold change for the latter. The genes coding for the catalytic subunits behaved differently (Figures 4.22d, 4.22e and 4.22f): *PIK3CB* expression level was unchanged in ADPKD compared to normal cells, while *PIK3CD* was significantly down-regulated. Interestingly, *PIK3CA* expression was significantly increased in ADPKD cells by a fold change of 2.7.

To confirm the results of the (sq) RT-PCR at the protein level, Western blotting of PI3K-p110α (coded by *PIK3CA*) was performed in the same human cells, and the results are presented in Figure 4.23.

(a) Expression of PI3K-p110α in five normal and four cystic human kidney cell lines

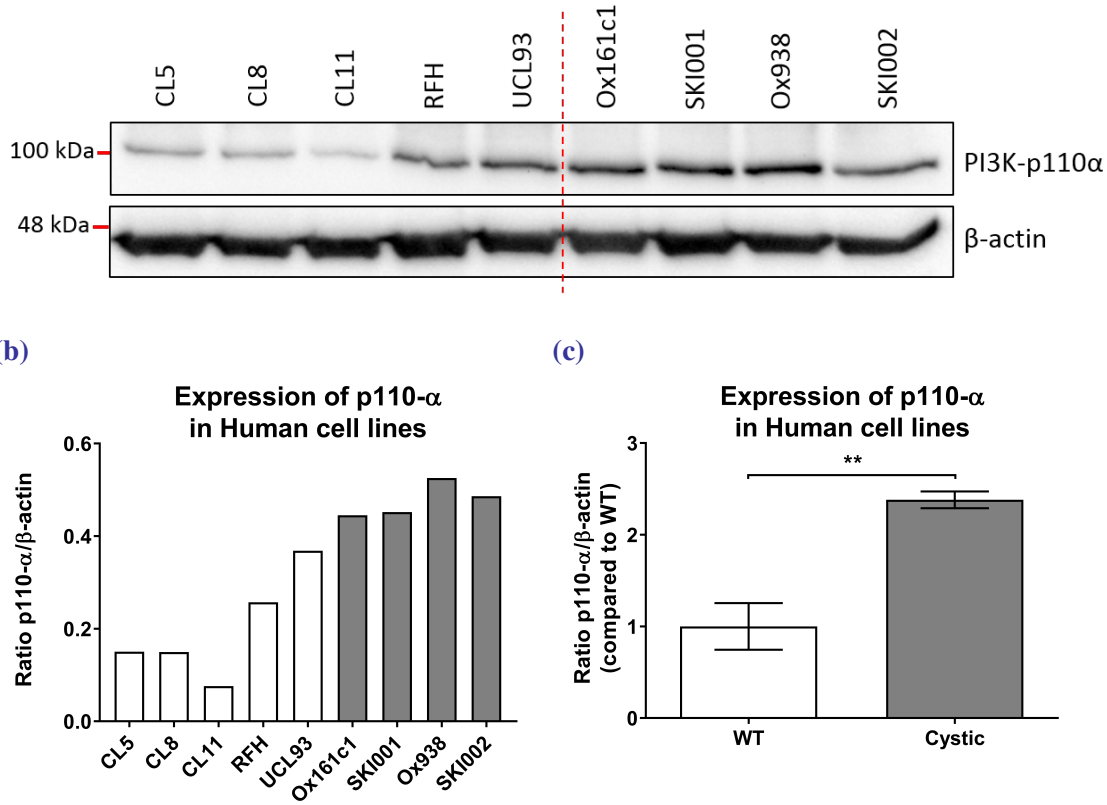

Figure 4.23: **Western blotting of PI3K-p110α in human normal and ADPKD cell lines.** (a) 20 μg of protein from five normal cell lines (CL5, CL8, CL11, RFH and UCL93, left) and four cystic cell lines (Ox161c1, SKI001, Ox938 and SKI002, right) were run in a 10 % SDS-PAGE gel and marked for β-actin (loading control, 110 kDa) or PI3K-p110α (110 kDa). (b) The p110-α/β-actin ratio was calculated for each cell line. (c) The p110-α/β-actin ratio was expressed as fold changes compared to the average value in WT cells.
*** p=0.006 (Unpaired t-test)*

While the levels of this protein were equivalent between the cystic cell lines, all of them over-expressing p110-α compared to the WT cells, there was more variability between the different normal cell lines, CL11 expressing it the least and UCL93 the most (Figure 4.23b), which is similar to the (sq) RT-PCR results. Globally, also similarly to what was observed at the mRNA level in Figure 4.22, the p110-α catalytic subunit was significantly up-regulated by 2.4-fold in cystic cells compared to normal (Figure 4.23c).

The over-expression of *PIK3CA*/PI3K-p110α in human ADPKD cells suggests that several combinations of regulatory and catalytic subunits can be up-regulated in ADPKD and an over-activation of the PI3K-linked pathway may not only be due to PI3K-p85α.

Table 4.3: Summary of all genes studied by bioinformatics analyses

Gene	Name	Selected from	Fold change microarray	FC human cells	FC mouse cells	FC mouse tissue	Luciferase Assay	Western Blotting	Reason for not taking further	miRNA
PIK3R1	Phosphoinositide-3-kinase Regulatory Subunit 1	Dot Plots	1.9	3.75 (****)	Up-regulation in MEK (FC = 5.8). Down-regulation in F1 (FC = 0.3)	Up-regulation in NeoLox (FC = 3.7 & 2.25) at 4 and 10 weeks	65 % reduction of signal, partially inhibited after mutagenesis	mir-193b transfection induces down-regulation of PI3K-85α	–	mir-193b
CELF2	CUGBP, Elav-Like Family Member 2	GSEA enrichment analysis	–	21.3 (****)	Non significant increase in F1/Cre. Down-regulation in MEK	Up-regulation (FC=3.4) in NeoLox at 4 weeks. No change at 10 weeks	Significant reduction of signal at 10 nM and 50 nM	–	Mutagenesis not successful	mir-582
IGFBP5	Insulin Like Growth Factor Binding Protein 5	GSEA enrichment analysis	–	328 (**)	FC = 20 (MEK), no significant increase (F1)	No change at 4 weeks, down-regulation at 10 weeks (FC = 0.46)	Significant reduction of signal partially inhibited after mutagenesis	–	No up-regulation in mouse. No consistency between batches	mir-193b
FSTL1	Follistatin-Like 1	GSEA enrichment analysis	–	1.87 (**)	Down-regulation in MEK and F1 (FC = 0.5)	No significant difference (4 weeks)	–	–	No consistent data between human cells and other models	mir-582

Summary of all genes studied by bioinformatics analyses (continued)

Gene	Name	Selected from	Fold change microarray	FC human cells	FC mouse cells	FC mouse tissue	Reason for not taking further	miRNA
KIF22	Kinesin Family Member 22	GSEA enrichment analysis	1.7	1.9	Up-regulation in MEK (FC = 1.2), trend up-regulation in F1	No significant difference (4 weeks and 10 weeks)	No consistent data between models	–
KRT19	Keratin 19, Type I	GSEA enrichment analysis	–	7.96 (*)	Not significant increase in F1, down-regulation in MEK	Up-regulation (FC=40) in NeoLox at 4 weeks	No consistent data between human cells and other models	–
PLAU	Plasminogen Activator, Urokinase	Direct comparison	1.7	1.42	Very strong down-regulation (FC = 0.01) in MEK. No change in F1	Trend to down-regulation (not significant)	Only SKI001 cells show a constant up-regulation. No consistent data between human cells and other models	mir-193b
SHROOM3	Shroom Family Member 3	Dot Plots	3.9	2.37 (**)	Up-regulation in MEK and F1 (FC = 2.2 & 1.2)	Trend to down-regulation (not significant). No change at 10 weeks	Only SKI001 cells show a constant up-regulation. No up-regulation in mouse kidney	mir-582
SLCO2A1	Solute Carrier Organic Anion Transporter Family Member 2A1	Dot Plots	4.5	7.3 (***)	Up-regulation in MEK (FC = 1.3)	No significant difference at 4 and 10 weeks	Only Ox161c1 cells show a constant up-regulation. No up-regulation in mouse kidneys	mir-193b

Summary of all genes studied by bioinformatics analyses (end)

Gene	Name	Selected from	Fold change microarray	FC human cells	FC mouse cells	FC mouse tissue	Reason for not taking further	miRNA
TES	Testin LIM Domain Protein	GSEA enrichment analysis	–	1.67	–	–	No consistent deregulation between human cells	mir-582
MCM5	Minichromosome Maintenance Complex Component 5	GSEA enrichment analysis	–	2.08 (*)	–	–	No consistent deregulation between human cells	mir-193b
MCM6	Minichromosome Maintenance Complex Component 6	GSEA enrichment analysis	–	0.8	–	–	Down-regulated in human cells	mir-193b
MCM7	Minichromosome Maintenance Complex Component 7	GSEA enrichment analysis	–	3.4	–	–	No consistent deregulation between human cells	mir-193b
POLE	Polymerase (DNA Directed), Epsilon, Catalytic Subunit	GSEA enrichment analysis	–	0.31	–	–	Down-regulated in human cells	mir-193b
CDK1	Cyclin Dependent Kinase 1	GSEA enrichment analysis	–	1.7 (*)	–	–	Not deregulated enough in human cells	mir-193b
CDKN1A	Cyclin-Dependent Kinase Inhibitor 1A (P21, Cip1)	GSEA enrichment analysis	–	0.43 (****)	–	–	Down-regulated in human cells	mir-582

4.5 Discussion

The aim of this section of the project was to identify new candidates related to the two miRNAs previously found down-regulated in ADPKD cells, while avoiding bias induced by focusing on only one model by studying dysregulation in different models as a criteria of selection. Through a collaboration with Dorien Peters' laboratory in Leiden (Netherlands), I had access to microarray data from a conditional *Pkd1*$^{-/-}$ mouse model, and used previously published datasets from a number of different disease models such as mouse (Menezes et al., 2012), human (Song et al., 2009) and rat (O' Meara et al., 2012). This allowed me to identify more consistent findings between models (hence their relevance in ADPKD). Furthermore, as the project developed, I also had access to kidney tissue from the *Pkd1*^{nl,nl} hypomorph model of mice from the start of the experiments.

4.5.1 Direct comparison approach and its limits

Initially, I worked on a direct comparison of datasets to try and identify common predicted targets of mir-193b-3p and mir-582-5p. The Leiden group had not yet generated their RNA-seq dataset so the results of this analysis were limited as our datasets did not have many up-regulated elements in common. Out of the four targets identified (*PLAU*, *SLC16A1*, *RNF145* and *BNIP2*), only *PLAU* had been experimentally validated as a target for mir-193b-3p according to the MirTarBase database. It was also interesting as it was found in the rat and the mouse studies. Because the function of the other targets did not appear particularly relevant for them to have a role in ADPKD, I decided to measure the expression of *PLAU* in our human cells to validate its dysregulation in the disease. Unfortunately, this gene was not up regulated in any of the models tested, whether it was human cells (over-expression in only one cell line), mouse cells (no change in F1 cells, strong down-regulation in MEK cells) or mouse kidney (non significant down-regulation). Hence, it was not possible to confirm *PLAU*'s up-regulation in ADPKD although it had been identified in several other studies. This illustrates yet again the difficulty to find a relevant candidate and the need to perform validation experiments in a number of models before selecting them for further studies.

4.5.2 Multiple pathways and gene processes identified by MSigDB/ GSEA analyses

Following this study, I was able to gain access to an unpublished high-throughput RNA-seq dataset of the conditional *Pkd1*$^{-/-}$ model from the Leiden group. I was able to utilise their 'PKD Signature' database, based on previously published studies as well as the RNA-seq data (Malas et al., 2017). This method had several advantages: first, the RNA-seq dataset being very large, the probability to find common targets was higher, but also because MSigDB and Gene Set Enrichment Analysis were used I could get a more global approach as I compared not only individual genes but entire pathways, gene sets and biological processes. This was interesting because it could suggest that a whole pathway could be enriched in ADPKD and not only a gene for which the relevance in the disease could be more difficult to find. Among the pathways that were found enriched in the disease, some were common to both miRNAs, such as the epithelial-mesenchymal transition (EMT), the response mechanism to oestrogens or the response to UV. EMT has already been shown to be a consequence of fibrosis in ADPKD (Chea and Lee, 2009) and linked to *Pkd1* deletion (Xu et al., 2014), which made it interesting to select genes involved in this mechanism (e.g. *FSTL1*). To narrow down the number of candidates, I chose to focus on several genes based on their known function and their previously reported link to ADPKD (e.g. the MCM proteins for mir-193b-3p or *CDKN1A* for mir-582-5p), and/or because they were previously suggested to have a role in ADPKD but not yet linked to my miRNAs of interest (*KRT19*, found up regulated in ADPKD (Schieren et al., 2006)). Furthermore, I also generated similar tables as the ones presented in Table 4.2 but considering not only the miRNAs predicted targets found up-regulated in our microarray or MirTarBase, but all predicted targets, which is a much longer list. I decided not to use these tables as they had only one connection with our preliminary study, i.e. the miRNAs, opposite to the two axes for the presented tables (i. e. miRNAs and mRNAs found dysregulated in ADPKD).

Altogether, I identified highly evidenced pathways and processes enriched in ADPKD and their respective targets up-regulated in at least two studies.

CELF2 and *IGFBP5* were chosen as two candidates of interest, based on the results of semi-quantitative real-time PCR in several human and mouse models. I chose not to focus on some of the genes that were found to be up-regulated in human as their over-expression was not conserved well across models (*KIF22*, *FSTL1*, *KRT19*) and their potential role in ADPKD was limited for example to the developmental stage (*KIF22*, see Kim and Shin (2016)). I generated plasmids containing these genes' 3'UTR sequence and performed dual-reporter luciferase assays to study their interaction with mir-582 and mir-193b. Although the transfection of HEK293 with mir-193b mimic induced a significant reduction of the fluorescent signal, the deregulation of *IGFBP5* and its interaction with mir-193b-3p was not consistent. Furthermore, although multiple protocols and couples of primers were used, it was not possible to mutate *CELF2* 3' UTR sequence, making it impossible for me to confirm its interaction with mir-582-5p.

The box plot analysis was a convenient visual tool to identify and select candidates based on their over-expression in ADPKD mice of different ages. Most of the targets actually showed a down-regulation in the most advanced stages of ADPKD (for example *CALB1* mentioned in the previous chapter, a segment-specific gene that appeared to be decreased with the destruction of the structures where it is expressed). I chose to validate the expression of three genes, *PIK3R1*, *SLCO2A1* and *SHROOM3* because they were globally and/or progressively increased over time in ADPKD. *SLCO2A1* (also known as Prostaglandins Receptor or *PGT*) showed a down-regulation compared to control at the moderate stages, but was nevertheless selected because of its role in prostaglandin E2 transport. Overall, *PIK3R1* expression was increased at all disease stages compared to normal mice, with a high increase at the late stages. Validating these observations in human cells, only this gene was increased in cystic cells compared to normal. Indeed, only one cell line consistently expressed *SHROOM3* (SKI001) or *SLCO2A1* (Ox161c1), while *PIK3R1* was increased in all the cystic cell lines, Ox161c1 being the most constant and SKI002 the one expressing it the lowest.

4.5.3 *PIK3R1* up-regulation in ADPKD is consistent across most models and an important factor of cysts progression

I also found that *PIK3R1* expression was increased in MEK (mouse) cells and in $Pkd1^{nl,nl}$ hypomorph mouse kidneys at 4 and 10 weeks. Its down-regulation in F1 cells is unclear but may represent developmental or strain specific changes in mice. Nevertheless, added to the RNA-seq quantifications in the Leiden group's $Pkd1^{-/-}$ mice, I showed its over-expression in four different models and at different stages of the disease. It is important to note that our hypomorph mouse model reaches its peak 2KW/BW ratio at 4 weeks before regressing (for unexplained reasons), meaning that the disease is already severe in the 4 weeks old mice.

Despite the use of different antibodies, immunohistochemistry stainings did not give any specific signal and thus did not allow me to validate the (sq) RT-PCR results in mice tissues at the protein level. However, an enrichment of the PI3K-p85α protein was shown in our human cystic cells by Western blotting. Interestingly, the over-expression levels in the different cystic cells were parallel to the mRNA levels (*i.e.* the protein was the most increased in Ox161c1 and SKI001 and the least increased in SKI002).

It was demonstrated for the first time that *PIK3R1* is a target for mir-193b-3p by dual-reporter luciferase assays and transfection of human cells with miRNA mimics or inhibitors, thus at the mRNA and protein levels. I suggest that the presence of other sequences complementary to mir-193b-3p, although not predicted by the algorithms, could explain the incomplete reversion of fluorescent signal after introduction of 4 mutations in the predicted seed sequence. Although the mir-193b-3p inhibitor's effect was less efficient, transfecting cystic cells with mir-193b-3p mimic had a significant effect on *PIK3R1* and p85-α expressions. Furthermore, although these experiments were performed on human cells, a third of the miRNA targets prediction algorithms also predict this interaction to happen in mouse. The fact that all these algorithms had - rightly - predicted this interaction in human as well is an encouraging suggestion that it does occur in mouse, which could be interesting to show in future studies.

Using 3-Dimensional cyst assays, I demonstrated that *PIK3R1* is important for cyst progression as its knock-down prevented cyst growth in human cells after activation by IGF-1. This finding, associated with the fact that transfecting these cells with mir-193b-3p mimic decreases cysts progression (experiment from A. Streets, data not shown), is a good evidence that mir-193b-3p targets *PIK3R1* and limits cyst growth.

Because the effects of IGF-1 were expected to be partially masked by the insulin present in ITS, the first step consisted in optimising the protocol by comparing cysts growth in a ”full” medium containing EGF. ITS and HC and in a ”poor” medium not containing these compounds. While the cells capacity to be activated by IGF-1 treatment was similar between the ”full” and the ”poor” media, the cysts cultured in the ”poor” medium did not look healthy. Therefore, I chose to work with the ”full” medium but not adding ITS. The activation being higher in the following experiment than in the preliminary one shows that removing the ITS did not have detrimental effects on cysts growth and that the activation of the pathway leading to cysts growth is exclusively due to the addition of IGF-1.

The PI3-K inhibitor induced a reduced cyst size compared to vehicle-treated control cells, indicating a strong effect on cyst formation.

In a recent study, Booij et al. studied the effects of PI3-K and mTOR inhibitors on cyst growth in murine IMCD3 *Pkd1*$^{-/-}$ cells and reported that PI3-K is not involved in cyst growth induced by forskolin (Booij et al., 2017). Our study was different as I worked on human cells and studied the effects of *PIK3R1* knock-down on cyst growth induced by IGF-1 activation, opposite to their approach that focused on the effects of PI3-K inhibitor after forskolin stimulation. Forskolin treatments induce an increase in cAMP levels which in return will activate not only the PI3-K/Akt pathway but also other pathways such as the Epac proteins (Bos, 2006) or the cyclic nucleotide-gated ion channels (Kaupp and Seifert, 2002). Hence, they studied the effects of a PI3-K inhibitor while activating multiple other pathways, which could mask the effects of the compound. I did not see a significant difference in cysts area at basal levels between siRNA Neg control and *PIK3R1* siRNA, suggesting that I reported exclusively the inhibition of the pathway’s activation by IGF-1.

In summary, I showed for the first time that specific siRNA-mediated knock-down of *PIK3R1* induced an insensitivity to an activation of the PI3-K/Akt pathway by IGF-1 in human ADPKD cells.

Since *PIK3R1* is a major component of the PI3-K/Akt signalling pathway, I looked at the difference between normal and cystic human cells' capacity to activate Akt or ERK1/2 phosphorylation with exposure to IGF-1.

The results indicate a consistent greater stimulation by IGF-1 in ADPKD cells than in normal cells, both for Akt or ERK1/2. The return to basal pERK levels after an hour was an expected result as it had previously been shown in several studies that IGF-1 activation of ERK was reaching its peak after a few minutes before declining to basal levels after 30 min (Webster et al., 1994; Foncea et al., 1997). The maintained phosphorylation of Akt over time was also shown previously in various other cell models (Zheng and Quirion, 2006, Ma and Bai, 2012, Sivaprasad et al., 2004). The basal levels of pAkt seemed higher in UCL93 compared to SKI001, which was also what could be expected from the literature as it was reported that *PKD1* over-expression in MDCK cells induced an increased basal pAkt expression (Boca et al., 2006) and similar results can be seen in Parker et al.'s 2007 paper. However, pAkt expression was increased in another study of *Pkd1* null kidney (Nishio et al., 2005), which suggests that depending on their *PKD1* mutation, not all models of PC1 deficiency may show the same reactivity to IGF-1 activation. The higher basal levels of pERK in normal cells have not been reported. My results show that the Akt and ERK pathways are more sensitive to IGF-1 activation in cystic cells, which is similar to what was shown by Parker et al. - in which paper they also reported that a deficiency in PC1 leads to a higher sensitivity to IGF-1 but not to an increased independent cell proliferation, also supporting the possibility of a difference in basal levels as previously shown (Parker et al., 2007). This confirmed that our model behaves as expected and defined technical practicalities such as the IGF-1 concentration and ideal time to induce a visible phosphorylation of the two pathways.

Because *PIK3R1* was found up-regulated in human and mouse cells and mouse tissue and the Akt and ERK pathways were found to be more sensitive to IGF-1 treatment in cystic cells compared to normal, I surmised that the two may be directly linked and that a knock-down of *PIK3R1* would lead to an inhibition of their phosphorylation. As 15 min of IGF-1 treatment showed the maximal level of ERK phosphorylation in the previous experiment, this time point was chosen for the knock-down experiment. The cells were transfected with a negative siRNA in order to check any off-target effect of the transfection or with an anti-*PIK3R1* siRNA. The p85-α subunit was blotted in each repeat of the experiment in order to check the effective knock-down of the protein. Calnexin served as a loading control to confirm the same amount of proteins were loaded in each well and to quantify the amount of phospho-proteins related to the quantity of total proteins. Unexpectedly, in some blots such as the one presented as an example, the total amount of Akt and ERK varied between the wells even when the loading control indicated equivalent amounts of proteins loaded. This was visible in blots re-probed for total proteins after revelation of phospho-proteins but also in cases where two different membranes were loaded and probed for the phosphorylated or the total protein. Hence, this variation can not be explained by the loss of proteins during re-probing of the membranes. Whether this is a technical or a biological observation would need to be investigated further.

Since Akt is a major downstream effector of the same pathway as PI3-Kinase, the knock-down of the main regulatory subunit p85-α was anticipated to have an effect on its phosphorylation. As expected, the cells transfected with anti-*PIK3R1* siRNA showed a significantly reduced phosphorylation of Akt. Although this reduction was incomplete (30.3 %), it was consistent in four independents experiments, supporting the role of the PI3K-p85α subunit in particular in the hyper-sensitivity of the cystic cells to IGF-1 treatment. Unexpectedly, the levels of phospho-ERK were also affected by *PIK3R1* knock-down in these cells. Although there was more variability between repeats, which is shown by the larger error bar, this reduction was significant. Noticeably, the transfection with the negative control siRNA led to a significant off-target effect on pERK relative expression levels in a consistent manner between batches.

The underlying causes of this effect are not understood, however transfection of small RNAs into cells have been reported to trigger off-target increases or decreases in some genes expression in different studies (Jackson and Linsley, 2004; Fedorov et al., 2005; Scacheri et al., 2004; Snove and Holen, 2004; Caffrey et al., 2011), highlighting the need to use a negative siRNA control condition as a reference for the study of siRNA effects. In the case of my experiments, this off-target effect casts a doubt on the interpretation for the significant reduction of ERK phosphorylation after p85-α knock-down. However, as the anti-*PIK3R1* siRNA also is a small RNA of the same nature than the negative control, I considered that the effect seen with the former was due to the knock-down of p85-α in this condition compared to the negative control. The use of a chemical PI3-K inhibitor could confirm or infirm this result. As IGF-1 is known to be an activator of the Ras/ERK pathway (Stewart et al., 1990; Jacobo and Kazlauskas, 2015), the higher phospho-ERK levels in the IGF-1-treated cells was anticipated. However, the reduction in relative pERK levels after knock-down of PI3-K (involved in the PI3K/Akt/mTOR pathway) was less expected and suggests a direct cross-talk between the two pathways. The relationship between the PI3-K/Akt and the Ras/ERK pathways is complex; they have been shown to both cross-inhibit each other and on the contrary cross-activate each other. For example, inhibitors of MEK (part of the Ras/ERK pathway) lead to a higher activation of the Akt pathway by EGF (Won et al., 2012) and Akt or PKA have been shown to negatively regulate ERK phosphorylation via activation of inhibitory sites in Raf (Dhillon et al., 2002b; Guan et al., 2000), while a strong activation of the Ras/ERK pathway has been linked to mTORC1 activation and Ras was shown to directly bind and activate PI3-K (Kodaki et al., 1994; Suire et al., 2002; Zoncu et al., 2011). Although IGF-1-mediated activation of the pathway has been reported to activate Akt and in return inhibit the Ras/ERK pathway in breast cancer cells MCF-7 when used at high doses (Moelling et al., 2002), IGF-1 treatments have also been reported to activate ERK/Ras in colon cancer cells MC38 (Teng et al., 2016) or in adrenocortical carcinoma H295R cells (Tong et al., 2016), which hints that the reciprocal interactions between the two pathways may vary depending on the IGF-1 concentration, cell type (thus amounts of available IGF receptors), or disease state.

Furthermore, the two pathways can also converge and act on the same substrates such as the Bcl-2 family member BAD, GSK3 (glycogen synthase 3) or FOXO3A (forkhead box OA3), which suggests a complex mutual regulation between the two (Yang et al., 2008b; She et al., 2005; Ding et al., 2005; Fang et al., 2000). More importantly, a number of studies have proposed a model in which PI3-K directly regulates the MEK/ERK pathway by interacting with Rac and/or Cdc42 which in return will stimulate the MEK/ERK pathway (Rul et al., 2002; Eblen et al., 2002; Ebi et al., 2013; Castellano and Downward, 2011; Welch et al., 2003; Dillon et al., 2015; Chu et al., 2016). In particular Chu et al. recently suggested the existence of what they called a ”non-canonical PI3K-Cdc42-Pak-Mek-Erk signalling pathway” in neutrophils in which PI3-K activates ERK via activation of Cdc42 (Chu et al., 2016) and Hussain et al. recently reported that the specific inhibitor of PI3-K led to reduced levels of phospho-ERK in colorectal carcinoma (Hussain et al., 2016). These results support my findings that the reduction of PI3-K levels in the cells may directly or indirectly lead to reduced phosphorylation of ERK and thus less activation of the Ras/MEK/ERK pathway and even more dysregulation of cell proliferation and apoptosis.

In order to understand the mechanisms affecting Akt phosphorylation in *PIK3R1* knock-down conditions, in particular the potential parallel up-regulation of a catalytic subunit and the reason for the incomplete blockade of the pathway, the relative expression levels of the genes coding for the two other regulatory subunits (*PIK3R2* and *PIK3R3*) and the three catalytic subunits (*PIK3CA*, *PIK3CB* and *PIK3CD*) were measured in five normal and four cystic human cell lines. Interestingly, *PIK3R2* and *PIK3R3* showed an up-regulation in the cystic cells, albeit lower than *PIK3R1*. This suggests that PI3K-p85α, the major PI3-K regulatory subunit coded by *PIK3R1*, is not solely responsible for the increased sensitivity of the cystic SKI001 human cells to IGF-1 activation and the resulting increased Akt and ERK phosphorylation, and that the two other regulatory subunits PI3K-p85β and PI3K-p55γ's over-expression can partly compensate the knock-down of p85-α in these cells. This would explain the incomplete inhibition of the pathway that was observed in the anti-*PIK3R1* siRNA-transfected cells.

The over-expression of the regulatory subunits of PI3-Kinase was expected to be found in conjunction with an increased expression of at least one of their associated catalytic subunits as their association with each other is essential to the kinase's activity (Jean and Kiger, 2015). Noticeably, *PIK3CA*, coding for the most common catalytic subunit p110-α, was highly significantly over-expressed by 2.7-fold in cystic cells compared to normal, while *PIK3CB* was unchanged and *PIK3CD* was significantly down-regulated. As *PIK3CD* is almost specific to immune cells and expressed at very low levels in the kidney (Chantry et al., 1997), the significance of this observation is limited in the context of ADPKD. Western blotting of p110-α in the nine human cell lines confirmed the results of the (sq) RT-PCR by showing a significant over-expression of this protein by 2.4-fold in cystic cells compared to normal. Although its expression was variable between the normal cells, UCL93 being the most p110-α-rich, this was similar to what was seen at the mRNA level by (sq) RT-PCR and all the cystic cells expressed the protein at levels above UCL93. The reasons for this gene's up-regulation remain to be understood as *PIK3CA* was suggested to be a target for mir-193b by only two algorithms, giving little support to the theory of an interaction between the two. Interestingly, *PIK3CA* was also found up-regulated in Song et al. (2009)'s study on human cysts, supporting my findings and therefore giving a more precise insight into the mechanisms ruling the dysregulation of the PI3-K/Akt pathway in ADPKD.

In summary, a comparison of our parallel miRNA/mRNA dataset to several other datasets and the Leiden 'PKD Signature' identified several new candidate genes up-regulated in several models of ADPKD and potentially targeted by mir-193b-3p or mir-582-5p that we showed down-regulated in the disease. Among these genes, *PIK3R1* was up-regulated in human and mouse cell and kidney models of ADPKD, was shown to have a novel interaction with mir-193-3p and functionally regulates ligand (IGF-1)-stimulated cyst growth. The mechanisms ruling this hypersensitivity of ADPKD cells to IGF-1 treatment, in particular the links between the Akt and the ERK pathways, need to be characterised further. Additionally, over-expression of the catalytic subunit p110-α, coded by *PIK3CA*, is likely to contribute to increase PI3K activity. This is summarised in the following Figure 4.24.

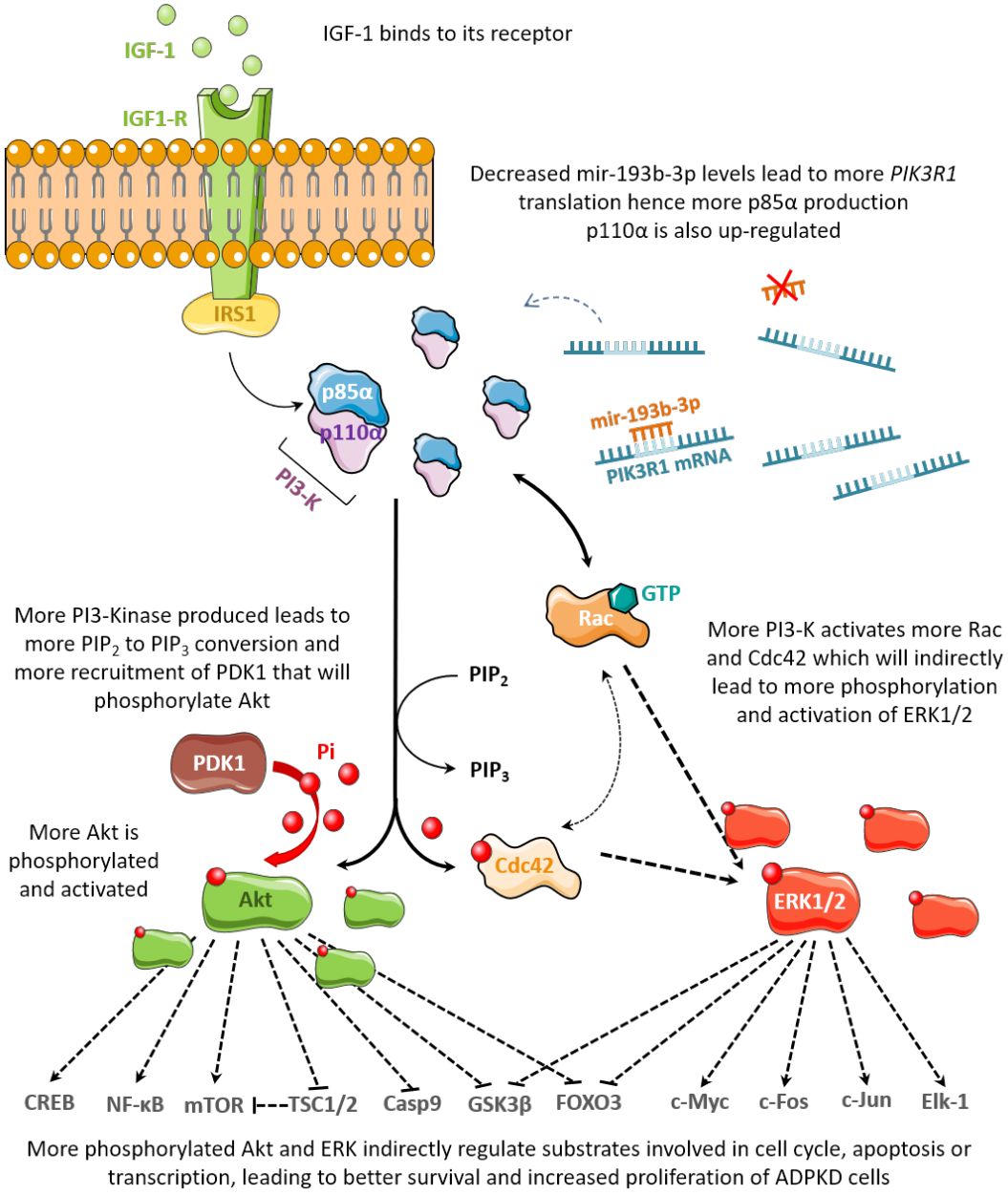

Figure 4.24: **Summary and hypotheses on the role of mir-193b and *PIK3R1* in ADPKD.** The down-regulation of mir-193b-3p in ADPKD (an hypothesis on what could explain miRNAs down-regulation in ADPKD is proposed in chapter 5) leads to less repression of *PIK3R1* expression and thus higher PI3K-p85α levels than in the healthy kidney. As *PIK3CA* is also up-regulated by undefined mechanisms, more active PI3-Kinase is present in the cell. IGF-1 binds to its receptor, activates and recruits PI3-Kinase which will mediate more conversion of phosphatidylinositol (3,4)-bisphosphate (PIP_2) to PIP_3 and more recruitment of PDK1 that will phosphorylate Akt and therefore more highly regulate its multiple substrates including NF-κB or mTOR. In parallel, I suggest that higher PI3-K levels result in more activation of Ras and/or Cdc42 via its "non-canonical pathway" and subsequently more phosphorylation of ERK and its substrates.
Altogether, the down-regulation of mir-193b-3p and consequential p85-α increase in ADPKD leads to the up-regulation of targets involved in cell proliferation, cell cycle and the repression of apoptosis, leading to cysts growth in the disease.

Chapter 5

Mechanisms of miRNA dysregulation in ADPKD

5.1 Introduction

The main aim of this chapter is to understand the mechanisms governing the down-regulation of miRNAs observed in ADPKD cells and the factors that could influence their expression *in vivo*. Indeed, although the general miRNA maturation mechanisms are known, less is understood about their biology in disease especially in ADPKD.
The first part of this chapter will focus on the effects of steroids (sexual hormones) on the pathogenesis of ADPKD.

Gender effect on the prognosis of ADPKD Many studies have reported that males ADPKD patients necessitate renal replacement therapy and transplantation earlier than women, and male gender is now well known as a risk factor for the disease (Choukroun et al., 1995; Johnson and Gabow, 1997; Gabow et al., 1992; Alves et al., 2014; Reed et al., 2008). This protective effect of the female gender was also observed in rat models of ADPKD (Gretz et al., 1995; Cowley Jr et al., 1993; Stringer et al., 2005; Cowley Jr et al., 1997). Moreover, sexual hormones were suggested to modulate cystogenesis and kidney function in PKD models. Indeed, administrating 5α-dihydrotestosterone (DHT, male hormone) to female Han:SPRD rats induced an increased kidney weight in both ovariectomised and healthy animals and reversed the protective effect observed after castration in males of the same model (Cowley Jr et al., 1997). Similarly, castration of male Han:SPRD rats limited the decline of eGFR observed in these animals as well as the decline in effective renal plasma flow (ERPF), while ovariectomy resulted in reduced eGFR and ERPF in female Han:SPRD rats (Stringer et al., 2005). Female hormones such as 17β-estradiol (E2) or 2-hydroxyestradiol (2-OHE), on the contrary, have a nephroprotective effect as male Han:SPRD rats treated with these E2 metabolites presented smaller kidney cysts and a better renal function (Anderson et al., 2012). These are many proofs that female hormones may have a protective role on ADPKD pathogenesis although the mechanisms by which E2 mediates its effect on cysts growth and kidney function is not known.

Effects of steroids on miRNAs expression Additionally, steroids have been suggested to influence miRNAs expression in several models. Maillot et al. showed that the expression of some miRNAs was increased after treatment of breast cancer cell lines (MCF-17) with 17β-estradiol, including mir-200c and mir-193b, and that the artificial expression of these miRNAs repressed oestrogens-mediated cell growth (Maillot et al., 2009).
However, Wang et al. found that mir-193b and other miRNAs' expression was increased with E2 treatment in these same cells (Wang et al., 2010d). Bhat-Nakshatri et al identified 21 miRNAs up-regulated and 7 down-regulated by E2 in the same cells (Bhat-Nakshatri et al., 2009). Paris et al. found 73 miRNAs differentially expressed (29 repressed, 44 increased) between cells possessing the ERβ receptor and ERβ- MCF-7 cells (Paris et al., 2012). Becker et al. studied the effects of anabolic steroids (trenbolone acetate + E2) on miRNAs expression in bovine liver and found 22 significantly down-regulated and 14 significantly up-regulated miRNAs in the treated animals' livers compared to untreated (Becker et al., 2011). Androgens effects are less known as fewer studies have analysed their effects on miRNAs; Wang et al. identified four down-regulated (including mir-17 for example) and eleven up-regulated miRNAs in prostate cells treated with 1,25$(OH)_2D_3$ and testosterone, and other individual miRNAs such as mir-21, mir-32, mir-27a, mir-135a and the mir-99a/let-7c/mir-125b-2 cluster were found down- or up-regulated by androgen treatments in prostate cells (Sun et al., 2014a; Ribas et al., 2009; Fletcher et al., 2012; Jalava et al., 2012; Kroiss et al., 2014). Altogether, these studies suggest that the expression of some miRNAs can be affected by steroids and depend on gender.
The question remains whether the gender difference in ADPKD outcome and the differential modulation of miRNAs by sexual hormones are connected, as gender-dependent miRNAs remain to be identified in this disease.

The second part of this chapter will aim at understanding the defects in the miRNAs machinery leading to the down-regulation of some miRNAs in ADPKD.

First of all, the expression levels of my two miRNAs of interest were measured in the NeoLox *Pkd1*^{nl,nl} hypomorph model at different stages of the disease to investigate if their down-regulation in ADPKD was a consistent finding.

5.2 Validation of mir-193b-3p and mir-582-5p deregulation in 2, 4 and 10 weeks old NeoLox mice

RNA samples from 2, 4 and 10 weeks old male and female NeoLox mice kidneys were analysed for the expression of mir-193b-3p and mir-582-5p, as shown in Figure 5.1 below.

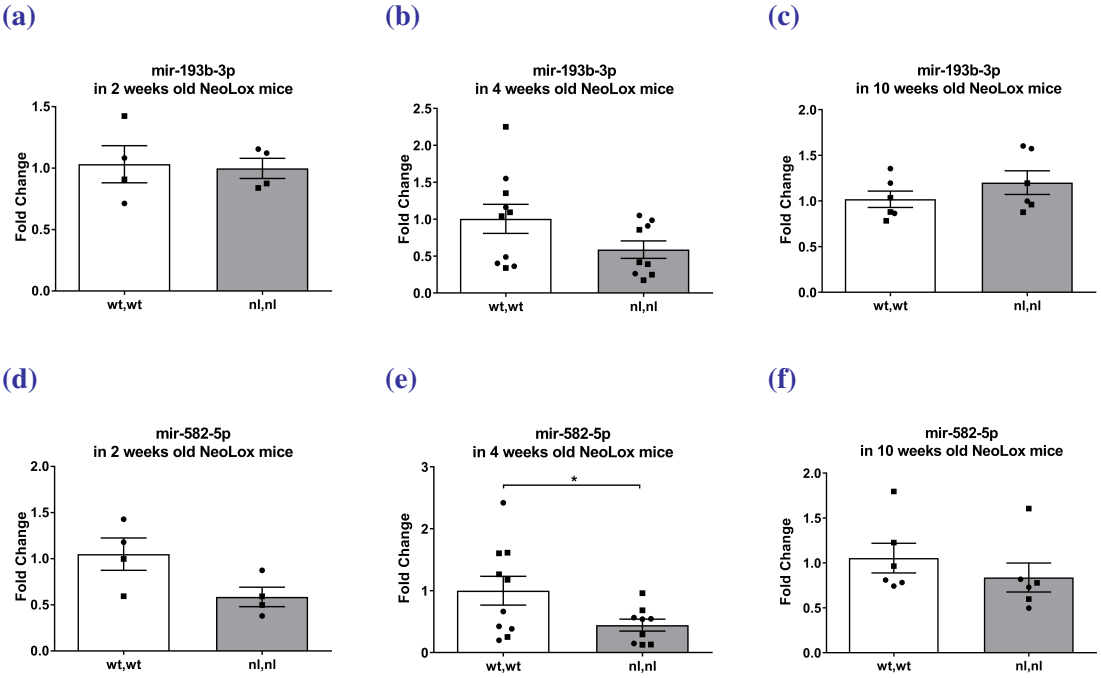

***Figure 5.1:* Differential expression of mir-193b-3p and mir-582-5p in the kidney of 2, 4 and 10 weeks old NeoLox mice.**
The values are represented as fold changes compared to all WT mice. Kidneys were extracted from (a) two males and two females wt,wt as well as two males and two females nl,nl mice at 2 weeks, (b) five males and five females wt,wt as well as five males and five females nl,nl mice at 4 weeks of age and (c) three males and three females wt,wt as well as three males and three females nl,nl mice at 10 weeks of age. Males are symbolised as squares and females as circles.
** p=0.047 (Unpaired t-test with Welch's correction)*

Mir-193b-3p did not show any change between WT and ADPKD mice at 2 or 10 weeks (Figures 5.1a and 5.1c). It showed a non-significant decrease of 0.59-fold in 4 weeks old mice (Figure 5.1b). In contrast, mir-582-5p showed a trend towards a down-regulation as early as 2 weeks of age (Figure 5.1d), which became significant at 4 weeks (Figure 5.1e) with a 0.44 fold change value. There was no change at 10 weeks (Figure 5.1f).

When analysing the results at the most severe stage of the model (4 weeks of age), I noticed that there seemed to be a difference in the two miRNAs' deregulation between males and females. Indeed, as shown in Figure 5.2 below, the down-regulation of mir-193b-3p became significant in males with a fold change of 0.38 between the WT and the ADPKD mice (Figure 5.2b), while there was no change between females WT and ADPKD (Figure 5.2c). Similarly, mir-582-5p showed a clear trend to a down-regulation in males ADPKD (Figure 5.2h) while no change was seen for the females (Figure 5.2i).

Furthermore, when the two-kidneys-weight-to-body-weight (2KW/BW) ratios were plotted against mir-193b-3p or mir-582-5p expression for the mice at all ages, the difference between males and females was clear. Taking all mice into consideration (Figures 5.2d and 5.2j), the correlation between 2KW/BW ratio and miRNA expression was significant ($p= 0.01$ and $p= 0.01$ for mir-193b-3p and mir-582-5p respectively) with a correlation coefficient of -0.5 for mir-193b-3p and -0.41 for mir-582-5p. However, while the correlation was significant for the males (Figures 5.2e: coefficient of -0.55 and p-value at 0.01 and 5.2k: $r= -0.46$ and $p= 0.04$), it was not significant for the females (Figures 5.2f: $p= 0.053$ and 5.2l $p= 0.22$) and the correlation coefficients were lower (-0.46 for females against -0.55 for males for mir-193b-3p and -0.35 against -0.46 for mir-582-5p). Summarised, my data showed that mir-193b-3p down-regulation was more important in ADPKD and more significantly correlated with the 2KW/BW ratio in males compared to females.

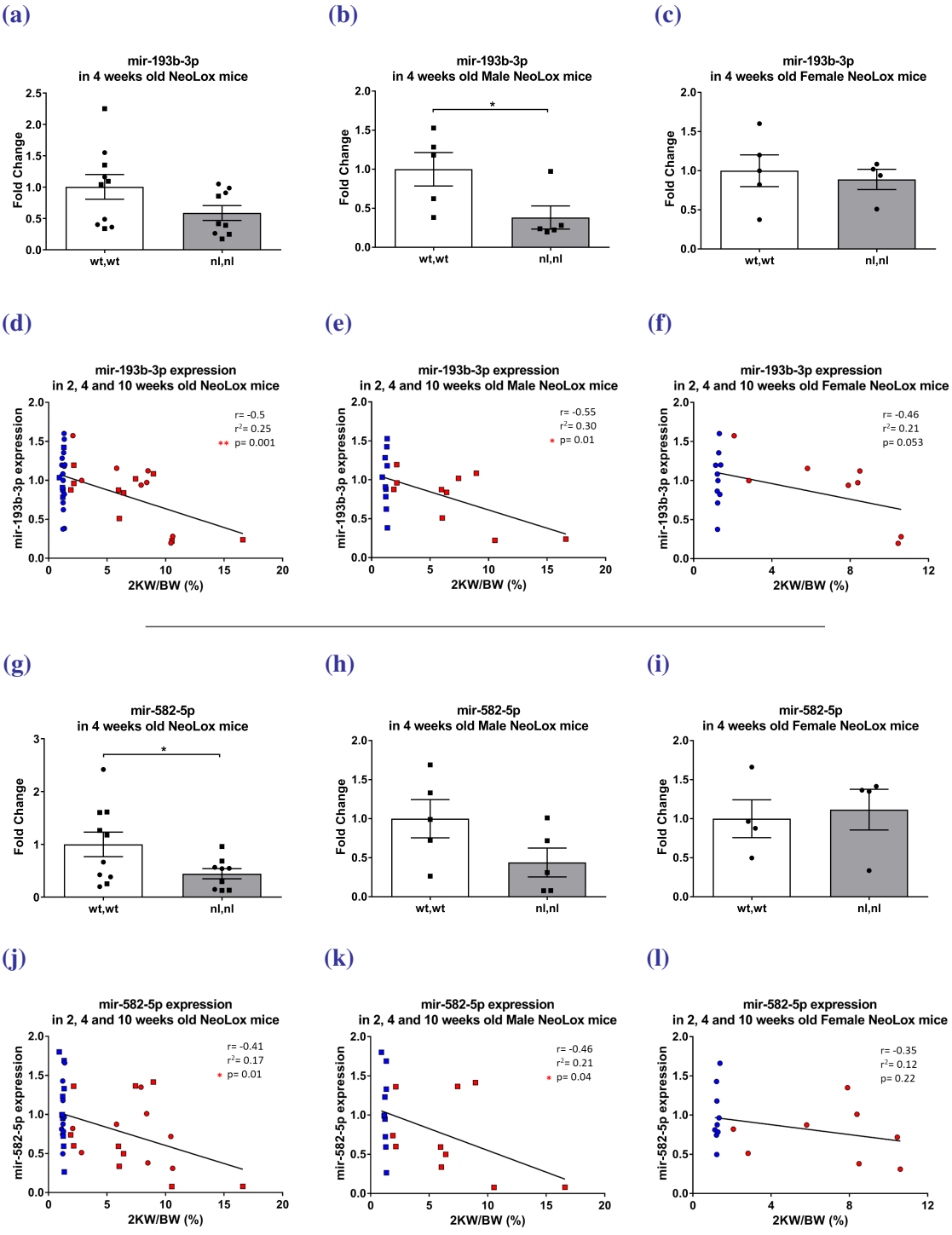

Figure 5.2: **Differential expression of mir-193b-3p (top panel) and mir-582-5p (bottom panel) in the kidney of 4 weeks old males and females NeoLox mice.**
The measurements are the same as the above Figure 5.1, split between males (b), (h) and females (c), (i) and recalculated as fold changes compared to the WT mice of the relevant gender. (d, j) 2KW/BW ratios plotted against miRNA expression for 2, 4 and 10 weeks old male (e, k) or female (f, l) mice. Males are symbolised as squares and females as circles. Blue and red symbols represent WT and ADPKD mice, respectively.
Linear regression curves are materialised. r: correlation coefficient, p: significance of correlation

This led us to think that there might be a gender effect in the deregulation of miRNAs expression in our model of ADPKD mice. Next I decided to analyse five other miRNAs found to be deregulated from another project from our lab.

5.3 Validation of the deregulation of five miRNAs selected from a human urinary exosomes RNA-seq dataset

A parallel study in our group (Magayr, 2017) identified several dysregulated miRNAs in ADPKD human urine exosomes by RNA-seq. From this, five new miRNAs were selected for study in addition to mir-193b-3p. These were mir-30a-5p, mir-30d-5p, mir-30e-5p, mir-192-5p and mir-194-5p. The expression levels of these five miRNAs were measured in *Pkd1*^{nl,nl} mouse kidneys at 4 and 10 weeks (Figure 5.3).

As shown in Figures 5.3a and 5.3b, mir-30a-5p was not found down-regulated in ADPKD mice at any time point. mir-30d-5p and mir-30e-5p were significantly down-regulated in *Pkd1*^{nl,nl} mice at 4 weeks by 0.5-fold and 0.7-fold respectively (Figures 5.3c and 5.3e), but not at 10 weeks (Figures 5.3d and 5.3f). Mir-192-5p and mir-194-5p were significantly under-expressed in ADPKD at both time points by 0.45-fold (4 weeks, Figure 5.3g) and 0.6-fold (10 weeks, Figure 5.3h) for the former and by 0.39-fold (4 weeks, Figure 5.3i) and 0.6-fold (10 weeks, Figure 5.3j) for the latter. This hierarchy in miRNAs down-regulation was parallel to what was found by T. Magayr in human urinary exosomes (Magayr, 2017), mir-192-5p and mir-194-5p being the two miRNAs whose expression was the most decreased in ADPKD patients.

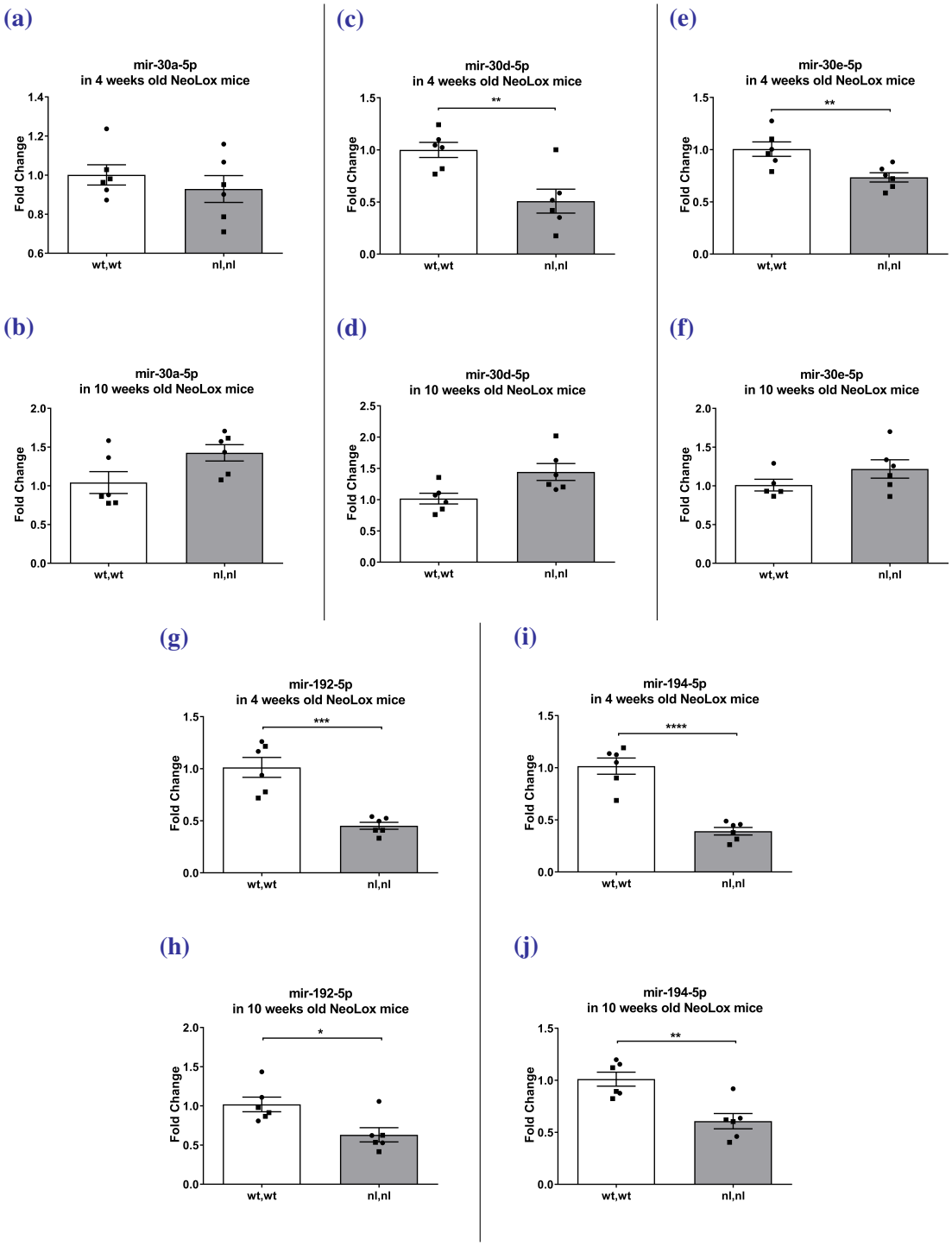

Figure 5.3: **Real-time PCR for the differential expression of mir-30a-5p, mir-30d-5p, mir-30e-5p, mir-192-5p and mir-194-5p in the kidney of 4 and 10 weeks old NeoLox mice.**
The values are represented as fold changes compared to all WT mice. Kidneys were extracted from (a, c, e, g, i) three males and three females wt,wt as well as three males and three females nl,nl mice at 4 weeks of age and (b, d, f, h, j) three males and three females wt,wt as well as three males and three females nl,nl mice at 10 weeks of age. Males are symbolised as squares and females as circles.
** p=0.03 (b), * p=0.015 (e), ** p=0.003 (c), **** p<0.0001 (Unpaired t-test)*

As shown in Figure 5.4, these two miRNAs also showed a difference in deregulation between 4 weeks old male and female ADPKD mice, but opposite to what was seen for mir-193b-3p and mir-582-5p. Indeed, mir-192-5p and mir-194-5p were more significantly down-regulated in ADPKD in females than in males, with p-values of 0.03 and 0.003 for males and females for mir-192-5p (Figures 5.4b and 5.4c) and p-values of 0.015 and 0.0001 for males and females for mir-194-5p (Figures 5.4e and 5.4e).

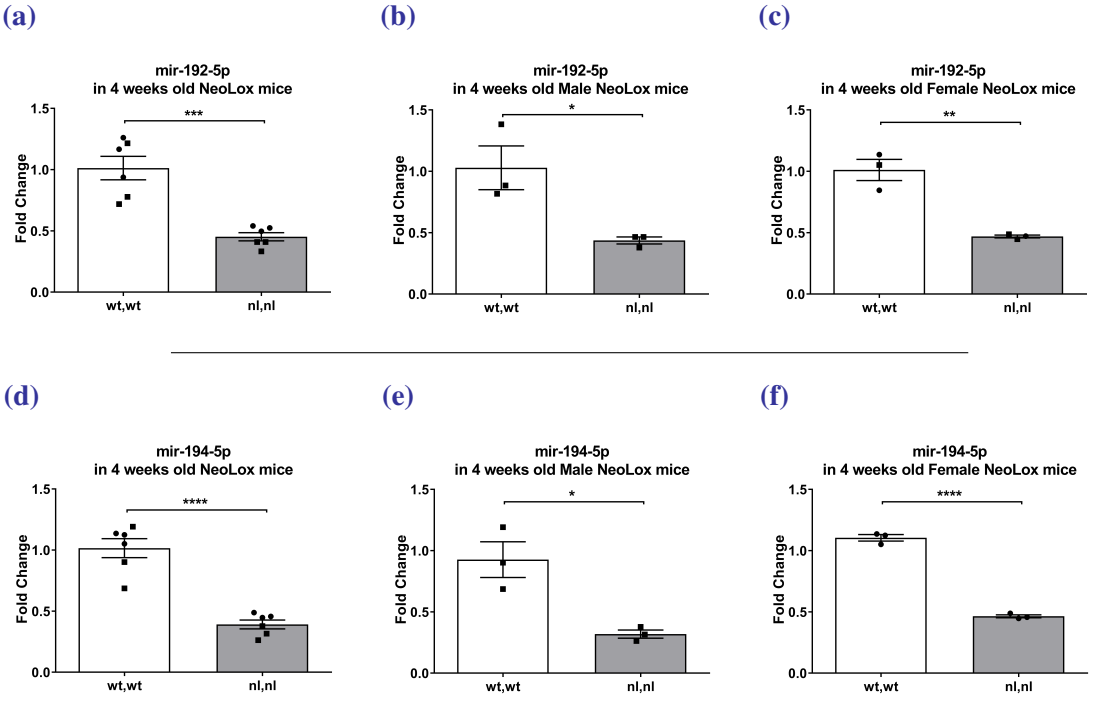

***Figure 5.4:* Real-time PCR for the differential expression of mir-192-5p (top panel) and mir-194-5p (bottom panel) in the kidney of 4 weeks old males and females NeoLox mice.**
The measurements are the same as the above Figure 5.3, split between males (b), (e) and females (c), (f) and recalculated as fold changes compared to the WT mice of the relevant gender. Males are symbolised as squares and females as circles.
** p=0.01 ** p=0.008 (e), ** p=0.0046 (c), ** p=0.0023 (j) and *** p=0.0002 **** p<0.0001 (Unpaired t-test)*

From these results, I decided to study the effects of the male and female hormones dihydrotestosterone (DHT) and β-estradiol (E2) on the expression of mir-192-5p, mir-193b-3p, mir-194-5p and mir-582-5p in human ADPKD cells, to understand if these are responsible for the difference observed in $Pkd1^{nl,nl}$ mice.

5.4 Effects of steroids on miRNA expression in ADPKD

5.4.1 Characterisation of human ADPKD cells potential sensitivity to steroids

Before analysing the influence of steroids on miRNAs expression, I first characterised the gender of origin and expression of steroids receptors in the human cell lines. To determine gender, PCR was performed on their genomic DNA in order to amplify the Y-chromosome-specific gene *SRY*, using DNA from a male and a female volunteer as controls. The expected product size from the primers was 310 kb (see Figure 5.5a). I also performed (sq) RT-PCR on our nine human cell lines to determine Androgen Receptor (*AR*) and Estrogen Receptors 1 and 2 (*ESR1* and *ESR2*) expression in these cells (see Figures 5.5b and 5.5c).

As shown in Figure 5.5a, a band of the expected size was detected in the male control DNA while there was no PCR product from the female gDNA. Out of nine cell lines, only UCL93 (normal cells) showed a PCR product band after amplification of *SRY* in their genome. This experiment was repeated on another batch of cells and showed the same results (data not shown). I concluded that only UCL93 had originated from a male patient while all the other cell lines were derived from female patients.

AR, *ESR1* and *ESR2* expression levels in the nine cell lines were measured in three different batches of the nine human ADPKD cell lines. In the three batches, *ESR1* did not show any amplification in any of the cell lines, suggesting that this gene is not expressed in these cells. *AR*, the male hormone receptor, was only expressed in the CL5, CL8, CL11 (normal) and Ox938 and SKI002 (cystic) cells (Figure 5.5b), and not in the other four cell lines, in all three batches. *ESR2*, one of the oestrogen receptors, was expressed in all the cell lines (Figure 5.5c). In the cell lines where I could see an amplification, the genes were expressed at similar levels between the cell lines. Hence, although the relative quantification experiment did not allow concluding on the potential reactivity of cells to the sexual hormones treatments, the genotyping of these cell lines suggested that UCL93 only would react differently to these treatments.

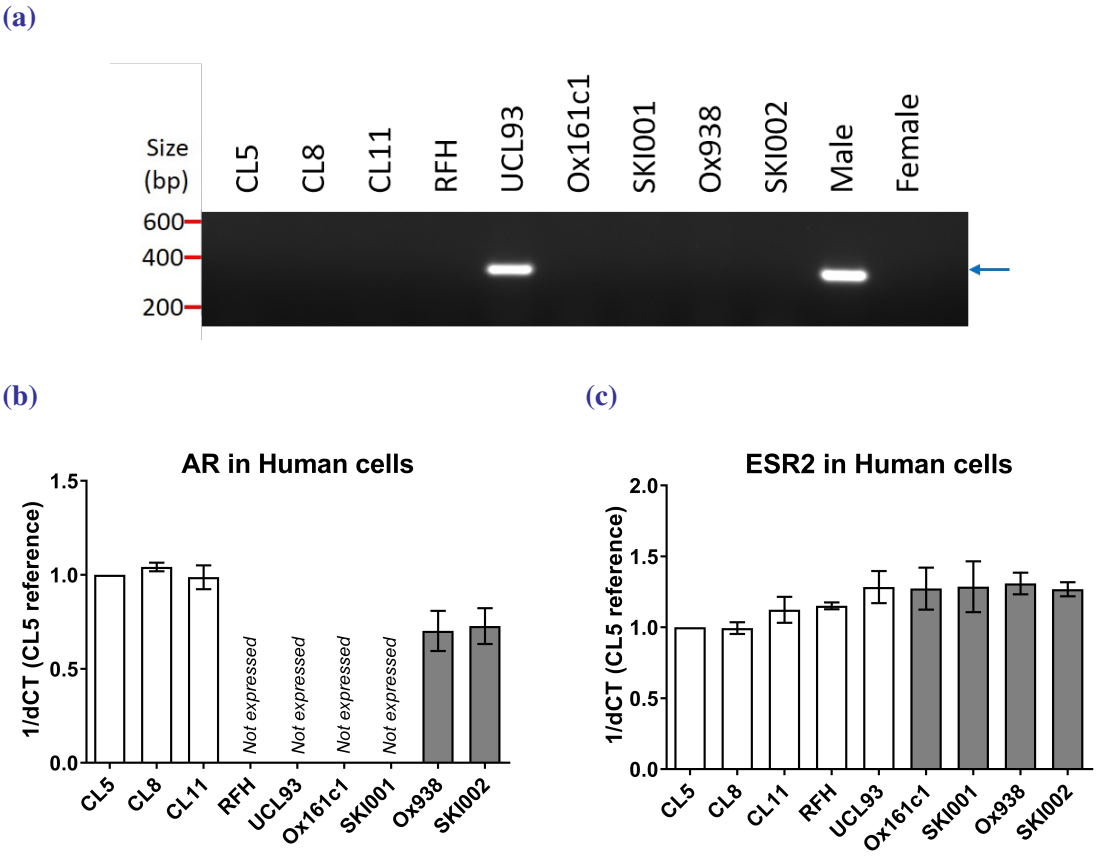

Figure 5.5: **Characterisation of human ADPKD cell lines gender.**
(a) *SRY* was amplified by PCR from genomic DNA extracted from nine ADPKD human cell lines and run into an agarose gel by electrophoresis. A male and female volunteers' gDNA was used as control of the PCR efficiency. The blue arrow indicates the correct amplification product. (b, c) *AR* and *ESR2* relative expression was measured by (sq) RT-PCR in three batches of the nine cell lines, expressed as 1/dCT and reported to the value of the CL5 cell line. White bars represent normal cells while grey bars represent ADPKD cells.

5.4.2 Treatments with steroids and effects on miRNAs expression

Because the phenol red present in most tissue culture medium has been reported to act as a weak oestrogen (Berthois et al., 1986), a pilot experiment was performed to investigate the difference miRNAs expression between cells cultured in "classic" DMEM F-12 medium containing phenol red and "clear" DMEM F-12 not containing phenol red. Two normal (RFH, UCL93) and two cystic (Ox161c1, SKI001) human kidney cell lines were cultured the same way in one medium or the other for 10 days before plating and their miRNAs were extracted a few days later to analyse mir-193b-3p and mir-582-5p expression.

(a) **(b)**

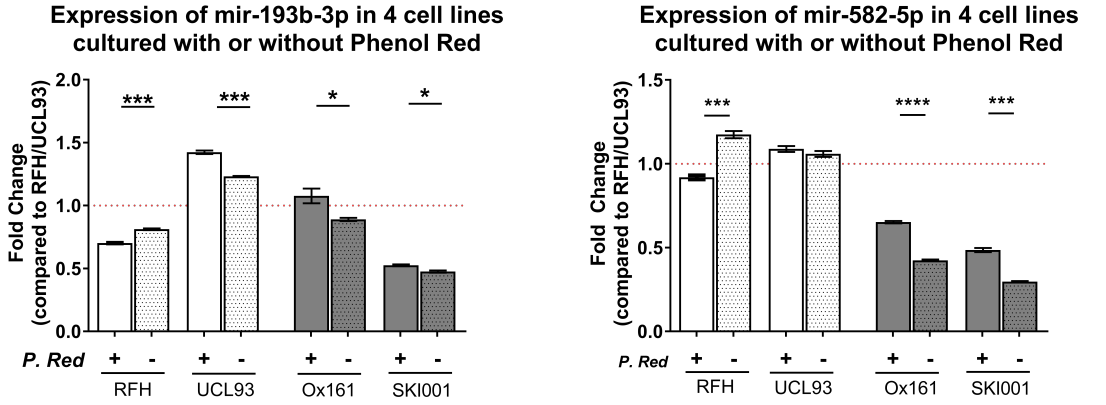

Figure 5.6: **Effects of phenol red on miRNA expression.**
RFH and UCL93 (normal, white bars) and Ox161c1 and SKI001 (cystic, grey bars) cells were cultured in phenol red-containing medium (plain bars) or phenol red-free medium (shaded bars) for 14 days in total. (a) Mir-193b-3p and (b) mir-582-5p expression was then measured in all the conditions and expressed as a fold change of the average of the two normal cell lines (RFH and UCL93) in phenol red medium. The dotted line materialises a fold change of 1 (no change compared to normal cells).
*n=3, * 0.03>p>0.001 *** 0.0005>p>0.0001 **** p<0.0001 (Unpaired t-test)*

For both miRNAs, removing the phenol red in their culture medium induced a low but significant down-regulation of mir-193b-3p (Figure 5.6a) and mir-582-5p (Figure 5.6b) expression in Ox161c1 and SKI001 and a significantly decreased mir-582-5p expression in UCL93 while it led to an up-regulation in RFH. Unexpectedly, mir-193b-3p was not down-regulated in Ox161c1 compared to the normal cells in this batch of cells. It was however under-expressed in SKI001 (Figure 5.6a). Mir-582-5p expression was lower in both cystic cell lines compared to normal (Figure 5.6b). Since phenol red is a weak oestrogen, the decreased expression of the miRNAs when deprived of phenol red suggests that oestrogens could increase their expression.

UCL93 and SKI001 were incubated with oestrogens or DHT for four days and the effects of these steroids on mir-193b-3p, mir-582-5p, mir-192-5p and mir-194-5p expression were analysed. I incubated the cells in phenol red free medium and added E2 or DHT at 20 nM or 100 nM for 4 days. Treatment with steroids at 100 nM having an erratic effect on the cells (inconsistent and seemingly random effects on miRNAs expression levels), only the results at 20 nM are presented (Figure 5.7).

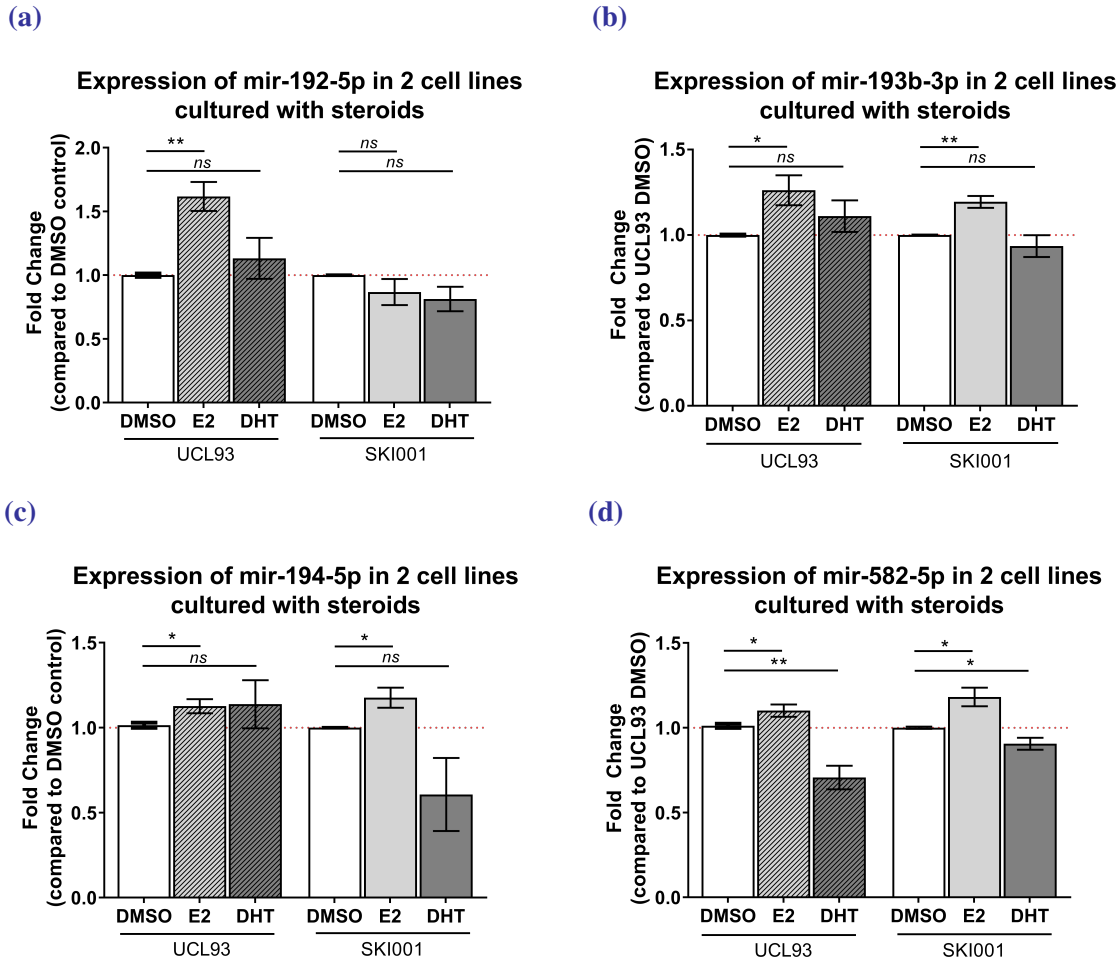

Figure 5.7: **Effects of steroids on miRNA expression.**
UCL93 (normal) and SKI001 (cystic) cells were cultured in phenol red-free medium and oestrogens (E2) or dihydrotestosterone (DHT) at 20 nM for 4 days in two independent batches of cells. (a) Mir-193b-3p, (b) mir-582-5p, (c) mir-192-p and (d) mir-194-5p expression was then measured in all the conditions and expressed as a fold change of the control (DMSO) condition. The dotted line materialises a fold change of 1 (no change compared to control).
** 0.037>p>0.01 ** 0.005>p>0.003 (Unpaired t-test with Welch's correction)*

From what was observed in the previous experiments, expected results would be an increased expression of miRNAs in the E2-treated conditions and a decreased expression in the DHT-treated conditions. Mir-582-5p (Figure 5.7d) showed expected results: in UCL93 and SKI001 oestrogens induced a low but significant up-regulation by 1.1 and 1.2-fold respectively while male hormones (DHT) led to a significantly lower expression of the miRNA to values of 0.7 and 0.9 respectively. For all other miRNAs however, UCL93, previously characterised as male origin cells showed no significant dysregulation of the miRNAs when treated with DHT.

Mir-192-5p (Figure 5.7a) expression was only affected by E2 treatments in UCL93 (fold change 1.6). Mir-193b-3p (Figure 5.7b) and mir-194-5p (Figure 5.7c) showed similar results: treating the normal or cystic cells with females hormones (E2) induced a significant 1.26 or 1.19-fold increase for mir-193-3p and 1.12 or 1.18-fold for mir-194-5p, while treatment of cystic cells with male hormones (DHT) induced no significant change in miRNA expression with a trend to a down-regulation.
Taken all together, oestrogens tended to have an effect on miRNAs expression while DHT's effects were more limited.

5.5 Dysregulation of miRNA maturation in ADPKD

Another aspect of the dysregulation of miRNAs that I aimed at understanding was what part of the miRNA maturation process was affected in our cells and mouse. Indeed, 10 out of 11 mature miRNAs identified from our microarray were consistently down-regulated in the cystic cells, which suggested that a global mechanism affecting most miRNAs maturation could be affected in ADPKD. MiRNAs are transcribed into primary miRNAs (pri-miRNAs) which are then exported out of the nucleus and cleaved into precursor-miRNAs (pre-miRNAs). These pre-miRNAs then go under a maturation process by the Dicer/TRBP complex to give a mature miRNA strand and a complementary passenger strand that will later be degraded.
First of all I measured the expression of the three intermediary miRNAs molecules (pri-miRNA, pre-miRNA and mature miRNA) in our cells to see what step of the maturation was deficient.

5.5.1 Expression of primary, precursor and mature miRNAs in human ADPKD cells

Small RNAs were specifically extracted from three independent batches of the nine human ADPKD cells and the expression of pri-miRNAs, pre-miRNAs and mature miRNAs was measured by (sq) RT-PCR. For both candidates, I measured the expression of the main strands (mir-193b-3p and mir-582-5p) but also of their complementary strands mir-193b* and mir-582-3p.

(a)

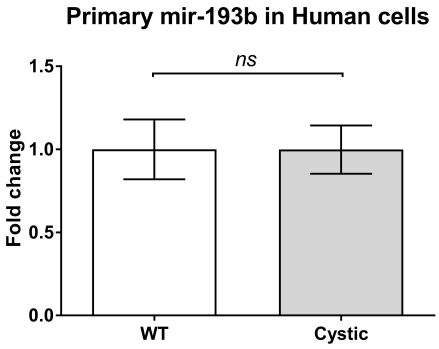
Primary mir-193b in Human cells
ns
Fold change
1.5
1.0
0.5
0.0
WT
Cystic

(b)

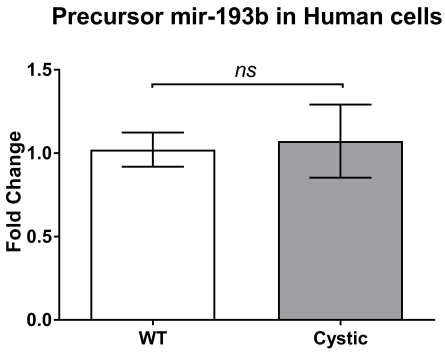
Precursor mir-193b in Human cells
ns
Fold Change
1.5
1.0
0.5
0.0
WT
Cystic

(c)

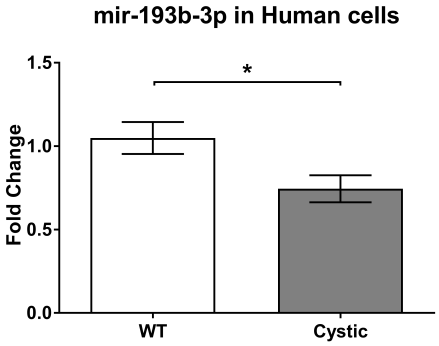
mir-193b-3p in Human cells
*
Fold Change
1.5
1.0
0.5
0.0
WT
Cystic

(d)

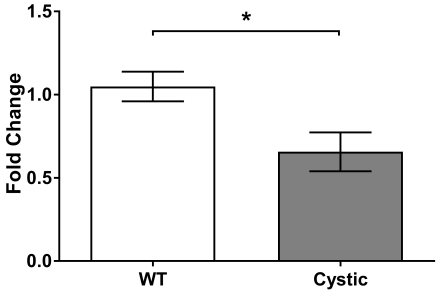
mir-193b* in Human cells
*
Fold Change
1.5
1.0
0.5
0.0
WT
Cystic

(e)

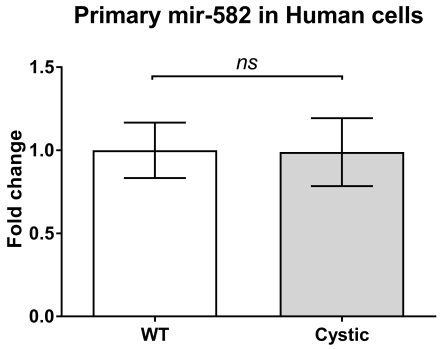
Primary mir-582 in Human cells
ns
Fold change
1.5
1.0
0.5
0.0
WT
Cystic

(f)

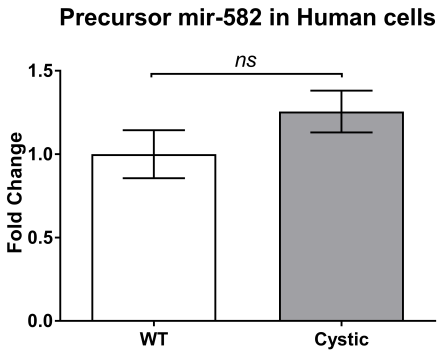
Precursor mir-582 in Human cells
ns
Fold Change
1.5
1.0
0.5
0.0
WT
Cystic

(g)

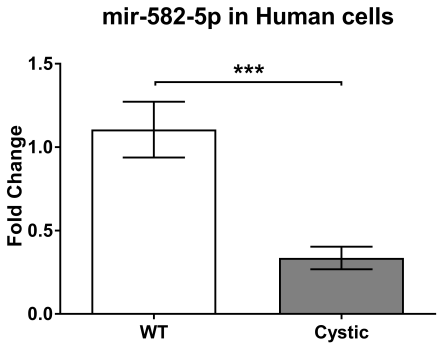
mir-582-5p in Human cells
***
Fold Change
1.5
1.0
0.5
0.0
WT
Cystic

(h)

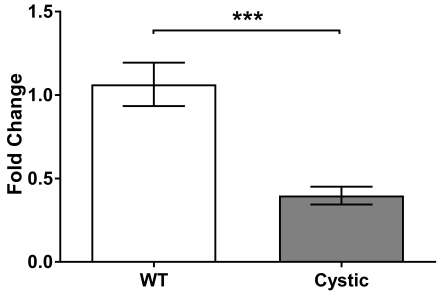
mir-582-3p in Human cells
***
Fold Change
1.5
1.0
0.5
0.0
WT
Cystic

←—***Figure 5.8*: Relative expression of primary, precursor and mature mir-193b and mir-582 in human cells.**
(Left panel) Relative expression levels of (a) primary, (b) precursor and (c, d) mature mir-193b and (right panel) expression of (e) primary, (f) precursor and (g, h) mature mir-582 in three independent batches of human cell lines, expressed as a fold change compared to normal cells (CL8, CL11, RFH, UCL93).
** 0.023>p>0.013 *** 0.007>p>0.003 (Unpaired t-test with Welch's correction)*

I excluded CL5 cells from all my analyses as this cell line was a consistent outlier in the three batches (very strong down-regulation of the mature miRNAs compared to the other normal cells). The primary miRNAs pri-mir-193b (Figure 5.8a) and pri-mir-582 (Figure 5.8e) showed no change between normal and cystic cells. Similarly, the precursors miRNAs pre-mir-193b (Figure 5.8b) and pre-mir-582 (Figure 5.8f) were not dysregulated in ADPKD cells compared to normal either. However, mature miRNAs mir-193b-3p and its complementary strand mir-193b* (Figures 5.8c and 5.8d) as well as mir-582-5p and its complementary strand mir-582-3p (Figures 5.8g and 5.8h) were significantly down-regulated in all cystic cells compared to all normal. Mir-193b-3p and mir-193b* were down-regulated by 0.74 and 0.66-fold, respectively, while mir-582-5p and mir-582-3p showed a 0.34 and 0.4-fold decrease in cystic cells.
The deregulation appearing between the precursor and mature miRNAs stages suggests that the defect in the miRNAs maturation occurs after the precursor maturation phase. Furthermore, because both strands were similarly down-regulated in both cases, I surmised that it was not due to a higher degradation of the mature strands but rather to a defective maturation process.

To confirm this hypothesis, RFH and Ox161c1 were treated with actinomycin D to inhibit RNA transcription in the cells and the miRNAs expression levels were measured at different time points.

5.5.2 Stability of mature miRNAs over time in normal and cystic cells

Actinomycin D is a compound that inhibits mRNA and miRNA transcription *in vitro*. I used *C-MYC* as a control of this reagent's efficiency on my two cell lines as its mRNA is known to have a short half life *in vitro*. I performed (sq) RT-PCR to measure the expression of this gene and my two miRNAs of interest mir-193b-3p and mir-582-5p.

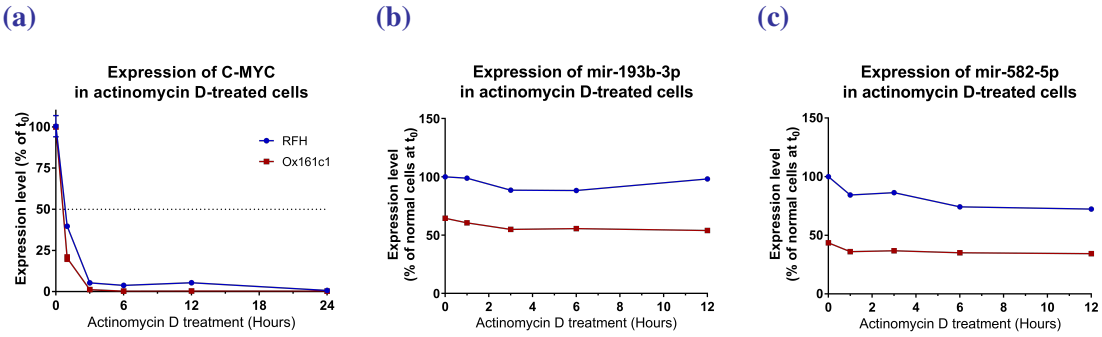

Figure 5.9: **Stability of *C-MYC*, mir-193b-3p and mir-582-5p over time in actinomycin D-treated human cells.**
RFH (normal, blue) and Ox161c1 (cystic, red) cells were cultured with actinomycin D for 1, 3, 6, 12 and 24 h. (a) *C-MYC* was used as a control of actinomycin D efficiency in the cells. Its expression was measured at all time points and expressed as percentage of the expression level at t_0. The dotted line materialises an expression level of 50 %. (b) mir-193b-3p and (c) mir-582-5p expression was measured between time points 1 hour and 12 hours and expressed as a percentage of the expression level in normal cells at t_0.

C-MYC expression levels decreased very quickly over time when the cells were treated with actinomycin D (Figure 5.9a), with a half-life of 0.63 hour (38 min) in Ox161c1 and 0.83 hour (50 min) in RFH and levels getting close to 0 % from two hours of incubation. The basal levels of mir-193b-3p (Figure 5.9b) and mir-582-5p (Figure 5.9c) were lower in Ox161c1 (cystic) compared to RFH (normal) by 35.5 points and 66.7 points respectively, confirming the relevance of this batch of cells for the experiment. As shown, levels of both miRNAs were constant in both cell lines over time, showing no difference in their evolution between the two cell lines and far from reaching their half life levels. The lowest mir-193b-3p levels were at 88 % and 83 % of their respective t_0 value in RFH and Ox161c1, while mir-582-5p expression levels reached 72 % and 78 % of t_0 in these two cell lines.

Altogether, the results presented in Figure 5.9 indicate that expression of miRNAs was very constant in the human cell lines and that their basal levels were different with no evidence of changes in degradation. This suggests that the process deregulated in our cells is the maturation step of their precursor miRNAs, leading to the production of less mature miRNAs.

5.5.3 Expression levels of mRNAs coding for proteins involved in miRNA maturation

As I hypothesised that pre-miRNAs were not correctly going through their maturation process in our cells, I measured the expression level of all the genes coding for the proteins playing a role in this step. These proteins are the different Argonaute proteins but also Dicer, TRBP and MCPIP1. I performed (sq) RT-PCR in three independent batches of our nine human cell lines to determine their relative expression between normal and ADPKD conditions.

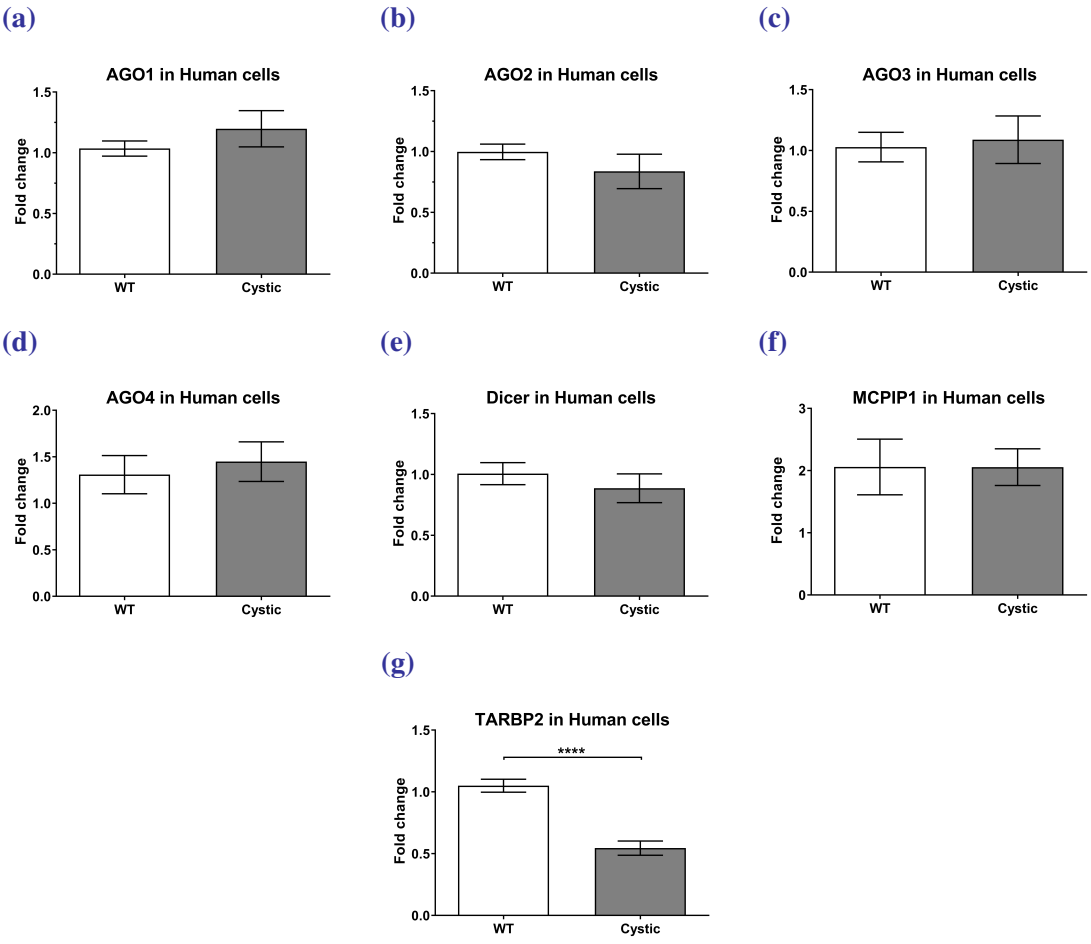

Figure 5.10: **Relative expression levels of genes coding for proteins involved in miRNAs maturation in nine human cell lines.**
(a) *AGO1*, (b) *AGO2*, (c) *AGO3*, (d) *AGO4*, (e) *Dicer*, (f) *MCPIP1* and (g) *TARBP2* expression levels were measured in three independent batches of five normal (white bars) and four cystic (grey bars) human cell lines. Values are expressed as fold change compared to all normal cells.
***** $p<0.0001$ (Unpaired t-test with Welch's correction)*

The genes coding for the Argonaute proteins *AGO1* (Figure 5.10a), *AGO2* (5.10b), *AGO3* (5.10c) and *AGO4* (5.10d), as well as Dicer (Figure 5.10e), did not show any dysregulation between normal and cystic cells. *MCPIP1* (Figure 5.10f), a protein whose role is the cleavage of the pre-miRNA terminal loop, was not changed either in ADPKD cells compared to normal. However, one gene's expression was significantly lower in cystic cells compared to normal: *TARBP2* coding for the TRBP protein (Figure 5.10g). Indeed, the *TARBP2* expression level was decreased to 0.55-fold of the normal cells level.

Western blotting was then performed on the nine human cell lines in order to confirm the down-regulation of TRBP at the protein level:

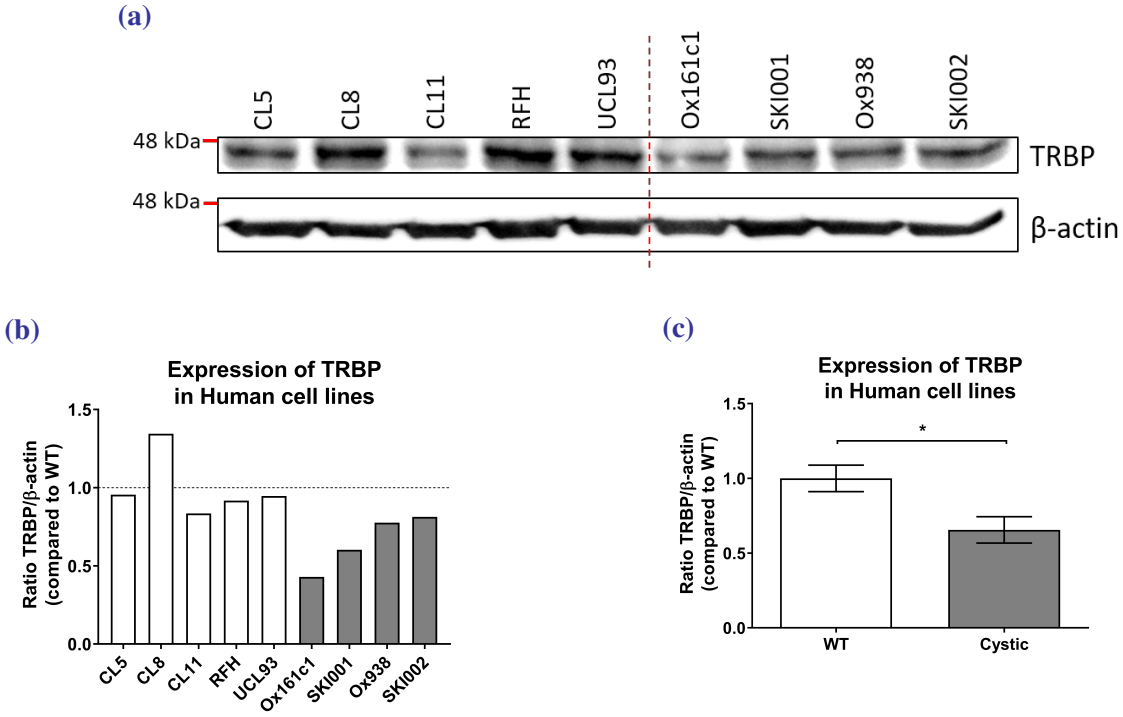

***Figure 5.11:* Western blotting of TRBP in normal and cystic human kidney cells.**
(a) TRBP (expected size 40 kDa) was stained in proteins extracted from five normal (CL5, CL8, CL11, RFH and UCL93, left) and four cystic (Ox161c1, SKI001, Ox938 and SKI002, right) human ADPKD cells. β-actin was used as a loading control (expected size 42 kDa). (b) The TRBP/β-actin ratio was measured for each cell line to quantify its expression levels and reported to the average value in WT cells. (c) TRBP expression levels were expressed as fold change in cystic cells (grey bars) compared to normal cells (white bars).
** p= 0.03 (Unpaired t-test).*

As seen in Figures 5.11a and 5.11b, TRBP was down-regulated in all the cystic cell lines compared to the average of the normal cells. Indeed, the protein levels were reduced by 57 % in Ox161c1, 40 % in SKI001, 22 % in Ox938 and 19 % in SKI002. Globally, when the values were combined by cells phenotype (WT or ADPKD), TRBP was significantly under-expressed by 35 % in the cystic cells compared to normal, in line with what was observed at the mRNA level by (sq) RT-PCR.
I then aimed at confirming the expression pattern of the primary and precursor miRNAs in the *Pkd1*^{nl,nl} mouse model.

5.5.4 Deregulation of primary and precursor miRNAs in the mouse model

I used (sq) RT-PCR to measure the relative expression of pri-mir-193b, pre-mir-193b and pri-mir-582 and pre-mir-582 in four weeks old NeoLox mice kidneys.
As shown in Figure 5.12, none of the primary and precursor miRNAs studied were significantly dysregulated in ADPKD mice. The trend for pri-mir-193b (Figure 5.12a), pri-mir-582 (Figure 5.12c), pre-mir-193b (Figure 5.12b) and pre-mir-582 (Figure 5.12d) was towards an up-regulation rather than the trend to the down-regulation observed for mature mir-193b-3p (Figure 5.1b or the significant down-regulation observed for mature mir-582-5p (Figure 5.1e) in the same mice. This was similar to what was found in human cells: the down-regulation of miRNAs in ADPKD occurs between the precursor and the mature miRNAs stages.

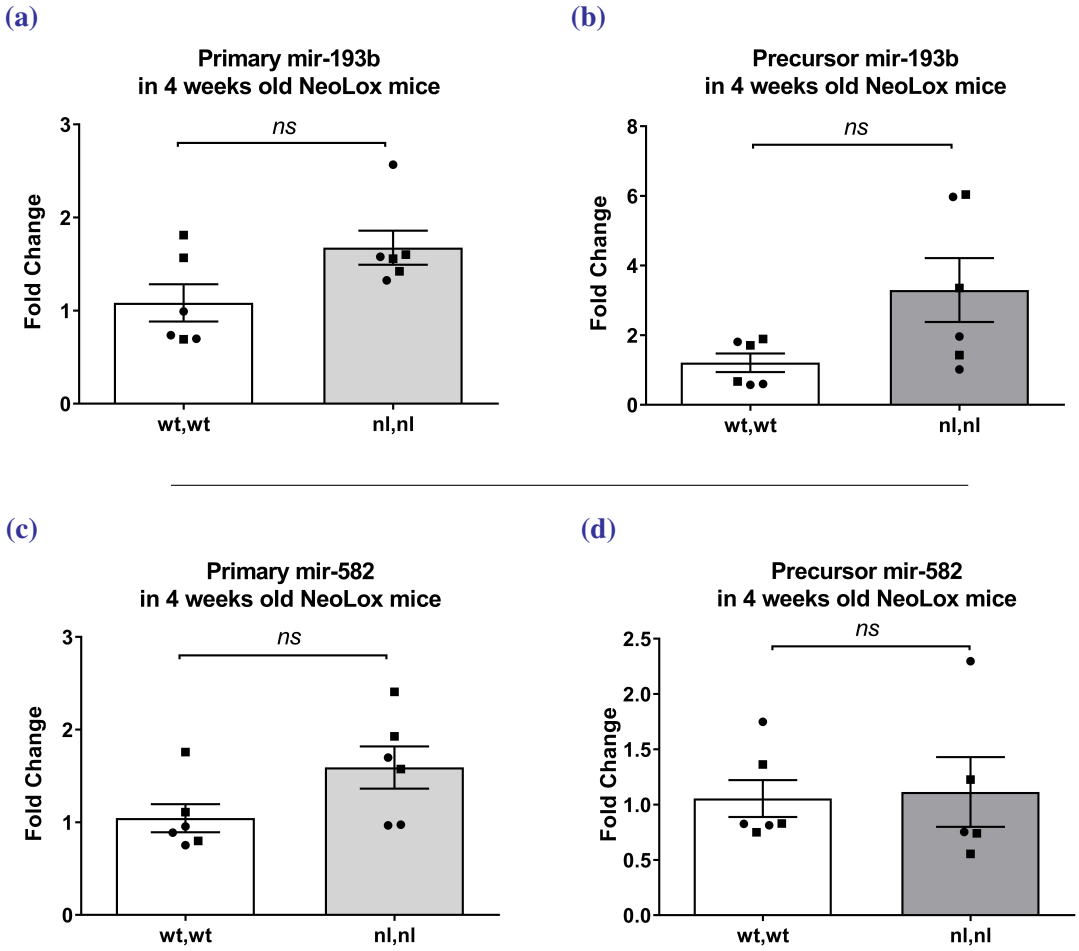

Figure 5.12: **Relative expression of primary and precursor miRNAs in 4 weeks old *Pkd1*^{nl,nl} mice.**
(a) Pri-mir-193b, (b) Pre-mir-193b, (c) Pri-mir-582 and (d) Pre-mir-582 expression levels were measured by (sq) RT-PCR in kidneys from three males and three females wt,wt (white bars) as well as three males and three females nl,nl (grey bars) mice of 4 weeks of age. The values are expressed as fold change compared to all WT mice. Males are symbolised as squares and females as circles.
ns: p>0.05 (Unpaired t-test with Welch's correction)

The last step of my study was then to study if the TRBP protein was under-expressed, similarly to what was found in human cells.

5.5.5 Down-regulation of TRBP in the NeoLox mouse model

Tarbp2 expression levels were measured in the same 4 weeks old *Pkd1*$^{nl.nl}$ mice as previously.

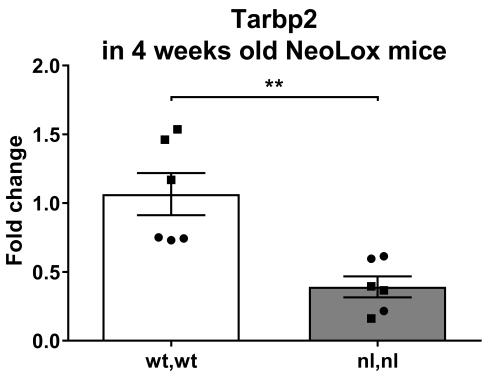

***Figure 5.13:* Relative expression of *Tarbp2* in 4 weeks old *Pkd1*^{nl,nl} mice.**
Tarbp2 expression levels were measured in kidneys from three males and three females wt,wt (white bars) as well as three males and three females nl,nl (grey bars) mice of 4 weeks of age. The values are expressed as fold change compared to all WT mice or WT cells. Males are symbolised as squares and females as circles.
*** p=0.0028 (Unpaired t-test)*

Similarly to what was shown above in human cells (Figure 5.10), *Tarbp2* was significantly down-regulated in NeoLox mice (Figure 5.13). Indeed, the *Pkd1*$^{nl.nl}$ mice expressed *Tarbp2* at a 0.39-fold proportion of the *Pkd1*^{wt,wt}.

5.6 Discussion

The aim of the experiments from this chapter was to understand part of the mechanisms regulating miRNA expression in ADPKD. The two factors I studied were the steroid hormones estradiol and dihydrotestosterone's effects on our human cells and the integrity of the miRNAs maturation process in human cells and mouse kidney.

5.6.1 Gender difference and role of steroids in miRNAs deregulation in ADPKD

Measurements of mir-193b-3p and mir-582-5p expression in *Pkd1*^{nl,nl} hypomorph mice confirmed that the latter was significantly down-regulated in ADPKD mice at the most severe stage (4 weeks). Although mir-193b-3p dysregulation was not significant in the *Pkd1*^{nl,nl} mice, there was a clear trend towards a lower expression level in the 4 weeks old ADPKD mice. Furthermore, in our recent paper, we reported that this miRNA was significantly down-regulated in 4 months old conditional *Pkd1* KO mice (Streets et al., 2017). Another study from our laboratory also found mir-193b-3p significantly down-regulated in ADPKD patients' urinary exosomes by RNA seq (Magayr, 2017).

When the expression levels of mir-193b-3p and mir-582-5p in the 4 weeks old Neo-Lox mice were measured, lower expression was generally present in males compared to females. Plotting these values against the 2KW/BW ratio allowed to determine the correlation between miRNAs expression levels and the severity of the disease. Again, in males these correlation levels were higher and more significant than in females.
It has been reported previously that female CKD patients are protected from renal failure compared to males (Iseki, 2008), and it is known that males ADPKD patients tend to be subjected to haemodialysis earlier than their female counterparts (Gabow et al., 1992; Reed et al., 2008). Furthermore, some miRNAs have been found to be influenced by gender and hormones in the kidney (Kwekel et al., 2015). The relationship of mir-193b-3p with oestrogens is still debated in the literature: it was reported to be induced by E2 in breast cancer cells by Wang et al., 2010d, but found down-regulated by the same hormone and in the same cells by Maillot et al., 2009. Because of these contradictory results and the fact that mir-193b-3p's link with E2 and DHT has not yet been reported in the kidney, and mir-582-5p function in ADPKD is still unknown, my project aimed at getting a better understanding of these processes and bringing new knowledge about these miRNAs' functions in this disorder and in particular their involvement with gender differences in disease outcome.

The differential expression of five miRNAs identified by RNA-seq from human urinary exosomes were confirmed in a mouse model and a similar pattern of gender imbalance shown. Although in the 10 weeks old $Pkd1^{nl,nl}$ mice only mir-192-5p and mir-194-5p were confirmed under-expressed, in the 4 weeks old mice (most severe stage) all but one of the tested miRNAs were validated. More interestingly, the hierarchy (from the least to the most down-regulated) in which these miRNAs were dysregulated in ADPKD (mir-30a-5p<mir-30e-5p<mir-30d-5p<mir-194-5p<mir-192-5p) was parallel to what was found in human urine exosomes. As mir-192-5p and mir-194-5p dysregulation seemed to be depending on gender as well, albeit the opposite of mir-193b-3p and mir-582-5p, *i.e.* more under-expressed in females than in males, I decided to focus on these four miRNAs for the study of the effects of steroid hormones on miRNA expression.

In order to determine the gender of origin of the cell lines and thus their potential ability to respond to steroid hormones, genotyping for *SRY* and qPCR for the oestrogens and androgen receptors were performed. I characterised UCL93 as the only male cell line and could measure the relative expression of *ESR2* and *AR* in all or some of the cell lines (*ESR1* was not amplified, which cannot be explained by tubule segment origin of the cells as the ERα protein was reported to be expressed in distal and proximal renal tubules (Wells et al., 2005; Burris et al., 2015)). I arbitrarily chose to represent the data compared to the CL5 cell line because it was the most constant between batches, but this only has a role of visually representing the data and does not aim at representing absolute mRNA quantities. Surprisingly, *AR* could not be amplified in four of the cell lines, in particular UCL93 which are of male origin. While a non-specificity of the qPCR primers was excluded as the dissociation curves in the cell lines expressing the gene showed a single peak, I suggest several other potential reasons for this lack of amplification; the primers may have only amplified the mRNA coding for the most common AR isoform, AR-A, or the amounts of *AR* mRNA could be too low to be detectable in the samples. Indeed, even in the cell lines where the gene could be amplified, the dCT values were rather low (around 15 compared to around 5 for *ESR2*). A solution could be to redesign the primers in order to amplify all the existing AR isoforms. Furthermore, depending on the studies *AR* has been reported to be expressed in the proximal tubules and cortical collecting duct in rats (Boulkroun et al., 2005) or in the proximal tubules in mouse and human (Ouar et al., 1998; Quinkler et al., 2005), suggesting a segment-specific localisation of this receptor that could depend on the segment origin of our human cell lines. Finally, immortalised cell lines tend to lose their markers or some proteins which could be the case here. This experiment did not allow me to conclude on the capacity of cells to respond to steroid hormones, but knowing that UCL93 were of male origin was important to try and understand the following results.

It is well known that the phenol red commonly added to tissue culture media can act as a weak oestrogen (Berthois et al., 1986). I wanted to know if removing phenol red would be sufficient to see a difference in miRNAs expression in our cell lines. After 10 days in phenol red-free medium, mir-193b-3p and mir-582-5p expression was reduced.

Surprisingly, RFH behaved the opposite way than the other cell lines.
This difference with the other normal cell line UCL93 could be due to a global variability in the cell lines themselves or to their difference of gender, although the two other cell lines studied (Ox161c1 and SKI001) were also of female origin. We could hypothesise that normal female cells behave the opposite way as cystic cells of the same gender, but this would require further experiments to be confirmed. Furthermore, mir-193b-3p was not down-regulated in Ox161c1 compared to the average of the two normal cells. This could be explained by the fact that in the original array the parental line Ox161 was used, while the present experiment was performed on the Ox161c1 cell line derived from a unique clone, or suggest a batch variability that insists on the importance of validating miRNAs and genes expression quantification in several independent batches, which I did all along this project. Overall, this experiment had the interests of confirming that using phenol red-free medium had to be used for a more neutral observation of miRNAs expression, but also indicating which cell lines were the best to show the effects of steroid hormones, and finally what could be expected from these treatments (*i.e.* oestrogens induce an increased miRNAs expression in the cells, suggesting the addition of DHT could on the contrary decrease their expression).

E2 and DHT treatments were performed at 20 nM and 100 nM, for 4 days, on two independent batches of cells. At 100 nM (very high concentration), β-estradiol and DHT showed erratic and non consistent effects between cells, miRNAs and batches (data not shown). An excessive dose of steroid hormones can cause adverse effects and probably explains this observation. Furthermore, typical doses used on cells range from 1 nM to 30 nM of DHT (Gupta et al., 2008; Zhu and Kyprianou, 2010), which is a good indicator that 20 nM was the best dose to study between the two. The normal/male cell line UCL93 did not behave the same under DHT treatment as the cystic/female cell line SKI001; DHT induced a trend to an increase in UCL93 for three of the miRNAs studied while it led to a trend to a down-regulation in SKI001 for all miRNAs. Whether this is due to the gender of the cells or their phenotype is difficult to conclude from these experiments and it would be worth repeating it in other cell lines. In three out of four miRNAs, however, the effect of DHT was not significant.

This may be linked to the fact that its receptor AR was not detected in these cell lines, hence limiting its ability to activate pathways in these, and shows the limits of our model for this study compared to *in vivo* models where cells are issued from all segments. However, A. Metzner reported that DHT increased *Pkd2*$^{-/-}$ zebrafish's cystic phenotype and showed an effect of this compound on Ox161c1 cysts area in 3D cultures. From her data she also suggested that DHT and androstanedione act via alternative pathways than Androgen Receptor, which could support the hypothesis of differences between males and females in part due to male hormones and the action of pathways poorly or not characterised yet (Metzner, 2016).

The fact that E2 and DHT only had consistent and significant effects on mir-582-5p suggests that this miRNA is the most susceptible to hormonal changes, while mir-192-5p and mir-194-5p's reactivity to these are less in line with what was found in the mouse kidneys (maybe because I had less samples which could bias the results). Finally, no significant gender effect could be seen in the normal phenotype as the WT mice did not show any difference in expression between males and females, hinting that there may be other factors or compensation mechanisms in the healthy conditions that regulate miRNAs expression. Interestingly, oestrogen receptor α (ERα) was shown to be activated by PI3-K and Akt, among others, that I showed up-regulated in ADPKD. This suggests that the over-activation of this pathway in ADPKD may not affect females as much as males as the former will in parallel become more sensitive to the protective effect of these steroids (Campbell et al., 2001; Gururaj et al., 2006).

Globally, I reported that 17β-oestrogen (E2) may induce an increase in miRNAs expression, suggesting that females are less likely to show a miRNA down-regulation in ADPKD which is in line with the idea that females are protected from ESRD compared to males.

5.6.2 Mechanisms of miRNAs maturation in ADPKD

The mechanisms regulating miRNAs maturation are very complex and far from being fully understood. I aimed at defining what part of the miRNAs processing and maturation processes is deregulated in our human ADPKD cells in order to pinpoint the factors that could govern the down-regulation of miRNAs that was observed in the disease.

Firstly the expression of the three intermediary forms of miRNAs was measured: primary, precursor and mature miRNA. Data from three independent batches of cells showed no dysregulation of pri-miRNAs or pre-miRNAs but a significant down-regulation of the two mature strands. If anything, the pre-miRNAs showed a trend to an up-regulation, which can suggest an accumulation of this form of miRNAs because of less processing into mature miRNAs. Interestingly, both mature strands of mir-193b and mir-582 were significantly down-regulated to equivalent levels, strongly suggesting the defect in the maturation process occurs between the precursor and mature miRNAs stages and is not due to a higher miRNAs degradation. Indeed, miRNAs degradation would be expected to target only one of the strands while both are at equivalent levels in our cystic cells.

To confirm this, actinomycin D was used to block all mRNA and miRNA transcription which allowed me to analyse degradation of mature miRNAs present in the cells. Indeed, because no new miRNA could be transcribed, the miRNAs measured were exclusively the ones produced before actinomycin D treatment hence a reduction of miRNAs levels would suggest a degradation of these mature miRNAs. The control *C-MYC* showed a very efficient effect of the actinomycin D treatment allowing me to analyse the results of the miRNAs quantification. We could very clearly observe that expression levels of mir-193b-3p and mir-582-5p were very stable over time and that their under-expression in cystic cells was visible from t_0, once again suggesting that this phenomenon is due to less miRNA maturation and not to more miRNA degradation.

I wanted to try and pinpoint which of the miRNA-processing proteins could induce a defect in miRNA maturation in ADPKD cells. Potential candidates were the Argonaute proteins AGO1 to AGO4, Dicer, TRBP and MCPIP1. Since the function and specificity of the different AGO proteins are being debated, some papers reporting no specificity between miRNAs and these proteins (Dueck et al., 2012) while others suggesting that a few subgroups of miRNAs interact specifically with certain Argonaute proteins in particular (Burroughs et al., 2011), I decided to measure the relative expression of the four existing human AGO involved in miRNA processing. These targets, however, did not show any dysregulation between normal and cystic human cells in three independent batches. Similarly, Dicer and MCPIP1 did not show any change.

Interestingly, I showed that *TARBP* was strongly and significantly down-regulated in these cells, which was consistent between batches. This was confirmed at the protein level by Western blotting. TRBP is an essential member of the RNA-Induced Silencing (RISC) complex responsible for the cleavage of precursor miRNAs and therefore its deregulation would directly affect miRNAs maturation.

Even more interestingly, I was able to confirm these results in mouse *Pkd1*^{nl,nl} kidneys: primary and precursor mir-193b and primary mir-582 expression levels were not down-regulated in ADPKD mice compared to WT. On the contrary, there was a trend to an increase which is quite similar to the cells and suggests that there may be an accumulation of the two intermediate miRNAs forms because less mature miRNA is produced.

Altogether, as *Trbp* was also significantly down-regulated in these mice, I have many clues indicating that in human ADPKD cells and 4 weeks old mice *Pkd1*^{nl,nl}, TRBP is down-regulated which leads to a reduced processing of precursor miRNAs by the RISC complex and less production of mature miRNAs.

Although this hypothesis seems convincing from my data, some elements still need to be elucidated. First of all, what causes *TARBP*'s down-regulation in ADPKD cells and *Pkd1*^{nl,nl} mice is not known. Prediction algorithms suggest that, despite the short length of *TARBP2*'s mRNA, several miRNAs could be targeting this gene. Interestingly, mir-196a-5p was predicted by 4 algorithms out of 10 and the microrna.org website, and was the only miRNA found over-expressed in our microarray.

Moreover, this miRNA was also up-regulated in human *PKD1* cysts in an unpublished dataset we had access to (kindly shared by Dr York Pei, Toronto GHRI, Canada), which supports the idea that an increase in mir-196a-5p could lead to *TARBP* repression. Other miRNAs are predicted by more algorithms and could also repress *TARBP2*'s expression. Lower *TARBP2* levels could also be due to a reduced stability of this mRNA by unknown mechanisms, therefore analysing the difference in this mRNA's stability between normal and ADPKD cells could be an interesting experiment to perform.

Furthermore, as TRBP is a constitutive protein in the kidney, the reason why not all miRNAs are affected in ADPKD needs to be understood. Not much is known about TRBP's specificity to miRNAs. However, De Vito et al. reported that the reduced *TARBP2* expression and disrupted TRBP activity observed in cancer stem cells of Ewing sarcoma family tumours affected some miRNAs clusters in particular (interestingly mir-193b was down-regulated in these cells compared to mesenchymal stem cells) (De Vito et al., 2012). Moreover, deletion of TRBP in mice cardiomyocytes only affected the expression levels of 60 miRNAs out of 594 total cardiac miRNAs, including mir-194-5p (Ding et al., 2015), and Kim et al. showed that some but not all miRNAs' (13 out of their 92 candidates) maturation was affected in *TARBP2* KO cells, generating iso-miRNAs with shifted seed sequences from pre-miRNAs (Kim et al., 2014b). This is in line with my findings suggesting that not all miRNAs are affected by a TRBP deficiency and would also explain why pre-miRNAs were not more highly accumulated in the cells. The deregulation at the protein level also remains to be understood. Indeed, TRBP's interaction with Dicer is essential for protein stability (Chendrimada et al., 2005), suggesting that although Dicer's mRNA levels are unchanged in ADPKD, the protein itself might not be stable and not able to process the miRNAs properly. Additionally, TRBP truncating mutations have been detected in gastric and colorectal cancers, suggesting that lower expression levels of this protein or insufficient amounts of full length TRBP could result in hyper-proliferation and survival, phenomena observed both in cancer and ADPKD (Garre et al., 2010; Kim et al., 2010).

Furthermore, TRBP may not only be differentially expressed but also undergo differential post-transcriptional modification. Indeed, it has been shown to carry over 14 different potential phosphorylation sites and to be more stable when hyper-phosphorylated (Kim et al., 2014b; Paroo et al., 2009). Paroo et al. also reported that this phosphorylation was regulated by the MAPK/ERK machinery, which makes my results complementary with those of the previous chapter focused on the PI3-K/Akt and ERK pathways in ADPKD. Indeed, at basal levels a reduced ERK phosphorylation in ADPKD cells would induce less phosphorylation of TRBP hence a deficient RISC-loading complex. The increase in ERK activity *e.g.* after IGF-1 stimulation could result in increased TRBP phosphorylation and increased protein stability although lower protein levels were actually measured. This hypothesis would need to be confirmed by checking the activation levels of TRBP in IGF-1-stimulated ADPKD cells. Interestingly, a recent study (Warner et al., 2016) reported a possible phosphorylation of TRBP by S6K2. S6K2 kinase is a substrate of pERK and of p-mTOR and its phosphorylation would induce a subsequent phosphorylation of TRBP, which also goes along with the hypothesis I suggested. Furthermore, a few recent studies have suggested that IGF-1 can affect some miRNAs expression levels in breast cancer cells and skeletal muscle cells (Martin et al., 2012; Meyer et al., 2015), and that it would be relevant to study whether miRNAs levels are influenced by treatment with IGF-1 in ADPKD. Finally, other post-transcriptional modifications may be taking place such as a SUMOylation (by Small Ubiquitin-like Modifier proteins), which has been reported to increase TRBP's stability *in vitro* and *in vivo*. However, this SUMOylation of TRBP does not affect miRNAs production but regulates their efficiency (Chen et al., 2015), suggesting that the impact of this post-transcriptional modification would take place at later stages.

As a summary, I propose the following: in ADPKD cells, *TARBP2* levels are strongly reduced by mechanisms such as an over-expression of miRNAs (for example mir-196) targeting this gene or a reduced stability of its mRNA. This leads to reduced expression levels of the protein TRBP in the disease hence to a defect in some miRNAs maturation including mir-193b-3p. Furthermore, the lower basal levels of pERK in ADPKD may induce lower levels of pS6K2 and pTRBP hence a reduced activity of this protein added to its lower expression levels. The increased ERK phosphorylation after IGF-1 activation and thus the potentially higher activation of TRBP would not compensate for its greatly reduced expression levels, hence the miRNAs dysregulation would still be present in ADPKD cells. Interestingly, 10 out of 11 of the miRNAs that came out of our microarray were down-regulated, suggesting that a major deregulation in miRNAs in ADPKD due in part to TRBP down-regulation is likely.
Figures 5.14 and 5.15 summarise the findings and hypotheses of how the down-regulation of TRBP may be a reason for the down-regulation of some miRNAs in ADPKD.

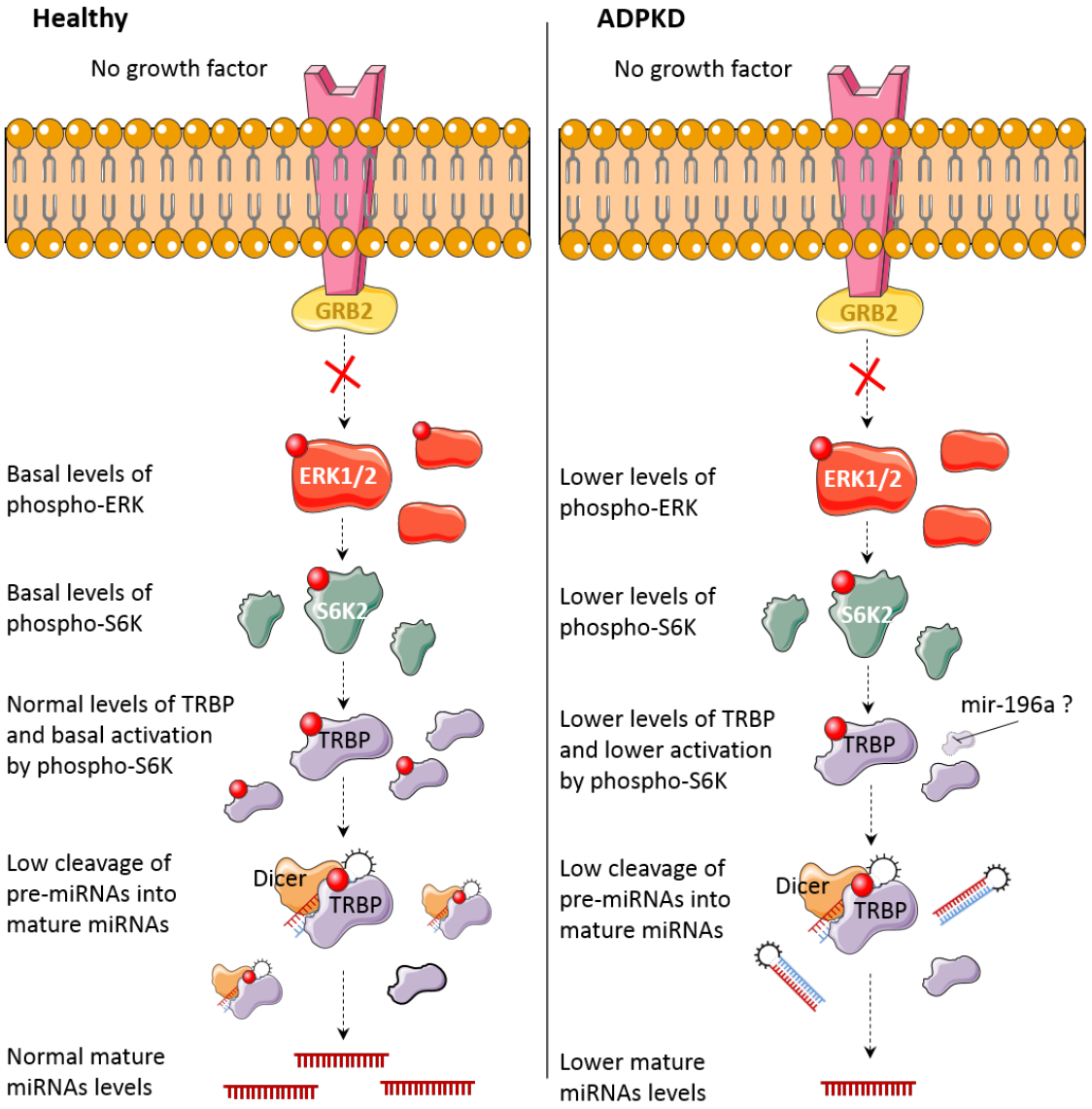

Figure 5.14: **Summary and hypotheses on the down-regulation of TRBP in ADPKD at basal levels.** In healthy kidneys (left), TRBP levels are normal and the lack of growth factors leads to basal Ras/MEK/ERK pathway activation and thus basal phosphorylation of ERK. This will lead to basal TRBP phosphorylation by S6 Kinase 2 and basal processing of pre-miRNAs into mature miRNAs by the TRBP/Dicer complex. In ADPKD (right), TRBP levels are strongly reduced by unknown mechanisms suggested to be miRNAs or defects in mRNA stability. Furthermore, the Ras/MEK/ERK pathway is less activated at the basal levels compared to normal, which suggests lower phospho-ERK and p-S6K2 levels, thus lower phosphorylation of TRBP. Less active TRBP/Dicer levels in ADPKD will lead to the processing of less pre-miRNAs and the production of less mature miRNAs such as mir-193b-3p.

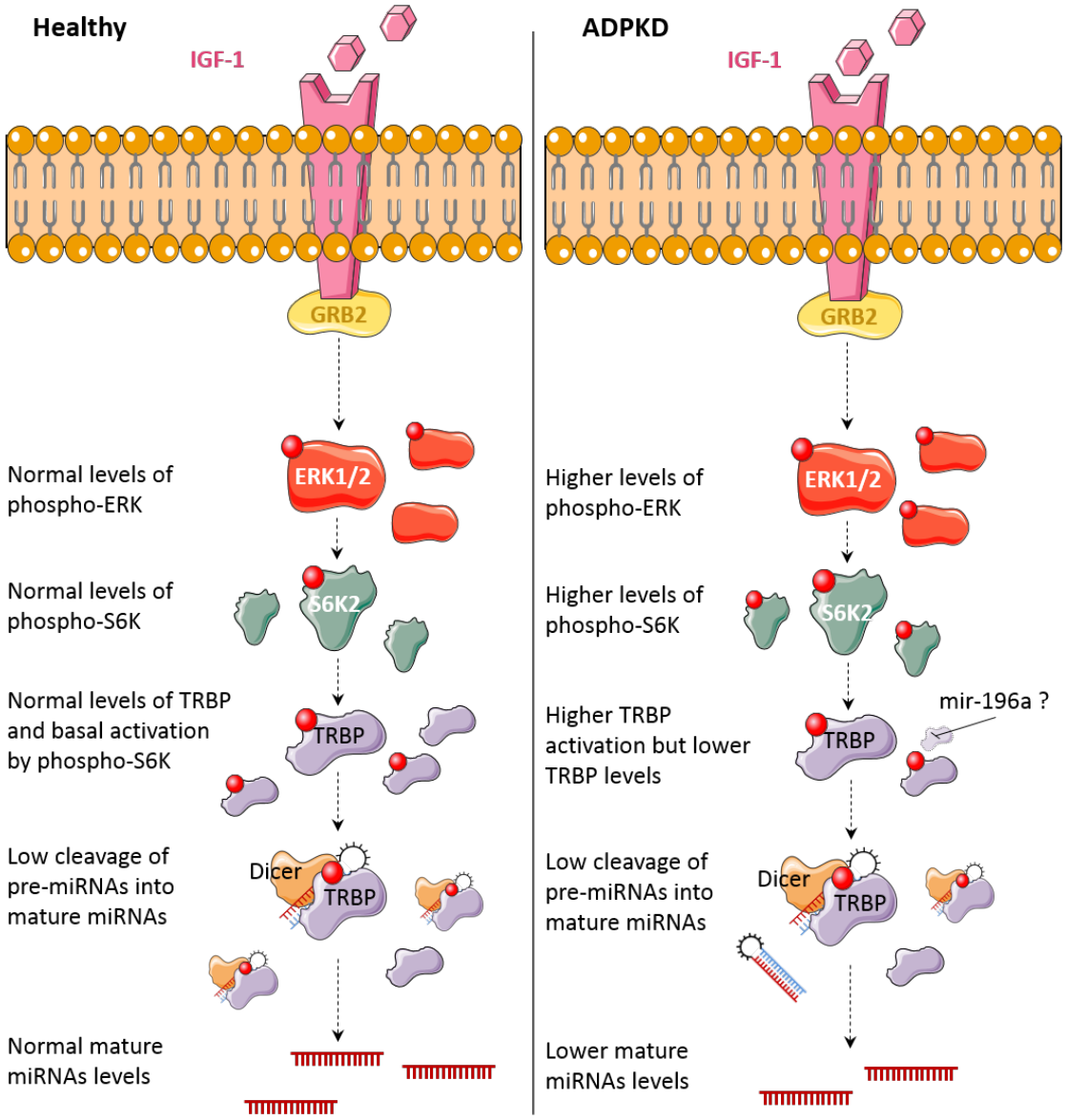

Figure 5.15: **Summary and hypotheses on the down-regulation of TRBP in ADPKD with IGF-1 stimulation.** When IGF-1 binds to its receptor, it activates the Akt and ERK pathways by successive phosphorylation steps. In a healthy kidney (left), the normal pS6K2 levels will activate TRBP and result in the production of normal levels of miRNAs. In ADPKD (right), although pERK levels were suggested to be increased, potentially resulting in higher phosphorylation levels of TRBP, TRBP itself is expressed about twice less than in normal cells. As a result, the total amount of p-TRBP remains lower in ADPKD compared to normal, still leading to reduced maturation of some miRNAs such as mir-193b.

Chapter 6

Summary and conclusions

Autosomal Dominant Polycystic Kidney Disease affects many people worldwide and is a major cause of kidney failure. The underlying mechanisms responsible for the pathogenesis of this disorder remain to be fully understood. Indeed, although mutations in *PKD1* and *PKD2* are absolute requirements for the development of disease, other genetic, epigenetic and environmental factors have been suggested to modify the disease phenotype. miRNAs are a group of small non-coding nucleic acids acting as post-transcriptional modulators of gene expression and have been shown to affect the outcome of other human diseases. Indeed, miRNA-based treatments are in advanced clinical development for diseases such as hepatitis C, cancer and scleroderma (*http://www.miragen.com/clinical-trials/*, Janssen et al., 2013; Zandwijk et al., 2015). As few miRNAs have been linked to ADPKD so far and the phenotypic variability of ADPKD can be high even between patients carrying the same germline mutation of *PKD1* or *PKD2*, I hypothesised that differentially regulated miRNAs could play an important role in disease expression, notably by modulating the expression of genes involved in major biological processes and pathways.

My first aim was to identify new genes both enriched in ADPKD and regulated by mir-193b-3p or mir-582-5p using data from a parallel mRNA/miRNA microarray performed on several conditionally immortalised normal and ADPKD human cell lines generated by our group from healthy or ADPKD kidneys. This approach seemed promising as it allowed us to characterize *ERBB4* as a target of mir-193-3p and to demonstrate its effect on cyst expansion *in vitro* (Streets et al., 2017).

The initial step consisted in grouping the candidates by biological process in order to identify targets regulating mechanisms known to be altered in ADPKD. Through this, twenty-two candidate genes involved in processes such as cell cycle, cell proliferation and metabolic processes were identified. Five of these genes were validated by semi-quantitative PCR and their 3' UTR sequence cloned into pmirGLO vectors to study their interaction with mir-193b-3p and mir-582. Among them, *CALB1* and *CLIC5* showed a reduction of fluorescent signal suggesting a binding of the miRNA, reversed by mutagenesis of the seed sequence. Furthermore, the interaction of *CALB1* with mir-193b-3p was confirmed by (sq) RT-PCR in cells transfected with the mimic or inhibitor of this miRNA.

This provided the first experimental evidence that mir-193b-3p targets *CALB1 in vitro*.
The interaction between mir-582-5p and *CLIC5* was less obvious, possibly due to the existence of two different isoforms of this protein that may show a different affinity for this miRNA, or to a stronger interaction between mir-582-5p and an unidentified protein regulating CLIC5. Hence, a sequencing of the 3'UTR of the two *CLIC5* isoforms as well as experiments to better characterise proteins regulating *CLIC5* such as by RNA co-immunoprecipitation or mass spectrometry would help to characterise further the nature of the relationship between this gene and mir-582-5p.
Although a consistent dysregulation of *CALB1* was shown in human ADPKD cells at the mRNA and protein level, this was not reproduced in other models such as murine cells and kidneys. A likely explanation for these discrepant findings is that *CALB1* expression is highly restricted to the distal tubules, segments that may be more selectively lost in disease. A screen for segment-specific markers in our cell lines did not clarify whether there was enrichment for distal tubule cells in the majority suggesting that dedifferentiation at least in part could have occurred.
The results with *CLIC5* were less consistent between models, some showing an increased expression of this gene while it was reduced in others. This led me to perform validation steps in the different models before carrying out further experiments on the next targets.
By focusing on the most highly enriched genes from our microarray, I identified a further 8 genes which I validated in multiple disease models. This led me to the identification of *ANO1*, encoding anoctamin, as a consistently enriched gene in ADPKD. This is the first evidence that this gene is up-regulated in the disease compared to normal in human and mouse ADPKD cells as well as in an *in vivo* murine model of the disease. Validation of *ANO1* as a target of mir-582-5p was however inconclusive suggesting that it could be regulated by other miRNAs such as mir-194-5p that was also found down-regulated in our array. It will be interesting to confirm this in future experiments. Chemical inhibitors of anoctamin or knock-down of its expression by siRNA had a significant effect on human ADPKD cyst growth *in vitro* confirming previous results in MDCK cells (Buchholz et al., 2014). In addition, a mir-582-5p mimic was similarly effective although its effect may be on multiple genes apart from *ANO1*.

As a result, I suggest a model in which anoctamin over-expression in ADPKD affects cysts progression, potentially affected by increased glycolysis known to occur in the disease and is reported to alter channel activity. Identifying why ANO1 expression is so highly increased (for example finding other relevant miRNAs) and confirming its functional role on downstream signalling pathways (*e.g.* MAPK) would be logical next steps. Identifying relevant candidates targeted by the mir-582-5p mimic would also clarify its effect and point to new areas for study. As anoctamin knock-down showed prolonged effects on cysts growth, it shows potential to be developed as a new drug target and tested in preclinical and clinical studies.

The second aim of this project was to identify candidates using bioinformatics analyses and comparisons with other datasets. Although directly comparing our dataset to the Leiden group's microarray data proved limited, using Gene Set Enrichment Analyses (GSEA) and its Molecular Signature Database (MSigDB) across ours and other datasets compiled in the Leiden group's 'PKD signature' (Malas et al., 2017) allowed me to identify individual genes but also more global dysregulated mechanisms, giving a wider approach to my characterisation of ADPKD pathogenesis due to miRNAs. The two candidates selected (*CELF2* and *IGFBP5*) could not be studied further but the results obtained using this bioinformatics approach suggested several other targets or general biological processes that could be interesting to study.

Furthermore, using box plots of the over time expression of genes common to our and the Leiden group's RNA-seq allowed me to identify a consistent up-regulation in the main regulatory subunit of the PI3-Kinase type I_A, *PIK3R1*. *PIK3R1* was shown to be specifically regulated by mir-193b-3p. I also demonstrated that knock-down of *PIK3R1* inhibited IGF-1 stimulated cyst growth *in vitro*. Over-expression of both regulatory and catalytic subunits of PI3-Kinase in ADPKD could underlie the increased sensitivity of both Akt and ERK pathways to IGF-1 stimulation - potentially by a non canonical pathway in which both pathways cross-activate each other - and the resulting over-proliferation and survival of cystic cells. Future experiments to validate the functional importance of a mir-193b-3p/*PIK3R1*/Akt axis in ADPKD pathogenesis could include artificially over-expressing *PIK3R1* or inhibiting mir-193b-3p in normal cells and study their capacity to form cysts

and the activation of the Akt pathway, validating the up-regulation of *PIK3CA* in mouse and further *in vivo* experiments on rodent disease models.

My third objective was to characterise the mechanisms governing miRNAs dysregulation in ADPKD. Mir-193b-3p and mir-582-5p's differential expression between male and female mice suggested an effect of sexual hormones on these miRNAs expression in ADPKD. Although no effect of the male hormone dihydrotestosterone could be shown, I demonstrated a small but significant increase of 17-β-oestradiol E2 on the expression of these miRNAs expression in cells. These results suggest that the protective phenotype seen in female ADPKD patients may be in part due to the effects of oestradiol on limiting miRNAs down-regulation and hence lessening their impact on the ADPKD phenotype. This would need to be studied further on other models of ADPKD and on other miRNAs known to be involved in this disease such as mir-17 or mir-21. The mechanisms of action of E2 on the cells would also need to be elucidated. Furthermore, I confirmed that two miRNAs identified by RNA-seq as differentially expressed in ADPKD patients' urinary exosomes, mir-192-5p and mir-194-5p, were also strongly down-regulated in the *Pkd1* hypomorph mouse model. This is the first time that the under-expression of these two miRNAs was linked to ADPKD in both a mouse model and in patients, and would be interesting to be taken further by validating relevant targets similarly to what was done in this project for mir-193b-3p and mir-582-5p, and by studying the effects of their over-expression or knock-down on cysts progression or cells proliferation.

Finally, I found that the dysregulation of both mir-193b-3p and mir-582-5p was due to a defect in miRNA maturation, a novel finding. This finding was associated with a selective and consistent decrease in *TARBP2*/TRBP expression suggesting a possible causal relationship. As TRBP is a constitutive protein, the mechanisms by which only some miRNAs including our miRNAs of interest are affected by its down-regulation remain to be understood. It is of interest that studies have reported a selectivity of TRBP deficiency for some miRNAs clusters in *TARBP2* KO cells, including mir-193b or mir-194 (Ding et al., 2015; Kim et al., 2014b; De Vito et al., 2012).

The next steps would be to characterise the mechanisms of this repression and identify the miRNAs targeted by this protein. Because TRBP is down-regulated at the mRNA level, I suggest that the transcription levels of *TARBP2* or its stability are affected, for example by the over-expression of some miRNAs such as mir-196a-5p that we found enriched in our microarray. Identifying these regulating factors by dual-reporter luciferase assays or analysis of *TARBP*'s mRNA stability similarly to what was done in this project, as well as studying potential post-transcriptional modifications affecting TRBP's activity in ADPKD, would be a major progress in characterising the basis for miRNAs dysregulation in this disorder.

In conclusion, this project validated the selective down-regulation of four miRNAs - mir-193b-3p, mir-582-5p, mir-192-5p and mir-194-5p - in ADPKD, identified three targets for mir-193b-3p - *ERBB4*, *CALB1* and *PIK3R1* - and generated a list of other predicted genes and pathways by bioinformatics analyses. Functional evidence of two candidates (*ANO1*, *PIK3R1*) on cyst growth was obtained using human 3D cyst assays. I found evidence that oestrogens may alter miRNA expression, and importantly showed for the first time that their dysregulation occurs at the maturation stage associated with a down-regulation of TRBP expression.

Bibliography

Aboualaiwi, Wissam A et al. (2009). 'Ciliary polycystin-2 is a mechanosensitive calcium channel involved in nitric oxide signaling cascades'. In: *Circulation Research* 104.7, pp. 860–869.

Adam, Liana et al. (2009). 'miR-200 expression regulates epithelial-to-mesenchymal transition in bladder cancer cells and reverses resistance to epidermal growth factor receptor therapy'. In: *Clinical Cancer Research* 15.16, pp. 5060–5072.

Agarwal, Vikram et al. (2015). 'Predicting effective microRNA target sites in mammalian mRNAs'. In: *eLife* 4.AUGUST2015, pp. 1–38.

Akers, Johnny C et al. (2013). 'Biogenesis of extracellular vesicles (EV): Exosomes, microvesicles, retrovirus-like vesicles, and apoptotic bodies'. In: *Journal of Neuro-Oncology* 113.1, pp. 1–11.

Alexiou, Panagiotis et al. (2009). 'miRGen 2.0: A database of microRNA genomic information and regulation'. In: *Nucleic Acids Research* 38.SUPPL.1, pp. 137–141.

Allegra, Danilo et al. (2014). 'Defective DROSHA processing contributes to downregulation of MiR-15/-16 in chronic lymphocytic leukemia'. In: *Leukemia* 28.1, pp. 98–107.

Allen, Erica et al. (2006). 'Loss of polycystin-1 or polycystin-2 results in dysregulated apolipoprotein expression in murine tissues via alterations in nuclear hormone receptors'. In: *Human Molecular Genetics* 15.1, pp. 11–21.

Allen, Mark D et al. (2014). 'A high-resolution structure of the EF-hand domain of human polycystin-2'. In: *Protein Science* 23.9, pp. 1301–1308.

Alves, Everton Fernando et al. (2014). 'Autosomal dominant polycystic kidney disease in hemodialysis patients in southern Brazil'. In: *Jornal Brasileiro de Nefrologia* 36.1, pp. 18–25.

Ameres, Stefan L and Phillip D Zamore (2013). 'Diversifying microRNA sequence and function'. In: *Nature Reviews Molecular Cell Biology* 14.8, pp. 475–88.

Anderson, Sharon et al. (2012). '2-Hydroxyestradiol slows progression of experimental polycystic kidney disease'. In: *American Journal of Physiology - Renal Physiology* 302.5, F636–F645.

Anglicheau, Dany et al. (2009). 'MicroRNA expression profiles predictive of human renal allograft status'. In: *Proceedings of the National Academy of Sciences* 106.13, pp. 5330–5335.

Anjum, Rana and John Blenis (2008). 'The RSK family of kinases: emerging roles in cellular signalling'. In: *Nature Reviews Molecular Cell Biology* 9.10, pp. 747–758.

Anyatonwu, Georgia I et al. (2007). 'Regulation of ryanodine receptor-dependent calcium signaling by polycystin-2'. In: *Proceedings of the National Academy of Sciences* 104.15, pp. 6454–6459.

Aqeilan, Rami I, George A Calin and Carlo M Croce (2010). 'miR-15a and miR-16-1 in cancer: discovery, function and future perspectives'. In: *Cell Death and Differentiation* 17.2, pp. 215–220.

Arac, Demet et al. (2012). 'A novel evolutionarily conserved domain of cell-adhesion GPCRs mediates autoproteolysis'. In: *EMBO Journal* 31.6, pp. 1364–1378.

Ariza, Manuela et al. (1997). 'A family with a milder form of adult dominant polycystic kidney disease not linked to the PKD1 (16p) or PKD2 (4q) genes'. In: *Journal of Medical Genetics* 34, pp. 587–589.

Asati, Vivek, Debarshi Kar Mahapatra and Sanjay Kumar Bharti (2016). 'PI3K / Akt / mTOR and Ras / Raf / MEK / ERK signaling pathways inhibitors as anticancer agents: Structural and pharmacological perspectives'. In: *European Journal of Medicinal Chemistry* 109, pp. 314–341.

Assistance Publique - Hôpitaux de Paris (2017). *The efficacy of Everolimus in reducing total native kidney volume in Polycystic Kidney Disease transplanted recipients (EVERKYSTE). NCT02134899.*

Avci, Edibe and Banu Balci-Peynircioglu (2016). 'An overview of exosomes: From biology to emerging roles in immune response'. In: *Acta Medica* 5.January, pp. 2–10.

Azuma-Mukai, Asuka et al. (2008). 'Characterization of endogenous human Argonautes and their miRNA partners in RNA silencing'. In: *Proceedings of the National Academy of Sciences* 105.23, pp. 7964–9.

Babich, Victor et al. (2004). 'The N-terminal extracellular domain is required for polycystin-1-dependent channel activity'. In: *Journal of Biological Chemistry* 279.24, pp. 25582–25589.

Bader, Andreas G (2012). 'MiR-34 - a microRNA replacement therapy is headed to the clinic'. In: *Frontiers in Genetics* 3.JUL, pp. 1–9.

Bae, Kyongtae T et al. (2006). 'Magnetic resonance imaging evaluation of hepatic cysts in early Autosomal-Dominant Polycystic Kidney Disease: the Consortium for Radiologic Imaging Studies of Polycystic Kidney Disease cohort'. In: *Clinical Journal of the American Society of Nephrology* 1.1, pp. 64–69.

Bahn, Jae Hoon et al. (2015). 'Genomic analysis of ADAR1 binding and its involvement in multiple RNA processing pathways'. In: *Nature Communications* 6, p. 6355.

Bai, Dong, Lynn Ueno and Peter K Vogt (2009). 'Akt-mediated regulation of NFkB and the essentialness of NFkB for the oncogenicity of PI3K and Akt'. In: *International Journal of Cancer* 125.12, pp. 2863–2870.

Bansal, Rahul Kumar and Anil Kapoor (2014). 'Laparoscopic nephrectomy for massive Polycystic Kidney Disease: Updated technique and outcomes'. In: *Journal of the Canadian Urological Association* 8.9-10, pp. 341–345.

Bao, Hao et al. (2013). 'MiR-223 downregulation promotes glomerular endothelial cell activation by up-regulating importin alpha4 and alpha5 in IgA nephropathy'. In: *Kidney International* 85.3, pp. 624–635.

Barman, Bahnisikha and Suvendra N. Bhattacharyya (2015). 'mRNA targeting to endoplasmic reticulum precedes ago protein interaction and MicroRNA (miRNA)-mediated translation repression in mammalian cells'. In: *Journal of Biological Chemistry* 290.41, pp. 24650–24656.

Baroukh, Nadine et al. (2007). 'MicroRNA-124a regulates foxa2 expression and intracellular signaling in pancreatic β-cell lines'. In: *Journal of Biological Chemistry* 282.27, pp. 19575–19588.

Bartel, David P (2004). 'MicroRNAs: Genomics, biogenesis, mechanism, and function'. In: *Cell* 116.2, pp. 281–297.

Bartram, Malte P et al. (2015). 'Loss of Dgcr8-mediated microRNA expression in the kidney results in hydronephrosis and renal malformation'. In: *BMC nephrology* 16.1, p. 55.

Baskerville, Scott and David P Bartel (2005). 'Microarray profiling of microRNAs reveals frequent coexpression with neighboring miRNAs and host genes'. In: *RNA* 11.3, pp. 241–7.

Becker, Christiane et al. (2011). 'Changes in the miRNA profile under the influence of anabolic steroids in bovine liver'. In: *Analyst* 136.6, pp. 1204–9.

Beg, Muhammad S et al. (2017). 'Phase I study of MRX34, a liposomal miR-34a mimic, administered twice weekly in patients with advanced solid tumors'. In: *Investigational New Drugs* 35.2, pp. 180–188.

Behm-Ansmant, Isabelle et al. (2006). 'mRNA degradation by miRNAs and GW182 requires both CCR4 : NOT deadenylase and DCP1 : DCP2 decapping complexes'. In: *Genes & Development* 20, 1885–1898 ST –MRNA degradation by miRNAs and GW1.

Ben-Dov, Iddo Z et al. (2014). 'Urine microRNA as potential biomarkers of Autosomal Dominant Polycystic Kidney Disease progression: description of miRNA profiles at baseline'. In: *PLoS ONE* 9.1, e86856.

Berezikov, Eugene et al. (2007). 'Mammalian mirtron genes'. In: *Molecular Cell* 28.2, pp. 328–336.

Bergmann, Carsten et al. (2011). 'Mutations in multiple PKD genes may explain early and severe Polycystic Kidney Disease'. In: *Journal of the American Society of Nephrology* 22.11, pp. 2047–56.

Berthois, Yolande et al. (1986). 'Phenol red in tissue culture media is a weak estrogen: implications concerning the study of estrogen-responsive cells in culture'. In: *Proceedings of the National Academy of Sciences* 83.8, pp. 2496–500.

Betancur, Juan G and Yukihide Tomari (2012). 'Dicer is dispensable for asymmetric RISC loading in mammals'. In: *RNA* 18.1, pp. 24–30.

Betancur, Juan G, Mayuko Yoda and Yukihide Tomari (2012). 'miRNA-like duplexes as RNAi triggers with improved specificity'. In: *Frontiers in Genetics* 3.JUL, pp. 2008–2013.

Betel, Doron et al. (2010). 'Comprehensive modeling of microRNA targets predicts functional non- conserved and non-canonical sites'. In: *Genome Biology* 11.8, R90.

Bhat-Nakshatri, Poornima et al. (2009). 'Estradiol-regulated microRNAs control estradiol response in breast cancer cells'. In: *Nucleic Acids Research* 37.14, pp. 4850–4861.

Blaszczyk, Jaroslaw et al. (2001). 'Crystallographic and modeling studies of RNase III suggest a mechanism for double-stranded RNA cleavage'. In: *Structure* 9.12, pp. 1225–1236.

Boca, Manila et al. (2006). 'Polycystin-1 induces resistance to apoptosis through the phosphatidylinositol 3-kinase/Akt signaling pathway'. In: *Journal of the American Society of Nephrology* 17.3, pp. 637–647.

Boehlke, Christopher et al. (2010). 'Primary cilia regulate mTORC1 activity and cell size through Lkb1'. In: *Nature Cell Biology* 12.11, pp. 1115–1122.

Boertien, Wendy E et al. (2013). 'Short-term renal hemodynamic effects of tolvaptan in subjects with Autosomal Dominant Polycystic Kidney Disease at various stages of chronic kidney disease'. In: *Kidney International* 84.6, pp. 1278–86.

Bohnsack, Markus T, Kevin Czaplinski and Dirk Gorlich (2004). 'Exportin 5 is a RanGTP-dependent dsRNA-binding protein that mediates nuclear export of pre-miRNAs'. In: *RNA* 10.2, pp. 185–91.

Booij, Tijmen H. et al. (2017). 'High-throughput phenotypic screening of kinase inhibitors to identify drug targets for Polycystic Kidney Disease'. In: *SLAS DISCOVERY: Advancing Life Sciences R&D*.

Boone, Michelle and Peter M.T. Deen (2008). 'Physiology and pathophysiology of the vasopressin-regulated renal water reabsorption'. In: *Pflugers Archiv European Journal of Physiology* 456.6, pp. 1005–1024.

Boor, Peter and Jürgen Floege (2011). 'Chronic kidney disease growth factors in renal fibrosis'. In: *Clinical and Experimental Pharmacology and Physiology* 38.7, pp. 391–400.

Bos, Johannes L (2006). 'Epac proteins: multi-purpose cAMP targets'. In: *Trends in Biochemical Sciences* 31.12, pp. 680–686.

Boulkroun, Sheerazed et al. (2005). 'Expression of androgen receptor and androgen regulation of NDRG2 in the rat renal collecting duct'. In: *Pflugers Archiv European Journal of Physiology* 451.2, pp. 388–394.

Brabletz, Simone and Thomas Brabletz (2010). 'The ZEB/miR-200 feedback loop–a motor of cellular plasticity in development and cancer?' In: *EMBO Reports* 11.9, pp. 670–677.

Brabletz, Simone et al. (2011). 'The ZEB1/miR-200 feedback loop controls Notch signalling in cancer cells'. In: *EMBO Journal* 30.4, pp. 770–82.

Braun, William E (2011). 'mTOR inhibitors and autosomal dominant polycystic kidney disease'. In: *New England Journal of Medicine* 364, pp. 287–288.

Braun, William E et al. (2014). 'Low-dose rapamycin (Sirolimus) effects in autosomal dominant polycystic kidney disease: An open-label randomized controlled pilot study'. In: *Clinical Journal of the American Society of Nephrology* 9.5, pp. 881–888.

Brennecke, Julius et al. (2005). 'Principles of microRNA-target recognition'. In: *PLoS Biology* 3.3, pp. 0404–0418.

Brown, C Titus et al. (2012). 'A Reference-Free Algorithm for Computational Normalization of Shotgun Sequencing Data'. In: pp. 1–18.

Brown, Samuel, Peter Lascarides and Susan Stickevers (2014). 'Treating pain in patients with Chronic Kidney Disease: A review of the literature'. In: *Practical Pain Management* 14.9.

Bu, Pengcheng et al. (2013). 'A microRNA mir-34a regulaed bimodal switch targets Notch in colon cancer stem cells'. In: *Cell Stem Cell* 12.5, pp. 602–615.

Buchholz, Bjoern et al. (2013). 'Anoctamin 1 induces calcium-activated chloride secretion and proliferation of renal cyst-forming epithelial cells'. In: *Kidney International* 85.5, pp. 1–10.

Buchholz, Bjoern et al. (2014). 'Anoctamin 1 induces calcium-activated chloride secretion and proliferation of renal cyst – forming epithelial cells'. In: *Kidney International* 85.5, pp. 1058–1067.

Burk, Ulrike et al. (2008). 'A reciprocal repression between ZEB1 and members of the miR-200 family promotes EMT and invasion in cancer cells'. In: *EMBO Reports* 9.6, pp. 582–9.

Burris, D et al. (2015). 'Estrogen directly and specifically downregulates NaPi-IIa through the activation of both estrogen receptor isoforms (ERα and ERβ) in rat kidney proximal tubule'. In: *American Journal of Physiology - Renal Physiology* 308.6, F522–F534.

Burroughs, Alexander Maxwell et al. (2011). 'Deep-sequencing of human Argonaute-associated small RNAs provides insight into miRNA sorting and reveals Argonaute association with RNA fragments of diverse origin'. In: *RNA Biology* 8.1, pp. 158–177.

Burtey, Stephane et al. (2005). 'Cloning and expression of the amphibian homologue of the human PKD1 gene'. In: *Gene* 357.1, pp. 29–36.

Butterworth, Michael B (2015). 'MicroRNAs and the regulation of aldosterone signaling in the kidney'. In: *American Journal of Physiology - Cell Physiology* 308, pp. C521–C527.

Butz, Henriett et al. (2012). 'Crosstalk between TGF-β signaling and the microRNA machinery'. In: *Trends in Pharmacological Sciences* 33.7, pp. 382–393.

Buzas, Edit I et al. (2014). 'Emerging role of extracellular vesicles in inflammatory diseases'. In: *Nature Reviews Rheumatology* 10, pp. 356–364.

Bycroft, Mark et al. (1999). 'The structure of a PKD domain from polycystin-1: implications for Polycystic Kidney Disease'. In: *EMBO Journal* 18.2, pp. 297–305.

Caby, Marie Pierre et al. (2005). 'Exosomal-like vesicles are present in human blood plasma'. In: *International Immunology* 17.7, pp. 879–887.

Caffrey, Daniel R. et al. (2011). 'Sirna off-target effects can be reduced at concentrations that match their individual potency'. In: *PLoS ONE* 6.7.

Cagnazzo, Federico et al. (2017). 'Intracranial aneurysms in patients with Autosomal Dominant Polycystic Kidney Disease: prevalence, risk of rupture, and management. A systematic review'. In: *Acta Neurochirurgica* 159.5, pp. 811–821.

Cai, Yiqiang et al. (1999). 'Identification and characterisation of polycystin-2, the PKD2 gene product'. In: *Journal of Biological Chemistry* 274.40, pp. 28557–28565.

Cai, Yiqiang et al. (2004). 'Calcium dependence of Polycystin-2 channel activity is modulated by phosphorylation at Ser812'. In: *Journal of Biological Chemistry* 279.19, pp. 19987–19995.
Cammaerts, Sophia et al. (2015). 'Genetic variants in microRNA genes: Impact on microRNA expression, function, and disease'. In: *Frontiers in Genetics* 6.MAY, pp. 1–12.
Campbell, Robert A et al. (2001). 'Phosphatidylinositol 3-kinase/AKT-mediated activation of estrogen receptor alpha: a new model for anti-estrogen resistance'. In: *Journal of Biological Chemistry* 276.13, pp. 9817–9824.
Cardone, Michael H et al. (1998). 'Regulation of cell death protease caspase-9 by phosphorylation'. In: *Science* 282.5392, pp. 1318–1321.
Caroli, Anna et al. (2013). 'Effect of longacting somatostatin analogue on kidney and cyst growth in Autosomal Dominant Polycystic Kidney Disease (ALADIN): A randomised, placebo-controlled, multicentre trial'. In: *The Lancet* 382.13, pp. 1485–1495.
Carpten, John D et al. (2007). 'A transforming mutation in the pleckstrin homology domain of AKT1 in cancer'. In: *Nature* 448.7152, pp. 439–44.
Castellano, Esther and Julian Downward (2011). 'RAS Interaction with PI3K: More Than Just Another Effector Pathway'. In: *Genes and Cancer* 2.3, pp. 261–74.
Chamberlain, M. Dean et al. (2008). 'Disrupted RabGAP function of the p85 subunit of phosphatidylinositol 3-kinase results in cell transformation'. In: *Journal of Biological Chemistry* 283.23, pp. 15861–15868.
Chan, Perry M., Louis Limsect and Edward Manser (2008). 'PAK is regulated by PI3K, PIX, CDC42, and PP2Cα and mediates focal adhesion turnover in the hyperosmotic stress-induced p38 pathway'. In: *Journal of Biological Chemistry* 283.36, pp. 24949–24961.
Chang, Hyeshik et al. (2014). 'TAIL-seq: Genome-wide determination of poly(A) tail length and 3' end modifications'. In: *Molecular Cell* 53.6, pp. 1044–1052.
Chang, Ming-Yang and Albert C M Ong (2008). 'Autosomal Dominant Polycystic Kidney Disease: recent advances in pathogenesis and treatment'. In: *Nephron. Physiology* 108.1, pp. 1–7.
Chang, Tsung-Cheng et al. (2007). 'Transactivation of miR-34a by p53 broadly influences gene expression and promotes apoptosis'. In: *Molecular cell* 26.5, pp. 745–52.
Chang, Zheng et al. (2015). 'Bridger: a new framework for de novo transcriptome assembly using RNA-seq data'. In: *Genome Biology* 16.1, p. 30.
Chantry, David et al. (1997). 'P110\(\delta\), a novel phosphatidylinositol 3-kinase catalytic subunit that associates with p85 and is expressed predominantly in leukocytes'. In: *Journal of Biological Chemistry* 272.31, pp. 19236–19241.
Chapin, Hannah C and Michael J Caplan (2010). 'The cell biology of Polycystic Kidney Disease'. In: *Journal of Cell Biology* 191.4, pp. 701–710.
Chau, B Nelson et al. (2012). 'MicroRNA-21 promotes fibrosis of the kidney by silencing metabolic pathways'. In: *Science Translational Medicine* 4.121.
Chea, Seung Wan and Kyu-Beck Lee (2009). 'TGF-β Mediated Epithelial-Mesenchymal Transition in Autosomal Dominant Polycystic Kidney Disease'. In: *Yonsei Medical Journal* 50.1, p. 105.
Chekulaeva, Marina and Witold Filipowicz (2009). 'Mechanisms of miRNA-mediated post-transcriptional regulation in animal cells'. In: *Current Opinion in Cell Biology* 21.3, pp. 452–460.
Chen, Cheng et al. (2015). 'SUMOylation of TARBP2 regulates miRNA/siRNA efficiency'. In: *Nature Communications* 6, pp. 1–15.
Chen, Chyi Ying A et al. (2009). 'Ago-TNRC6 triggers microRNA-mediated decay by promoting two deadenylation steps'. In: *Nature Structural and Molecular Biology* 16.11, pp. 1160–1166.
Chen, Hui and Zhiying Xu (2015). 'Hypermethylation-Associated Silencing of miR-125a and miR-125b: A Potential Marker in Colorectal Cancer'. In: *Disease Markers* 2015.
Chen, Jianfu, Fan Lai and Lee Niswander (2012). 'The ubiquitin ligase mLin41 temporally promotes neural progenitor cell maintenance through FGF signaling'. In: *Genes and Development* 26.8, pp. 803–815.
Chen, Shao-Yin et al. (2008a). 'The genomic analysis of erythrocyte microRNA expression in sickle cell diseases'. In: *PLoS ONE* 3.6, e2360.
Chen, Wen-Cheng, Yi-Shiuan Tzeng and Hung Li (2008b). 'Gene expression in early and progression phases of Autosomal Dominant Polycystic Kidney Disease'. In: *BMC Research Notes* 1, p. 131.
Chen, Xian-Ming (2009). 'MicroRNA signatures in liver diseases'. In: *World Journal of Gastroenterology* 15.14, p. 1665.
Chen, Ying et al. (2014). 'A DDX6-CNOT1 complex and W-binding pockets in CNOT9 reveal direct links between miRNA target recognition and silencing'. In: *Molecular Cell* 54.5, pp. 737–750.
Chendrimada, Thimmaiah P et al. (2005). 'TRBP recruits the Dicer complex to Ago2 for microRNA processing and gene silencing'. In: *Nature* 436.7051, pp. 740–744.

Cheung, Lydia W T et al. (2011). 'High frequency of PIK3R1 and PIK3R2 mutations in endometrial cancer elucidates a novel mechanism for regulation of PTEN protein stability'. In: *Cancer Discovery* 1.2, pp. 170–185.

Chiang, H. Rosaria et al. (2010). 'Mammalian microRNAs: Experimental evaluation of novel and previously annotated genes'. In: *Genes and Development* 24.10, pp. 992–1009.

Chivet, Mathilde et al. (2012). 'Emerging role of neuronal exosomes in the central nervous system'. In: *Frontiers in Physiology* 3 MAY.May, pp. 1–6.

Cho, Chun-yu et al. (2016). 'Negative feedback regulation of AXL by miR-34a modulates apoptosis in lung cancer cells'. In: *RNA* 22, pp. 303–315.

Choi, Yeon Ho et al. (2011). 'The extracellular signal-regulated kinase mitogen-activated protein kinase / ribosomal S6 protein kinase 1 cascade phosphorylates cAMP response element-binding protein to induce MUC5B gene expression via D-prostanoid receptor signaling'. In: *Journal of Biological Chemistry* 286.39, pp. 34199–34214.

Chou, Chih Hung et al. (2016). 'miRTarBase 2016: Updates to the experimentally validated miRNA-target interactions database'. In: *Nucleic Acids Research* 44.D1, pp. D239–D247.

Choukroun, Gabriel et al. (1995). 'Factors influencing progression of renal failure in autosomal dominant polycystic kidney disease'. In: *Journal of the American Society of Nephrology* 6.6, pp. 1634–42.

Christie, Mary et al. (2013). 'Structure of the PAN3 pseudokinase reveals the basis for interactions with the PAN2 deadenylase and the GW182 proteins'. In: *Molecular Cell* 51.3, pp. 360–373.

Chu, Julia Y et al. (2016). 'Non-canonical PI3K-Cdc42-Pak-Mek-Erk signaling promotes immune-complex induced apoptosis in human neutrophils'. In: *Cell Reports* 17.2, pp. 374–386.

Chung, Arthur C K et al. (2010). 'miR-192 mediates TGF-β / Smad3-driven renal fibrosis'. In: *Journal of the American Society of Nephrology* 21, pp. 1317–1325.

Cline, David M. (2004). 'Chronic pain: evaluation and treatment in the emergency department'. In: *Emergency Medicine Reports*.

Cloonan, Nicole (2015). 'Re-thinking miRNA-mRNA interactions: interwining issues confound targets discovery'. In: *Insights and Perspectives*, pp. 379–388.

Cohen, Philip and Sheelagh Frame (2001). 'The renaissance of GSK3'. In: *Nature Reviews Molecular Cell Biology* 2.10, pp. 769–776.

Compeau, Phillip E C, Pavel A Pevzner and Glenn Tesler (2011). 'How to apply de Bruijn graphs to genome assembly'. In: *Nature Biotechnology* 29.11, pp. 987–991.

Conkrite, Karina et al. (2011). 'Mir-17-92 cooperates with RB pathway mutations to promote retinoblastoma'. In: *Genes and Development* 25.16, pp. 1734–1745.

Cooke, Amy, Andrew Prigge and Marvin Wickens (2010). 'Translational repression by deadenylases'. In: *Journal of Biological Chemistry* 285.37, pp. 28506–28513.

Cornec-Le Gall, Emilie et al. (2013). 'Type of PKD1 mutation influences renal outcome in ADPKD'. In: *Journal of the American Society of Nephrology* 24.6, pp. 1006–1013.

Corsten, Maarten F. et al. (2010). 'Circulating MicroRNA-208b and MicroRNA-499 reflect myocardial damage in cardiovascular disease'. In: *Circulation: Cardiovascular Genetics* 3.6, pp. 499–506.

Cowley Jr, Benjamin D et al. (1993). 'Autosomal-Dominant Polycystic Kidney Disease in the rat'. In: *Kidney International* 43.3, pp. 522–534.

Cowley Jr, Benjamin D et al. (1997). 'Gender and the effect of gonadal hormones on the progression of inherited Polycystic Kidney Disease in rats'. In: *American Journal of Kidney Diseases* 29.2, pp. 265–272.

Craene, Bram De and Geert Berx (2013). 'Regulatory networks defining EMT during cancer initiation and progression'. In: *Nature Reviews Cancer* 13.2, pp. 97–110.

Cushing, Leah et al. (2011). 'miR-29 is a major regulator of genes associated with pulmonary fibrosis'. In: *American Journal of Respiratory Cell and Molecular Biology* 45.2, pp. 287–294.

Dahan, Diana et al. (2014). 'Induction of angiotensin-converting enzyme after miR-143/145 deletion is critical for impaired smooth muscle contractility'. In: *American Journal of Physiology - Cell Physiology* 307.12, pp. C1093–101.

Dai, Yong et al. (2009). 'Comprehensive analysis of microRNA expression patterns in renal biopsies of lupus nephritis patients'. In: *Rheumatology International* 29.7, pp. 749–754.

Davis, Brandi N et al. (2010). 'Smad proteins bind a conserved RNA sequence to promote MicroRNA maturation by Drosha'. In: *Molecular Cell* 39.3, pp. 373–384.

Davison, Sara N, Holly Koncicki and Frank Brennan (2014). 'Pain in chronic kidney disease: A scoping review'. In: *Seminars in Dialysis* 27.2, pp. 188–204.

De Vito, Claudio et al. (2012). 'A TARBP2-dependent miRNA expression profile underlies cancer stem cell properties and provides candidate therapeutic reagents in Ewing sarcoma'. In: *Cancer Cell* 21.6, pp. 807–821.

Dedes, Konstantin J et al. (2011). 'Down-regulation of the miRNA master regulators Drosha and Dicer is associated with specific subgroups of breast cancer'. In: *European Journal of Cancer* 47.1, pp. 138–150.

Delcommenne, Marc et al. (1998). 'Phosphoinositide-3-OH kinase-dependent regulation of glycogen synthase kinase 3 and protein kinase B/AKT by the integrin-linked kinase'. In: *Proceedings of the National Academy of Sciences* 95.19, pp. 11211–11216.

Delmas, Patrick et al. (2004). 'Gating of the polycystin ion channel signaling complex in neurons and kidney cells'. In: *FASEB Journal* 18.6, pp. 740–742.

Denby, Laura et al. (2014). 'MicroRNA-214 antagonism protects against renal fibrosis'. In: *Journal of the American Society of Nephrology* 25.1, pp. 65–80.

Denli, Ahmet M et al. (2004). 'Processing of primary microRNAs by the Microprocessor complex'. In: *Nature* 432.7014, pp. 231–235.

Deshpande, Supriya D et al. (2013). 'Transforming growth factor-β induced cross talk between p53 and a MicroRNA in the pathogenesis of diabetic nephropathy'. In: *Diabetes* 62.9, pp. 3151–3162.

Dhillon, Amardeep S et al. (2002a). 'Cyclic AMP-dependent kinase regulates Raf-1 kinase mainly by phosphorylation of serine 259.' In: *Molecular and cellular biology* 22.10, pp. 3237–46.

Dhillon, Amardeep S et al. (2002b). 'Regulation of Raf-1 activation and signalling by dephosphorylation'. In: *EMBO Journal* 21.1-2, pp. 64–71.

Di Carlo, Valerio et al. (2013). 'TDP-43 regulates the microprocessor complex activity during in vitro neuronal differentiation'. In: *Molecular Neurobiology* 48.3, pp. 952–963.

Di Leva, Gianpiero, Michela Garofalo and Carlo M Croce (2014). 'MicroRNAs in Cancer'. In: *Annual Review of Pathology: Mechanisms of Disease* 9.1, pp. 287–314.

Di Lullo, Luca et al. (2015). 'Chronic Kidney Disease and cardiovascular complications'. In: *Heart Failure Reviews* 20.3, pp. 259–272.

Diaz, Bruce et al. (1997). 'Phosphorylation of Raf-1 serine 338-serine 339 is an essential regulatory event for Ras-dependent activation and biological signaling.' In: *Molecular and cellular biology* 17.8, pp. 4509–16.

Diederichs, Sven and Daniel A. Haber (2007). 'Dual role for Argonautes in microRNA processing and posttranscriptional regulation of microRNA expression'. In: *Cell* 131.6, pp. 1097–1108.

Dillon, Lloye M et al. (2015). 'P-REX1 creates a positive feedback loop to activate growth factor receptor, PI3K/AKT and MEK/ERK signaling in breast cancer'. In: *Oncogene* 34.30, pp. 3968–76.

Ding, Jian et al. (2015). 'Trbp regulates heart function through microRNA-mediated Sox6 repression'. In: *Nature Genetics* 47.7, pp. 776–783.

Ding, Jun, Xiaoman Li and Haiyan Hu (2016). 'TarPmiR: A new approach for microRNA target site prediction'. In: *Bioinformatics* 32.18, pp. 2768–2775.

Ding, Qingqing et al. (2005). 'Erk associates with and primes GSK-3β for its inactivation resulting in upregulation of β-catenin'. In: *Molecular Cell* 19.2, pp. 159–170.

Distefano, Gianfranco et al. (2009). 'Polycystin-1 regulates extracellular signal-regulated kinase-dependent phosphorylation of tuberin to control cell size through mTOR and its downstream effectors S6K and 4EBP1.' In: *Molecular and cellular biology* 29.9, pp. 2359–71.

Donzelli, Sara et al. (2015). 'Epigenetic silencing of miR-145-5p contributes to brain metastasis'. In: *Oncotarget* 6.34, pp. 35183–35201.

Drake, Kylie M et al. (2009). 'Loss of heterozygosity at 2q37 in sporadic Wilms' tumor: Putative role for miR-562'. In: *Clinical Cancer Research* 15.19, pp. 5985–5992.

Du, Keyong and Marc Montminy (1998). 'CREB Is a Regulatory Target for the Protein Kinase Akt / PKB'. In: *Journal of Biological Chemistry* 273.9, pp. 32377–32379.

Dueck, Anne et al. (2012). 'MicroRNAs associated with the different human Argonaute proteins'. In: *Nucleic Acids Research* 40.19, pp. 9850–9862.

Dunlop, Elaine A and Andrew R Tee (2009). 'Mammalian target of rapamycin complex 1: Signalling inputs, substrates and feedback mechanisms'. In: *Cellular Signalling* 21.6, pp. 827–835.

Duvvuri, Umamaheswar et al. (2012). 'TMEM16A induces MAPK and contributes directly to tumorigenesis and cancer progression'. In: *Cancer Research* 72.13, pp. 3270–3281.

Dweep, Harsh and Norbert Gretz (2015). 'miRWalk2.0: a comprehensive atlas of microRNA-target interactions'. In: *Nature Methods* 12.8, p. 697.

Dweep, Harsh et al. (2013). 'Parallel analysis of mRNA and microRNA microarray profiles to explore functional regulatory patterns in Polycystic Kidney Disease : using PKD / Mhm rat model'. In: *PLoS ONE* 8.1, pp. 1–12.

Ebi, Hiromichi et al. (2013). 'PI3K regulates MEK/ERK signaling in breast cancer via the Rac-GEF, P-Rex1'. In: *Proceedings of the National Academy of Sciences* 110.52, pp. 21124–9.

Eblen, Scott T et al. (2002). 'Rac-PAK signaling stimulates extracellular signal-regulated kinase (ERK) activation by regulating formation of MEK1-ERK complexes'. In: *Molecular and Cellular Biology* 22.17, pp. 6023–6033.

Edlund, Anna et al. (2014). 'CFTR and Anoctamin 1 (ANO1) contribute to cAMP amplified exocytosis and insulin secretion in human and murine pancreatic beta-cells'. In: *BMC Medicine* 12, p. 87.

Eichhorn, Stephen W et al. (2014). 'MRNA Destabilization Is the dominant effect of mammalian microRNAs by the time substantial repression ensues'. In: *Molecular Cell* 56.1, pp. 104–115.

Eiring, Anna M et al. (2010). 'miR-328 Functions as an RNA Decoy to Modulate hnRNP E2 Regulation of mRNA Translation in Leukemic Blasts'. In: *Cell* 140.5, pp. 652–665.

El Andaloussi, Samir et al. (2013). 'Extracellular vesicles: biology and emerging therapeutic opportunities'. In: *Nature Reviews Drug Discovery* 12.5, pp. 347–357.

El Ouaamari, Abdelfattah et al. (2008). 'miR-375 targets 3'-phosphoinositide-dependent protein kinase-1 and regulated glucose-induced biological responses in pancreatic beta-cells'. In: *Diabetes* 57.October.

Elkayam, Elad et al. (2012). 'The structure of human argonaute-2 in complex with miR-20a'. In: *Cell* 150.1, pp. 100–110.

Elkon, Ran, Alejandro P Ugalde and Reuven Agami (2013). 'Alternative cleavage and polyadenylation: extent, regulation and function'. In: *Nature Reviews Genetics* 14.7, pp. 496–506.

Elliott, Justine, Nadezhda N Zheleznova and Patricia D Wilson (2011). 'c-Src inactivation reduces renal epithelial cell-matrix adhesion, proliferation, and cyst formation'. In: *American Journal of Physiology - Cell Physiology* 301.2, pp. C522–9.

Ellwanger, Daniel C. et al. (2011). 'The sufficient minimal set of miRNA seed types'. In: *Bioinformatics* 27.10, pp. 1346–1350.

Elmen, Joacim et al. (2008a). 'Antagonism of microRNA-122 in mice by systemically administered LNA-antimiR leads to up-regulation of a large set of predicted target mRNAs in the liver'. In: *Nucleic Acids Research* 36.4, pp. 1153–1162.

Elmen, Joacim et al. (2008b). 'LNA-mediated microRNA silencing in non-human primates'. In: *Nature* 452.7189, pp. 896–9.

Emamian, Seyed Alireza et al. (1993). 'Kidney dimensions at sonography: Correlation with age, sex, and habitus in 665 adult volunteers'. In: *American Journal of Roentgenology* 160.1, pp. 83–86.

Eminaga, Seda et al. (2013). 'Quantification of microRNA expression with next-generation sequencing'. In: *Current Protocols in Molecular Biology* July.

Endo, Kosuke et al. (2013). 'MicroRNA 210 as a biomarker for congestive heart failure.' In: *Biological and Pharmaceutical Bulletin* 36.1, pp. 48–54.

Engelman, Jeffrey A (2009). 'Targeting PI3K signalling in cancer: opportunities, challenges and limitations'. In: *Nature Reviews Cancer* 9.8, pp. 550–62.

Engelman, Jeffrey a, Ji Luo and Lewis C Cantley (2006). 'The evolution of phosphatidylinositol 3-kinases as regulators of growth and metabolism'. In: *Nature Reviews Genetics* 7.8, pp. 606–619.

Ersahin, Tulin, Nurcan Tuncbag and Rengul Cetin-atalay (2015). 'The PI3K/AKT/mTOR interactive pathway'. In: *Molecular BioSystems* 11.11, pp. 1946–1954.

Esau, Christine et al. (2006). 'miR-122 regulation of lipid metabolism revealed by in vivo antisense targeting'. In: *Cell Metabolism* 3.2, pp. 87–98.

Eulalio, Ana et al. (2007). 'Target-specific requirements for enhancers of decapping in miRNA-mediated gene silencing'. In: *Genes & Development* 21.20, pp. 2558–2570.

Fabian, John R, Ira 0 Daar and Deborah K Morrison (1993). 'Critical Tyrosine Residues Regulate the Enzymatic and Biological Activity of Raf-1 Kinase'. In: *Molecular and Cellular Biology* 13.11, pp. 7170–7179.

Fabian, Marc R et al. (2009). 'Mammalian miRNA RISC Recruits CAF1 and PABP to Affect PABP-Dependent Deadenylation'. In: *Molecular Cell* 35.6, pp. 868–880.

Fabian, Marc R et al. (2012). 'miRNA-mediated deadenylation is orchestrated by GW182 through two conserved motifs that interact with CCR4–NOT'. In: *Nature Structural and Molecular Biology* 19.3, pp. 1211–1217.

Fang, Xianjun et al. (2000). 'Phosphorylation and inactivation of glycogen synthase kinase 3 by protein kinase A'. In: *Proceedings of the National Academy of Sciences* 97.22, pp. 11960–11965.

Fang, Yun et al. (2010). 'MicroRNA-10a regulation of proinflammatory phenotype in athero-susceptible endothelium in vivo and in vitro.' In: *Proceedings of the National Academy of Sciences* 107.30, pp. 13450–5.

Fazi, Francesco et al. (2007). 'Epigenetic Silencing of the Myelopoiesis Regulator microRNA-223 by the AML1/ETO Oncoprotein'. In: *Cancer Cell* 12.5, pp. 457–466.

Fedorov, Yuriy et al. (2005). 'Different delivery methods—different expression profiles'. In: *Nature Methods* 2, p. 241.

Ferraresso, Manuela and E Favi (2016). 'Hypothermic machine perfusion in kidney transplantation: back to the future?' In: *Journal of Transplantation Technologie & Research* 6.1, pp. 1–4.
Fischer, Evelyne et al. (2006). 'Defective planar cell polarity in Polycystic Kidney Disease'. In: *Nature Genetics* 38.1, pp. 21–23.
Fletcher, Claire E et al. (2012). 'Androgen-regulated processing of the oncomir miR-27a, which targets prohibitin in prostate cancer'. In: *Human Molecular Genetics* 21.14, pp. 3112–3127.
Fletcher, Claire E et al. (2017). 'A novel role for GSK3β as a modulator of Drosha microprocessor activity and MicroRNA biogenesis'. In: *Nucleic Acids Research* 45.5, pp. 2809–2828.
Foncea, Rocio et al. (1997). 'Insulin-like growth factor-I rapidly activates multiple signal transduction pathways in cultured rat cardiac myocytes'. In: *Journal of Biological Chemistry* 272.31, pp. 19115–19124.
Forman, Joshua J, Aster Legesse-Miller and Hilary A Coller (2008). 'A search for conserved sequences in coding regions reveals that the let-7 microRNA targets Dicer within its coding sequence'. In: *Proceedings of the National Academy of Sciences* 105.39, pp. 14879–84.
Frank, Filipp, Nahum Sonenberg and Bhushan Nagar (2010). 'Structural basis for 5'-nucleotide base-specific recognition of guide RNA by human AGO2'. In: *Nature* 465.7299, pp. 818–822.
Franke, Thomas F et al. (1997). 'Direct regulation of the Akt proto-oncogene product by phosphatidylinositol-3,4-bisphosphate'. In: *Science* 275.5300, pp. 665–8.
Friedlander, Gerard and Claude Amiel (1986). 'Somatostatin and α2-adrenergic agonists selectively inhibit vasopressin-induced cyclic AMP accumulation in MDCK cells'. In: *FEBS Letters* 198.1, pp. 38–42.
Friedman, Robin C et al. (2009). 'Most mammalian mRNAs are conserved targets of microRNAs'. In: *Genome Research* 19.1, pp. 92–105.
Fruman, David A (1998). 'Phosphoinositide Kinases'. In: *Annual Review of Biochemistry* 67, pp. 481–507.
Fujita, Shuji and Hideo Iba (2008). 'Putative promoter regions of miRNA genes involved in evolutionarily conserved regulatory systems among vertebrates'. In: *Bioinformatics* 24.3, pp. 303–308.
Fukao, Akira et al. (2014). 'MicroRNAs trigger dissociation of eIF4AI and eIF4AII from target mRNAs in humans'. In: *Molecular Cell* 56.1, pp. 79–89.
Fuziwara, Cesar Seigi and Edna Teruko Kimura (2015). 'Insights into Regulation of the miR-17-92 Cluster of miRNAs in Cancer'. In: *Frontiers in Medicine* 2.September, p. 64.
Gabow, Patricia A et al. (1992). 'Factors affecting the progression of renal disease in Autosomal-Dominant Polycystic Kidney Disease'. In: *Kidney International* 41.5, pp. 1311–1319.
Gainullin, Vladimir G et al. (2015). 'Polycystin-1 maturation requires polycystin-2 in a dose-dependent manner'. In: *Journal of Clinical Investigation* 125.2, pp. 607–620.
Galicia-Vazquez, Gabriela, Jennifer Chu and Jerry Pelletier (2015). 'eIF4AII is dispensable for miRNA-mediated gene silencing'. In: *RNA* 21.10, pp. 1826–1833.
Gansevoort, Ron T et al. (2016). 'Recommendations for the use of tolvaptan in Autosomal Dominant Polycystic Kidney Disease: A position statement on behalf of the ERA-EDTA Working Groups on Inherited Kidney Disorders and European Renal Best Practice'. In: *Nephrology Dialysis Transplantation* 31.3, pp. 337–348.
Garibaldi, Francesca et al. (2016). 'Mutant p53 inhibits miRNA biogenesis by interfering with the microprocessor complex'. In: *Oncogene* 35.January, pp. 1–11.
Garre, Pilar et al. (2010). 'Reassessing the TARBP2 mutation rate in hereditary nonpolyposis colorectal cancer.' In: *Nature genetics* 42.10, 817–8, author reply 818.
Gebert, Luca F R et al. (2014). 'Miravirsen (SPC3649) can inhibit the biogenesis of miR-122'. In: *Nucleic Acids Research* 42.1, pp. 609–21.
Geng, Lin et al. (2006). 'Polycystin-2 traffics to cilia independently of polycystin-1 by using an N-terminal RVxP motif'. In: *Journal of Cell Science* 119.Pt 7, pp. 1383–1395.
Georgakilas, Georgios et al. (2014). 'microTSS: accurate microRNA transcription start site identification reveals a significant number of divergent pri-miRNAs'. In: *Nature Communications* 5.May, p. 5700.
Georgakilas, Georgios et al. (2016). 'DIANA-miRGen v3.0: Accurate characterization of microRNA promoters and their regulators'. In: *Nucleic Acids Research* 44.D1, pp. D190–D195.
Ghildiyal, Megha and Phillip D Zamore (2009). 'Small silencing RNAs: an expanding universe'. In: *Nature Reviews Genetics* 10.2, pp. 94–108.
Ghosh, Tanay et al. (2008). 'MicroRNA-mediated up-regulation of an alternatively polyadenylated variant of the mouse cytoplasmic b-actin gene'. In: *Nucleic Acids Research* 36.19, pp. 6318–6332.
Giamarchi, Aurélie et al. (2006). 'The versatile nature of the calcium-permeable cation channel TRPP2'. In: *EMBO Reports* 7.8, pp. 787–93.
Gingras, Anne Claude, Brian Raught and Nahum Sonenberg (1999). 'eIF4 initiation factors: effectors of mRNA recruitment to ribosomes and regulators of translation'. In: *Annual Review of Biochemistry* 68, pp. 913–963.

Glowacki, François et al. (2013). 'Increased circulating miR-21 levels are associated with kidney fibrosis'. In: *PLoS ONE* 8.2, pp. 1–11.
Golden, Ryan J et al. (2017). 'An Argonaute phosphorylation cycle promotes microRNA-mediated silencing.' In: *Nature* 542.7640, pp. 1–6.
Gonzales, Patricia A et al. (2010). *The urinary proteomes*. Ed. by Alex J Rai. Methods in. HumanaPress.
Gowda, Shivaraj et al. (2010). 'Markers of renal function tests'. In: *North American Journal of Medical Sciences* 2.4, pp. 2–5.
Grandori, Carla et al. (2000). 'The Myc/Max/Mad Network and the Transcriptional Control of Cell Behavior'. In: *Annual Review of Cell and Developmental Biology* 16.1, pp. 653–699.
Grantham, J J (1996). 'The etiology, pathogenesis, and treatment of Autosomal Dominant Polycystic Kidney Disease: recent advances'. In: *American Journal of Kidney Diseases* 28.6, pp. 788–803.
Gregory, Philip A et al. (2008). 'The miR-200 family and miR-205 regulate epithelial to mesenchymal transition by targeting ZEB1 and SIP1'. In: *Nature Cell Biology* 10.5, pp. 593–601.
Gregory, Philip A et al. (2011). 'An autocrine TGF-β/ZEB/miR-200 signaling network regulates establishment and maintenance of epithelial-mesenchymal transition'. In: *Molecular biology of the cell* 22.10, pp. 1686–98.
Gregory, Richard I et al. (2004). 'The Microprocessor complex mediates the genesis of microRNAs'. In: *Nature* 432.7014, pp. 235–240.
Gregory, Richard I et al. (2005). 'Human RISC couples microRNA biogenesis and posttranscriptional gene silencing'. In: *Cell* 123.4, pp. 631–640.
Gresh, Lionel et al. (2004). 'A transcriptional network in Polycystic Kidney Disease'. In: *EMBO Journal* 23.7, pp. 1657–1668.
Gretz, Norbert et al. (1995). 'Gender-dependent disease severity in autosomal polycystic kidney disease of rats'. In: *Kidney International* 48.0085-2538, pp. 496–500.
Grieben, Mariana et al. (2016). 'Structure of the polycystic kidney disease TRP channel Polycystin-2 (PC2)'. In: *Nature Structural and Molecular Biology* 24.2, pp. 114–122.
Grimson, Andrew et al. (2007). 'MicroRNA targeting specificity in mammals: determinants beyond seed pairing'. In: *Molecular Cell* 27.1, pp. 91–105.
Gu, Shuo et al. (2011). 'Thermodynamic stability of small hairpin RNAs highly influences the loading process of different mammalian Argonautes.' In: *Proceedings of the National Academy of Sciences* 108.22, pp. 9208–13.
Guan, Kun Liang et al. (2000). 'Negative regulation of the serine/threonine kinase B-Raf by Akt'. In: *Journal of Biological Chemistry* 275.35, pp. 27354–27359.
Guil, Sonia and Javier F Caceres (2007). 'The multifunctional RNA-binding protein hnRNP A1 is required for processing of miR-18a'. In: *Nature Structural and Molecular Biology* 14.7, pp. 591–6.
Guo, Fei et al. (2015). 'The Involvement of p53-miR-34a-CDK4 Signaling During the Development of Cervical Cancer'. In: *Cancer Translational Medicine* 1.2, p. 67.
Guo, Huili et al. (2010). 'Mammalian microRNAs predominantly act to decrease target mRNA levels'. In: *Nature* 466.7308, pp. 835–840.
Guo, Xiaofang et al. (2012). 'The microRNA-processing enzymes: Drosha and Dicer can predict prognosis of nasopharyngeal carcinoma'. In: *Journal of Cancer Research and Clinical Oncology* 138.1, pp. 49–56.
Gupta, Manveen K et al. (2013). 'miRNA-548c: a specific signature in circulating PBMCs from dilated cardiomyopathy patients'. In: *Journal of Molecular and Cellular Cardiology* 62, pp. 131–141.
Gupta, Vandana et al. (2008). 'Effects of dihydrotestosterone on differentiation and proliferation of human mesenchymal stem cells and preadipocytes'. In: *Molecular and Cellular Endocrinology* 296, pp. 32–40.
Gururaj, Anupama E et al. (2006). 'Novel mechanisms of resistance to endocrine therapy: genomic and nongenomic considerations'. In: *Clinical Cancer Research* 12.3 II, pp. 1001–1008.
Ha, Minju and V Narry Kim (2014). 'Regulation of microRNA biogenesis'. In: *Nature Reviews Molecular Cell Biology* 15.8, pp. 509–524.
Ha, Tai-You (2011). 'MicroRNAs in human diseases: from lung, liver and kidney diseases to infectious disease, sickle cell disease and endometrium disease'. In: *Immune Network* 11.6, pp. 309–323.
Hajarnis, Sachin et al. (2015). 'Transcription factor hepatocyte nuclear factor-1β (HNF-1β) regulates mir-200 expression through a long noncoding RNA'. In: *Journal of Biological Chemistry* 290.41, pp. 24793–24805.
Hajarnis, Sachin et al. (2017). 'microRNA-17 family promotes Polycystic Kidney Disease progression through modulation of mitochondrial metabolism'. In: *Nature Communications* 8, pp. 1–15.

Halvorson, Christian R, Matthew S Bremmer and Stephen C Jacobs (2010). 'Polycystic Kidney Disease: Inheritance, pathophysiology, prognosis, and treatment'. In: *International Journal of Nephrology and Renovascular Disease* 3, pp. 69–83.

Han, Jinju et al. (2006). 'Molecular basis for the recognition of primary microRNAs by the Drosha-DGCR8 complex'. In: *Cell* 125.5, pp. 887–901.

Han, Jinju et al. (2009). 'Posttranscriptional crossregulation between Drosha and DGCR8'. In: *Cell* 136.1, pp. 75–84.

Harris, Peter C et al. (2006). 'Cyst number but not the rate of cystic growth is associated with the mutated gene in Autosomal Dominant Polycystic Kidney Disease'. In: *Journal of the American Society of Nephrology* 17.11, pp. 3013–3019.

Hateboer, Nick et al. (1999). 'Comparison of phenotypes of Polycystic Kidney Disease types 1 and 2'. In: *The Lancet* 353.9147, pp. 103–107.

Havens, Mallory a et al. (2012). 'Biogenesis of mammalian microRNAs by a non-canonical processing pathway'. In: *Nucleic Acids Research* 40.10, pp. 4626–4640.

Hay, Nissim (2004). 'Upstream and downstream of mTOR'. In: *Journal of Biological Chemistry* 381.5-6, pp. 397–405.

He, Jin et al. (2011a). 'Identification of porcine polycystic kidney disease 1 (PKD1) gene: Molecular cloning, expression profile, and implication in disease model'. In: *Gene* 490.1-2, pp. 37–46.

He, Jin et al. (2013). 'Construction of a transgenic pig model overexpressing polycystic kidney disease 2 (PKD2) gene'. In: *Transgenic Research* 2.123, pp. 861–867.

He, Quanhua et al. (2011b). 'Activation of the basolateral membrane Cl- conductance essential for electrogenic K+ secretion suppresses electrogenic Cl- secretion'. In: *Experimental Physiology* 96.3, pp. 305–316. arXiv: 003.

Head, Steven et al. (2014). 'Library construction for next-generation sequencing: Overviews and challenges'. In: *Biotechniques* 56.2, p. 61.

Hendrickson, David G et al. (2009). 'Concordant regulation of translation and mRNA abundance for hundreds of targets of a human microRNA'. In: *PLoS Biology* 7.11, pp. 25–29.

Hennessy, Erica et al. (2010). 'Identification of microRNAs with a role in glucose stimulated insulin secretion by expression profiling of MIN6 cells'. In: *Biochemical and Biophysical Research Communications* 396.2, pp. 457–462.

Herbert, Kristina M. et al. (2013). 'Phosphorylation of DGCR8 increases its intracellular stability and induces a progrowth miRNA profile'. In: *Cell Reports* 5.4, pp. 1070–1081.

Herbert, Terence P, Andrew R Tee and Christopher G Proud (2002). 'The extracellular signal-regulated kinase pathway regulates the phosphorylation of 4E-BP1 at multiple sites'. In: *Journal of Biological Chemistry* 277.13, pp. 11591–11596.

Hibio, Naoki et al. (2012). 'Stability of miRNA 5'terminal and seed regions is correlated with experimentally observed miRNA-mediated silencing efficacy.' In: *Scientific Reports* 2, p. 996.

Hidaka, Sumi et al. (2004). 'PIGEA-14, a novel coiled-coil protein affecting the intracellular distribution of polycystin-2'. In: *Journal of Biological Chemistry* 279.33, pp. 35009–35016.

Hiesberger, Thomas et al. (2004). *Mutation of hepatocyte nuclear factor-1β inhibits Pkhd1 gene expression and produces renal cysts in mice*.

Ho, Jacqueline et al. (2011). 'The pro-apoptotic protein Bim is a microRNA target in kidney progenitors'. In: *Journal of the American Society of Nephrology* 22.6, pp. 1053–1063.

Hofherr, Alexis et al. (2014). 'N-glycosylation determines the abundance of the transient receptor potential channel TRPP2'. In: *Journal of Biological Chemistry* 289.21, pp. 14854–14867.

Hogan, Marie C et al. (2010). 'Randomized clinical trial of long-acting somatostatin for Autosomal Dominant Polycystic Kidney and Liver Disease'. In: *Journal of the American Society of Nephrology* 21.216, pp. 1052–1061.

Hon, Lawrence S. and Zemin Zhang (2007). 'The roles of binding site arrangement and combinatorial targeting in microRNA repression of gene expression'. In: *Genome Biology* 8.8, R166.

Hopp, Katharina et al. (2014). 'Tolvaptan plus Pasireotide shows enhanced efficacy in a PKD1 model'. In: *Journal of the American Society of Nephrology* JULY 2014, pp. 1–9.

Horie, Takahiro et al. (2010). 'MicroRNA-33 encoded by an intron of sterol regulatory element-binding protein 2 (Srebp2) regulates HDL in vivo'. In: *Proceedings of the National Academy of Sciences* 107.40, pp. 17321–17326.

Horman, Shane R et al. (2013). 'Akt-mediated phosphorylation of argonaute 2 downregulates cleavage and upregulates translational repression of MicroRNA targets'. In: *Molecular Cell* 50.3, pp. 356–367.

Https://clinicaltrials.gov/ (2017). *ClinicalTrials.gov*.

Hu, Yibing et al. (2015). 'Fibroblast-derived exosomes contribute to chemoresistance through priming cancer stem cells in colorectal cancer'. In: *PLoS ONE* 10.5, pp. 1–17.

Huang, Edmund et al. (2009). 'DNA testing for live kidney donors at risk for Autosomal Dominant Polycystic Kidney Disease'. In: *Transplantation* 87.1, pp. 133–7.
Huang, Vera et al. (2012). 'Upregulation of Cyclin B1 by miRNA and its implications in cancer'. In: *Nucleic Acids Research* 40.4, pp. 1695–1707.
Huangfu, Danwei et al. (2003). 'Hedgehog signalling in the mouse requires intraflagellar transport proteins'. In: *Nature* 426.November, pp. 83–87.
Hughes, Jim et al. (1995). 'The polycystic kidney disease 1 (PKD1) gene encodes a novel protein with multiple cell recognition domains'. In: *Nature Genetics* 10, pp. 151–160.
Humphreys, David T et al. (2005). 'MicroRNAs control translation initiation by inhibiting eukaryotic initiation factor 4E/cap and poly(A) tail function'. In: *Proceedings of the National Academy of Sciences* 102.47, pp. 16961–6.
Hurd, Paul J and Christopher J Nelson (2009). 'Advantages of next-generation sequencing versus the microarray in epigenetic research'. In: *Briefings in Functional Genomics and Proteomics* 8.3, pp. 174–183.
Hussain, Aashiq et al. (2016). 'A novel PI3K axis selective molecule exhibits potent tumor inhibition in colorectal carcinogenesis'. In: *Molecular Carcinogenesis* 55.12, pp. 2135–2155.
Husson, Hervé et al. (2004). 'New insights into ADPKD molecular pathways using combination of SAGE and microarray technologies'. In: *Genomics* 84.3, pp. 497–510.
Iki, Taichiro et al. (2010). 'In vitro assembly of plant RNA-induced silencing complexes facilitated by molecular chaperone HSP90'. In: *Molecular Cell* 39.2, pp. 282–291.
Iliou, Maria S et al. (2014). 'Impaired DICER1 function promotes stemness and metastasis in colon cancer'. In: *Oncogene* 33.30, pp. 4003–15.
Ingham, Philip W and Andrew P McMahon (2001). 'Hedgehog signaling in animal development : paradigms and principles Hedgehog signaling in animal development : paradigms and principles'. In: *Genes and Development* 15.23, pp. 3059–3087.
Inoki, Ken et al. (2002). 'TSC2 is phosphorylated and inhibited by Akt and suppresses mTOR signalling'. In: *Nature Cell Biology* 4.9, pp. 648–57.
Iseki, Kunitoshi (2008). 'Gender differences in Chronic Kidney Disease'. In: *Kidney International* 74.4, pp. 415–417.
Iwasaki, Shintaro, Tomoko Kawamata and Yukihide Tomari (2009). 'Drosophila Argonaute1 and Argonaute2 Employ Distinct Mechanisms for Translational Repression'. In: *Molecular Cell* 34.1, pp. 58–67.
Iwasaki, Shintaro et al. (2010). 'Hsc70/Hsp90 chaperone machinery mediates ATP-dependent RISC loading of small RNA duplexes'. In: *Molecular Cell* 39.2, pp. 292–299.
Iwasaki, Yuka W et al. (2013). 'Global microRNA elevation by inducible Exportin 5 regulates cell cycle entry'. In: *RNA* 19.4, pp. 490–7.
Jackson, Aimee L and Peter S Linsley (2004). 'Noise amidst the silence: Off-target effects of siRNAs?' In: *Trends in Genetics* 20.11, pp. 521–524.
Jackson, Richard J, Christopher U T Hellen and Tatyana V Pestova (2010). 'The mechanism of eukaryotic translation initiation and principles of its regulation'. In: *Nature Reviews Molecular Cell Biology* 11.2, pp. 113–127.
Jacobo, Sarah Melissa P and Andrius Kazlauskas (2015). 'Insulin-like growth factor 1 (IGF-1) stabilizes nascent blood vessels'. In: *Journal of Biological Chemistry* 290.10, pp. 6349–6360.
Jaiswal, Bijay S et al. (2009). 'Somatic mutations in p85α promote tumorigenesis through class IA PI3K activation'. In: *Cancer Cell* 16.6, pp. 463–474.
Jalava, Sanni E et al. (2012). 'Androgen-regulated miR-32 targets BTG2 and is overexpressed in castration-resistant prostate cancer'. In: *Oncogene* 31.41, pp. 1–12.
Janssen, Harry L a et al. (2013). 'Treatment of HCV infection by targeting microRNA'. In: *New England Journal of Medicine* 368.18, pp. 1685–94.
Jardine, Meg J et al. (2013). 'mTOR inhibition in Autosomal Dominant Polycystic Kidney Disease (ADPKD) : the question remains open'. In: *Nephrology Dialysis Transplantation* 28.2, pp. 242–244.
Jean, Steve and Amy A Kiger (2015). 'Classes of phosphoinositide 3-kinases at a glance'. In: *Journal of Cell Science* 127, pp. 923–928.
Jiang, Fan et al. (2014). 'NADPH oxidase-dependent redox signaling in TGF-β-mediated fibrotic responses'. In: *Redox Biology* 2.1, pp. 267–272.
Joglekar, Mugdha V. et al. (2007). 'MicroRNA profiling of developing and regenerating pancreas reveal post-transcriptional regulation of neurogenin3'. In: *Developmental Biology* 311.2, pp. 603–612.
Johnson, Ann M and Patricia A Gabow (1997). 'Identification of patients with autosomal dominant polycystic kidney disease at highest risk for end-stage renal disease'. In: *Journal of the American Society of Nephrology* 8.10, pp. 1560–1567.

Johnson, Steven M et al. (2005). 'RAS is regulated by the let-7 microRNA family'. In: *Cell* 120.5, pp. 635–647.

Johnstone, Rose M et al. (1987). 'Vesicle formation during reticulocyte maturation. Association of plasma membrane activities with released vesicles (exosomes)'. In: *Journal of Biological Chemistry* 262.19, pp. 9412–9420.

Jonas, Stefanie and Elisa Izaurralde (2013). 'The role of disordered protein regions in the assembly of decapping complexes and RNP granules'. In: *Genes and Development* 27.24, pp. 2628–2641.

— (2015). 'Towards a molecular understanding of microRNA-mediated gene silencing'. In: *Nature Reviews Genetics* 16.7, pp. 421–433.

Jopling, Catherine L et al. (2005). 'Modulation of hepatitis C virus RNA abundance by a liver-specific MicroRNA'. In: *Science* 309.5740, pp. 1577–81.

Kadener, Sebastian et al. (2009). 'Genome-wide identification of targets of the drosha-pasha/DGCR8 complex.' In: *RNA* 15.4, pp. 537–545.

Karube, Yoko et al. (2005). 'Reduced expression of Dicer associated with poor prognosis in lung cancer patients'. In: *Cancer Science* 96.2, pp. 111–115.

Kato, Mitsuo et al. (2007). 'MicroRNA-192 in diabetic kidney glomeruli and its function in TGF-β-induced collagen expression via inhibition of E-box repressors'. In: *Proceedings of the National Academy of Sciences* 104.9, pp. 3432–7.

Kato, Mitsuo et al. (2009). 'TGF-β activates Akt kinase through a microRNA-dependent amplifying circuit targeting PTEN'. In: *Nature Cell Biology* 11.7, pp. 881–889.

Kaupp, U. Benjamin and Reinhard Seifert (2002). 'Cyclic nucleotide-gated ion channels'. In: *Physiological Reviews* 82.3, pp. 769–824.

Keklikoglou, Ioanna et al. (2012). 'MicroRNA-520/373 family functions as a tumor suppressor in estrogen receptor negative breast cancer by targeting NF-κB and TGF-β signaling pathways'. In: *Oncogene* 31.37, pp. 4150–4163.

Keller, Sandro et al. (2007). 'CD24 is a marker of exosomes secreted into urine and amniotic fluid'. In: *Kidney international* 72.9, pp. 1095–1102.

Kelly, Rodney W et al. (1991). 'Extracellular organelles (prostasomes) are immunosuppressive components of human semen'. In: *Clinical and Experimental Immunology* 86.3, pp. 550–556.

Kertesz, Michael et al. (2007). 'The role of site accessibility in microRNA target recognition'. In: *Nature Genetics* 39 VN - r.10, pp. 1278–1284.

Khalid, Usman et al. (2016). 'MicroRNA-21 (miR-21) expression in hypothermic machine perfusate may be predictive of early outcomes in kidney transplantation'. In: *Clinical Transplantation* 30.2, pp. 99–104.

Khvorova, Anastasia, Angela Reynolds and Sumedha D Jayasena (2003). 'Functional siRNAs and miRNAs exhibit strand bias'. In: *Cell* 115.2, pp. 209–216.

Kim, Chong-Su and Dong-Mi Shin (2016). 'Improper hydration induces global gene expression changes associated with renal development in infant mice'. In: *Genes & Nutrition* 11.1, p. 28.

Kim, Hyunho et al. (2014a). 'Ciliary membrane proteins traffic through the Golgi via a Rabep1/GGA1/Arl3-dependent mechanism'. In: *Nature Communications* 5.May, p. 5482.

Kim, Keetae et al. (2000). 'Polycystin 1 is required for the structural integrity of blood vessels'. In: *Proceedings of the National Academy of Sciences* 97.4, pp. 1731–6.

Kim, Min S et al. (2008). 'Mutational analysis of oncogenic AKT E17K mutation in common solid cancers and acute leukaemias'. In: *British journal of cancer* 98.9, pp. 1533–5.

Kim, Min S et al. (2010). 'Somatic mutations and losses of expression of microRNA regulation-related genes AGO2 and TNRC6A in gastric and colorectal cancers'. In: *Journal of Pathology* 221.2, pp. 139–146.

Kim, Seokho et al. (2016). 'The polycystin complex mediates Wnt/Ca2+ signalling'. In: *Nature Cell Biology* 18.7, pp. 752–764.

Kim, V N, J Han and M C Siomi (2009). 'Biogenesis of small RNAs in animals'. In: *Nature Reviews Molecular Cell Biology* 10.2, pp. 126–139.

Kim, Yoosik et al. (2014b). 'Deletion of human tarbp2 reveals cellular microRNA targets and cell-cycle function of TRBP'. In: *Cell Reports* 9.3, pp. 1061–1074.

Klawitter, Jelena et al. (2013). 'Bioactive lipid mediators in Polycystic Kidney Disease'. In: *Journal of Lipid Research* 55.6, pp. 1139–1149.

Klippel, Anke et al. (1997). 'A specific product of phosphatidylinositol 3-kinase directly activates the protein kinase Akt through its pleckstrin homology domain'. In: *Molecular and cellular biology* 17.1, pp. 338–44.

Kloosterman, Wigard P. et al. (2007). 'Targeted inhibition of miRNA maturation with morpholinos reveals a role for miR-375 in pancreatic islet development'. In: *PLoS Biology* 5.8, pp. 1738–1749.

Kobe, Bostjan and Andrey V. Kajava (2001). 'The leucine-rich repeat as a protein recognition motif'. In: *Current Opinion in Structural Biology* 11.6, pp. 725–732.
Kodaki, Tsutomu et al. (1994). 'The activation of phosphatidylinositol 3-kinase by Ras'. In: *Current Biology* 4.9, pp. 798–806.
Koptides, M et al. (2000). 'Genetic evidence for a trans-heterozygous model for cystogenesis in Autosomal Dominant Polycystic Kidney Disease'. In: *Human Molecular Genetics* 9.3, pp. 447–52.
Korpal, Manav et al. (2008). 'The miR-200 family inhibits epithelial-mesenchymal transition and cancer cell migration by direct targeting of E-cadherin transcriptional repressors ZEB1 and ZEB2'. In: *Journal of Biological Chemistry* 283.22, pp. 14910–14914.
Köttgen, Michael and Gerd Walz (2005). 'Subcellular localization and trafficking of polycystins'. In: *Pflugers Archiv European Journal of Physiology* 451.1, pp. 286–293.
Köttgen, Michael et al. (2005). 'Trafficking of TRPP2 by PACS proteins represents a novel mechanism of ion channel regulation'. In: *EMBO Journal* 24.4, pp. 705–716.
Kozminski, Keith G, Peter L Beech and Joel L Rosenbaum (1995). 'The Chlamydomonas kinesin-like protein FLA10 is involved in motility associated with the flagellar membrane'. In: *Journal of Cell Biology* 131.6 I, pp. 1517–1527.
Kozomara, Ana and Sam Griffiths-Jones (2014). 'MiRBase: Annotating high confidence microRNAs using deep sequencing data'. In: *Nucleic Acids Research* 42.D1, pp. 68–73.
Kraus, Andre et al. (2016). 'Glucose promotes secretion-dependent renal cyst growth'. In: *Journal of Molecular Medicine* 94.1, pp. 107–117.
Kriegsheim, Alex von et al. (2006). 'Regulation of the Raf–MEK–ERK pathway by protein phosphatase 5'. In: *Nature Cell Biology* 8.9, pp. 1011–1016.
Kroiss, A et al. (2014). 'Androgen-regulated microRNA-135a decreases prostate cancer cell migration and invasion through downregulating ROCK1 and ROCK2'. In: *Oncogene* August 2013, pp. 1–10.
Krol, Jacek, Inga Loedige and Witold Filipowicz (2010). 'The widespread regulation of microRNA biogenesis, function and decay'. In: *Nature Reviews Genetics* 11.9, pp. 597–610.
Krol, Jacek et al. (2004). 'Structural features of microRNA (miRNA) precursors and their relevance to miRNA biogenesis and small interfering RNA/short hairpin RNA design'. In: *Journal of Biological Chemistry* 279.40, pp. 42230–42239.
Krstic, Radivoj V (1997). *Human microscopic anatomy: an atlas for students of medicine and biology*. Springer-Verlag.
Krugmann, Sonja et al. (2002). 'Identification of ARAP3, a novel PI3K effector regulating both Arf and Rho GTPases, by selective capture on phosphoinositide affinity matrices'. In: *Molecular Cell* 9.1, pp. 95–108.
Krupa, Aleksandra et al. (2010). 'Loss of microRNA-192 promotes fibrogenesis in diabetic nephropathy'. In: *Journal of the American Society of Nephrology* 21.3, pp. 438–447.
Kumar, Sandeep et al. (2014). 'Role of flow-sensitive microRNAs in endothelial dysfunction and atherosclerosis mechanosensitive athero-miRs'. In: *Arteriosclerosis, Thrombosis, and Vascular Biology* 34.10, pp. 2206–2216.
Kunzelmann, Karl et al. (2011). 'Expression and function of epithelial anoctamins'. In: *Experimental Physiology* 92.2, pp. 184–192.
Kunzelmann, Karl et al. (2012). 'Airway epithelial cells - Functional links between CFTR and anoctamin dependent Cl- secretion'. In: *International Journal of Biochemistry and Cell Biology* 44.11, pp. 1897–1900.
Kurts, Christian et al. (2013). 'The immune system and kidney disease: basic concepts and clinical implications'. In: *Nature Reviews Immunology* 13.10, pp. 738–53.
Kwekel, Joshua C. et al. (2015). 'Sex and age differences in the expression of liver microRNAs during the life span of F344 rats'. In: *Biology of Sex Differences* 8.1, p. 6.
Ladewig, Erik et al. (2012). 'Discovery of hundreds of mirtrons in mouse and human small RNA data'. In: *Genome Research* 22, pp. 1634–1645.
Lagos-Quintana, Mariana et al. (2001). 'Identification of novel genes coding for small expressed RNAs'. In: *Science* 294.5543, pp. 853–858.
Lake, David, Sonia A L Corrêa and Jürgen Müller (2016). 'Negative feedback regulation of the ERK1/2 MAPK pathway'. In: *Cellular and Molecular Life Sciences* 73.23, pp. 4397–4413.
Lakhia, Ronak et al. (2016). 'MicroRNA-21 aggravates cyst growth in a model of Polycystic Kidney Disease'. In: *Journal of the American Society of Nephrology* 27.8, pp. 2319–30.
Lal, Mark et al. (2008). 'Polycystin-1 C-terminal tail associates with β-catenin and inhibits canonical Wnt signaling'. In: *Human Molecular Genetics* 17.20, pp. 3105–3117.
Lam, Jenny K W et al. (2015). 'siRNA versus miRNA as therapeutics for gene silencing'. In: *Molecular Therapy - Nucleic Acids* 4.9, e252.

Lan, Hui Yao (2012). 'Transforming growth factor-β/Smad signalling in diabetic nephropathy'. In: *Clinical and Experimental Pharmacology and Physiology* 39.8, pp. 731–738.
Landgraf, Pablo et al. (2007). 'A ammalian microRNA expression atlas based on small RNA library sequencing'. In: *Cell* 129.7, pp. 1401–1414.
Landthaler, Markus, Abdullah Yalcin and Thomas Tuschl (2004). 'The human DiGeorge syndrome critical region gene 8 and its D. melanogaster homolog are required for miRNA biogenesis'. In: *Current Biology* 14, pp. 2162–2167.
Lantinga-van Leeuwen, Irma S et al. (2004). 'Lowering of Pkd1 expression is sufficient to cause Polycystic Kidney Disease'. In: *Human Molecular Genetics* 13.24, pp. 3069–3077.
Lantinga-van Leeuwen, Irma S et al. (2007). 'Kidney-specific inactivation of the Pkd1 gene induces rapid cyst formation in developing kidneys and a slow onset of disease in adult mice'. In: *Human Molecular Genetics* 16.24, pp. 3188–3196.
Laplante, Mathieu and David M. Sabatini (2012). 'mTOR signaling in growth control and disease'. In: *Cell* 149.2, pp. 274–293.
Lavoie, Hugo and Marc Therrien (2015). 'Regulation of RAF protein kinases in ERK signalling'. In: *Nature Reviews Molecular Cell Biology* 16.5, pp. 281–298.
Lee, Inhan et al. (2009). 'New class of microRNA targets containing simultaneous 5'-UTR and 3'-UTR interaction sites'. In: *Genome Research* 19, pp. 1175–1183.
Lee, Jae Eun, Min Ha Park and Jong Hoon Park (2004a). 'The gene expression profile of cyst epithelial cells in Autosomal Dominant Polycystic Kidney Disease patients'. In: *Journal of Biochemistry and Molecular Biology* 37.5, pp. 612–617.
Lee, Kyung et al. (2015). 'Inactivation of integrin-β1 prevents the development of Polycystic Kidney Disease after the loss of polycystin-1'. In: *Journal of the American Society of Nephrology* 26.4, pp. 888–95.
Lee, Rosalind C, Rhonda L Feinbaum and Victor Ambros (1993). 'The C. elegans heterochronic gene lin-4 encodes small RNAs with antisense complementarity to & II-14'. In: *Cell* 75.5, pp. 843–854.
Lee, Seung-Ok et al. (2008). 'MicroRNA15a modulates expression of the cell-cycle regulator Cdc25A and affects hepatic cystogenesis in a rat model of Polycystic Kidney Disease'. In: *Journal of Clinical Investigation* 118.11, pp. 3714–3724.
Lee, Wen-Chin et al. (2017). 'Chronic Kidney Disease-mineral and bone disorder'. In: *BioMed Research International* 2017.
Lee, Yoontae et al. (2003). 'The nuclear RNase III Drosha initiates microRNA processing'. In: *Nature* 425.6956, pp. 415–419.
Lee, Yoontae et al. (2004b). 'MicroRNA genes are transcribed by RNA polymerase II'. In: *EMBO Journal* 23, pp. 4051–4060.
Leppä, Sirpa et al. (1998). 'Differential regulation of c-Jun by ERK and JNK during PC12 cell differentiation'. In: *EMBO Journal* 17.15, pp. 4404–4413.
Leuenroth, Stephanie J et al. (2008). 'Triptolide reduces cystogenesis in a model of ADPKD'. In: *Journal of the American Society of Nephrology* 19.9, pp. 1659–1662.
Leung, Anthony K L et al. (2011). 'Poly(ADP-Ribose) regulates stress responses and microRNA activity in the cytoplasm'. In: *Molecular Cell* 42.4, pp. 489–499.
Leuschner, Philipp J F et al. (2006). 'Cleavage of the siRNA passenger strand during RISC assembly in human cells'. In: *EMBO Reports* 7.3, pp. 314–320.
Levey, Andrew S and Josef Coresh (2012). 'Chronic Kidney Disease'. In: *The Lancet* 379.9811, pp. 165–180.
Levey, Andrew S, Lesley A Stevens and Christopher H Schmid (2009). 'A new equation to estimate glomerular filtration rate'. In: *Annals of Internal Medicine* 150.9, pp. 35604–602.
Levey, Andrew S et al. (2007). 'Chronic Kidney Disease as a global public health problem: Approaches and initiatives – a position statement from Kidney Disease Improving Global Outcomes'. In: *Kidney International* 72.3, pp. 247–259.
Li, Laisheng et al. (2013a). 'MiR-34a inhibits proliferation and migration of breast cancer through down-regulation of Bcl-2 and SIRT1'. In: *Clinical and Experimental Medicine* 13.2, pp. 109–117.
Li, Qianbin et al. (2010). 'Discovery of 3-(2-aminoethyl)-5-(3-phenyl-propylidene)-thiazolidine-2,4-dione as a dual inhibitor of the Raf/MEK/ERK and the PI3K/Akt signaling pathways'. In: *Bioorganic and Medicinal Chemistry Letters* 20.15, pp. 4526–30.
Li, Rong et al. (2013b). 'The microRNA miR-433 promotes renal fibrosis by amplifying the TGF-β/Smad3-Azin1 pathway'. In: *Kidney International* 84.6, pp. 1129–1144.
Li, Xiaoduan and Xipeng Wang (2017). 'The emerging roles and therapeutic potential of exosomes in epithelial ovarian cancer'. In: *Molecular cancer* 16.1, p. 92.
Li, Xiaogang (2015). *Polycystic Kidney Disease*. Ed. by Xiaogang Li. Codon Publications, p. 514.

Liberzon, Arthur et al. (2011). 'Molecular signatures database (MSigDB) 3.0'. In: *Bioinformatics* 27.12, pp. 1739–1740.
Lichner, Zsuzsanna et al. (2015). 'miR-17 inhibition enhances the formation of kidney cancer spheres with stem cell/ tumor initiating cell properties'. In: *Oncotarget* 6.8, pp. 5567–81.
Lin, Chun-Liang et al. (2014). 'MicroRNA-29a promotion of nephrin acetylation ameliorates hyperglycemia induced podocyte dysfunction'. In: *Journal of the American Society of Nephrology* 25.8, pp. 1698–709.
Littler, Dene R et al. (2010). 'The enigma of the CLIC proteins: Ion channels, redox proteins, enzymes, scaffolding proteins?' In: *FEBS Letters* 584.10, pp. 2093–2101.
Liu, Gang et al. (2010). 'miR-21 mediates fibrogenic activation of pulmonary fibroblasts and lung fibrosis'. In: *Journal of Experimental Medicine* 207.8, pp. 1589–1597.
Liu, Haoming et al. (2016). 'HP1BP3, a chromatin retention factor for co-transcriptional microRNA processing'. In: *Molecular Cell* 63.3, pp. 420–432.
Livak, Kenneth J and Thomas D Schmittgen (2001). 'Analysis of relative gene expression data using real-time quantitative PCR and the 2-DDCt method'. In: *Methods* 25, pp. 402–408.
Livshts, Mikhail A et al. (2015). 'Isolation of exosomes by differential centrifugation: Theoretical analysis of a commonly used protocol'. In: *Scientific Reports* 5.May, p. 17319.
Llave, Cesar et al. (2002). 'Cleavage of Scarecrow-like mRNA targets directed by a class of Arabidopsis miRNA'. In: *Science* 297.5589, pp. 2053–2056.
Loghman-Adham, Mahmoud et al. (2004). 'The intrarenal renin-angiotensin system in Autosomal Dominant Polycystic Kidney Disease'. In: *American Journal of Physiology - Renal Physiology* 287.4, F775–F788.
Loher, Phillipe and Isidore Rigoutsos (2012). 'Interactive exploration of RNA22 microRNA target predictions'. In: *Bioinformatics* 28.24, pp. 3322–3323.
Long, Jianyin et al. (2010). 'Identification of microRNA-93 as a novel regulator of vascular endothelial growth factor in hyperglycemic conditions'. In: *Journal of Biological Chemistry* 285.30, pp. 23457–23465.
— (2011). 'MicroRNA-29c is a signature MicroRNA under high glucose conditions that targets sprouty homolog 1, and its in vivo knockdown prevents progression of diabetic nephropathy'. In: *Journal of Biological Chemistry* 286.13, pp. 11837–11848.
López-Hernández, Francisco J. and Jose M. López-Novoa (2012). 'Role of TGF-β in chronic kidney disease: An integration of tubular, glomerular and vascular effects'. In: *Cell and Tissue Research* 347.1, pp. 141–154.
Low, Seng Hui et al. (2006). 'Polycystin-1, STAT6, and P100 function in a pathway that transduces ciliary mechanosensation and is activated in Polycystic Kidney Disease'. In: *Developmental Cell* 10.1, pp. 57–69.
Lund, Elsebet et al. (2004). 'Nuclear export of microRNA precursors'. In: *Science* 303.5654, pp. 95–98.
Ma, Li et al. (2005). 'Phosphorylation and functional inactivation of TSC2 by Erk: Implications for tuberous sclerosis and cancer pathogenesis'. In: *Cell* 121.2, pp. 179–193.
Ma, Xiaoju Max and John Blenis (2009). 'Molecular mechanisms of mTOR-mediated translational control'. In: *Nature Reviews Molecular Cell Biology* 10, pp. 307–318.
Ma, Xiumei and Yongrui Bai (2012). 'IGF-1 activates the PI3K/AKT signaling pathway via upregulation of secretory clusterin'. In: *Molecular Medicine Reports* 6.6, pp. 1433–1437.
MacRae, Ian J, Kaihong Zhou and Jennifer A Doudna (2007). 'Structural determinants of RNA recognition and cleavage by Dicer'. In: *Nature Structural and Molecular Biology* 14.10, pp. 934–940.
MacRae, Ian J et al. (2008). 'In vitro reconstitution of the human RISC-loading complex'. In: *Proceedings of the National Academy of Sciences* 105.2, pp. 512–517.
MacRae, Ian et al. (2006). 'Structural Basis for Double-Stranded RNA Processing by Dicer'. In: *Science* 311.5758, pp. 195–198.
Magayr, Tajdida (2017). 'Identification of new biomarkers for disease progression in Autosomal Dominant Polycystic Kidney Disease'. PhD thesis. University of Sheffield.
Maillot, Gerard et al. (2009). 'Widespread estrogen-dependent repression of microRNAs involved in breast tumor cell growth'. In: *Cancer Research* 69.21, pp. 8332–8340.
Malanga, Donatella et al. (2008). 'Activating E17K mutation in the gene encoding the protein kinase AKT1 in a subset of squamous cell carcinoma of the lung'. In: *Cell Cycle* 7.5, pp. 665–669.
Malas, Tareq B et al. (2017). 'Meta-analysis of Polycystic Kidney Disease expression profiles defines strong involvement of injury repair processes'. In: *American Journal of Physiology - Renal Physiology* 312, F806–F817.

Malhas, Ashraf N, Ramadan A Abuknesha and Robert G Price (2002). 'Interaction of the leucine-rich repeats of polycystin-1 with extracellular matrix proteins: possible role in cell proliferation'. In: *Journal of the American Society of Nephrology* 13.1, pp. 19–26.

Mandelker, Diana et al. (2009). 'A frequent kinase domain mutation that changes the interaction between PI3Kα and the membrane.' In: *Proceedings of the National Academy of Sciences* 106.40, pp. 16996–7001.

Mangolini, Alessandra et al. (2016). 'Role of calcium in Polycystic Kidney Disease: From signaling to pathology'. In: *World Journal of Nephrology* 5.1, pp. 76–83.

Mao, Zhiguo, Guoqiang Xie and Albert C M Ong (2014). 'Metabolic abnormalities in Autosomal Dominant Polycystic Kidney Disease'. In: *Nephrology Dialysis Transplantation*, pp. 1–7.

Marais, Richard, Judy Wynne and Richard Treisman (1993). 'The SRF accessory protein Elk-1 contains a growth factor-regulated transcriptional activation domain'. In: *Cell* 73.2, pp. 381–393.

Marais, Richard et al. (1995). 'Ras recruits Raf-1 to the plasma membrane for activation by tyrosine phosphorylation'. In: *EMBO Journal* 1413.13, pp. 3136–3145.

Margolis, B and E Y Skolnik (1994). 'Activation of Ras by receptor tyrosine kinases.' In: *Journal of the American Society of Nephrology* 5.6, pp. 1288–1299.

Marioni, John C et al. (2008). 'RNA-seq : An assessment of technical reproducibility and comparison with gene expression arrays'. In: pp. 1509–1517.

Maroni, Paola et al. (2017). 'In bone metastasis miR-34a-5p absence inversely correlates with Met expression, while Met oncogene is unaffected by miR-34a-5p in non-metastatic and metastatic breast carcinomas'. In: *Carcinogenesis* 38.5, pp. 492–503.

Marsico, Annalisa et al. (2013). 'PROmiRNA: a new miRNA promoter recognition method uncovers the complex regulation of intronic miRNAs'. In: *Genome Biology* 97.1, pp. 1–6.

Marson, Alexander et al. (2008). 'Connecting microRNA genes to the core transcriptional regulatory circuitry of embryonic stem cells'. In: *Cell* 134.3, pp. 521–533.

Martello, Graziano et al. (2010). 'A microRNA targeting dicer for metastasis control'. In: *Cell* 141.7, pp. 1195–1207.

Martin, Elizabeth C. et al. (2012). 'Insulin-like growth factor-1 signaling regulates miRNA expression in MCF-7 breast cancer cell line'. In: *PLoS ONE* 7.11, pp. 3–8.

Martinez-Castelao, Alberto et al. (2014). 'Consensus document for the detection and management of Chronic Kidney Disease'. In: *Aten Primaria* 46.9, pp. 501–519.

Mathews, David H et al. (1999). 'Expanded sequence dependence of thermodynamic parameters improves prediction of RNA secondary structure.' In: *Journal of Molecular Biology* 288.5, pp. 911–40.

Mathonnet, Géraldine et al. (2007). 'MicroRNA inhibition of translation initiation in vitro by targeting the cap-binding complex eIF4F'. In: *Science* 317.5845, pp. 1764–1767.

Mathys, Hansruedi et al. (2014). 'Structural and Biochemical Insights to the Role of the CCR4-NOT Complex and DDX6 ATPase in MicroRNA Repression'. In: *Molecular Cell* 54.5, pp. 751–765.

Matsushita, Kunihiro et al. (2012). 'Comparison of risk prediction using the CKD-EPI equation and the MDRD study equation for estimated glomerular filtration rate'. In: *Journal of the American Medical Association* 307.18, pp. 1941–1951.

Mattiske, Sam et al. (2012). 'The oncogenic role of miR-155 in breast cancer'. In: *Cancer Epidemiology Biomarkers and Prevention* 21.8, pp. 1236–1243.

Mayo Clinic (2016). *Mayo Clinic - Chronic Kidney Disease*.

— (2017). *Mayo Clinic - Autosomal Dominant Polycystic Kidney Disease*.

McCain, Jack (2013). 'The MAPK (ERK) Pathway: Investigational Combinations for the Treatment Of BRAF-Mutated Metastatic Melanoma'. In: *Pharmacology and Therapeutics* 38.2, pp. 96–108.

McLendon, Roger et al. (2008). 'Comprehensive genomic characterization defines human glioblastoma genes and core pathways'. In: *Nature* 455.7216, pp. 1061–1068.

Meijer, Hedda A et al. (2013). 'Translational Repression and eIF4A2 Activity Are Critical for MicroRNA-Mediated Gene Regulation'. In: *Science* 340.April, pp. 82–85.

Meister, Gunter et al. (2004). 'Human Argonaute2 mediates RNA cleavage targeted by miRNAs and siRNAs'. In: *Molecular Cell* 15.2, pp. 185–197.

Melo, Sonia A. et al. (2010). 'A genetic defect in exportin-5 traps precursor MicroRNAs in the nucleus of cancer cells'. In: *Cancer Cell* 18.4, pp. 303–315.

Mendell, Joshua T (2008). 'miRiad Roles for the miR-17-92 Cluster in Development and Disease'. In: *Cell* 133.2, pp. 217–222.

Mendoza, Michelle C, E. Emrah Er and John Blenis (2011). 'The Ras-ERK and PI3K-mTOR pathways: Cross-talk and compensation'. In: *Trends in Biochemical Sciences* 36.6, pp. 320–328.

Menezes, Luis F et al. (2012). 'Network analysis of a Pkd1-mouse model of Autosomal Dominant Polycystic Kidney Diseaseidentifies HNF4α as a disease modifier'. In: *PLoS Genetics* 8.11, pp. 1–14.

Menezes, Luis F et al. (2016). 'Fatty acid oxidation is impaired in an orthologous mouse model of Autosomal Dominant Polycystic Kidney Disease'. In: *EBioMedicine* 5, pp. 183–92.
Merritt, William M et al. (2008). 'Dicer, Drosha and Outcomes in patients with ovarian cancer'. In: *New England Journal of Medicine* 359.25, pp. 2641–2650.
Metzner, Aylin (2016). 'A study of ADPKD pathogenesis and treatment in zebrafish models'. PhD thesis. University of Sheffield.
Meyer, Swanhild U et al. (2015). 'TNF-α and IGF1 modify the microRNA signature in skeletal muscle cell differentiation'. In: *Cell Communication and Signaling* 13.1, p. 4.
Misso, Gabriella et al. (2014). 'Mir-34: a new weapon against cancer?' In: *Molecular Therapy - Nucleic Acids* 3.9, e194.
Moelling, Karin et al. (2002). 'Regulation of Raf-Akt cross-talk'. In: *Journal of Biological Chemistry* 277.34, pp. 31099–31106.
Molina, Kimberley and Vincent DiMaio (2012). 'Normal organ weights in men: Part II—the brain, lungs, liver, spleen, and kidneys'. In: *American Journal of Forensic Medicine & Pathology* 33.4, pp. 368–372.
Monteys, Alex Mas et al. (2010). 'Structure and activity of putative intronic miRNA promoters.' In: *RNA* 16.3, pp. 495–505.
Mora, Alfonso et al. (2004). 'PDK1, the master regulator of AGC kinase signal transduction'. In: *Seminars in Cell and Developmental Biology* 15.2, pp. 161–170.
Morrison, Deborah K et al. (1993). 'Identification of the major phosphorylation sites of the Raf-1 kinase'. In: *Journal of Biological Chemistry* 268.23, pp. 17309–17316.
Mount, David B (2014). 'Thick ascending limb of the loop of henle'. In: *Clinical Journal of the American Society of Nephrology* 9.11, pp. 1974–1986.
Moura, Joao, Elisabet Borsheim and Eugenia Carvalho (2014). 'The role of micrornas in diabetic complications—special emphasis on wound healing'. In: *Genes* 5.4, pp. 926–956.
Mullany, Lila E. et al. (2016). 'MicroRNA seed region length impact on target messenger RNA expression and survival in colorectal cancer'. In: *PloS one* 11.4, e0154177.
Murphy, Leon O et al. (2002). 'Molecular interpretation of ERK signal duration by immediate early gene products'. In: *Nature Cell Biology* 4.8, pp. 556–564.
Nagalakshmi, Vidya K et al. (2011). 'Dicer regulates the development of nephrogenic and ureteric compartments in the mammalian kidney'. In: *Kidney international* 79.3, pp. 317–330.
Nair, Jayaprakash K et al. (2014). 'Multivalent N -acetylgalactosamine-conjugated siRNA localizes in hepatocytes and elicits robust RNAi-mediated gene silencing'. In: *Journal of the American Chemical Society* 136.49, pp. 16958–16961.
Nam, Yunsun et al. (2012). 'Molecular basis for interaction of let-7 microRNAs with Lin28'. In: *Cell* 147.5, p. 1091.
Namkung, Wan et al. (2010). 'Inhibition of Ca2+-activated Cl- channels by gallotannins as a possible molecular basis for health benefits of red wine and green tea'. In: *FASEB Journal* 24.11, pp. 4178–4186.
Nature Education (2017). *Nature Glossary - Microarray*.
Nauli, Surya M et al. (2003). 'Polycystins 1 and 2 mediate mechanosensation in the primary cilium of kidney cells'. In: *Nature Genetics* 33, pp. 129–137.
Nauli, Surya M et al. (2008). 'Endothelial cilia are fluid shear sensors that regulate calcium signaling and nitric oxide production through polycystin-1'. In: *Circulation* 117.9, pp. 1161–1171.
New England Biolabs (2017). *NEB website - RNA-seq*.
Newby, Linda J et al. (2002). 'Identification, characterization, and localization of a novel kidney polycystin-1-polycystin-2 complex'. In: *Journal of Biological Chemistry* 277.23, pp. 20763–20773.
NHS (2016a). *NHS - Autosomal Dominant Polycystic Kidney Disease*.
— (2016b). *NHS - Chronic Kidney Disease*.
Nishio, Saori et al. (2005). 'Pkd1 regulates immortalized proliferation of renal tubular epithelial cells through p53 induction and JNK activation'. In: *Journal of Clinical Investigation* 115.4, pp. 910–918.
NKF (2002). *K/DOQI clinical practice guidelines for Chronic Kidney Disease: evaluation, classification and stratification*. Vol. 39, S1–S266.
Norman, Jill (2011). 'Fibrosis and progression of Autosomal Dominant Polycystic Kidney Disease (ADPKD)'. In: *Biochimica et Biophysica Acta - Molecular Basis of Disease* 1812.10, pp. 1327–1336.
Novalic, Zlata et al. (2012). 'Dose-dependent effects of sirolimus on mTOR signaling and polycystic kidney disease'. In: *Journal of the American Society of Nephrology* 23.5, pp. 842–53.
Nykänen, Antti, Benjamin Haley and Phillip D Zamore (2001). 'ATP requirements and small interfering RNA structure in the RNA interference pathway'. In: *Cell* 107.3, pp. 309–321.
O Donnell, Kathryn a et al. (2005). 'c-Myc-regulated microRNAs modulate E2F1 expression'. In: *Nature* 435.7043, pp. 839–43.

O' Meara, Caitlin C et al. (2012). 'Role of genetic modifiers in an orthologous rat model of ARPKD'. In: *Physiological Genomics* 44.15, pp. 741–753.
Ogawa, Yuko et al. (2011). 'Proteomic analysis of two types of exosomes in human whole saliva'. In: *Biological and Pharmaceutical Bulletin* 34.1, pp. 13–23.
Oh, Uhtaek and Jooyoung Jung (2016). 'Cellular functions of TMEM16/anoctamin'. In: *Pflugers Archiv European Journal of Physiology* 468.3, pp. 443–453.
Okada, Nobuhiro et al. (2014). 'A positive feedback between p53 and miR-34 miRNAs mediates tumor suppression'. In: *Genes and Development* 28.5, pp. 438–450.
Okamura, Katsutomo et al. (2007). 'The mirtron pathway generates microRNA-class regulatory RNAs in Drosophila'. In: *Cell* 130.1, pp. 89–100.
Olayioye, Monilola et al. (1999). 'ErbB Receptor-induced Activation of Stat Transcription Factors Is Mediated by Src Tyrosine Kinases'. In: *Journal of Biological Chemistry* 274.24, pp. 17209–17218.
Olivieri, Fabiola et al. (2013). 'Diagnostic potential of circulating miR-499-5p in elderly patients with acute non ST-elevation myocardial infarction'. In: *International Journal of Cardiology* 167.2, pp. 531–536.
Ong, Albert C M and Peter C Harris (2015). 'A polycystin-centric view of cyst formation and disease: the polycystins revisited'. In: *Kidney International* 88.4, pp. 699–710.
Orom, Ulf Andersson, Finn Cilius Nielsen and Anders H. Lund (2008). 'MicroRNA-10a binds the 5'UTR of ribosomal protein mRNAs and enhances their translation'. In: *Molecular Cell* 30.4, pp. 460–471.
Ouar, Zahia et al. (1998). 'Pleiotropic effects of dihydrotestosterone in immortalized mouse proximal tubule cells'. In: *Kidney International* 53.1, pp. 59–66.
Ousingsawat, Jiraporn et al. (2011). 'CFTR and TMEM16A are separate but functionally related Cl - channels'. In: *Cellular Physiology and Biochemistry* 28.4, pp. 715–724.
Outeda, Patricia et al. (2014). 'Polycystin signaling is required for directed endothelial cell migration and lymphatic development'. In: *Cell Reports* 7.3, pp. 634–644.
Ouyang, H et al. (2014). 'microRNA-10b enhances pancreatic cancer cell invasion by suppressing TIP30 expression and promoting EGF and TGF-β actions.' In: *Oncogene* 33.38, pp. 4664–74.
Pacold, Michael E et al. (2000). 'Crystal structure and functional analysis of Ras binding to its effector phosphoinositide 3-kinase gamma'. In: *Cell* 103.6, pp. 931–43.
Pandey, Priyanka et al. (2008). 'Microarray-based approach identifies microRNAs and their target functional patterns in Polycystic Kidney Disease'. In: *BMC genomics* 9, p. 624.
Pandey, Priyanka et al. (2011). 'Systems biology approach to identify transcriptome reprogramming and candidate microRNA targets during the progression of Polycystic Kidney Disease'. In: *BMC Systems Biology* 5.1, p. 56.
Paris, Ornella et al. (2012). 'Direct regulation of microRNA biogenesis and expression by estrogen receptor beta in hormone-responsive breast cancer'. In: *Oncogene* 31.38, pp. 4196–4206.
Park, Jong-Eun et al. (2011). 'Dicer recognizes the 5' end of RNA for efficient and accurate processing'. In: *Nature* 475.7355, pp. 201–205. arXiv: 15334406.
Park, Sun Mi et al. (2008). 'The miR-200 family determines the epithelial phenotype of cancer cells by targeting the E-cadherin repressors ZEB1 and ZEB2'. In: *Genes and Development* 22.7, pp. 894–907.
Parker, Emma et al. (2007). 'Hyperproliferation of PKD1 cystic cells is induced by insulin-like growth factor-1 activation of the Ras/Raf signalling system'. In: *Kidney International* 72.2, pp. 157–65.
Parnell, Stephen C et al. (1998). 'The polycystic kidney disease-1 protein, polycystin-1, binds and activates heterotrimeric G-proteins in vitro'. In: *Biochemical and biophysical research communications* 251.2, pp. 625–631.
Parnell, Stephen C et al. (2002). 'Polycystin-1 activation of c-Jun N-terminal kinase and AP-1 is mediated by heterotrimeric G proteins'. In: *Journal of Biological Chemistry* 277.22, pp. 19566–19572.
Paroo, Zain et al. (2009). 'Phosphorylation of the human microRNA-generating complex mediates MAPK/Erk signaling'. In: *Cell* 139.1, pp. 112–122.
Patel, Vishal et al. (2012). 'MicroRNAs regulate renal tubule maturation through modulation of Pkd1'. In: *Journal of the American Society of Nephrology* 23.12, pp. 1941–8.
Patel, Vishal et al. (2013). 'miR-17-92 miRNA cluster promotes kidney cyst growth in Polycystic Kidney Disease'. In: *Proceedings of the National Academy of Sciences* 110.26, pp. 10765–10770.
Paul, Binu M et al. (2014). 'Evidence of a third ADPKD locus is not supported by re-analysis of designated PKD3 families'. In: *Kidney international* 85.2, pp. 383–92.
Pazour, Gregory J., Curtis G. Wilkerson and George B. Witman (1998). 'A dynein light chain is essential for the retrograde particle movement of intraflagellar transport (IFT)'. In: *Journal of Cell Biology* 141.4, pp. 979–992.
Pedersen, Irene M et al. (2007). 'Interferon modulation of cellular microRNAs as an antiviral mechanism'. In: *Nature* 449.7164, pp. 919–922.

Pei, York (2001). 'A "two-hit" model of cystogenesis in Autosomal Dominant Polycystic Kidney Disease?' In: *Trends in Molecular Medicine* 7.4, pp. 151–6.
— (2006). 'Diagnostic approach in Autosomal Dominant Polycystic Kidney Disease'. In: *Clinical Journal of the American Society of Nephrology* 1.5, pp. 1108–1114.
Pei, York et al. (1999). 'Somatic PKD2 mutations in individual kidney and liver cysts support a "two-hit" model of cystogenesis in type 2 Autosomal Dominant Polycystic Kidney Disease'. In: *Journal of the American Society of Nephrology* 10.7, pp. 1524–1529.
Pei, York et al. (2009). 'Unified criteria for ultrasonographic diagnosis of ADPKD'. In: *Journal of the American Society of Nephrology* 20.1, pp. 205–212.
Pema, Monika et al. (2016). 'mTORC1-mediated inhibition of polycystin-1 expression drives renal cyst formation in tuberous sclerosis complex.' In: *Nature Communications* 7, p. 10786.
Peng, Tao et al. (2016). 'MIR-506 functions as a tumor suppressor in glioma by targeting STAT3'. In: *Oncology Reports* 35.2, pp. 1057–1064.
Peral, Belen et al. (1996). 'A stable, nonsense mutation associated with a case of infantile onset polycystic kidney disease 1 (PKD1)'. In: *Human Molecular Genetics* 5.4, pp. 539–542.
Perico, Norberto and Giuseppe Remuzzi (2012). 'Chronic Kidney Disease: A research and public health priority'. In: *Nephrology Dialysis Transplantation* 27.
Persu, Alexandre et al. (2004). 'Comparison between siblings and twins supports a role for modifier genes in ADPKD'. In: *Kidney International* 66.6, pp. 2132–2136.
Pham, John W et al. (2004). 'A Dicer-2-dependent 80S complex cleaves targeted mRNAs during RNAi in Drosophila'. In: *Cell* 117.1, pp. 83–94.
Philp, Amanda J et al. (2001). 'The phosphatidylinositol 3'-kinase p85α gene is an oncogene in human ovarian and colon tumors.' In: *Cancer research* 61.20, pp. 7426–7429.
Piazzon, Nathalie et al. (2012). 'Bicc1 links the regulation of cAMP signaling in polycystic kidneys to microRNA-induced gene silencing'. In: *Journal of Molecular Cell Biology* 4.6, pp. 398–408.
Pierchala, Brian a (2010). 'Proteomic analysis of the slit diaphragm complex: CLIC5 is a protein critical for podocyte morphology and function'. In: *Kidney International* 78, pp. 868–882.
Pillai, Ramesh S et al. (2005). 'Inhibition of translational initiation by Let-7 MicroRNA in human cells'. In: *Science* 309.5740, pp. 1573–1576.
Piontek, Klaus et al. (2007). 'A critical developmental switch defines the kinetics of kidney cyst formation after loss of Pkd1'. In: *Nature Medicine* 13.12, pp. 1490–1495.
Pirson, Yves, J L Christophe and E Goffin (1996). 'Outcome of renal replacement therapy in Autosomal Dominant Polycystic Kidney Disease'. In: *Nephrology Dialysis Transplantation* 11 Suppl 6, pp. 24–8.
Pisitkun, Trairak, Rong-Fong Shen and Mark A. Knepper (2004). 'Identification and proteomic profiling of exosomes in human urine'. In: *Proceedings of the National Academy of Sciences* 101.36, pp. 13368–73.
Podsypanina, Katrina et al. (1999). 'Mutation of Pten/Mmac1 in mice causes neoplasia in multiple organ systems'. In: *Proceedings of the National Academy of Sciences* 96.4, pp. 1563–1568.
Ponticelli, Claudio and Francesco Locatelli (2010). 'Autosomal Dominant Polycystic Kidney Disease and mTOR inhibitors: the narrow road between hope and disappointment'. In: *Nephrology Dialysis Transplantation* 25.12, pp. 3809–3812.
Ponting, C P, K Hofmann and Peer Bork (1999). 'A latrophilin/CL-1-like GPS domain in polycystin-1'. In: *Current biology* 9.16, R585–R588.
Porath, Binu et al. (2016). 'Mutations in GANAB, encoding the glucosidase II a subunit, cause Autosomal-Dominant Polycystic Kidney and Liver Disease'. In: *American Journal of Human Genetics* 98, pp. 1193–1207.
Poy, Matthew N et al. (2004). 'A pancreatic islet-specific microRNA regulates insulin secretion.' In: *Nature* 432.November, pp. 226–230.
Poy, Matthew N et al. (2009). 'miR-375 maintains normal pancreatic alpha- and beta-cell mass'. In: *Proceedings of the National Academy of Sciences* 106.14, pp. 5813–5818.
Pumiglia, Kevin et al. (1995). 'Raf-1 N-terminal sequences necessary for Ras-Raf interaction and signal transduction'. In: *Molecular and cellular biology* 15.1, pp. 398–406.
Putta, Sumanth et al. (2012). 'Inhibiting microRNA-192 ameliorates renal fibrosis in diabetic nephropathy'. In: *Journal of the American Society of Nephrology* 23.3, pp. 458–469.
Pyronnet, Stéphane et al. (2008). 'Antitumor effects of somatostatin'. In: *Molecular and Cellular Endocrinology* 286.1-2, pp. 230–237.
Qi, Hank H et al. (2008). 'Prolyl 4-hydroxylation regulates Argonaute 2 stability'. In: *Nature* 455.7211, pp. 421–424.
Qian, Feng et al. (1996). 'The molecular basis of focal cyst formation in human Autosomal Dominant Polycystic Kidney Disease type I'. In: *Cell* 87.6, pp. 979–987.

Qian, Feng et al. (2002). 'Cleavage of polycystin-1 requires the receptor for egg jelly domain and is disrupted by Autosomal-Dominant Polycystic Kidney Disease 1-associated mutations'. In: *Proceedings of the National Academy of Sciences* 99.26, pp. 16981–16986.

Qian, Feng et al. (2005). 'The nanomechanics of polycystin-1 extracellular region'. In: *Journal of Biological Chemistry* 280.49, pp. 40723–40730.

Qin, Shan et al. (2012). 'c-Met and NF-\(\kappa\)B-dependent overexpression of Wnt7a and -7b and Pax2 promotes cystogenesis in Polycystic Kidney Disease'. In: *Journal of the American Society of Nephrology* 23.8, pp. 1309–1318.

Qin, Wei et al. (2011). 'TGF-β/Smad3 Signaling Promotes Renal Fibrosis by Inhibiting miR-29'. In: *Journal of the American Society of Nephrology* 22.8, pp. 1462–1474.

Quévillon Huberdeau, Miguel et al. (2017). 'Phosphorylation of Argonaute proteins affects mRNA binding and is essential for microRNA-guided gene silencing in vivo'. In: *EMBO Journal* 36.14, e201696386.

Quick-Cleveland, Jen et al. (2014). 'The DGCR8 RNA-binding heme domain recognizes primary microRNAs by clamping the hairpin'. In: *Cell Reports* 7.6, pp. 1994–2005.

Quinkler, Marcus et al. (2005). 'Androgen receptor-mediated regulation of the alpha-subunit of the epithelial sodium channel in human kidney'. In: *Hypertension* 46.4, pp. 787–798.

Ragelle, Heloise, Gaelle Vandermeulen and Veronique Preat (2013). 'Chitosan-based siRNA delivery systems'. In: *Journal of Controlled Release* 172.1, pp. 207–218.

Rand, Tim A. et al. (2005). 'Argonaute2 cleaves the anti-guide strand of siRNA during RISC activation'. In: *Cell* 123.4, pp. 621–629.

Raphael, Kalani L et al. (2009). 'Inactivation of Pkd1 in principal cells causes a more severe cystic kidney disease than in intercalated cells'. In: *Kidney International* 75.6, pp. 626–633.

Raposo, Graca et al. (1996). 'B lymphocytes secrete antigen-presenting vesicles'. In: *Journal of Experimental Medicine* 183, pp. 1161–1172.

Raver-Shapira, Nina et al. (2007). 'Transcriptional Activation of miR-34a Contributes to p53-Mediated Apoptosis'. In: *Molecular Cell* 26.5, pp. 731–743.

Ravichandran, Kameswaran et al. (2014). 'An mTOR anti-sense oligonucleotide decreases polycystic kidney disease in mice with a targeted mutation in Pkd2'. In: *Human Molecular Genetics* 23.18, pp. 4919–4931.

Ravine, David et al. (1994). 'Evaluation of ultrasonographic diagnostic criteria for autosomal dominant polycystic kidney disease 1'. In: *Lancet* 343.8901, pp. 824–827.

Reed, Berenice Y et al. (2008). 'Variation in age at ESRD in Autosomal Dominant Polycystic Kidney Disease'. In: *American Journal of Kidney Diseases* 51.2, pp. 173–183.

Rehwinkel, Jan et al. (2005). 'miRNA-mediated gene silencing A crucial role for GW182 and the DCP1 : DCP2 decapping complex in miRNA-mediated gene silencing'. In: *RNA* 11, pp. 1640–1647.

Remenyi, Judit et al. (2016). 'The loop structure and the RNA helicase p72/DDX17 influence the processing efficiency of the mice miR-132'. In: *Scientific Reports* 6.February, p. 22848.

Ren, Dong et al. (2017). 'Oncogenic miR-210-3p promotes prostate cancer cell EMT and bone metastasis via NF-κB signaling pathway'. In: *Molecular Cancer* 16.1, p. 117.

Reusch, H. Peter et al. (2001). 'Regulation of Raf by Akt controls growth and differentiation in vascular smooth muscle cells'. In: *Journal of Biological Chemistry* 276.36, pp. 33630–33637.

Ribas, Judit et al. (2009). 'miR-21: An androgen receptor-regulated microRNA that promotes hormone-dependent and hormone-independent prostate cancer growth'. In: *Cancer Research* 69.18, pp. 7165–7169.

Riegersperger, Markus et al. (2015). 'Pulsed oral sirolimus in advanced autosomal-dominant polycystic kidney disease (Vienna RAP Study): study protocol for a randomized controlled trial'. In: *Trials* 16.1, p. 182.

Riffo-Campos, Ángela L., Ismael Riquelme and Priscilla Brebi-Mieville (2016). 'Tools for sequence-based miRNA target prediction: What to choose?' In: *International Journal of Molecular Sciences* 17.12.

Ro, Seungil et al. (2007). 'Tissue-dependent paired expression of miRNAs'. In: *Nucleic Acids Research* 35.17, pp. 5944–5953.

Rodriguez-Viciana, Pablo et al. (1996). 'Activation of phosphoinositide 3-kinase by interaction with Ras and by point mutation'. In: *EMBO Journal* 15.10, pp. 2442–2451.

Romaine, Simon P R et al. (2015). 'MicroRNAs in cardiovascular disease: an introduction for clinicians'. In: *Heart (British Cardiac Society)* 101.12, pp. 921–8.

Rossetti, Sandro et al. (2001). 'Mutation analysis of the entire PKD1 gene: genetic and diagnostic implications'. In: *American Journal of Human Genetics* 68.1, pp. 46–63.

Roth, Carina et al. (2011). 'Screening for circulating nucleic acids and caspase activity in the peripheral blood as potential diagnostic tools in lung cancer'. In: *Molecular Oncology* 5.3, pp. 281–291.

Roush, Sarah and Frank J Slack (2008). 'The let-7 family of microRNAs'. In: *Trends in Cell Biology* 18.10, pp. 505–516.
Roux, Philippe P et al. (2004). 'Tumor-promoting phorbol esters and activated Ras inactivate the tuberous sclerosis tumor suppressor complex via p90 ribosomal S6 kinase.' In: *Proceedings of the National Academy of Sciences* 101.37, pp. 13489–94.
Rouya, Christopher et al. (2014). 'Human DDX6 effects miRNA-mediated gene silencing via direct binding to CNOT1'. In: *RNA* 20.9, pp. 1398–1409.
Rowe, Isaline et al. (2013). 'Defective glucose metabolism in Polycystic Kidney Disease identifies a new therapeutic strategy'. In: *Nature Medicine* 19.4, pp. 488–93.
Ruby, J Graham, Calvin H Jan and David P Bartel (2007). 'Intronic microRNA precursors that bypass Drosha processing'. In: *Nature* 448.7149, pp. 83–86.
Ruggenenti, Piero et al. (2005). 'Safety and efficacy of long-acting somatostatin treatment in Autosomal Dominant Polycystic Kidney Disease'. In: *Kidney International* 68.1, pp. 206–216.
Ruggenenti, Piero et al. (2016). 'Effect of Sirolimus on disease progression in patients with Autosomal Dominant Polycystic Kidney Disease and CKD stages 3b-4'. In: *Clinical Journal of the American Society of Nephrology*, pp. 785–794.
Rul, Wilfrid et al. (2002). 'Activation of ERK, controlled by Rac1 and Cdc42 via Akt, is required for anoikis'. In: *Annals of the New York Academy of Sciences* 973, pp. 145–148.
Rundle, Dana R, Gary Gorbsky and Leonidas Tsiokas (2004). 'PKD2 interacts and co-localizes with mDia1 to mitotic spindles of dividing cells: role of mDia1 IN PKD2 localization to mitotic spindles'. In: *Journal of Biological Chemistry* 279.28, pp. 29728–29739.
Rupaimoole, Rajesha and Frank J. Slack (2017). 'MicroRNA therapeutics: towards a new era for the management of cancer and other diseases'. In: *Nature Reviews Drug Discovery* 16.3, pp. 203–221.
Rupaimoole, Rajesha et al. (2016). 'Hypoxia-upregulated microRNA-630 targets Dicer, leading to increased tumor progression'. In: *Oncogene* April 2015, pp. 1–9.
Saigusa, Takamitsu and P. D. Bell (2015). 'Molecular pathways and therapies in Autosomal-Dominant Polycystic Kidney Disease'. In: *Physiology* 30.3, pp. 195–207.
Saini, Sharanjot et al. (2011). 'MicroRNA-708 induces apoptosis and suppresses tumorigenicity in renal cancer cells'. In: *Cancer Research* 71.19, pp. 6208–6219.
Salvadori, Maurizio and Aris Tsalouchos (2017). 'New therapies targeting cystogenesis in Autosomal Dominant Polycystic Kidney Disease'. In: *European Medical Journal* July, pp. 102–111.
Salzman, David W., Jonathan Shubert-Coleman and Henry Furneaux (2007). 'P68 RNA helicase unwinds the human let-7 microRNA precursor duplex and is required for let-7-directed silencing of gene expression'. In: *Journal of Biological Chemistry* 282.45, pp. 32773–32779.
Sammels, Eva et al. (2010). 'Polycystin-2 activation by inositol 1,4,5-trisphosphate-induced Ca2+ release requires its direct association with the inositol 1,4,5-trisphosphate receptor in a signaling microdomain'. In: *Journal of Biological Chemistry* 285.24, pp. 18794–18805.
Samuels, Yardena and Kajsa Ericson (2006). 'Oncogenic PI3K and its role in cancer'. In: *Current Opinion in Oncology* 18.1, pp. 77–82.
Sarbassov, Dos D et al. (2005). 'Phosphorylation and regulation of Akt/PKB by the rictor-mTOR complex'. In: *Science* 307.5712, pp. 1098–1101.
Scacheri, Peter C et al. (2004). 'Short interfering RNAs can induce unexpected and divergent changes in the levels of untargeted proteins in mammalian cells.' In: *Proceedings of the National Academy of Sciences* 101.7, pp. 1892–1897.
Schertel, Claus et al. (2012). 'Functional characterization of Drosophila microRNAs by a novel in vivo library'. In: *Genetics* 192.4, pp. 1543–1552.
Schieren, Gisela et al. (2006). 'Gene profiling of polycystic kidneys'. In: *Nephrology Dialysis Transplantation* 21.7, pp. 1816–1824.
Schirle, Nicole T and Ian J MacRae (2012). 'The crystal structure of human Argonaute2'. In: *Science* 86.3, pp. 514–535.
Schmidt, Hartmut (2012). 'Three functional facets of calbindin D-28k'. In: *Frontiers in Molecular Neuroscience* 5.March, pp. 1–7.
Schrier, Robert W et al. (2014). 'Blood pressure in early Autosomal Dominant Polycystic Kidney Disease'. In: *New England Journal of Medicine* 371.24, pp. 2255–66.
Schwarz, Dianne S et al. (2003). 'Asymmetry in the assembly of the RNAi enzyme complex'. In: *Cell* 115.2, pp. 199–208.
Sears, Rosalie et al. (2000). 'Multiple Ras-dependent phosphorylation pathways regulate Myc protein stability'. In: *Genes and Development* 14.19, pp. 2501–2514.
Seco, Celia Zazo et al. (2015). 'Progressive hearing loss and vestibular dysfunction caused by a homozygous nonsense mutation in CLIC5'. In: *European Journal of Human Genetics* 23.23, pp. 189–194.

Selistre, Luciano et al. (2012). 'Early renal abnormalities in children with postnatally diagnosed Autosomal Dominant Polycystic Kidney Disease'. In: *Pediatric nephrology* 27.9, pp. 1589–1593.
Sepramaniam, Sugunavathi et al. (2010). 'MicroRNA 320a functions as a novel endogenous modulator of aquaporins 1 and 4 as well as a potential therapeutic target in cerebral ischemia'. In: *Journal of Biological Chemistry* 285.38, pp. 29223–29230.
Serino, Grazia et al. (2012). 'Abnormal miR-148b expression promotes aberrant glycosylation of IgA1 in IgA nephropathy'. In: *Journal of the American Society of Nephrology* 23.5, pp. 814–24.
Serra, Andreas L et al. (2010). 'Sirolimus and kidney growth in Autosomal Dominant Polycystic Kidney Disease'. In: *New England Journal of Medicine* 363.9, pp. 820–829.
Shan, Zhi Xin et al. (2010). 'MiR-1/miR-206 regulate Hsp60 expression contributing to glucose-mediated apoptosis in cardiomyocytes'. In: *FEBS Letters* 584.16, pp. 3592–3600.
Shanmugam, Narkunaraja, Marpadga A. Reddy and Rama Natarajan (2008). 'Distinct roles of heterogeneous nuclear ribonuclear protein K and microRNA-16 in cyclooxygenase-2 RNA stability induced by S100b, a ligand of the receptor for advanced glycation end products'. In: *Journal of Biological Chemistry* 283.52, pp. 36221–36233.
Shapiro, Paul S and Natalie G Ahn (1998). 'Feedback Regulation of Raf-1 and Mitogen-activated Protein Kinase (MAP) Feedback Regulation of Raf-1 and Mitogen-activated Protein Kinase (MAP) Kinase Kinases 1 and 2 by MAP Kinase'. In: *Journal of Biological Chemistry* 1.3, pp. 1788–1793.
She, Qing Bai et al. (2005). 'The BAD protein integrates survival signaling by EGFR/MAPK and PI3K/Akt kinase pathways in PTEN-deficient tumor cells'. In: *Cancer Cell* 8.4, pp. 287–297.
Shen, Jia et al. (2013). 'EGFR modulates microRNA maturation in response to hypoxia through phosphorylation of AGO2'. In: *Nature* 497.7449, pp. 383–387.
Shen, Peter S et al. (2016). 'The structure of the Polycystic Kidney Disease channel PKD2 in lipid nanodiscs'. In: *Cell* 167.3, 763–773.e11.
Sheppard, Karen E. et al. (2013). 'Synergistic inhibition of ovarian cancer cell growth by combining selective PI3K/mTOR and RAS/ERK pathway inhibitors'. In: *European Journal of Cancer* 49.18, pp. 3936–3944.
Shillingford, Jonathan M et al. (2006). 'The mTOR pathway is regulated by polycystin-1, and its inhibition reverses renal cystogenesis in polycystic kidney disease'. In: *Proceedings of the National Academy of Sciences* 103.14, pp. 1–6.
Si, Min-Liang et al. (2007). 'miR-21-mediated tumor growth'. In: *Oncogene* 26.19, pp. 2799–2803.
Simpson, Kate et al. (2016). 'MicroRNAs in diabetic nephropathy: from biomarkers to therapy'. In: *Current Diabetes Reports* 16.3, pp. 1–7.
Singh, Harpreet, Michael A Cousin and Richard H Ashley (2007). 'Functional reconstitution of mammalian 'chloride intracellular channels' CLIC1, CLIC4 and CLIC5 reveals differential regulation by cytoskeletal actin'. In: *FEBS Journal* 274, pp. 6306–6316.
Singla, Veena and Jeremy F Reiter (2006). 'The primary cilium as the cell's antenna: signaling at a sensory organelle'. In: *Science* 313.5787, pp. 629–633.
Sîrbu, Alina et al. (2012). 'RNA-seq vs dual- and single-channel microarray data: sensitivity analysis for differential expression and clustering'. In: *PLoS ONE* 7.12.
Sivaprasad, Usha et al. (2004). 'Stimulation of Insulin-Like Growth Factor (IGF) binding protein-3 synthesis by IGF-I and transforming growth factor-alpha is mediated by both phosphatidylinositol-3 kinase and mitogen-activated protein kinase pathways in mammary epithelial cells'. In: *Endocrinology* 145.9, pp. 4213–4221.
Smibert, Peter et al. (2013). 'Homeostatic control of Argonaute stability by microRNA availability.' In: *Nature Structural and Molecular Biology* 20.7, pp. 789–95.
Snove, Jr O and Torgeir Holen (2004). 'Many commonly used siRNAs risk off-target activity'. In: *Biochemical and Biophysical Research Communications* 319.1, pp. 256–263.
Song, Xuewen et al. (2009). 'Systems biology of Autosomal Dominant Polycystic Kidney Disease (ADPKD): computational identification of gene expression pathways and integrated regulatory networks'. In: *Human Molecular Genetics* 18.13, pp. 2328–2343.
Stayner, Cherie et al. (2006). 'Pax2 gene dosage influences cystogenesis in Autosomal Dominant Polycystic Kidney Disease'. In: *Human Molecular Genetics* 15.24, pp. 3520–3528.
Stefano, George B (2014). 'Comparing bioinformatic gene expression profiling methods: microarray and RNA-seq'. In: *Medical Science Monitor Basic Research* 20, pp. 138–142.
Stephanis, Lucia de et al. (2017). 'Double inhibition of cAMP and mTOR signalling may potentiate the reduction of cell growth in ADPKD cells'. In: *Clinical and Experimental Nephrology* 21.2, pp. 203–211.
Stevens, Lesley A et al. (2006). 'Assessing kidney function — measured and estimated glomerular filtration rate'. In: *New England Journal of Medicine* 354.23, pp. 2473–2483.

Stewart, Alistair J et al. (1990). 'Role of Insulin-like Growth Factors and the Type I Insulin-like Growth Factor Receptor in the Estrogen-stimulated Proliferation Human Breast Cancer Cells *'. In: 265.34, pp. 21172–21178.

Streets, Andrew J et al. (2003). 'Functional Analysis of PKD1 Transgenic Lines Reveals a Direct Role for Polycystin-1 in Mediating Cell-Cell Adhesion'. In: *Journal of the American Society of Nephrology* 14.7, pp. 1804–1815.

Streets, Andrew J et al. (2006). 'Identification of an N-terminal glycogen synthase kinase 3 phosphorylation site which regulates the functional localization of polycystin-2 in vivo and in vitro'. In: *Human Molecular Genetics* 15.9, pp. 1465–1473.

Streets, Andrew J et al. (2009). 'Homophilic and heterophilic polycystin 1 interactions regulate E-cadherin recruitment and junction assembly in MDCK cells'. In: *Journal of Cell Science* 122.10, pp. 1702–1702.

Streets, Andrew J et al. (2013). 'Hyperphosphorylation of polycystin-2 at a critical residue in disease reveals an essential role for polycystin-1-regulated dephosphorylation'. In: *Human Molecular Genetics* 22.10, pp. 1924–1939.

Streets, Andrew J et al. (2017). 'Parallel microarray profiling identifies ErbB4 as a determinant of cyst growth in ADPKD and a prognostic biomarker for disease progression'. In: *American Journal of Physiology - Renal Physiology* 12, ajprenal.00607.2016.

Stringer, Kenneth D et al. (2005). 'Gender hormones and the progression of experimental polycystic kidney disease'. In: *Kidney International* 68.4, pp. 1729–1739.

Su, Hong et al. (2009). 'Essential and overlapping functions for mammalian argonautes in microRNA silencing'. In: *Genes and Development* 23.3, pp. 304–317.

Su, Xiaohua et al. (2010). 'TAp63 suppresses metastasis through coordinate regulation of Dicer and miRNA'. In: *Nature* 467.7318, pp. 986–990.

Subramanian, Aravind et al. (2005). 'Gene set enrichment analysis : A knowledge-based approach for interpreting genome-wide'. In: *Proceedings of the National Academy of Sciences* 102.43, pp. 15545–15550.

Subramanya, Arohan R and David H Ellison (2014). 'Distal convoluted tubule'. In: *Clinical Journal of the American Society of Nephrology* 9.12, pp. 2147–2163.

Sui, Weiguo et al. (2008). 'Microarray analysis of MicroRNA expression in acute rejection after renal transplantation'. In: *Transplant Immunology* 19.1, pp. 81–85.

Suire, Sabine, Phillip Hawkins and Len Stephens (2002). 'Activation of phosphoinositide 3-kinase gamma by Ras'. In: *Current biology* 12.13, pp. 1068–1075.

Sun, Dandan et al. (2014a). 'Regulation of several androgen-induced genes through the repression of the miR-99a let-7 miR-125b-2 miRNA cluster in prostate cancer cells'. In: *Oncogene* 33.11, pp. 1448–57.

Sun, Fang et al. (2008). 'Downregulation of CCND1 and CDK6 by miR-34a induces cell cycle arrest'. In: *FEBS Letters* 582.10, pp. 1564–1568.

Sun, Huan et al. (2010). 'MicroRNA-17 post-transcriptionally regulates polycystic kidney disease-2 gene and promotes cell proliferation'. In: *Molecular Biology Reports* 37.6, pp. 2951–2958.

Sun, T et al. (2014b). 'MiR-221 promotes the development of androgen independence in prostate cancer cells via downregulation of HECTD2 and RAB1A'. In: *Oncogene* 33.21, pp. 2790–800.

Sun, Yingqing et al. (2004). 'Development of a microarray to detect human and mouse microRNAs and characterization of expression in human organs'. In: *Nucleic acids research* 32.22.

Suzuki, Hiroshi I. et al. (2011). 'MCPIP1 ribonuclease antagonizes dicer and terminates microRNA biogenesis through precursor microRNA degradation'. In: *Molecular Cell* 44.3, pp. 424–436.

Suzuki, Hiroshi I et al. (2015). 'Small-RNA asymmetry is directly driven by mammalian Argonautes'. In: *Nature Structural and Molecular Biology* 22.7, pp. 512–21.

Syed, Fraz, Haiying Grunenwald and Nicholas Caruccio (2009). 'Summary of the online focus on next-generation sequencing data analysis'. In: *Nature Methods* 6.11, pp. 802–803.

Szeto, Cheuk-Chun et al. (2012). 'Micro-RNA expression in the urinary sediment of patients with chronic kidney diseases'. In: *Disease markers* 33.3, pp. 137–44.

't Hoen, Peter A C (2003). 'Fluorescent labelling of cRNA for microarray applications'. In: *Nucleic Acids Research* 31.5, 20e–20.

Tack, Ivan (2010). 'Effects of water consumption on kidney function'. In: *Nutrition Today* 45.6, S37–S40.

Takahashi-Yanaga, Fumi and Toshiyuki Sasaguri (2008). 'GSK-3beta regulates cyclin D1 expression: A new target for chemotherapy'. In: *Cellular Signalling* 20.4, pp. 581–589.

Takakura, Ayumi et al. (2009). 'Renal injury is a third hit promoting rapid development of adult Polycystic Kidney Disease'. In: *Human Molecular Genetics* 18.14, pp. 2523–2531.

Tan, Ying-Cai, Jon Blumenfeld and Hanna Rennert (2011). 'Autosomal Dominant Polycystic Kidney Disease: Genetics, mutations and microRNAs'. In: *Biochimica et Biophysica Acta* 1812.10, pp. 1202–1212.

Tanaka, Tetsuhiro and Masaomi Nangaku (2014). 'ANO1: an additional key player in cyst growth'. In: *Kidney international* 85.5, pp. 1007–9.

Tang, Guo Qing and E. Stuart Maxwell (2008). 'Xenopus microRNA genes are predominantly located within introns and are differentially expressed in adult frog tissues via post-transcriptional regulation'. In: *Genome Research*.

Tang, Xiaoli et al. (2013). 'Acetylation of Drosha on the N-terminus inhibits its degradation by ubiquitination'. In: *PLoS ONE* 8.8.

Tang, Xiaoqing et al. (2009). 'Identification of glucose-regulated miRNAs from pancreatic β-cells reveals a role for miR-30d in insulin transcription'. In: *RNA* 15.2, pp. 287–93.

Tang, Yanping et al. (2011). 'Quantitative analysis of miRNA expression in seven human foetal and adult organs'. In: *PLoS ONE* 6.12, pp. 1–6.

Tarasov, Valery et al. (2007). 'Differential regulation of microRNAs by p53 revealed by massively parallel sequencing: miR-34a is a p53 target that induces apoptosis and G 1-arrest'. In: *Cell Cycle* 6.13, pp. 1586–1593.

Tay, Yvonne et al. (2008). 'MicroRNAs to Nanog, Oct4 and Sox2 coding regions modulate embryonic stem cell differentiation'. In: *Nature* 455.7216, pp. 1124–1128.

Taylor, Alan N, James E McIntosh and James E Bourdeau (1982). 'Immunocytochemical localization of vitamin D-dependent calcium-binding protein in renal tubules of rabbit, rat, and chick'. In: *Kidney International* 21.5, pp. 765–773.

Taylor, Karin et al. (2015). 'Nanocell targeting using engineered bispecific antibodies'. In: *mAbs* 7.1, pp. 53–65.

Teng, Jia An et al. (2016). 'The activation of ERK1/2 and JNK MAPK signaling by Insulin/IGF-1 is responsible for the development of colon cancer with type 2 diabetes mellitus'. In: *PLoS ONE* 11.2.

Terryn, Sara et al. (2011). 'Fluid transport and cystogenesis in Autosomal Dominant Polycystic Kidney Disease'. In: *Biochimica et Biophysica Acta* 1812.10, pp. 1314–21.

The Cancer Genome Atlas Network (2013). 'Comprehensive molecular characterization of clear cell renal cell carcinoma'. In: *Nature* 499.7456, pp. 43–9.

ThermoFisher (2017). *ThermoFisher - Microarray*.

Thomas, Robert, Abbas Kanso and John R Sedor (2008). 'Chronic Kidney Disease and its complications'. In: *Primary Care* 35.2, pp. 329–44, vii.

Thum, Thomas et al. (2008). 'MicroRNA-21 contributes to myocardial disease by stimulating MAP kinase signalling in fibroblasts'. In: *Nature* 456.7224, pp. 980–984.

Tian, Yu et al. (2007). 'TAZ promotes PC2 degradation through a SCFbeta-Trcp E3 ligase complex'. In: *Molecular and cellular biology* 27.18, pp. 6383–95.

Tian, Zhongmin et al. (2008). 'MicroRNA-target pairs in the rat kidney identified by microRNA microarray, proteomic, and bioinformatic analysis'. In: *Genome Research* 18.3, pp. 404–411.

Tokumaru, Shogo et al. (2008). 'let-7 regulates Dicer expression and constitutes a negative feedback loop'. In: *Carcinogenesis* 29.11, pp. 2073–2077.

Tomankova, Tereza, Martin Petrek and Eva Kriegova (2010). 'Involvement of microRNAs in physiological and pathological processes in the lung'. In: *Respiratory research* 11.1, p. 159.

Tong, An Li et al. (2016). 'Interaction between Angiotensin II and Insulin/IGF-1 Exerted a Synergistic Stimulatory Effect on ERK1/2 Activation in Adrenocortical Carcinoma H295R Cells'. In: *International Journal of Endocrinology* 2016.

Torres, Anna et al. (2011). 'Major regulators of miRNAs biogenesis Dicer and Drosha are down-regulated in endometrial cancer'. In: *Tumor Biology* 32.4, pp. 769–776.

Torres, Vicente E and Peter C Harris (2009). 'Autosomal Dominant Polycystic Kidney Disease: the last 3 years'. In: *Kidney International* 76.2, pp. 149–168.

— (2014). 'Strategies targeting cAMP signaling in the treatment of Polycystic Kidney Disease'. In: *Journal of the American Society of Nephrology* 25.1, pp. 18–32.

Torres, Vicente E et al. (2004). 'Effective treatment of an orthologous model of autosomal Autosomal Dominant Polycystic Kidney Disease'. In: *Nature Medicine* 10.4, pp. 363–4.

Torres, Vicente E et al. (2012). 'Tolvaptan in patients with Autosomal Dominant Polycystic Kidney Disease'. In: *New England Journal of Medicine* 367.25, pp. 2407–2418.

Torres, Vicente E et al. (2014). 'Angiotensin blockade in late Autosomal Dominant Polycystic Kidney Disease'. In: *New England Journal of Medicine* 371.24, pp. 2267–2276.

Torres, Vicente E et al. (2016). 'Effect of Tolvaptan in Autosomal Dominant Polycystic Kidney Disease by CKD Stage: Results from the TEMPO 3:4 Trial'. In: *Clinical Journal of the American Society of Nephrology* February 2015, pp. 1–9.

Torres, Vicente E et al. (2017). 'Multicenter, open-label, extension trial to evaluate the long-term efficacy and safety of early versus delayed treatment with tolvaptan in Autosomal Dominant Polycystic Kidney Disease: the TEMPO 4:4 Trial'. In: *Nephrology Dialysis Transplantation*, pp. 1–13.

Trabucchi, Michele et al. (2009). 'The RNA-binding protein KSRP promotes the biogenesis of a subset of microRNAs'. In: *Nature* 459.7249, pp. 1010–1014.

Tran, Uyen et al. (2010). 'The RNA-binding protein bicaudal C regulates polycystin 2 in the kidney by antagonizing miR-17 activity'. In: *Development* 137, pp. 1107–1116.

Trang, Phong et al. (2011). 'Systemic delivery of tumor suppressor microRNA mimics using a neutral lipid emulsion inhibits lung tumors in mice'. In: *Molecular Therapy* 19.6, pp. 1116–22.

Trionfini, Piera, Ariela Benigni and Giuseppe Remuzzi (2014). 'MicroRNAs in kidney physiology and disease'. In: *Nature Reviews Nephrology* 11.1, pp. 23–33.

Trudel, Marie, Qin Yao and Feng Qian (2016). 'The Role of G-protein-coupled receptor proteolysis site cleavage of polycystin-1 in renal physiology and Polycystic Kidney Disease'. In: *Cells* 5.1, p. 3.

Turco, Alberto E et al. (1996). 'An Italian family with Autosomal Dominant Polycystic Kidney Disease unlinked to either the PKD1 or PKD2 gene'. In: *American Journal of Kidney Diseases* 28.5, pp. 759–761.

University of Oregon (2017). *RNA-seqlopedia*.

University of Utah (2017). *Learn.Genetics*.

Valencia-Sanchez, Marco Antonio et al. (2006). 'Control of translation and mRNA degradation by miRNAs and siRNAs'. In: *Genes and Development* 20.5, pp. 515–524.

Van Den Beucken, Twan et al. (2014). 'Hypoxia promotes stem cell phenotypes and poor prognosis through epigenetic regulation of DICER'. In: *Nature Communications* 5, p. 5203.

Vanhaesebroeck, Bart et al. (2001). 'Synthesis and function of 3-phosphorylated inositol lipids'. In: *Annual Review of Biochemistry* 70, pp. 535–602.

Vanhaesebroeck, Bart et al. (2010). 'The emerging mechanisms of isoform-specific PI3K signalling'. In: *Nature Reviews Molecular Cell Biology* 11.5, pp. 329–341.

Vassilev, Peter M et al. (2001). 'Polycystin-2 is a novel cation channel implicated in defective intracellular Ca(2+) homeostasis in polycystic kidney disease'. In: *Biochemical and biophysical research communications* 282.1, pp. 341–50.

Vasudevan, Shobha, Yingchun Tong and Joan A. Steitz (2007). 'Switching from repression to activation: microRNAs can up-regulate translation'. In: *Science* 318.December, pp. 1931–1934.

Veikkolainen, Ville et al. (2012). 'ErbB4 modulates tubular cell polarity and lumen diameter during kidney development'. In: *Journal of the American Society of Nephrology* 23.1, pp. 112–22.

Ventura, Andrea et al. (2008). 'Targeted deletion reveals essential and overlapping functions of the miR-17-92 family of miRNA clusters'. In: *Cell* 132.5, pp. 875–886.

Vermeulen, Annaleen et al. (2005). 'The contributions of dsRNA structure to Dicer specificity and efficiency'. In: *RNA* 11.5, pp. 674–82.

Veronese, Angelo et al. (2010). 'Oncogenic role of miR-483-3p at the IGF2/483 locus'. In: *Cancer Research* 70.8, pp. 3140–3149.

Vlachos, Ioannis S et al. (2014). 'DIANA-TarBase v7.0: indexing more than half a million experimentally supported miRNA:mRNA interactions'. In: *Nucleic Acids Research* 43.D1, pp. D153–D159.

Vogel, Britta et al. (2013). 'Multivariate miRNA signatures as biomarkers for non-ischaemic systolic heart failure'. In: *European Heart Journal* 34.36, pp. 2812–2822.

Voulgari, Angeliki and Alexander Pintzas (2009). 'Epithelial-mesenchymal transition in cancer metastasis: Mechanisms, markers and strategies to overcome drug resistance in the clinic'. In: *Biochimica et Biophysica Acta - Reviews on Cancer* 1796.2, pp. 75–90.

Wada, Taeko, Jiro Kikuchi and Yusuke Furukawa (2012). 'Histone deacetylase 1 enhances microRNA processing via deacetylation of DGCR8'. In: *EMBO Reports* 13.2, pp. 142–149.

Wahle, Elmar and G. Sebastiaan Winkler (2013). 'RNA decay machines: Deadenylation by the Ccr4-Not and Pan2-Pan3 complexes'. In: *Biochimica et Biophysica Acta - Gene Regulatory Mechanisms* 1829.6-7, pp. 561–570.

Walz, Gerd et al. (2010). 'Everolimus in patients with Autosomal Dominant Polycystic Kidney Disease'. In: *New England Journal of Medicine* 363.9, pp. 830–840.

Wang, Bo et al. (2010a). 'E-cadherin expression is regulated by miR-192 / 215 by a mechanism that is independent of the profibrotic effects of transforming growth factor-β'. In: *Diabetes* 59.7, pp. 1794–1802.

Wang, Gang et al. (2010b). 'Expression of microRNAs in the urinary sediment of patients with IgA nephropathy'. In: *Disease Markers* 28.2, pp. 79–86.

Wang, Gang et al. (2010c). 'Intra-renal expression of microRNAs in patients with IgA nephropathy'. In: *Laboratory Investigation* 90, pp. 98–103.

Wang, Gang et al. (2011a). 'Elevated levels of miR-146a and miR-155 in kidney biopsy and urine from patients with IgA nephropathy'. In: *Disease Markers* 30.4, pp. 171–179.
Wang, Guohua et al. (2010d). 'RNA polymerase II binding patterns reveal genomic regions involved in microRNA gene regulation'. In: *PLoS ONE* 5.11.
Wang, Hong-Wei et al. (2009a). 'Structural insights into RNA processing by the human RISC-loading complex'. In: *Nature Structural and Molecular Biology* 16.11, pp. 1148–1153.
Wang, Jin et al. (2014a). 'Circulating microRNAs in pancreatic juice as candidate biomarkers of pancreatic cancer'. In: *Journal of Cancer* 5.8, pp. 696–705.
Wang, Peng et al. (2014b). 'Methylation-mediated silencing of the miR-124 genes facilitates pancreatic cancer progression and metastasis by targeting Rac1'. In: *Oncogene* 33.October 2012, pp. 514–24.
Wang, Qiang et al. (2008a). 'MicroRNA-377 is up-regulated and can lead to increased fibronectin production in diabetic nephropathy'. In: *FASEB Journal* 22.12, pp. 4126–4135.
Wang, Wenzhang et al. (2011b). 'Human tumor microRNA signatures derived from large-scale oligonucleotide microarray datasets'. In: *International Journal of Cancer* 129.7, pp. 1624–1634.
Wang, X. H. et al. (2009b). 'MicroRNA-320 expression in myocardial microvascular endothelial cells and its relationship with insulin-like growth factor-1 in type 2 diabetic rats'. In: *Clinical and Experimental Pharmacology and Physiology* 36.2, pp. 181–188.
Wang, Xiaowei (2014). 'Composition of seed sequence is a major determinant of microRNA targeting patterns'. In: *Bioinformatics* 30.10, pp. 1377–1383.
— (2016). 'Improving microRNA target prediction by modeling with unambiguously identified miRNA-target pairs from CLIP-ligation studies'. In: *Bioinformatics* 32.9, pp. 1316–1322.
Wang, X et al. (2009c). 'High-resolution human core-promoter prediction with CoreBoost_HM'. In: *Genome research* 19.2, pp. 266–275.
Wang, Yanli et al. (2008b). 'Structure of an argonaute silencing complex with a seed-containing guide DNA and target RNA duplex'. In: *Nature* 456.7224, pp. 921–926.
Warner, Matthew J. et al. (2016). 'S6K2-mediated regulation of TRBP as a determinant of miRNA expression in human primary lymphatic endothelial cells'. In: *Nucleic Acids Research* 44.20, pp. 9942–9955.
Watnick, Terry J et al. (1998). 'Somatic mutation in individual liver cysts supports a two-hit model of cystogenesis in Autosomal Dominant Polycystic Kidney Disease'. In: *Molecular Cell* 2.2, pp. 247–251.
Watnick, Terry J et al. (2000). 'Mutations of PKD1 in ADPKD2 cysts suggest a pathogenic effect of trans-heterozygous mutations'. In: *Nature Genetics* 25.2, pp. 143–144.
Weber, Martina et al. (2014). 'MiRNA-155 targets myosin light chain kinase and modulates actin cytoskeleton organization in endothelial cells.' In: *American Journal of Physiology - Heart and Circulatory Physiology* 306, H1192–203.
Webster, Jonathan, Diane Prager and Shlomo Melmed (1994). 'Insulin-like growth factor-1 activation of extracellular signal-related kinase-1 and -2 in growth hormone-secreting cells'. In: *Molecular Endocrinology* 8.5, pp. 539–544.
Welch, Heidi C E et al. (2003). 'Phosphoinositide 3-kinase-dependent activation of Rac'. In: *FEBS Letters* 546.1, pp. 93–97.
Welling, L. W. (1990). 'Pathogenesis of cysts and cystic kidneys'. In: *The Cystic Kidney*. Ed. by K.D. Gardne and J. Bernstein, pp. 99–116.
Wells, Corinne C et al. (2005). 'Diabetic nephropathy is associated with decreased circulating estradiol levels and imbalance in the expression of renal estrogen receptors'. In: *Gender Medicine* 2.4, pp. 227–237.
Wen, Jessica and Joshua R Friedman (2012). 'miR-122 regulates hepatic lipid metabolism and tumor suppression'. In: *Journal of Clinical Investigation* 31.8, pp. 2773–2776.
Weston, Benjamin S. et al. (2001). 'The polycystin-1 C-type lectin domain binds carbohydrate in a calcium-dependent manner, and interacts with extracellular matrix proteins in vitro'. In: *Biochimica et Biophysica Acta - Molecular Basis of Disease* 1536.2-3, pp. 161–176.
Whitmarsh, Alan J et al. (1995). 'Integration of MAP kinase signal transduction pathways at the serum response element'. In: *Science* 269.5222, pp. 403–7.
Wienholds, Erno et al. (2005). 'MicroRNA expression in zebrafish embryonic development'. In: *Science* 309.5732, pp. 310–311.
Wilkes, Martin et al. (2017). 'Molecular insights into lipid-assisted Ca2+ regulation of the TRP channel Polycystin-2'. In: *Nature Structural and Molecular Biology* 24.2, pp. 123–130.
Wilson, Patricia D (2001). 'Polycystin : new aspects of structure, function, and regulation'. In: *Journal of the American Society of Nephrology* 12, pp. 834–845.
Won, Jae Kyung et al. (2012). 'The crossregulation between ERK and PI3K signaling pathways determines the tumoricidal efficacy of MEK inhibitor'. In: *Journal of Molecular Cell Biology* 4.3, pp. 153–163.

Wu, Chunlei et al. (2016). 'BioGPS: Building your own mash-up of gene annotations and expression profiles'. In: *Nucleic Acids Research* 44.D1, pp. D313–D316.
Wu, Guanqing et al. (2000). 'Cardiac defects and renal failure in mice with targeted mutations in Pkd2'. In: *Nature Genetics* 24.1, pp. 75–78.
Wu, Ming-Ming et al. (2014). 'Hypoxia augments the Ca2+-activated chloride current carried by anoctamin-1 in cardiac vascular endothelial cells of neonatal mice'. In: *British Journal of Pharmacology* 171.15, pp. 3680–3692.
Xia, Hua Qiang et al. (2011). 'Over-expression of miR375 reduces glucose-induced insulin secretion in Nit-1 cells'. In: *Molecular Biology Reports* 38.5, pp. 3061–3065.
Xiao, Zhousheng et al. (2006). 'Cilia-like structures and polycystin-1 in osteoblasts/osteocytes and associated abnormalities in skeletogenesis and Runx2 expression'. In: *Journal of Biological Chemistry* 281.41, pp. 30884–30895.
Xiong, Mingxia et al. (2012). 'The miR-200 family regulates TGF-β1-induced renal tubular epithelial to mesenchymal transition through Smad pathway by targeting ZEB1 and ZEB2 expression'. In: *American Journal of Physiology - Renal Physiology* 302.3, F369–79.
Xu, Chang et al. (2007). 'Human ADPKD primary cyst epithelial cells with a novel, single codon deletion in the PKD1 gene exhibit defective ciliary polycystin localization and loss of flow-induced Ca2+ signaling'. In: *American Journal of Physiology - Renal Physiology* 292.3.
Xu, Jen Xin et al. (2014). 'Polycystin-1 and Gα12 regulate the cleavage of E-cadherin in kidney epithelial cells'. In: *Physiological Genomics* 02115.59, physiolgenomics.00090.2014.
Xu, Yaoxian et al. (2016). 'The polycystin-1, lipoxygenase, and alpha-toxin domain regulates polycystin 1 trafficking'. In: *Journal of the American Society of Nephrology* 27.4, pp. 1159–1173.
Yamamura, Soichiro et al. (2012). 'Microrna-34a modulates c-Myc transcriptional complexes to suppress malignancy in human prostate cancer cells'. In: *PLoS ONE* 7.1, pp. 1–12.
Yang, Baoxue et al. (2008a). 'Small-molecule CFTR inhibitors slow cyst growth in Polycystic Kidney Disease'. In: *Journal of the American Society of Nephrology* 19.7, pp. 1300–10.
Yang, Jer-Yen et al. (2008b). 'ERK promotes tumorigenesis by inhibiting FOXO3a via MDM2-mediated degradation'. In: *Nature Cell Biology* 10.2, pp. 138–48.
Ye, Yan et al. (2013). 'PI(4,5)P2 5-phosphatase A regulates PI3K/Akt signalling and has a tumour suppressive role in human melanoma'. In: *Nature Communications* 4, p. 1508.
Yeom, Kyu Hyeon et al. (2006). 'Characterization of DGCR8/Pasha, the essential cofactor for Drosha in primary miRNA processing'. In: *Nucleic Acids Research* 34.16, pp. 4622–4629.
Yi, Rui et al. (2003). 'Exportin-5 mediates the nuclear export of pre-microRNAs and short hairpin RNAs'. In: *Genes and Development* 17.24, pp. 3011–3016.
Yim, Hyungshin et al. (2011). 'Nek1 and TAZ interact to maintain normal levels of polycystin 2'. In: *Journal of the American Society of Nephrology* 22.5, pp. 832–837.
Yin, Liangjie et al. (2014). 'Glucose stimulates calcium-activated chloride secretion in small intestinal cells'. In: *American Journal of Physiology - Cell Physiology* 306.7, pp. C687–96.
Yoda, Mayuko et al. (2010). 'ATP-dependent human RISC assembly pathways'. In: *Nature Structural and Molecular Biology* 17.1, pp. 17–23.
Yoder, Bradley K, Xiaoying Hou and Lisa M Guay-Woodford (2002). 'The Polycystic Kidney Disease proteins, polycystin-1, polycystin-2, polaris, and cystin, are co-localized in renal cilia'. In: *Journal of the American Society of Nephrology* 13, pp. 2508–2516.
Younger, Scott T and David R Corey (2011a). 'Transcriptional gene silencing in mammalian cells by miRNA mimics that target gene promoters'. In: *Nucleic Acids Research* 39.13, pp. 5682–5691.
— (2011b). 'Transcriptional regulation by miRNA mimics that target sequences downstream of gene termini'. In: *Molecular BioSystems* 7, pp. 2383–2388.
Yu, Bin et al. (2005). 'Methylation as a crucial step in plant microRNA biogenesis'. In: *Science* 307.5711, pp. 932–935.
Yu, Fengyan et al. (2007). 'let-7 regulates self renewal and tumorigenicity of breast cancer cells'. In: *Cell* 131.6, pp. 1109–1123.
Yu, Jinghua et al. (1998). 'Regulation of the p85/p110 phosphatidylinositol 3'-Kinase: stabilization and inhibition of the p110α catalytic subunit by the p85 regulatory subunit'. In: *Molecular and Cellular Biology* 18.3, pp. 1379–1387.
Yu, Yadong, Xiaoying Lü and Fei Ding (2015). 'microRNA regulatory mechanism by which PLLA aligned nanofibers influence PC12 cell differentiation'. In: *Journal of Neural Engineering* 12.4, p. 046010.
Zandwijk, Nico van et al. (2015). 'Mesomir 1: a phase I study of Targomirs in patients with refractory malignant pleural mesothelioma (Mpm) and lung cancer (Nsclc)'. In: *Annals of Oncology* 26.Supplement 2, p. 16.

Zawada, Adam M. et al. (2014). 'Massive analysis of cDNA Ends (MACE) and miRNA expression profiling identifies proatherogenic pathways in chronic kidney disease'. In: *Epigenetics* 9.1, pp. 161–172.
Zeisberg, Michael et al. (2003). 'BMP-7 counteracts TGF-β1-induced epithelial-to-mesenchymal transition and reverses chronic renal injury'. In: *Nature medicine* 9.7, pp. 964–968.
Zeng, Yan, Rui Yi and Bryan R Cullen (2005). 'Recognition and cleavage of primary microRNA precursors by the nuclear processing enzyme Drosha'. In: *EMBO Journal* 24.1, pp. 138–48.
Zeng, Yan et al. (2008). 'Phosphorylation of Argonaute 2 at serine-387 facilitates its localization to processing bodies.' In: *Biochemical Journal* 413.3, pp. 429–36.
Zhang, Haidi et al. (2002). 'Human Dicer preferentially cleaves dsRNAs at their termini without a requirement for ATP'. In: *EMBO Journal* 21.21, pp. 5875–5885.
Zhang, Haidi et al. (2004). 'Single processing center models for human Dicer and bacterial RNase III'. In: *Cell* 118.1, pp. 57–68.
Zhang, Jin et al. (2013). 'Up-regulation of Ago2 expression in gastric carcinoma'. In: *Medical Oncology* 30.3, pp. 1–7.
Zhang, Lin et al. (2006). 'microRNAs exhibit high frequency genomic alterations in human cancer'. In: *Proceedings of the National Academy of Sciences* 103.24, pp. 9136–9141.
Zhang, Xinbo et al. (2011a). 'Akt, FoxO and regulation of apoptosis'. In: *Biochimica et Biophysica Acta - Molecular Cell Research* 1813.11, pp. 1978–1986.
Zhang, Xinna et al. (2011b). 'The ATM Kinase Induces MicroRNA Biogenesis in the DNA Damage Response'. In: *Molecular Cell* 41.4, pp. 371–383.
Zhang, Zheng et al. (2009). 'MicroRNA-21 protects from mesangial cell proliferation induced by diabetic nephropathy in db/db mice'. In: *FEBS Letters* 583.12, pp. 2009–2014.
Zhao, Luqing et al. (2016). 'DDX3X promotes the biogenesis of a subset of miRNAs and the potential roles they played in cancer development'. In: *Scientific Reports* 6.
Zhao, Yuming et al. (2017). 'Methods of MicroRNA promoter prediction and transcription factor mediated regulatory network'. In: *BioMed Research International* 2017.
Zhdanova, Olga et al. (2011). 'The inducible deletion of Drosha and miRNAs in mature podocytes results in a collapsing glomerulopathy'. In: *Kidney International* 80.7, pp. 719–730.
Zheng, Wen-Hua and Remi Quirion (2006). 'Insulin-like growth factor-1 (IGF-1) induces the activation/phosphorylation of Akt kinase and cAMP response element-binding protein (CREB) by activating different signaling pathways in PC12 cells'. In: *BMC Neuroscience* 7.1, p. 51.
Zhong, Xiang et al. (2011). 'Smad3-mediated upregulation of miR-21 promotes renal fibrosis'. In: *Journal of the American Society of Nephrology* 22.9, pp. 1668–1681.
Zhong, Xiang et al. (2013). 'MiR-21 is a key therapeutic target for renal injury in a mouse model of type 2 diabetes'. In: *Diabetologia* 56.3, pp. 663–674.
Zhou, Hua et al. (2013). 'miR-150 promotes renal fibrosis in lupus nephritis by downregulating SOCS1'. In: *Journal of the American Society of Nephrology* 24.7, pp. 1073–1087.
Zhou, Songyang et al. (1993). 'SH2 domains recognize specific phosphopeptide sequences'. In: *Cell* 72.5, pp. 767–778.
Zhou, Xuefeng et al. (2007). 'Characterization and identification of microRNA core promoters in four model species'. In: *PLoS Computational Biology* 3.3, pp. 0412–0423.
Zhu, Meng-Lei and Natasha Kyprianou (2010). 'Role of androgens and the androgen receptor in epithelial-mesenchymal transition and invasion of prostate cancer cells'. In: *FASEB Journal* 24.3, pp. 769–777.
Zhu, Y. Y. et al. (2001). 'Reverse transcriptase template switching: A SMART approach for full-length cDNA library construction'. In: *BioTechniques* 30.4, pp. 892–897.
Zhuo, Jia L. and Xiao C. Li (2013). 'Proximal nephron'. In: *Comprehensive Physiology* 3.3, pp. 1079–1123.
Zimmermann, Sven and Karin Moelling (1999). 'Phosphorylation and regulation of Raf by Akt (protein kinase B)'. In: *Science* 286.5445, pp. 1741–1744.
Zoncu, Roberto, Alejo Efeyan and David M Sabatini (2011). 'mTOR: from growth signal integration to cancer, diabetes and ageing'. In: *Nature Reviews Molecular Cell Biology* 12.1, pp. 21–35.